Ghent University - Faculty of Sciences

Department of Biology

Research Group of Protistology & Aquatic Ecology

Photoprotection in intertidal benthic diatoms

Blommaert Lander

Promotor: Prof. Dr. Koen Sabbe

Co-promotor: Prof. Dr. Wim Vyverman

Thesis submitted in fulfillment of the requirements for the degree of Doctor in Science - Biology

Academic year 2016-2017

Dutch translation of the title

Fotoprotectie bij intertidale benthische kiezelwieren

Lander Blommaert

Cover illustration

Cover front: The high light setup used in Chapters 3 and 5.

To refer to this work

Blommaert, L., 2017. Photoprotection in intertidal benthic diatoms.

Ph.D. dissertation. Ghent University, Ghent, Belgium.

Publically defended on 30/06/2017

Members of the examination committee

Prof. Dr. Koen Sabbe – Ghent University (Promotor)*

Prof. Dr. Wim Vyverman – Ghent University (Co-promotor)*

Prof. Dr. Bart Braeckman – Ghent University (Chairman)

Prof. Dr. Olivier De Clerck – Ghent University (Secretary)

Prof Dr. Graham J. C. Underwood – Essex University

Prof. Dr. Lieven De Veylder – VIB / Ghent University

Dr. Bruno Jesus – Nantes University

* non-voting members

Thesis defended in public

Friday, June 30th 2017 at 16:00 h

Auditorium Valere Billet

Campus Sterre

Financial support

(FWO project G.0222.09N), Ghent University (BOF-GOA 01G01911) and the Egide/Campus France-PHC Tournesol (n128992UA) exchange program

Table of contents

Glossary

Ax	Antheraxanthin, a xanthophyll pigment
Chl *a*	Chlorophyll *a*, a green pigment
Ddx	Diadinoxanthin, a xanthophyll pigment
Ddx + Dtx	Total Ddx and Dtx xanthophyll cycle pool
DES	De-epoxidation state, the amount of de-epoxidized xanthophyll cycle pigments divided by the total xanthophyll cycle pigment pool size multiplied by 100
Dtx	Diatoxanthin, a xanthophyll pigment
ECS	ElectroChromic Shift, an electric field induced absorption change of pigments
Epipelon	Microalgae living in loose association with the sediments
Epipsammon	Microalgae living in close association with individual sand particles
De-epoxidation	Removal of an epoxide group, a three-atom ring containing oxygen (a cyclic ether)
FCP	Fucoxanthin Chlorophyll *a*/*c* binding Protein
LHCR	Light-Harvesting Complex Red lineage protein
LHCX	Light-Harvesting Complex X protein
NPQ	Non-Photochemical Quenching of chlorophyll fluorescence
NPQs	Sustained quenching NPQ component
Phytoplankton	Microalgae that live suspended in the water column
PMF	Proton Motive Force, a gradient that drives ATP synthesis, comprising an electric (ΔΨ) and an osmotic (ΔpH) component
PSI and PSII	Photosystem I and II, functional and structural units of protein complexes involved in photosynthesis
qE	Energy dependent quenching NPQ component
qI	'Photoinhibitory' quenching, slowly relaxing NPQ component
Tychoplankton	Microalgae occurring both in or on the sediments as suspended in the water column
Vx	Violaxanthin, a xanthophyll pigment
Vx + Ax + Zx	Total Vx, Ax, and Zx xanthophyll cycle pool
Xanthophylls	Pigments that play an important role in photoprotection
XC	Xanthophyll cycle, alternation of epoxidized and de-epoxidized xanthophylls
Zx	Zeaxanthin, a xanthophyll pigment
$\Delta F/F_m'$	Effective quantum efficiency of PSII photochemistry
ΔΨ	A gradient of electric potential (in this context across the thylakoid membrane)
ΔpH	Proton gradient across the thylakoid membrane

Chapter 1: General introduction and outline

This introduction provides the reader with information about the intertidal sediment habitat and their main primary producers: intertidal benthic diatoms. In addition, it introduces the main mechanisms by which these organisms protect themselves against oversaturating light conditions at low tide and more specifically excess light energy dissipation as heat, or non-photochemical quenching (NPQ), involving the xanthophyll cycle (XC), Light-harvesting complex X (LHCX) proteins and the build-up of a proton gradient across the thylakoid membrane. Finally, it provides background information on optical techniques which allow the probing of photosynthesis in vivo: chlorophyll fluorescence monitoring and electrochromism.

Intertidal sediments

Estuaries and coastal zones, which form the interface between the terrestrial and marine environment, are ecologically and economically valuable environments. They are highly productive ecosystems, partly due to the contribution of microphytobenthic (MPB) biofilms thriving on intertidal sediments (Underwood and Kromkamp 1999) and macroalgae on rocky shores (Migné et al. 2015). Especially in turbid systems, primary production in sediments may equal or even surpass the primary production of algae suspended in the water column (phytoplankton), (Underwood and Kromkamp 1999). Microphytobenthic organisms, are a major food source for grazing meiofauna (Pinckney et al. 2003). In addition MPB may also be a food source for benthic suspension feeders such as commercially cultivated bivalves (oysters, mussels) when resuspended in the water column (Riera 1998). Moreover, in both nutrient replete and nutrient limited conditions, a considerable fraction of the photosynthetically assimilated carbon is released (Cook et al. 2007) and incorporated in higher trophic levels. As such, the MPB plays a central role in the food web of intertidal sediments (Middelburg et al. 2000). Exudated polymeric substances of these organisms, in addition, contribute to the stability and increase the erosion thresholds of intertidal sediments which may serve as a natural coastal defense (Stal 2010; Gerbersdorf and Wieprecht 2015). Sediment stabilization by diatoms also allows new species to colonize the sediments. As such, they can be regarded as ecosystem engineers (Boogert et al. 2006; Gerbersdorf et al. 2009; Passarelli et al. 2014). Finally, MPB plays an important role in lowering dissolved inorganic nitrogen in estuarine waters (Cabrita and Brotas 2000), a process which is dependent on MPB photosynthesis (Thornton et al. 2007).

Intertidal sediments consist of muddy, sandy sediments and mixed sediment types, which all differ in sediment grain size composition. In sandy sediments, grain size is generally larger than 62.5 µm and sediment particles are spherical (Paterson and Hagerthey 2001). As such there is not much attraction between particles, which act as individual units. When sediment particles become smaller, the surface to volume ratio increases, together with the Van der Waals attraction forces between them. As a result muddy sediments are more cohesive than sandy sediments (Paterson and Hagerthey 2001). Large sediment particles can settle in highly hydrodynamic conditions whereas smaller particles are swept away and mainly accumulate in less dynamic conditions. As hydrodynamic conditions are not constant, most natural intertidal sediments are poorly sorted and comprise a mix of particles of different sizes (Yallop et al. 1994). Grain size also changes the optical properties of intertidal sediments, which influences the experienced light climate for primary producers. Light attenuation, for instance is much stronger in muddy sediments, resulting in a very thin photic zone, whereas it can penetrate deeper (a couple of mm) in coarse sandy sediments (Kuhl et al. 1994; Cartaxana et al. 2016b). Another important difference between muddy and sandy sediments is nutrient availability: whereas nutrients are sequestered onto fine sediments and are available for the MPB, sandy sediments are generally low in nutrients (Paterson and Hagerthey 2001).

Microphytobenthic communities

The microphytobenthos from intertidal sediments in temperate zones is usually dominated by diatoms, even though cyanobacteria and euglenophytes can also be common (Underwood and Barnett 2006). Microphytobenthic diatom communities differ according to sediment type (mud or sand) (Sabbe and Vyverman 1991; Hamels et al. 1998; Méléder et al. 2007; Ribeiro et al. 2013). Three major growth forms of sediment inhabiting diatoms can be distinguished (Fig. 1): (1) The tychoplankton comprises both centric and pennate diatom species, which live on intertidal sediments, but also thrive suspended in the water column; (2) epipelic (literally 'living on mud') species live in loose association with the sediment matrix and are mostly biraphid pennate diatoms. Raphid diatoms possess a raphe structure through which mucilage is secreted. As such they are able to move (Round et al. 1990; Aumeier and Menzel 2012) and position themselves in the sediment light gradient (Cartaxana et al. 2016a). (3) the epipsammon (literally 'living on sand') comprises mostly araphid and small monoraphid diatoms which are largely immotile and live in close association with single sand grains (free-living or attached, Sabbe 1997). Therefore, they are subject to the mixing and transport of their substratum (Admiraal 1984). The names epipelon and epipsammon are often used to describe the whole communities living on muddy or sandy sediments, respectively. Indeed, epipelic species tend to dominate sheltered muddy areas whereas epipsammic species prevail in

more dynamic sandy sediments (Sabbe and Vyverman 1991). There are, however, many exceptions. Several large motile species, for instance, thrive on unstable sandy sediments (Admiraal 1984).

Diatom communities on muddy and sandy sediments differ in species diversity, seasonal variability and vertical distribution. Whereas muddy sediments are dominated by communities of epipelic diatoms which show lower diversity and display seasonal blooms, communities on sandy sediments are often more diverse and show less seasonal variation (Sabbe 1993; Hamels et al. 1998; Ribeiro et al. 2013). As in muddy sediments diatoms are generally motile and light penetration into the sediment is limited to the uppermost 200 µm, dense photosynthetic biofilms mainly occur near the sediment surface (Cartaxana et al. 2016b). In sandy sediments, diatoms are much more sparse and distributed over a greater depth (viable diatoms are found up to 0.5 m deep) (Yallop et al. 1994; Jewson et al. 2006). Diatoms in these habitats show adaptations against strong hydrodynamic conditions. They are generally smaller to avoid being crushed by collisions between sand grains (Delgado et al. 1991) and live adnate to or stalked on sand grains (Paterson and Hagerthey 2001) (Fig. 1). As the sediment is constantly reworked in these dynamic conditions, Miller et al. (1987) hypothesized that these communities are retained in a pioneer state and no species have the ability to gain dominance, as such decreasing interspecific competition. In addition, niche differentiation (adnate, small motile, stalked) also reduces strong interspecific species competition (Miller et al. 1987; Jewson et al. 2006). In very high disturbance conditions, only a low number of highly adapted diatoms can survive, usually showing strong attachment and or hiding in crevices on sand grains such as small motile diatoms (Paterson and Hagerthey 2001; Ribeiro et al. 2013).

Due to the different light gradients in sandy vs. muddy sediments and the different capabilities of motility in epipsammic vs. epipelic diatoms, it can be expected that these different growth forms possess contrasting strategies to cope with excess light energy.

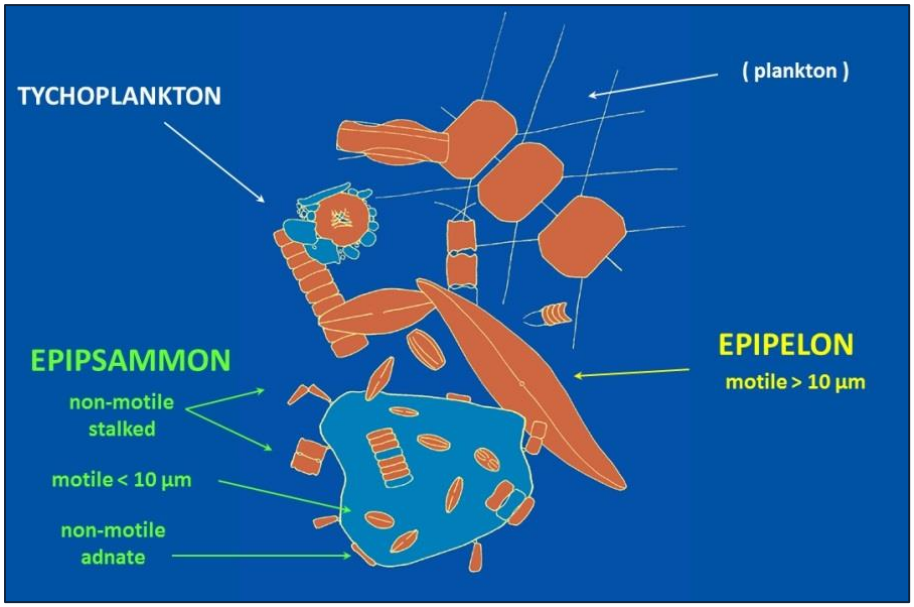

Figure 1: Diatom growth forms in intertidal sediments (Sabbe 1997), see text for details.

Photosynthesis

General model of oxygenic photosynthesis

During oxygenic photosynthesis, light energy is captured by light harvesting complexes (Fig. 2) (LHC), which funnel the energy (called exitons) to the reaction centers of photosystem I (PSI) and photosystem II (PSII) (Lyu and Lazár 2017). Here, special subsets of chlorophyll molecules in PSI (P700) and PSII (P680) become exited and donate an electron to a nearby electron acceptor in a process called charge separation. In the case of P700, the electron is transported through PSI to ferredoxin (Fd). Fd is again oxidized by the ferredoxin-$NADP^+$-oxidoreductase (FNR) complex, with $NADP^+$ being reduced to NADPH. In P680, the separated electron is transported through PSII, via the first (Q_A) and second (Q_B) electron acceptor, the plastoquinone pool (PQ), the cytochrome b6f complex (cytb6f) and plastocyanin (PC) to reduce the oxidized P700. The electron separated from P680 is replaced by an electron coming from H_2O, which is split into protons and oxygen in the oxygen evolving complex (OEC). During this linear electron transport (LET) protons are translocated across the thylakoid membrane (TM) from the stroma to the thylakoid lumen. In addition, protons are consumed in the chloroplast stroma during the Calvin-Benson cycle (CBC) which assimilates CO_2 into glucose. As a result of the above processes, light establishes an electrochemical gradient of protons across the thylakoidal membrane (Bailleul et al. 2010a; Lyu and Lazár 2017). This gradient is called the proton motive force (PMF), comprising both an electric field ($\Delta\Psi$) and a proton concentration gradient (ΔpH). The PMF drives ATP synthesis (Mitchell 1961) which together with NADPH is essential for carbon fixation. Besides LET, cyclic

electron transport (CET) around PSI is contributes to the PMF (Kramer et al. 2003), see further.

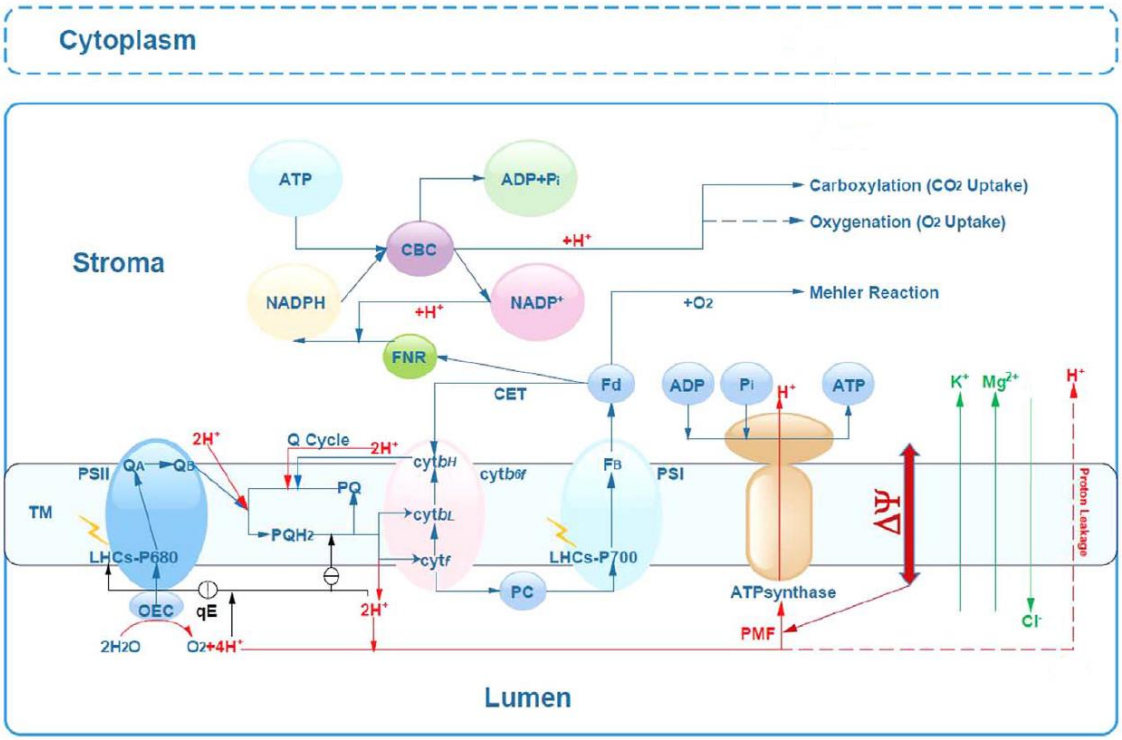

Figure 2: A model of oxygenic photosynthesis(Lyu and Lazár 2017), see text for details.

Monitoring photosynthesis in vivo

Chlorophyll fluorescence

Light energy that is absorbed by PSII or its light harvesting complexes ends up in one of three competing pathways which sum up to 100% (Fig. 3): (1) photochemistry, comprising a charge separation and the transfer of an electron from the reaction center to the primary electron acceptor Q_A, (2) dissipation as heat and (3) re-emission of a photon with a longer wavelength (fluorescence). In case of Chlorophyll *a* molecules, a fluorescence peak can be observed in the red region (~685 nm). At ambient temperatures, most chlorophyll fluorescence is considered to originate from PSII (Krause and Weis 1991). As the three pathways by which the absorbed photon is used/dissipated are considered to sum up to 100%, changes in fluorescence yield reflect changes in the complementary pathways which decrease fluorescence. A commonly used method to discriminate between photochemistry (photochemical quenching) and energy dissipation as heat (non-photochemical quenching) is the saturation pulse method which uses a short (< 1s) light pulse of high intensity (= a saturating pulse) to fully reduce the primary electron acceptor of P680, Q_A (Fig. 4).

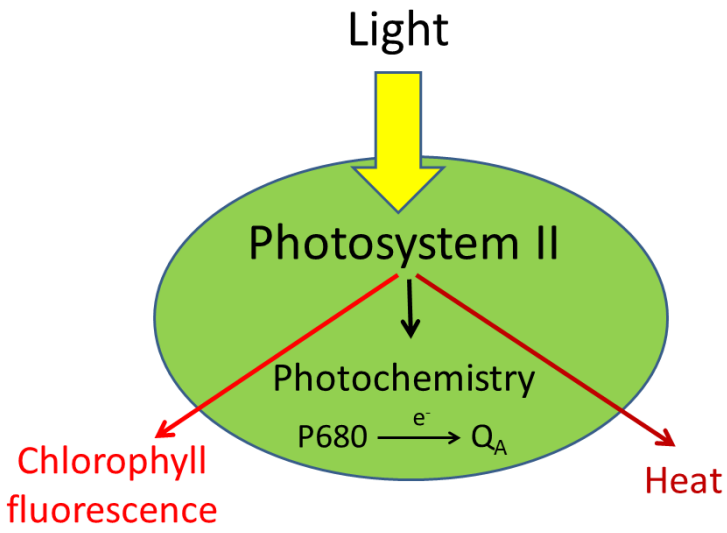

Figure 3: The possible fate of absorbed photons at PSII, after Baker (2008).

When a leaf (or algal sample) is kept in darkness, Q_A becomes fully oxidized. As such the PSII reaction centers are capable of photochemistry (using light energy to reduce Q_A) and are referred to as being 'open'. When weak measuring light pulses are applied (which keep the Q_A pool maximally oxidized), the fluorescence yield of this measuring light will be minimal and called F_0. When the sample is exposed to a saturating pulse, Q_A will become fully reduced and PSII reaction centers will not be able to perform additional charge separations (i.e. they are 'closed'). As a result, the fluorescence yield will now reach a maximal level, F_m. When the difference between both minimal (all PSII reaction centers open) and maximal fluorescence (all PSII reaction centers closed) yields is calculated (i.e. the variable fluorescence, F_m- F_0 or F_v) and is divided by F_m, the maximal quantum yield of PSII can be estimated as (F_v/F_m). This value reflects the relative amount of fluorescence that is quenched photochemically due to the reaction centers.

When samples are light adapted, a similar set of parameters can be determined, now denoted with prime ('). The basal fluorescence yield in the light adapted state is called F' (or sometimes as F_s). This is usually higher than F_0 due to a significant reduction of the Q_A pool upon light exposure. When the actinic light (driving photosynthesis) is sufficiently high, a lowering in the maximum fluorescence (now called F_m') is also observed. As during saturating pulses photochemistry is saturated, the observed decline in maximum fluorescence, which is related to heat dissipation, is called non-photochemical quenching of chlorophyll fluorescence (NPQ). It is calculated as (F_m-F_m')/F_m' (Krause and Weis 1991).

In land plants, three NPQ components have been distinguished, based on the relaxation kinetics after high light exposure: the rapidly relaxing component qE (seconds to minutes), the slower state transitions qT (tens of minutes), and the so-called 'photoinhibitory' quenching qI, which relaxes in the range of hours (Horton and Hague

1988). qE is the major NPQ component and its mechanism is well-studied in plants (Demmig-adams et al. 2014; Ruban 2016), see further.

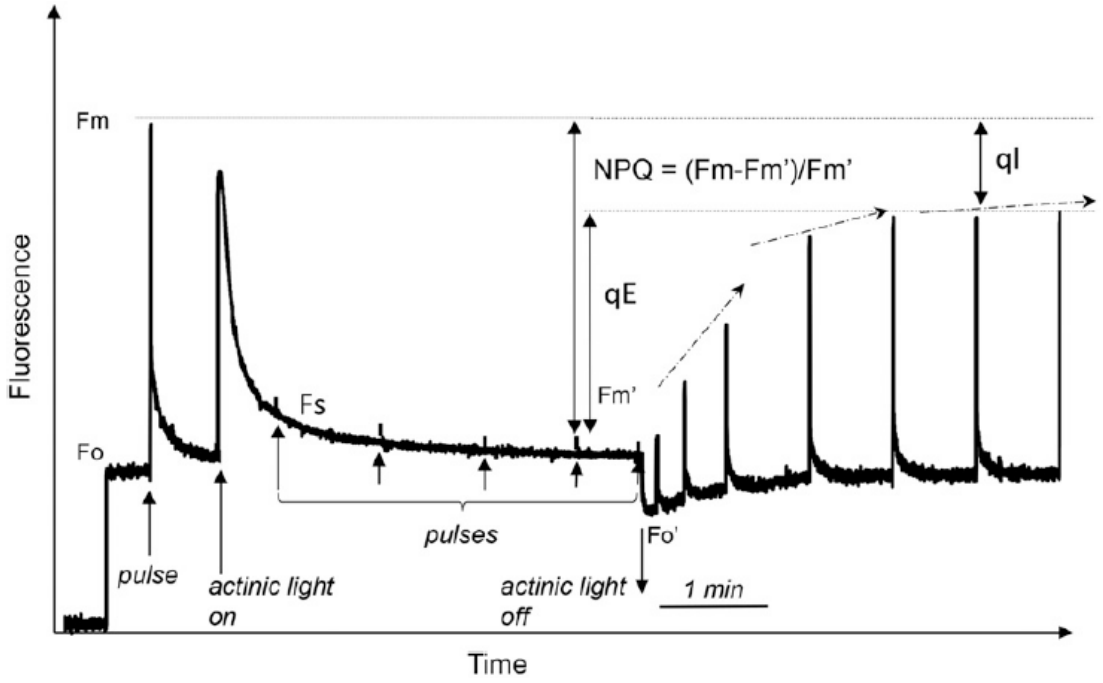

Figure 4: A PAM fluorescence trace of an *A. thaliana* leaf showing induction and relaxation of NPQ during actinic illumination with 1000 µmol photons $m^{-2}s^{-1}$. F_m and F_0 are the maximum and minimum fluorescence levels before actinic illumination, whereas F_s is the steady-state fluorescence level (denoted as F' in the rest of this thesis) and F_m' the maximum fluorescence during actinic illumination. qE and qI are the quickly and slowly reversible components of NPQ (Ruban 2016).

Electrochromic shift (ECS)

During oxygenic photosynthesis, electrons obtained from H_2O are transferred through photosystem II (PSII), the cytochrome b6f complex, PSI and ferrodoxin to NADPH. During this linear electron flow (LEF) protons are translocated to the thylakoid lumen (see above). As such light establishes an electrochemical gradient of protons across the thylakoid membrane (TM). This gradient is called the proton motive force (PMF), and it comprises both an electric field (ΔΨ) and a proton concentration gradient (ΔpH), which drives ATP synthesis (Mitchell 1961) (Fig. 2). The light-generated electric field across the thylakoid membrane shifts the absorption spectrum of pigments imbedded in this lipid membrane (Fig. 5a). This effect is called the ElectroChromic Shift (Bailleul et al. 2010a). A linear relationship between the ECS signal and the trans-thylakoidal electric field is usually observed in plants (Joliot and Joliot 1989). In addition, a linear as well as a quadratic ECS response have been observed in diatoms (Bailleul et al. 2015) (Fig. 5a).

this technique has multiple applications to monitor photosynthesis *in vivo*. Below, we briefly describe the ECS applications used in Chapter 6 of this dissertation.

Although mostly a linear response between the ECS signal and ΔΨ are observed (blue), pigments which become polarized as a result of the electric field across the TM will show an ECS signal with a quadratic response to ΔΨ. A major advantage of the presence of both a linear and quadratic ECS signal is that the transthykoidal electric field, present in the dark ($\Delta\Psi_d$), can now be quantified (Bailleul et al. 2015). A linear ECS signal will respond linearly to a given light stimulus, independent from an electric field before this stimulus. A quadratic ECS signal, however, is dependent on the pre-existing $\Delta\Psi_d$. As a consequence, by plotting the quadratic signal in function the linear ECS signal, we can determine $\Delta\Psi_d$ (Fig. 5b).

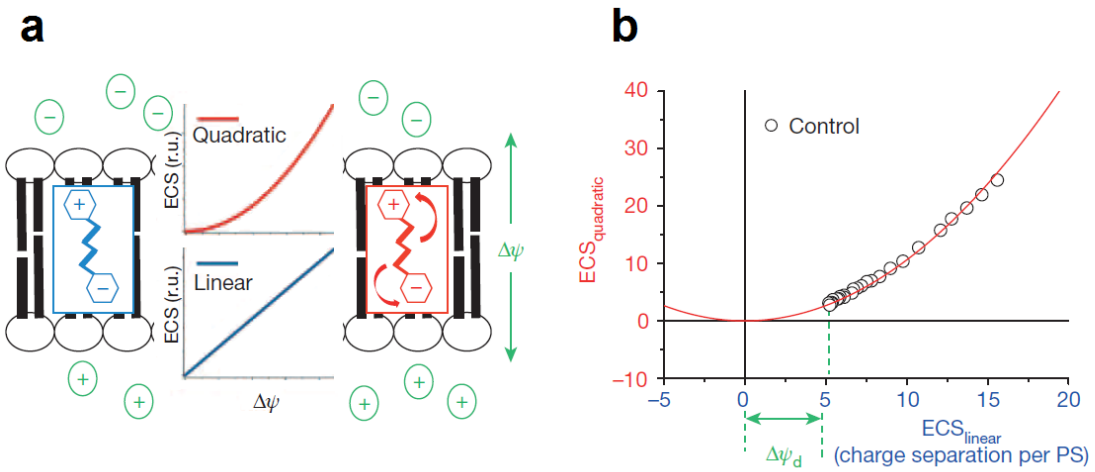

Figure 5: (a) Schematic representation of polar (blue) and polarizable (red) pigments and their respective linear and quadratic ECS response in diatoms. (b) The relationship between linear and quadratic ECS components during the decay of a light pulse induced electric field in *Phaeodactylum tricornutum*. The measured ECS signals do not reach the minimum of the parabola but rather remain positive, indicating the presence of a dark electric field $\Delta\Psi_d$. (Bailleul et al. 2015).

The activity of the different components contributing to the ΔΨ and as such to the ECS signal can be discriminated by kinetic analysis of the ECS signal after a single turnover (inducing only one charge separation in both PSI and PSII) xenon or laser flash (Joliot and Delosme 1974; Bailleul et al. 2010a) (Fig. 6). Three different phases are observed. A first phase (red) corresponds to an electric field change, related to a charge separation in PSI and PSII, whereas the following slower phase (blue) corresponds to the activity of cytochrome b6f. The decay phase (green) represents the breakdown of the electric field by ion fluxes and is related to the proton efflux through the ATP-synthase complex. In chapter 6, we used this technique to normalize ECS signals to one charge separation of PSII and PSI (red).

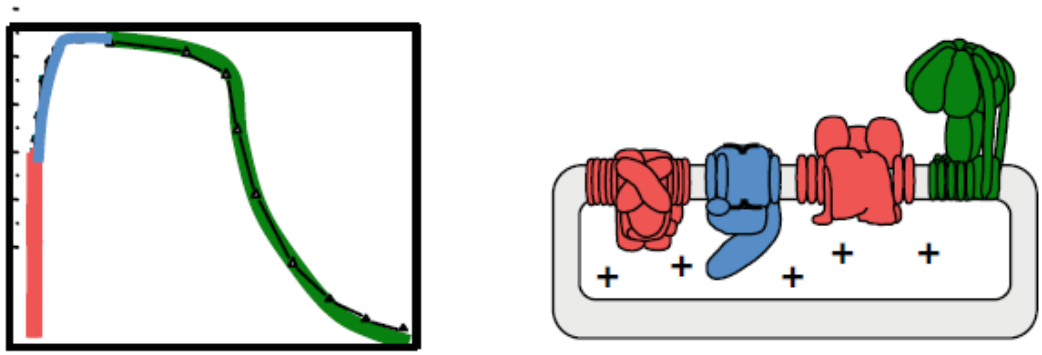

Figure 6: The different components contributing to ΔΨ (y-axis): PSI and PSII (red), cytochrome b6f (blue) and the ATP synthase complex (green) (Bailleul et al. 2010a).

In steady state conditions (Fig. 7), the rate at which ions leak (R_{leak}) across the thylakoid membrane, mainly by the ATP synthase complex and by which membrane potential is formed by PSII and PSI (R_{ph}, the rate of photochemistry) and the cytochrome b6f complex (R_{b6f}) are balanced and as such, the slope of the ECS signal in the light equals zero (S_l). When the light is switched off, charge separation of PSII and PSI immediately stops, whereas both ion leakage and cytochrome b6f still occur at the same rate, resulting in a slope S_d. Therefore, the contribution of photochemistry R_{ph} during light can be estimated as S_l - S_d (Joliot and Joliot 2002). In chapter 6, we used this approach to observe changes in the PSII and PSI photochemistry upon addition of the uncoupler nigericin.

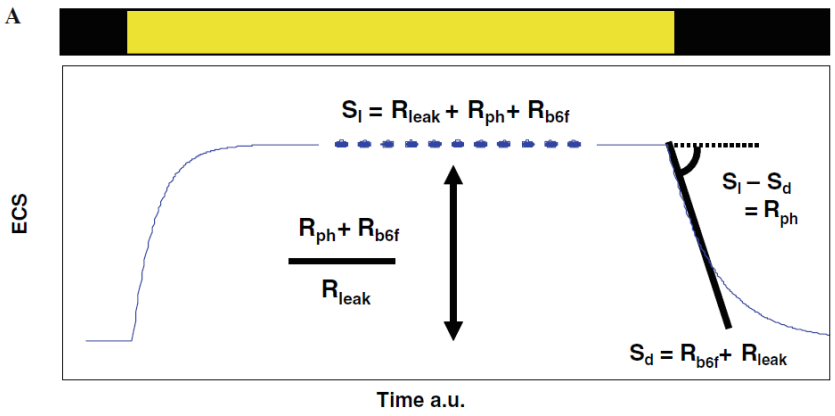

Figure 7: estimating the rate of photochemistry of PSI and PSII (R_{ph}) in steady-state conditions (Bailleul et al. 2010a).

The ECS signal, moreover, can be used to estimate the relative contributions of ΔpH and ΔΨ to the PMF in steady-state photosynthesis conditions (Fig. 8). The relaxation of both components upon an abrupt light-dark transition is thought to differ, which allows discrimination between both. The ΔΨ component relaxes more rapidly than the ΔpH component, due to a low electric capacitance of the thylakoid membrane, the high H^+ buffering capacity of the thylakoid lumen (Fig. 2) and the slow movement of counter ions (see Cruz et al. 2001). After the light-dark transition, fast proton efflux allows the

PMF to reach its dark-adapted state. As proton efflux continues when the PMF > 0, or comes into equilibrium with the ATP/(ADP + P) couple, the observed ECS signal representing ΔΨ, would be inverted (more positive charges on the stromal side) as proton efflux continues driven by ΔpH, resulting in an (inverted) ECS signal, below the dark baseline, which is indicative of the ΔpH contribution. In a second phase when protons are freed from the "buffering network", ΔpH decreases and the ΔΨ increases concomitantly (the PMF being constant). Since what ECS follows is ΔΨ, these two phases translate into an ECS inversion.

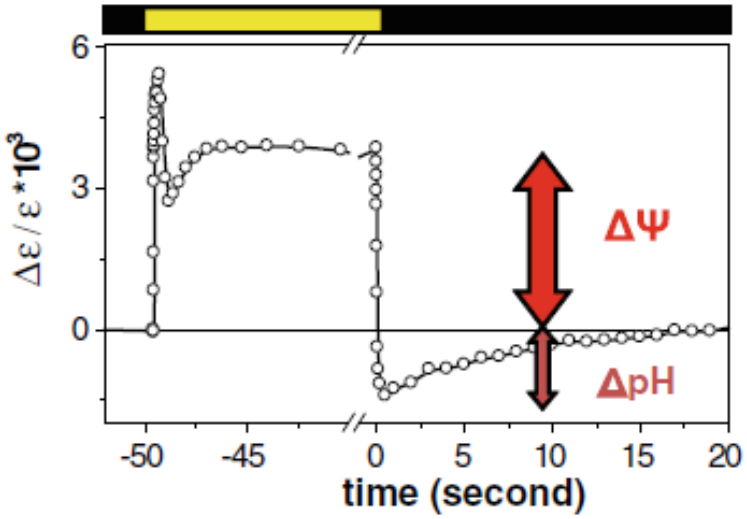

Figure 8: Using the ECS signal (y-axis) to parse PMF into ΔpH and ΔΨ after turning off light. During light onset the ECS signal rises rapidly, after which it decays partly by counter-ion fluxes to reach a steady state. When light is switched off, the ECS signal decays rapidly and even drops below the dark baseline, causing an inversion of the ECS signal after which the signal relaxes slowly to the dark adapted baseline (Bailleul et al. 2010a).

Photoprotection

In conditions of low photosynthetically available radiation (PAR), photosynthesis is light-limited and increases linearly with light absorption (Fig. 9). At increasing levels of PAR, however, the photosynthetic capacity becomes saturated (at P_{max}). As light absorption keeps increasing linearly with PAR, this results in an excess of light energy (Erickson et al. 2015). As the absorption of excess light energy can result in oxidative damage to, in particular, the PSII core, photosynthetic organisms possess various photoprotection mechanisms to cope with excess light (Fig. 10).

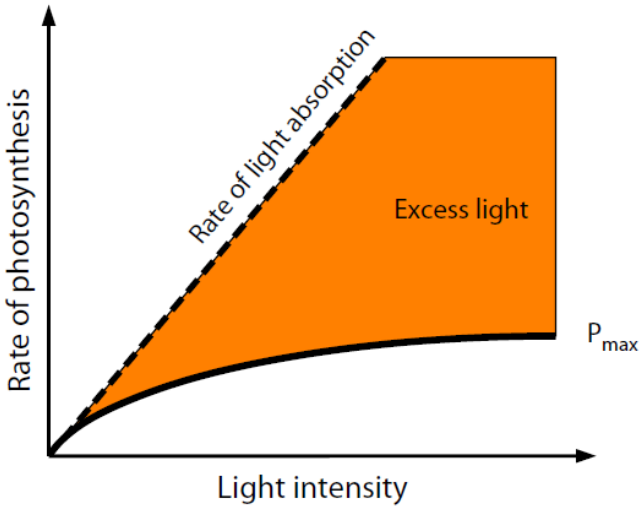

Figure 9: The rate of photosynthesis in function of light intensity (PAR) (Erickson et al. 2015).

Besides avoiding excess light absorption by movement of leaves, cells (see further), or chloroplasts, a decrease in light absorption can be accomplished by adjusting the light-harvesting antenna size. This process, however, is rather a long-term acclimation strategy to excess light. One of the fastest responses that photosynthetic organisms possess to cope with excess light, nonetheless, is excess light energy dissipation as heat (Demmig-adams et al. 2014) and is observed as Non-photochemical quenching of chlorophyll fluorescence (NPQ). The name 'Non-photochemical quenching' literally means that it is a process apart from photochemistry (non-photochemical) that consumes light energy (quenching) that would otherwise be emitted as fluorescence. A detailed description of how it is measured can be found above. Excess absorbed light energy, furthermore, can be removed by alternative electron transport pathways (See Fig. 2). These comprise cyclic electron transport around PSI (CET), which dissipates excess energy absorbed by PSI, by re-donating electrons to the acceptor site of PSI, instead of using it to reduce $NADP^+$. At PSI, oxygen can also be reduced to form superoxide radicals during the Mehler reaction (Claquin et al. 2004). Superoxide radicals are converted to hydrogen peroxide by superoxide dismutase (SOD). As the latter is then detoxified to H_2O by ascorbate peroxidase (APX), a water-to-water cycle is formed (as the electrons brought into the electron transport chain at the oxygen evolving complex

initially originate from H_2O). During photorespiration, oxygen rather than CO_2 is fixed by RUBISCO in a light-dependent manner. This leads to the production of phosphoglycolate which is either released in the form of glycolate or recycled in a wasteful process, releasing both CO_2 and NH_3. Photorespiration could maintain a high electron flow during high light conditions (Wingler et al. 2000). Under conditions of excess light, the production of reactive oxygen species (ROS) is inevitable (Takahashi and Badger 2011). At PSI, electron transfer to oxygen produces hydrogen peroxide (H_2O_2) via superoxide radicals (see above), whereas in PSII, singlet oxygen ($^1O_2$) is produced (Asada 2006). ROS can be scavenged by different enzymes or antioxidants such as ascorbate and carotenoids such as zeaxanthin (see further) (Takahashi and Badger 2011). Despite the above photoprotective defenses, damage to the photosynthetic machinery can still occur, mainly to the core of the PSII (D1 protein). This protein then has to be replaced to prevent a net loss of PSII reaction centers. If the D1 protein is not replaced, net photodamage will lead to a decrease in the efficiency and/or maximum rate of photosynthesis, termed photoinhibition (Niyogi 1999).

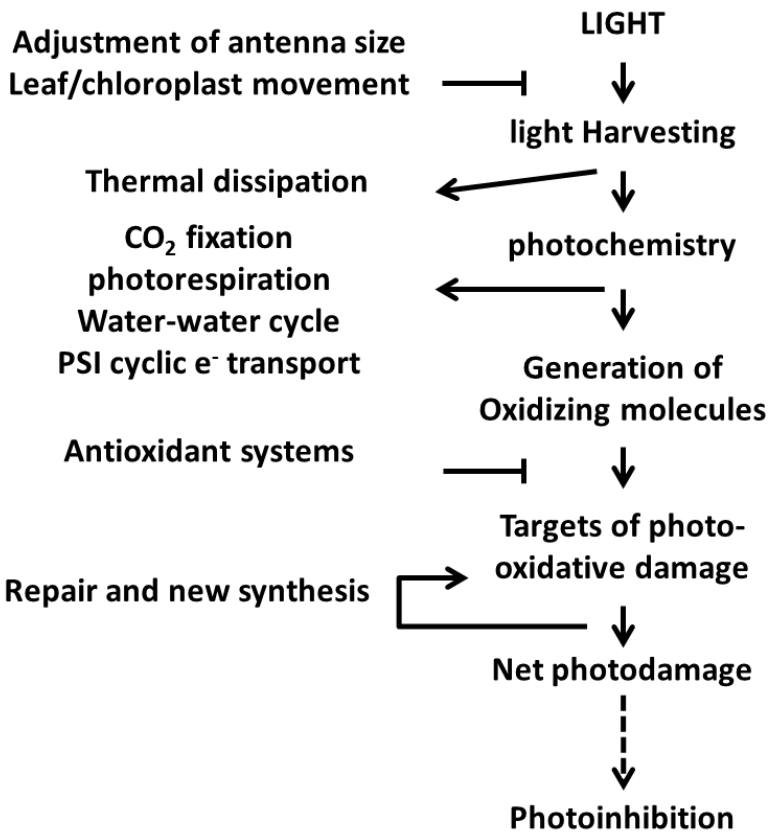

Figure 10: Schematic diagram of photoprotective processes in plants, after Niyogi (1999).

Photoprotection in diatoms

In diatoms, excess light energy absorption can be avoided by decreasing the cellular pigment content (MacIntyre et al. 2002). As a minor reduction in pigment content also decreases the 'packaging effect' (where densely packed pigments shade each other), only a drastic decrease in cell pigment content is effective (Wilhelm et al. 2014). A decrease in cell pigment content in concert with a decrease in LHC proteins, moreover, is considered to be a long-term acclimation process, instead of a mechanism to cope with a rapidly fluctuating light climate (Nymark et al. 2009). Raphid benthic diatoms, however, can reduce the amount of absorbed light energy more rapidly by migrating vertically into the sediment (in bulk or via microcycling) (Kromkamp et al. 1998; Serôdio 2004; Laviale et al. 2016). This 'behavioural' mechanism is considered to be a major photoprotection strategy (Perkins et al. 2010) and will be addressed in a separate section (see below and Chapter 4). Also NPQ and the associated xanthophyll cycle are major fast photoprotection mechanisms in diatoms (Lavaud and Goss 2014; Goss and Lepetit 2015) and hence, are explained in detail in its own section, see further.

Cyclic electron transport (CET) around PSI in occurs in diatoms (Grouneva et al. 2009). This process, however, was found to be rather insensitive to light intensity, thus questioning its potential as a photoprotection mechanism (Bailleul et al. 2015). Also a CET around PSII has been observed in diatoms (Lavaud et al. 2002, 2007): During cyclic electron transport around PSII, water is not split to produce oxygen, but electrons are re-donated to the PSII reaction centre. As such an oxygen deficit is observed during a sequence of single-turnover flashes (Lavaud et al. 2002). PSII CET functions as an energy-dissipating leak in PSII (Onno Feikema et al. 2006) which is activated during high light conditions and could prevent photoinhibition (Lavaud 2007). Planktonic as well as benthic diatoms photoreduce oxygen in the Mehler reaction (Waring et al. 2010). However, in the tychoplanktonic *Phaeodactylum tricornutum* the portion of the photosynthetic electron flow that is re-routed to an oxygen consuming pathway, is constant regardless of the light intensity (Bailleul et al. 2015).

Besides cyclic electron flows, photorespiration and nitrate reduction could also function as an alternative electron sink (instead of NADPH) in diatoms (Allen et al. 2005), and as such dissipate excess energy (Parker and Armbrust 2005). The release of glycolate (as a by-product of oxygen fixation, instead of CO_2 fixation by RUBISCO, see above) has indeed been observed when planktonic diatoms are shifted from low to oversaturating light conditions which might be due to a lag in upregulation of photorespiration enzymes (Parker et al. 2004). Glycolate release, additionally, is promoted in low temperature environments and low presence of nitrate, whereas nitrate reduction as an alternative electron sink is used in the presence of nitrate.

Scavenging of reactive oxygen species (ROS) (Janknegt et al. 2008, 2009a; b; Waring et al. 2010), which are produced as by-products of photosynthetic electron transport, especially occurs when the electron transport chain is over-reduced and electrons leak onto O_2. Scavenging can occur as in plants enzymatically by SOD and APX or by non-enzymatic scavengers such as glutathione. Janknegt et al. (2009b), nonetheless, concluded that in planktonic diatoms xanthophyll cycle related quenching is more important than scavenging by antioxidants. Waring et al. (2010), however, showed higher SOD and APX activity in a planktonic than in a benthic diatom, as the former photo-reduced more oxygen than the latter at saturating light intensities. In the case of microphytobenthic communities, the action of the xanthophyll cycle/NPQ is crucial to protect the D1 protein from damage, whereas addition of exogenous ROS scavengers can provide additional protection. The ROS scavenging mechanisms in MPB, nonetheless, seem sufficient to prevent lipid peroxidation after strong light exposure (Laviale et al. 2015).

If the above mechanisms are insufficient to protect the PSII core, it can be repaired, mainly by replacing the D1 protein (Lavaud et al. 2016). In MPB communities, total D1 protein content decreases when D1 synthesis is halted by addition of chloroplast protein synthesis inhibitors. However, blocking the xanthophyll cycle leads to a more severe reduction in D1 content (Cartaxana et al. 2013), indicating the xanthophyll cycle is more important than D1 replacement to avoid a net loss of functional D1 proteins.

Non-photochemical quenching

The NPQ scenario

The qE mechanism in plants is located in the antenna of PSII that undergoes a conformational change upon acidification of the thylakoid lumen (ΔpH). Due to this change, the quencher pigment(s) begin(s) receiving the harvested light energy from the light-harvesting complex (LHCII) antenna start dissipating the excess energy as heat (see the 'NPQ scenario' in Figure 11 (Ruban 2016). The trigger for qE is the transthylakoidal proton gradient ΔpH, which is built up during electron transport (ET) and consumed by the ATPase. It acts by activating the xanthophyll cycle, in which violaxanthin (Vx) is de-epoxidized (removal of an epoxide group, which is an oxygen atom cyclically bound to two carbon atoms) to zeaxanthin (Zx) via the intermediate antheraxanthin (Ax). At the same time, the pH sensor Photosystem II subunit S (PsbS) is activated through protonation (Ruban 2016). The protonated PsbS protein undergoes a conformational change, promoting dissociation of a Light-harvesting complex (LHC) subset from the PSII core, which leads to the formation of the qE quenching site (Demmig-adams et al. 2014). Even though in plants qE was found to correlate well with Zx content, it has also been observed in the absence of it. It is therefore suggested that Zx functions more as an allosteric regulator of the qE process than as a direct quencher (Horton 2012).

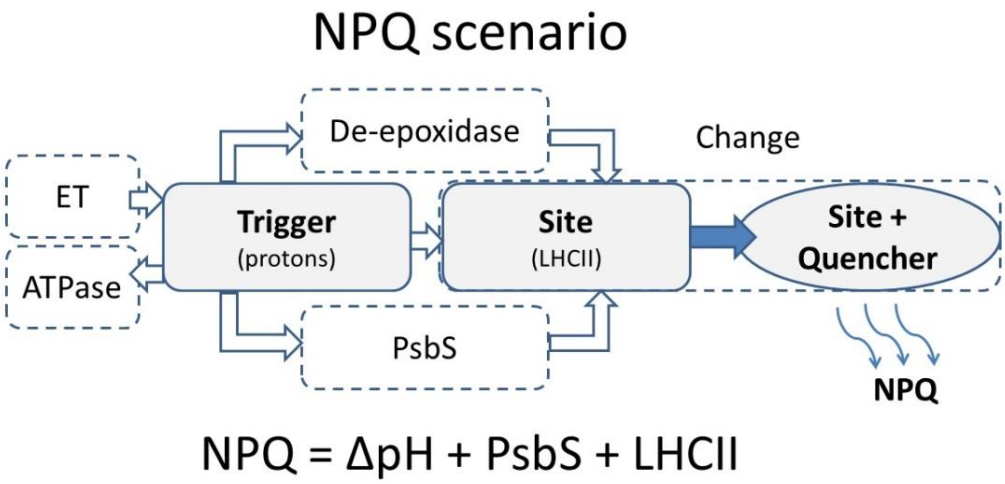

Figure 11: the NPQ scenario model proposed by Ruban (2016), see text for details.

As diatoms belong to a lineage that acquired photosynthesis by incorporating a plastid of red algal origin, while their genomes also contain traces of a possible earlier green endosymbiont, cf. Archibald (2009), the NPQ regulatory components differ from the green lineage (reviewed by Goss & Lepetit, 2015), see also Fig. 14 below for an overview. Diatoms lack the PsbS protein in their genomes (Armbrust et al. 2004), and the diadinoxanthin/diatoxanthin (Ddx/Dtx) cycle replaces the Vx cycle as major xanthophyll cycle (Lohr and Wilhelm 1999) (Fig. 11). Below we discuss the xanthophyll cycles (XC) and possible NPQ regulators (LHCX proteins) and the role of a proton gradient as trigger in diatoms in comparison with plants.

The xanthophyll cycle

Even though both the Ddx/Dtx as the Vx/Ax/Zx cycle are present in diatoms (Fig. 12), only the Ddx/Dtx cycle is considered to be important in the NPQ mechanism, whereas Vx/Ax/Zx cycle pigments are considered to be precursors which only become prominent after prolonged high light treatment when the total XC pool starts to increase (de novo synthesis) (Lohr and Wilhelm 1999, 2001; Dambek et al. 2012). A major difference between both XC is that the Ddx cycle requires only one de-epoxidation step (Fig. 12). The reverse reaction from Dtx to Ddx is an epoxidation step which occurs in low light conditions and is up to 20-fold faster in diatoms than in plants and chlorophytes (Goss et al. 2006b). The large differences in epoxidation rate between the major XC in diatoms and plants must be viewed in conjunction with the roles of Dtx and Zx in the respective NPQ mechanisms (Lavaud and Goss 2014). In contrast to higher plants, NPQ can be maintained when Dtx is present, even in the absence of ΔpH (Lepetit et al. 2013; Lavaud and Lepetit 2013), with the exception of a Zx-dependent quenching mechanism observed in evergreen plants during winter (Demmig-Adams and Adams 2006). As in diatoms the epoxidation reaction is nearly as fast as the de-epoxidation reaction, the

epoxidation is suppressed by a light-driven ΔpH, preventing a futile cycle (Mewes and Richter 2002; Goss et al. 2006b).

Even though generally a tight correlation between Dtx and NPQ is found, the quenching ability of Dtx decreases at high concentrations (Schumann et al. 2007). While Dtx is supposed to be protein-bound to participate in the NPQ mechanism, a portion of the Dtx pool is found to be lipid-dissolved and might function as an anti-oxidant.

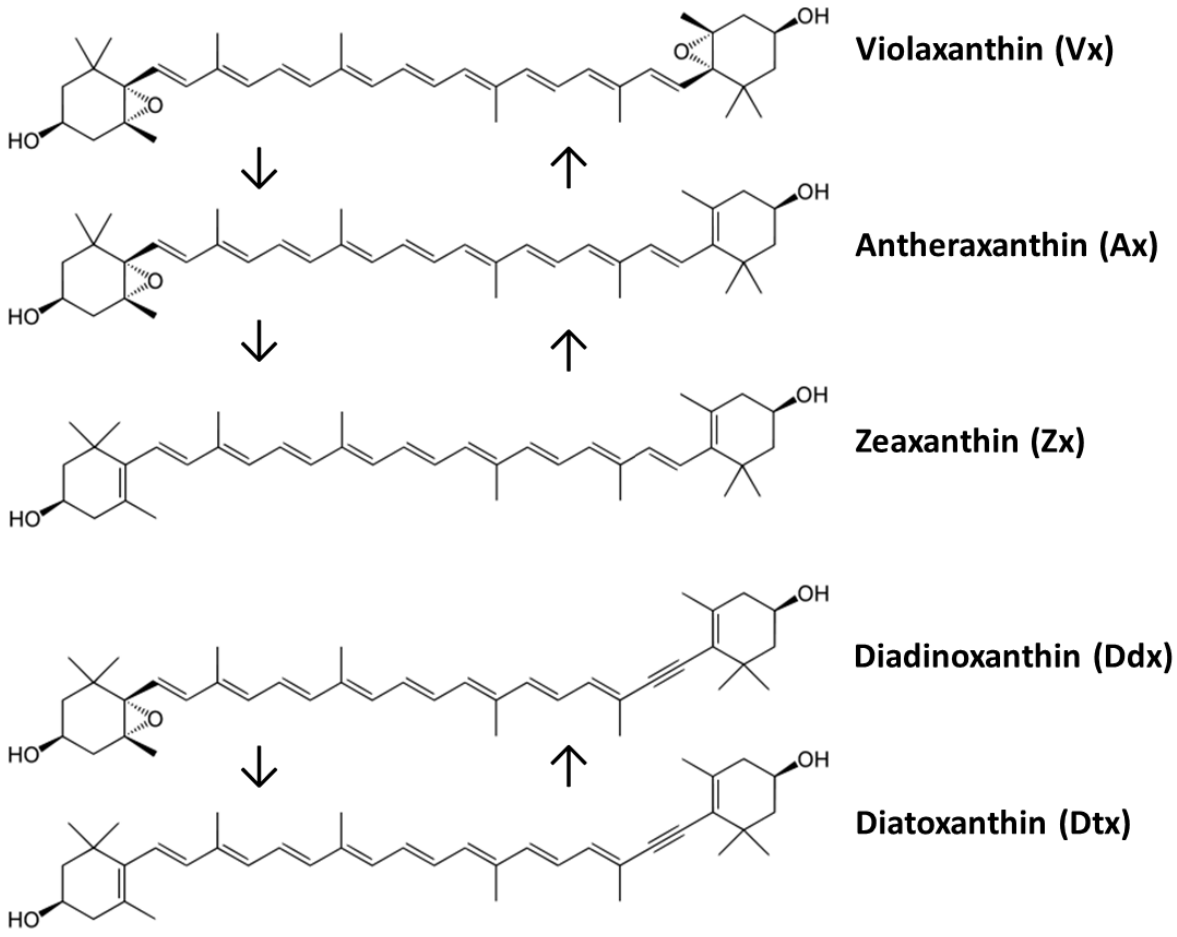

Figure 12: Xanthophyll cycles in diatoms, after Lohr and Wilhelm (1999).

LHCX proteins

In vascular plants both sensing excess light energy and quenching are exerted by different proteins: PsbS (absent from diatom genomes) as a sensor and LHC proteins as quenchers (Niyogi and Truong 2013). In algae, however, energy dissipating instead of light harvesting proteins diversified within the LHC proteins: Light-Harvesting Complex Stress-Related (LHCSR) proteins, called LHCX proteins in diatoms, which are absent in vascular plants (Niyogi et al. 2013), see Fig. 14. LHCSR proteins appear to function both as sensors of excess light and sites of quenching (Ballottari et al. 2016).

The function of LHCSR proteins is particularly well studied in the green alga *Chlamydomonas reinhardtii*. The LHCSR3 protein for instance is essential for NPQ (Peers et al. 2009). The exact mechanism by which it dissipates excess energy, however, is still under debate (Ballottari et al. 2016). Sensing of ΔpH is exerted by three thylakoid lumen-exposed acidic residues in the same protein molecule which are closely located to each other. Protonation of these residues might induce changes in the protein structure, as such influencing Chl-Chl and Chl *a*-carotenoid interactions necessary for fluorescence quenching (Ballottari et al. 2016).

In diatom genomes, several LHCX homologs can be found. Ranging from four (in *Phaeodactylum tricornutum*) or five (in *Thalassiosira pseudonana*, *Thalassiosira oceanica* and *Pseudo-nitzschia multiseries*) to 11 in *Fragilariopsis cylindrus*, (Taddei et al. 2016). High light induces changes in the LHCX content on both mRNA as well as protein level in both centric and pennate diatoms (Oeltjen et al. 2002; Nymark et al. 2009; Bailleul et al. 2010b; Park et al. 2010; Zhu and Green 2010; Lepetit et al. 2013; Taddei et al. 2016), suggesting a similar role for LHCX proteins in NPQ as LHCSR proteins in green algae. High light induced proteins might either confer higher NPQ capacity by binding newly synthetized Dtx molecules and/or are involved in sustained NPQ after prolonged high light exposure (Zhu and Green 2010; Lepetit et al. 2013).

The current ΔpH/qE paradigm

Lavaud and Goss (2014) proposed the following paradigm for NPQ regulation in pennate diatoms: (1) A certain magnitude of ΔpH is needed for NPQ induction; (2) When NPQ is established, the presence of Dtx alone is sufficient for maintaining a quenching state; (3) Dtx is mandatory: NPQ is always accompanied by Dtx, however a XC-independent NPQ component has been observed in *P. tricornutum* upon addition of substances that abolish ΔpH (Eisenstadt et al. 2008).

A molecular mechanism of NPQ in diatoms has been recently proposed (Lavaud and Goss 2014; Goss and Lepetit 2015) (Fig. 13). NPQ (qE) is believed to be based on two quenching sites (Q1&2) within the LHC antenna of PSII: (1) Q2, which is localized in the

part of the LHC that remains attached to the PSII and which directly depends on the synthesis and activation of Dtx, and (2) Q1, which is localized in the part of the LHC that detaches from PSII upon Dtx activation at Q2 and which forms an energy sink that amplifies Q2 quenching. It is believed that the persistence of Dtx, even in the dark, is responsible for keeping both quenching sites active and especially Q1. In other words, as long as Dtx is present at the Q2 site, Fucoxanthin Chlorophyll *a*/*c* binding Protein FCP oligomers cannot reconnect to PSII, generating sustained qI/NPQs (Lavaud and Goss 2014). The function of Dtx as an NPQ regulator is not entirely clear. Two mutually but not exclusive alternatives have been proposed (see Lavaud and Goss 2014 for more details): Dtx could directly quench excited Chl *a* molecules at the Q2 site, and/or together with proton binding it could support a conformational change of LHCF (Light-Harvesting Complex containing Fucoxanthin) and/or LHCX proteins, leading to their the disconnection of FCP oligomers and formation of the Q1 site.

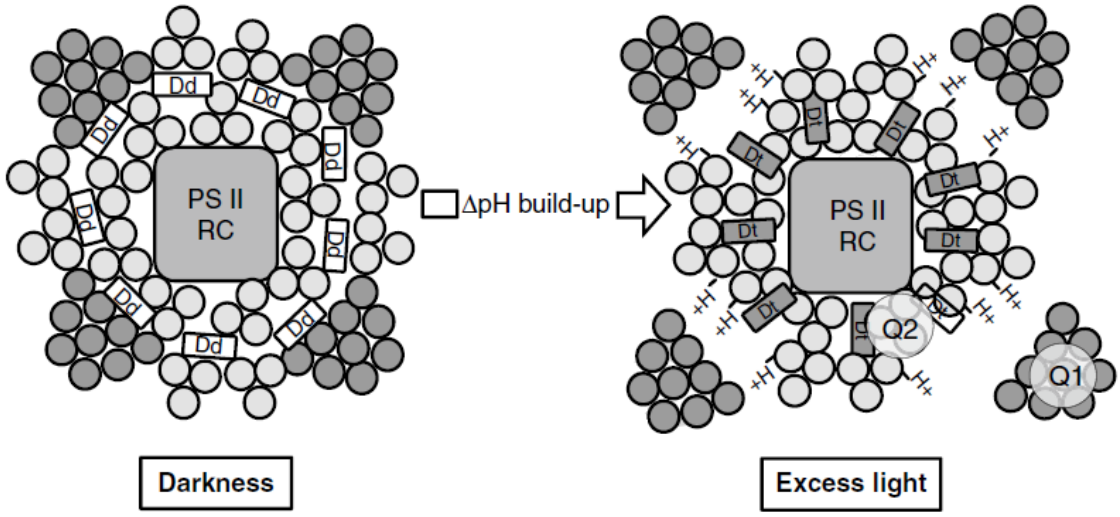

Figure 13: A working hypothesis for Dtx-dependent energy dissipation (resulting in NPQ) in pennate diatoms (mostly based on observations in *P. tricornutum*) depicting the organization of the PSII LHC antenna system in "low NPQ" and "high NPQ" cells dark acclimated and exposed to excess light conditions, respectively (Lavaud and Goss 2014). Light and dark-grey circles are FCP polypeptides forming trimers and higher FCP oligomeric complexes, respectively; the latter are loosely bound to the PSII LHC antenna system and can disconnect under excess light exposure. Ddx diadinoxanthin, Dtx diatoxanthin, H+ protons, PSII RC photosystem II reaction center, Q1/Q2 quenching sites 1 and 2, ΔpH trans-thylakoid proton gradient, The model depicted here aims to illustrate the effective involvement of Dtx as an allosteric regulator of a conformational change in the LHC antenna. The conformational change is believed to be an aggregation of part of the LHC antenna generated by the pronotation of FCP-binding sites (Goss et al. 2006a; Lavaud and Kroth 2006).

Even though the above model incorporates a similar function of a ΔpH in NPQ, its exact role is far from clear (see also Fig. 15): (1) LHCX proteins in diatoms only have two out of the three protonable residues that essential for ΔpH sensing in *C. reinhardtii* (LHCX4 in

Phaeodactylum tricornutum, even only has one residue, Ballottari et al. 2016; Taddei et al. 2016); (2) the Ddx epoxidase enzyme has a pH optimum which is shifted up in comparison with the optimum of the violaxanthin de-epoxidase (VDE) in plants and shows activity at a pH of 6.5 and higher (Jakob et al. 2001). De-epoxidation, moreover, has been observed around a neutral pH at high concentrations of the cofactor ascorbate (Grouneva et al. 2006); and (3) as a considerable PMF is present in darkness in diatoms (Bailleul et al. 2015), the thylakoid lumen might already be acidic in dark conditions. Therefore, the DDE enzyme might already be active in darkness and could thus need an alternative regulator to become active in high light conditions.

For the above reasons, measuring the ΔpH in diatoms in vivo would be a major step forward in understanding the NPQ mechanism and has not been done before.

Diversity and evolution of NPQ

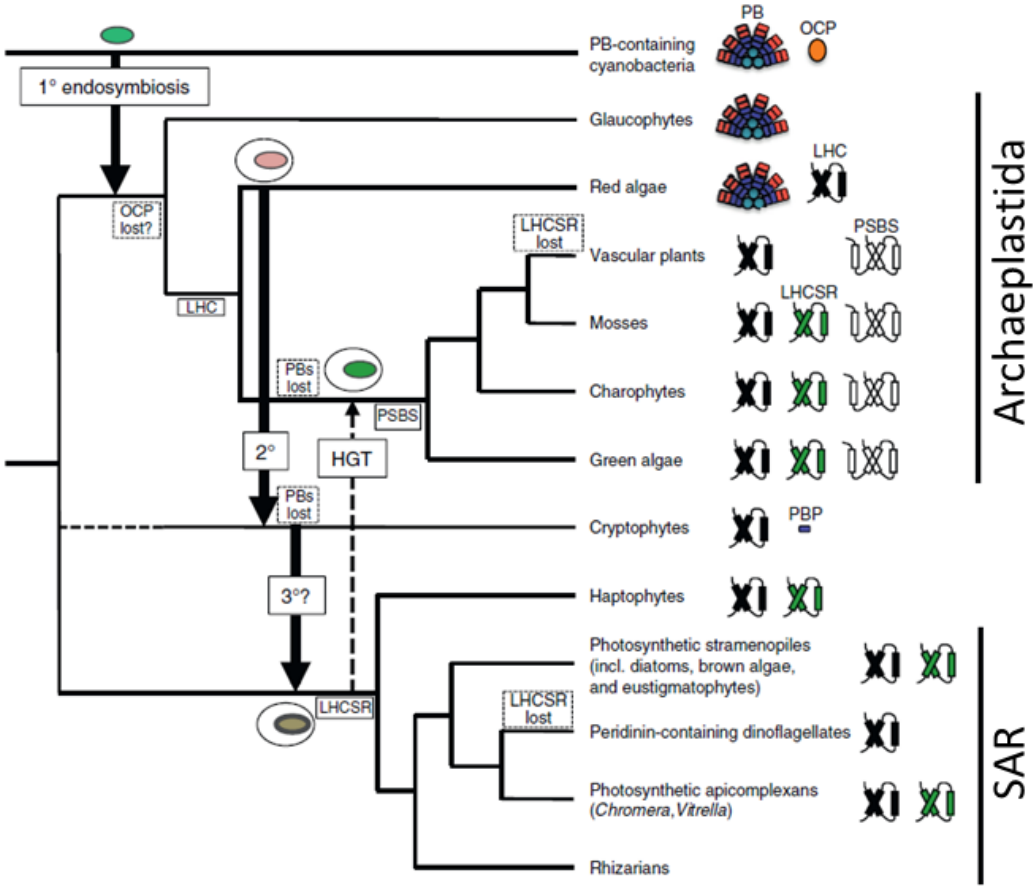

Figure 14: Schematic overview of the relationship between major groups of oxygenic photosynthetic organisms and the possible evolutionary steps towards flexible NPQ (Niyogi and Truong 2013). See text for details.

All oxygenic photosynthetic organisms exhibit NPQ capacity (Morosinotto and Bassi 2014). While the molecular mechanisms behind the observed NPQ differ between

groups of organisms, NPQ in all cases comprises a structural reorganization of antenna complexes (which differ strongly between clades, Fig. 14) and may involve different xanthophyll cycles (Goss and Lepetit 2015). Three different types of NPQ have been described in oxygenic photosynthetic organisms (Niyogi and Truong 2013). NPQ involving the orange carotenoid protein (OCP) is probably the oldest (Wilson et al. 2006) and arose in Cyanobacteria, which use phycobilisomes (PB) as their major light-harvesting antennae (Fig. 14). These proteins bind the xanthophyll 3'-hydroxyechinenone, which absorbs blue-green light. Upon blue-green light absorption, the OCP is activated and interacts with the PB to induce excitation-energy quenching, whereas the Fluorescence Recovery Protein is needed to relax the quenching mechanism (Kirilovsky and Kerfeld 2016), see Fig. 15.

The PB light-harvesting antennae were lost in the green lineage and the lineage which obtained a red plastid by secondary (and/or tertiary) endosymbiosis and replaced by three-helix Light-Harvesting Complex (LHC) antenna proteins, comprising LHCSR/LHCX proteins (Niyogi and Truong 2013). The phylogenetic distribution of LHCSR and LHCX proteins, as seen on Fig. 14, is still unclear and may be due to an ancient origin and subsequent loss in red algae, transfer from the green lineage to the lineage possessing a secondary red plastid or horizontal gene transfer (HGT) in the opposite direction (see Niyogi and Truong 2013 for more details). For a description of the function of LHCSR/LHCX proteins in NPQ in green algae and diatoms, respectively, see the section "LHCX proteins". The PsbS proteins likely evolved in the common ancestor of higher plants and green algae (Koziol et al. 2007). Whereas the PsbS gene is present in the genomes of green algae, the PsbS proteins do not seem to be involved in flexible NPQ of unicellular green algae (Bonente et al. 2008; Peers et al. 2009). The PsbS protein, however, been shown to accumulate in *C. reinhardtii* only under prolonged (several hours) periods of high light in combination with low CO_2 availability (Correa-Galvis et al. 2016). Interestingly, in mosses, LHCSR as well as PsbS seem to be involved in NPQ (Gerotto et al. 2011), whereas in flowering plants only the PsbS-dependent mechanism is retained (Morosinotto and Bassi 2014).

Besides specific proteins, see above, major differences in xanthophyll cycles are found in photosynthetic organisms (Goss and Jakob 2010; Lavaud and Goss 2014; Goss and Lepetit 2015). There is, for instance, no evidence for a functional xanthophyll cycle in cyanobacteria and red algae (Goss and Jakob 2010). Whereas the Vx cycle is the main XC in both the green lineage and brown algae, the Dtx cycle is the main cycle in diatoms, Xanthophyceae, Haptophyceae and Dinophyceae.

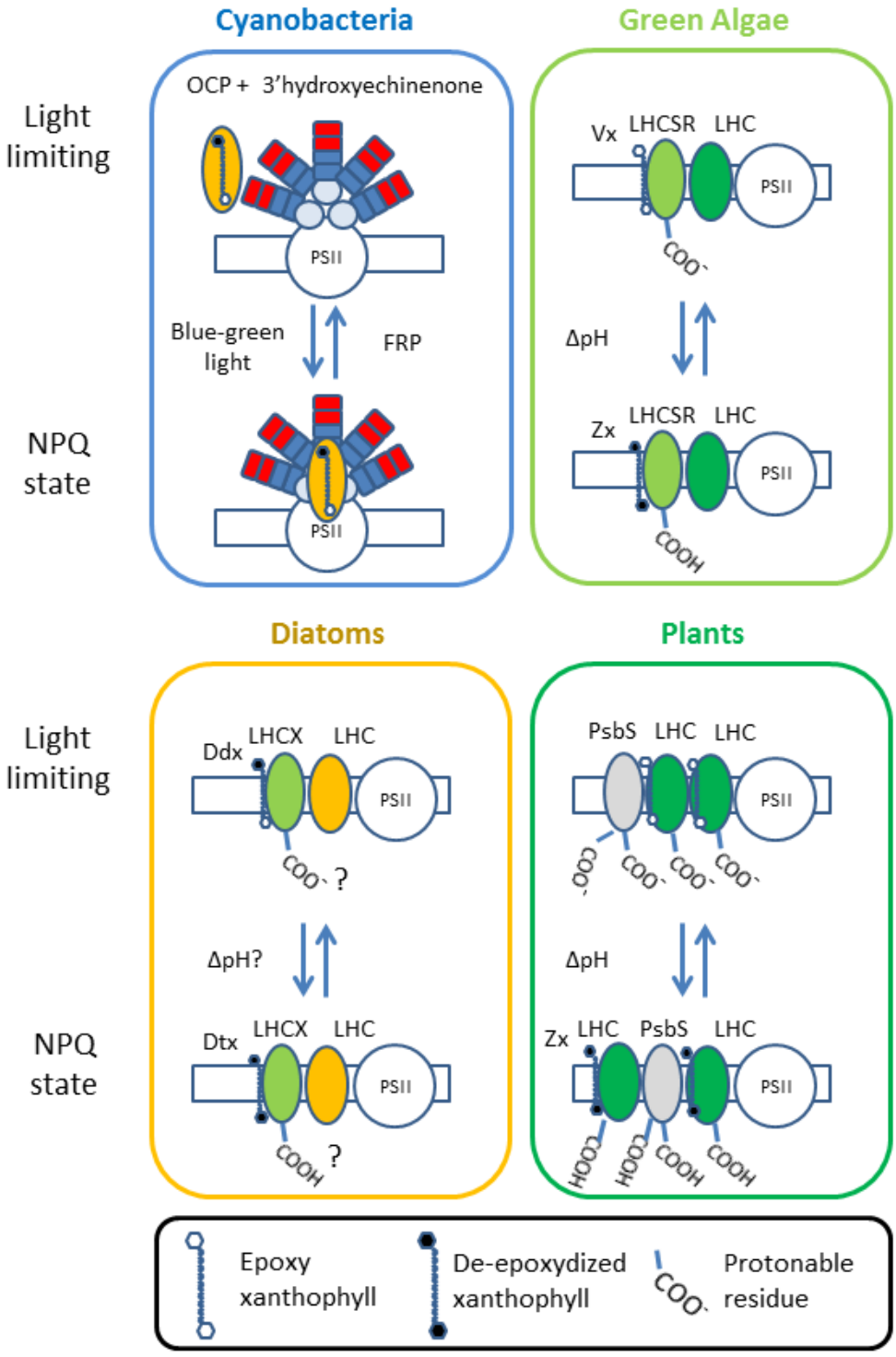

Figure 15: A schematic overview of the flexible NPQ mechanisms in major photosynthetic groups, modified after Niyogi and Truong (2013). See the sections 'The NPQ scenario', 'The xanthophyll cycle' and 'LHCX proteins' for details. Question marks express uncertainty.

Migration in epipelic diatoms

The migration of raphid diatoms in the uppermost sediment layers has been known for a long time (Fauvel and Bohn 1907; Perkins 1960; Round and Palmer 1966; Barranguet et al. 1998). In intertidal sediments, epipelic diatoms migrate to the surface during daytime low tide and migrate downwards during nighttime and immersion (Palmer and Round 1967). As these migratory patterns are maintained for a couple of days in vitro (i.e. in absence of actual environmental cues), it is hypothesized that epipelic diatoms have an internal clock, which is entrained by the day/night as well as by the tidal cycle (Palmer and Round 1967; Serôdio et al. 1997). Diatom emergence at the sediment surface seems to be species-specific, as a sequential species turnover was observed in laboratory mesocosms (Paterson 1986) and during an emersion period in the field (Underwood et al. 2005).

Besides following the tidal and diurnal cycles, epipelic diatoms can migrate within the light gradient of the surface sediments to avoid overexposure (Admiraal 1984). As such this 'behavioural photoprotection' mechanism could represent a rapid, flexible and energetically cheap way to optimize photosynthesis (Serôdio et al. 2001). Indeed, epipelic diatoms position themselves within sediment light gradients in order to maximize photosynthesis and/or avoid overexposure (Admiraal 1984; Serôdio et al. 2006; Cartaxana et al. 2016a). Besides bulk downward vertical migration, a continuous cycling of motile diatoms (microcycling) within the top layers of the sediments was proposed where cells migrating downwards in order to avoid photoinhibition are replaced by others (Kromkamp et al. 1998).

While in situ epipelic diatom communities also activate the XC as a response to high light (Chevalier et al. 2010), they use vertical migration and/or microcycling as their primary photoprotection mechanism when motility is allowed (Kromkamp et al. 1998; Serôdio 2004; Perkins et al. 2010; Cartaxana et al. 2011; Serôdio et al. 2012; Laviale et al. 2015). The total contribution of both vertical migration and xanthophyll-cycle based photoprotection, however, was estimated to be relatively low (~20%) in epipelic communities from the Tagus estuary (Serôdio et al. 2012; Laviale et al. 2015).

As vertical migration is fast enough to reduce the amount of absorbed photons and can operate simultaneously with NPQ induction (Laviale et al. 2016), a behavioural response could alleviate the need for physiological photoprotection (Serôdio et al. 2001; Raven 2011). Therefore, we suspected differences in physiological photoprotection (mainly in NPQ) between different MPB growth forms.

NPQ capacity differences between diatoms

Marked differences in NPQ capacity and kinetics were discovered between planktonic diatom species and even between ecotypes isolated from habitats experiencing different degrees of light fluctuations. These differences have been attributed either to variation in XC kinetics and/or the amount of LHCX proteins (Dimier and Corato 2007; Lavaud et al. 2007; Bailleul et al. 2010b; Petrou et al. 2011; Lavaud and Lepetit 2013). The picture emerging from these reports is a higher/faster Dtx synthesis supporting a faster NPQ induction and a higher level of NPQ activity in species/ecotypes adapted to habitats characterized by strong light fluctuations and/or on average higher irradiance (Lavaud and Goss 2014).

Species thriving in fluctuating light conditions, for instance, exhibit high de novo synthesis of Dtx molecules (accumulation of Dtx independently from Ddx de-epoxidation) which correlates well with NPQ development during strong light conditions, whereas species experiencing a more stable light climate in their natural habitat, synthetize additional Dtx which is not involved in NPQ but may rather have an antioxidant function (Lavaud and Lepetit 2013). To better cope with fluctuating light conditions need not only to exhibit high NPQ at high light levels, but also to carry out quick NPQ relaxation at low light (Lavaud et al. 2007). Finally, as Dtx molecules have to be epoxidized back to Ddx to switch the antenna system from an energy dissipating to a light harvesting mode, diatoms with a high Dtx epoxidation rate dissipate NPQ faster compared to diatoms with a lower epoxidation rate (Goss et al. 2006; Goss and Jakob 2010). Besides XC characteristics, NPQ capacity can also be attributed to differences in LHCX protein content. The low amount of LHCX1 protein, for instance, explains the limited NPQ capacity in a high latitude *Phaeodactylum tricornutum* ecotype isolated from a habitat which experiences lower average light intensity and less drastically fluctuating light conditions compared to other ecotypes (Bailleul et al. 2010b).

Aims

While our knowledge of NPQ regulation by the XC and LHCX proteins and possibly ΔpH is mostly based on studies in planktonic diatoms, whose light climate is mostly governed by water column turbulence, far less attention has been paid to NPQ regulation of truly benthic diatoms thriving in and on the sediments of intertidal flats (but see Jesus et al. 2009; Perkins et al. 2010; Cartaxana et al. 2011, 2016a; b; Serôdio et al. 2012; Lavaud and Goss 2014; Ezequiel et al. 2015; Pniewski et al. 2015; Laviale et al. 2015). As communities living on sandy sediments show no endogenous migration rhythms in situ and exhibited higher diatoxanthin/diadinoxanthin ratios than communities living on fine substrates a trade-off between behavioral photoprotection (vertical migration) and physiological photoprotection, conferred by the XC, was proposed (van Leeuwe et al. 2008; Jesus et al. 2009). However, at least the sandy sediments contain a mix of both epipsammic and epipelic forms (Jesus et al. 2009; Cartaxana et al. 2011), and even when the latter are not numerically dominant, they can still make a substantial contribution to biomass because of their much larger biovolumes (see for example, Hamels et al. 1998), which obscures differences between growth forms. Measurements of NPQ and vertical migration (VM) furthermore are rare and limited to natural communities (Perkins et al. 2010; Serôdio et al. 2012; Laviale et al. 2015, 2016). While LHCX proteins play a crucial role in the NPQ mechanism of diatoms (Bailleul et al. 2010b), they have rarely been investigated in benthic diatoms, with the exception of natural epipelic communities and the epipelic diatom *Navicula phyllepta* (Laviale et al. 2015). This study showed an increase in LHCX protein isoforms upon high light exposure and an even higher induction in combination with high temperature and inhibition of diatom motility. Information on LHCX identity and sequence characteristics, however, is largely lacking. Finally, the role of ΔpH in the regulation of NPQ is far from clear in diatoms and in vivo ΔpH measurements have not been conducted.

The general aim of this study is to provide a detailed comparative analysis of physiological (mainly NPQ) and behavioral photoprotective mechanisms in the major intertidal benthic diatom growth forms, with emphasis on epipelic and (non-motile) epipsammic forms, based on laboratory analyses of isolates. In addition this study aims to provide a comprehensive analysis of NPQ regulation (XC, LHCX and ΔpH) in intertidal benthic diatoms.

More specifically, we aim to:

1. **Characterize NPQ capacity in a set of unialgal isolates of the major intertidal benthic growth forms, viz. epipelon, motile and non-motile epipsammon, and tychoplankton.**

2. **Determine the xanthophyll cycle kinetics in an epipelic and a non-motile epipsammic diatom.**

3. **Quantify both vertical migration and NPQ for a set of epipelic as well as motile and non-motile epipsammic species.**

4. **Detect LHCX isoforms in an epipelic and an non-motile epipsammic diatom in low and high light conditions.**

5. **Identify *LHCX* genes present in the genome of a non-motile epipelic diatom and study their expression in relation to (high) light exposure.**

6. **Establish and apply a method to measure ΔpH in diatoms and study its relation to NPQ and the XC.**

Outline

Chapter 2

By comparing photophysiological traits in 15 microphytobenthic diatoms species belonging to the four main morphological growth forms we revealed a clear relationship between growth form and photoprotective capacity. Both NPQ and associated XC traits were stronger developed in less motile growth forms and indicate a trade-off between behavioral and physiological photoprotection.

Chapter 3

Here we studied the effect of 1 h high light exposure on the kinetics of the xanthophyll cycle and NPQ in both an epipelic (motile) diatom (*Seminavis robusta*) and an epipsammic (non-motile) diatom (*Opephora guenter-grassii*). This revealed that *O. guenter-grassii* could rapidly switch on and off NPQ by relying on fast XC kinetics. This species also demonstrated a high de novo synthesis of xanthophylls within a relatively short time period. In contrast, *S. robusta* showed slower NPQ and associated xanthophyll cycle kinetics, partly relying on additional NPQ conferred by *de novo* synthetized diatoxanthin molecules and synthesis of LHCX isoforms.

Chapter 4

We tested both the behavioral response (vertical migration, VM) and non-phototochemical quenching in epipsammic and epipelic strains acclimated to the same light climate. Our results revealed the clustering of both growth forms around a NPQ/VM trade-off curve and confirm that they can be seen as functional groups exhibiting different photoprotection strategies.

Chapter 5

The availability of the draft genome of *S. robusta* allowed us to identify 14 *LHCX* genes in the epipelic diatom *S. robusta*. Remarkably, all of the studied *LHCX* genes showed a clear response to a shift from low to high light and a transient induction during a dark to low light switch. Our data implicates the involvement of multiple fast-regulated *LHCX* genes during variable light conditions, allowing epipelic species to respond and/or acclimate to prolonged high light conditions

Chapter 6

In this study we attempted to investigate the relationship between NPQ and the trans-thylakoidal proton gradient by making use of the electro-chromatic shift (ECS) and tested the validity of this technique.

References

Admiraal, W. 1984. The ecology of estuarine sediment-inhabiting diatoms. Prog. Phycol. Res. **3**: 269–322.

Allen, A. E., B. B. Ward, and B. Song. 2005. Characterization of diatom (Bacillariophyceae) nitrate reductase genes and their detection in marine phytoplankton communities. J. Phycol. **41**: 95–104. doi:10.1111/j.1529-8817.2005.04090.x

Archibald, J. M. 2009. The Puzzle of Plastid Evolution. Curr. Biol. **19**: 81–88. doi:10.1016/j.cub.2008.11.067

Armbrust, E., J. Berges, and C. Bowler. 2004. The genome of the diatom *Thalassiosira pseudonana*: ecology, evolution, and metabolism. Science (80-.). **306**: 79–86.

Asada, K. 2006. Production and scavenging of reactive oxygen species in chloroplasts and their functions. Plant Physiol. **141**: 391–6. doi:10.1104/pp.106.082040

Aumeier, C., and D. Menzel. 2012. Secretion in the Diatoms, p. 221–250. *In* J.M. Vivanco and F. Baluška [eds.], Secretions and Exudates in Biological Systems. Springer Berlin Heidelberg.

Bailleul, B., N. Berne, O. Murik, and others. 2015. Energetic coupling between plastids and mitochondria drives CO_2 assimilation in diatoms. Nature **524**: 366–369. doi:10.1038/nature14599

Bailleul, B., P. Cardol, C. Breyton, and G. Finazzi. 2010a. Electrochromism: a useful probe to study algal photosynthesis. Photosynth. Res. **106**: 179–89. doi:10.1007/s11120-010-9579-z

Bailleul, B., A. Rogato, A. De Martino, S. Coesel, P. Cardol, C. Bowler, A. Falciatore, and G. Finazzi. 2010b. An atypical member of the light-harvesting complex stress-related protein family modulates diatom responses to light. Proc. Natl. Acad. Sci. **107**: 18214–18219. doi:10.1073/pnas.1007703107

Baker, N. R. 2008. Chlorophyll Fluorescence: A Probe of Photosynthesis In Vivo. Annu. Rev. Plant Biol. **59**: 89–113. doi:10.1146/annurev.arplant.59.032607.092759

Ballottari, M., T. B. Truong, E. De Re, E. Erickson, G. R. Stella, G. R. Fleming, R. Bassi, and K. K. Niyogi. 2016. Identification of pH-sensing Sites in the Light Harvesting Complex Stress-related 3 Protein Essential for Triggering Non-photochemical Quenching in *Chlamydomonas reinhardtii*. J. Biol. Chem. **291**: 7334–46. doi:10.1074/jbc.M115.704601

Barranguet, C., J. Kromkamp, and J. Peene. 1998. Factors controlling primary production and photosynthetic characteristics of intertidal microphytobenthos. Mar. Ecol. Prog. Ser. **173**: 117–126. doi:10.3354/meps173117

Bonente, G., F. Passarini, S. Cazzaniga, C. Mancone, M. C. Buia, M. Tripodi, R. Bassi, and S. Caffarri. 2008. The occurrence of the psbS gene product in *Chlamydomonas reinhardtii* and in other photosynthetic organisms and its correlation with energy quenching. Photochem. Photobiol. **84**: 1359–70. doi:10.1111/j.1751-1097.2008.00456.x

Boogert, N. J., D. M. Paterson, and K. N. Laland. 2006. The Implications of Niche Construction and Ecosystem Engineering for Conservation Biology. Bioscience **56**: 570. doi:10.1641/0006-3568(2006)56[570:TIONCA]2.0.CO;2

Cabrita, M., and V. Brotas. 2000. Seasonal variation in denitrification and dissolved nitrogen fluxes in intertidal sediments of the Tagus estuary, Portugal. Mar. Ecol. Prog. Ser. **202**: 51–

65. doi:10.3354/meps202051

Cartaxana, P., S. Cruz, C. Gameiro, and M. Kühl. 2016a. Regulation of intertidal microphytobenthos photosynthesis over a diel emersion period is strongly affected by diatom migration patterns. Front. Microbiol. **7**: 872. doi:10.3389/fmicb.2016.00872

Cartaxana, P., N. Domingues, S. Cruz, B. Jesus, M. Laviale, J. Serôdio, and J. Marques da Silva. 2013. Photoinhibition in benthic diatom assemblages under light stress. Aquat. Microb. Ecol. **70**: 87–92. doi:10.3354/ame01648

Cartaxana, P., L. Ribeiro, J. Goessling, S. Cruz, and M. Kühl. 2016b. Light and O_2 microenvironments in two contrasting diatom-dominated coastal sediments. Mar. Ecol. Prog. Ser. **545**: 35–47. doi:10.3354/meps11630

Cartaxana, P., M. Ruivo, C. Hubas, I. Davidson, J. Serôdio, and B. Jesus. 2011. Physiological versus behavioral photoprotection in intertidal epipelic and epipsammic benthic diatom communities. J. Exp. Mar. Bio. Ecol. **405**: 120–127. doi:10.1016/j.jembe.2011.05.027

Chevalier, E. M., F. Gévaert, and A. Créach. 2010. In situ photosynthetic activity and xanthophylls cycle development of undisturbed microphytobenthos in an intertidal mudflat. J. Exp. Mar. Bio. Ecol. **385**: 44–49. doi:10.1016/j.jembe.2010.02.002

Claquin, P., J. C. Kromkamp, and V. Martin-Jezequel. 2004. Relationship between photosynthetic metabolism and cell cycle in a synchronized culture of the marine alga *Cylindrotheca fusiformis* (Bacillariophyceae). Eur. J. Phycol. **39**: 33–41. doi:10.1080/0967026032000157165

Cook, P. L. M., B. Veuger, S. Böer, and J. J. Middelburg. 2007. Effect of nutrient availability on carbon and nitrogen incorporation and flows through benthic algae and bacteria in near-shore sandy sediment. Aquat. Microb. Ecol. **49**: 165–180.

Correa-Galvis, V., P. Redekop, K. Guan, A. Griess, T. B. Truong, S. Wakao, K. K. Niyogi, and P. Jahns. 2016. Photosystem II Subunit PsbS Is Involved in the Induction of LHCSR Protein-dependent Energy Dissipation in *Chlamydomonas reinhardtii*. J. Biol. Chem. **291**: 17478–87. doi:10.1074/jbc.M116.737312

Dambek, M., U. Eilers, J. Breitenbach, S. Steiger, C. Büchel, and G. Sandmann. 2012. Biosynthesis of fucoxanthin and diadinoxanthin and function of initial pathway genes in *Phaeodactylum tricornutum*. J. Exp. Bot. **63**: 5607–5612. doi:10.1093/jxb/ers211

Delgado, M., V. N. De Jonge, and H. Peletier. 1991. Effect of sand movement on the growth of benthic diatoms. J. Exp. Mar. Bio. Ecol. **145**: 221–231. doi:10.1016/0022-0981(91)90177-X

Demmig-Adams, B., and W. W. Adams. 2006. Photoprotection in an ecological context: the remarkable complexity of thermal energy dissipation. New Phytol. **172**: 11–21. doi:10.1111/j.1469-8137.2006.01835.x

Demmig-adams, B., C. M. Cohu, J. J. Stewart, W. W. A. III, and Govindjee. 2014. Non-Photochemical Quenching and Energy Dissipation in Plants, Algae and Cyanobacteria, B. Demmig-Adams, G. Garab, W. Adams III, and Govindjee [eds.]. Springer Netherlands.

Dimier, C., and F. Corato. 2007. Photoprotection and xanthophyll cycle activity in three marine diatoms. J. Phycol. **43**: 937–947.

Eisenstadt, D., I. Ohad, N. Keren, and A. Kaplan. 2008. Changes in the photosynthetic reaction

centre II in the diatom *Phaeodactylum tricornutum* result in non-photochemical fluorescence quenching. Environ. Microbiol. **10**: 1997–2007. doi:10.1111/j.1462-2920.2008.01616.x

Erickson, E., S. Wakao, and K. K. Niyogi. 2015. Light stress and photoprotection in *Chlamydomonas reinhardtii*. Plant J. **82**: 449–465. doi:10.1111/tpj.12825

Ezequiel, J., M. Laviale, S. Frankenbach, P. Cartaxana, and J. Serôdio. 2015. Photoacclimation state determines the photobehaviour of motile microalgae: The case of a benthic diatom. J. Exp. Mar. Bio. Ecol. **468**: 11–20. doi:10.1016/j.jembe.2015.03.004

Fauvel, P., and G. Bohn. 1907. Le rhythme des marées chez les diatomées litorales. C. R. Séanc. Soc. Biol **62**.

Gerbersdorf, S. U., R. Bittner, H. Lubarsky, W. Manz, and D. M. Paterson. 2009. Microbial assemblages as ecosystem engineers of sediment stability. J. Soils Sediments **9**: 640–652. doi:10.1007/s11368-009-0142-5

Gerbersdorf, S. U., and S. Wieprecht. 2015. Biostabilization of cohesive sediments: revisiting the role of abiotic conditions, physiology and diversity of microbes, polymeric secretion, and biofilm architecture. Geobiology **13**: 68–97. doi:10.1111/gbi.12115

Gerotto, C., A. Alboresi, G. M. Giacometti, R. Bassi, and T. Morosinotto. 2011. Role of PSBS and LHCSR in *Physcomitrella patens* acclimation to high light and low temperature. Plant. Cell Environ. **34**: 922–32. doi:10.1111/j.1365-3040.2011.02294.x

Goss, R., and T. Jakob. 2010. Regulation and function of xanthophyll cycle-dependent photoprotection in algae. Photosynth. Res. **106**: 103–122. doi:10.1007/s11120-010-9536-x

Goss, R., and B. Lepetit. 2015. Biodiversity of NPQ. J. Plant Physiol. **172**: 13–32. doi:10.1016/j.jplph.2014.03.004

Goss, R., B. Lepetit, and C. Wilhelm. 2006a. Evidence for a rebinding of antheraxanthin to the light-harvesting complex during the epoxidation reaction of the violaxanthin cycle. J. Plant Physiol. **163**: 585–590. doi:10.1016/j.jplph.2005.07.009

Goss, R., E. A. Pinto, C. Wilhelm, and M. Richter. 2006b. The importance of a highly active and ΔpH-regulated diatoxanthin epoxidase for the regulation of the PS II antenna function in diadinoxanthin cycle containing algae. J. Plant Physiol. **163**: 1008–1021. doi:10.1016/j.jplph.2005.09.008

Grouneva, I., T. Jakob, C. Wilhelm, and R. Goss. 2006. Influence of ascorbate and pH on the activity of the diatom xanthophyll cycle-enzyme diadinoxanthin de-epoxidase. Physiol. Plant. **126**: 205–211. doi:10.1111/j.1399-3054.2006.00613.x

Grouneva, I., T. Jakob, C. Wilhelm, and R. Goss. 2009. The regulation of xanthophyll cycle activity and of non-photochemical fluorescence quenching by two alternative electron flows in the diatoms *Phaeodactylum tricornutum* and *Cyclotella meneghiniana*. Biochim. Biophys. Acta **1787**: 929–38. doi:10.1016/j.bbabio.2009.02.004

Hamels, I., K. Sabbe, K. Muylaert, C. Barranguet, C. Lucas, P. Herman, and W. Vyverman. 1998. Organisation of microbenthic communities in intertidal estuarine flats, a case study from the molenplaat (Westerschelde estuary, The Netherlands). Eur. J. Protistol. **34**: 308–320. doi:10.1016/S0932-4739(98)80058-8

Horton, P. 2012. Optimization of light harvesting and photoprotection: molecular mechanisms and physiological consequences. Philos. Trans. R. Soc. Lond. B. Biol. Sci. **367**: 3455–65. doi:10.1098/rstb.2012.0069

Jakob, T., R. Goss, and C. Wilhelm. 2001. Unusual pH-dependence of diadinoxanthin de-epoxidase activation causes chlororespiratory induced accumulation of diatoxanthin in the diatom *Phaeodactylum tricornutum*. J. Plant Physiol. **158**: 383–390. doi:10.1078/0176-1617-00288

Janknegt, P. J., C. M. De Graaff, W. H. Van De Poll, R. J. W. Visser, E. W. Helbling, and A. G. J. Buma. 2009a. Antioxidative responses of two marine microalgae during acclimation to static and fluctuating natural uv radiation. Photochem. Photobiol. **85**: 1336–1345. doi:10.1111/j.1751-1097.2009.00603.x

Janknegt, P. J., C. M. De Graaff, W. H. Van De Poll, R. J. W. Visser, J. W. Rijstenbil, and A. G. J. Buma. 2009b. Short-term antioxidative responses of 15 microalgae exposed to excessive irradiance including ultraviolet radiation. Eur. J. Phycol. **44**: 525–539. doi:10.1080/09670260902943273

Janknegt, P. J., W. H. van de Poll, R. J. W. Visser, J. W. Rijstenbil, and A. G. J. Buma. 2008. Oxidative stress responses in the marine antarctic diatom *Chaetoceros Brevis* (Bacillariophyceae) during photoacclimation. J. Phycol. **44**: 957–966. doi:10.1111/j.1529-8817.2008.00553.x

Jesus, B., V. Brotas, L. Ribeiro, C. R. Mendes, P. Cartaxana, and D. M. Paterson. 2009. Adaptations of microphytobenthos assemblages to sediment type and tidal position. Cont. Shelf Res. **29**: 1624–1634. doi:10.1016/j.csr.2009.05.006

Jewson, D. H., S. F. Lowry, and R. Bowen. 2006. Co-existence and survival of diatoms on sand grains. Eur. J. Phycol. **41**: 131–146. doi:10.1080/09670260600652903

Joliot, P., and R. Delosme. 1974. Flash-induced 519 nm absorption change in green algae. Biochim. Biophys. Acta **357**: 267–84.

Joliot, P., and A. Joliot. 1989. Characterization of linear and quadratic electrochromic probes in Chlorella sorokiniana and *Chlamydomonas reinhardtii*. Biochim. Biophys. Acta - Bioenerg. **975**: 355–360. doi:10.1016/S0005-2728(89)80343-3

Joliot, P., and A. Joliot. 2002. Cyclic electron transfer in plant leaf. Proc. Natl. Acad. Sci. **99**: 10209–10214. doi:10.1073/pnas.102306999

Kirilovsky, D., and C. A. Kerfeld. 2016. Cyanobacterial photoprotection by the orange carotenoid protein. Nat. Plants **2**: 16180. doi:10.1038/nplants.2016.180

Koziol, A. G., T. Borza, K.-I. Ishida, P. Keeling, R. W. Lee, and D. G. Durnford. 2007. Tracing the Evolution of the Light-Harvesting Antennae in Chlorophyll *a*/*b*-Containing Organisms. Plant Physiol. **143**.

Kramer, D. M., J. A. Cruz, and A. Kanazawa. 2003. Balancing the central roles of the thylakoid proton gradient. Trends Plant Sci. **8**: 27–32. doi:10.1016/S1360-1385(02)00010-9

Krause, G. H., and E. Weis. 1991. Chlorophyll Fluorescence and Photosynthesis: The Basics. Annu. Rev. Plant Physiol. Plant Mol. Biol. **42**: 313–349. doi:10.1146/annurev.pp.42.060191.001525

Kromkamp, J. C., C. Barranguet, and J. Peene. 1998. Determination of microphytobenthos PSII quantum efficiency and photosynthetic activity by means of variable chlorophyll fluorescence. Mar. Ecol. Prog. Ser. **162**: 45–55. doi:10.3354/meps162045

Kuhl, M., C. Lassen, and B. B. Jorgensen. 1994. Light penetration and light intensity in sandy marine sediments measured with irradiance and scalar irradiance fiber-optic microprobes. Mar. Ecol. Prog. Ser. **105**: 139–148. doi:10.3354/meps105139

Lavaud, J. 2007. Fast regulation of photosynthesis in diatoms: mechanisms, evolution and ecophysiology. Funct. Plant Sci. Biotechonology **1**: 267–287. doi:http://dx.doi.org/

Lavaud, J., H. J. van Gorkom, and A.-L. Etienne. 2002. Photosystem II electron transfer cycle and chlororespiration in planktonic diatoms. Photosynth. Res. **74**: 51–59. doi:10.1023/A:1020890625141

Lavaud, J., and R. Goss. 2014. The peculiar features of the non-photochemical fluorescence quenching in diatoms and brown algae, p. 421–443. *In* B. Demmig-Adams, G. Garab, W. Adams III, and Govindjee [eds.], Non-Photochemical Quenching and Energy Dissipation in Plants, Algae and Cyanobacteria. Springer.

Lavaud, J., and B. Lepetit. 2013. An explanation for the inter-species variability of the photoprotective non-photochemical chlorophyll fluorescence quenching in diatoms. Biochim. Biophys. Acta **1827**: 294–302. doi:10.1016/j.bbabio.2012.11.012

Lavaud, J., C. Six, and D. A. Campbell. 2016. Photosystem II repair in marine diatoms with contrasting photophysiologies. Photosynth. Res. **127**: 189–199. doi:10.1007/s11120-015-0172-3

Lavaud, J., R. F. Strzepek, and P. G. Kroth. 2007. Photoprotection capacity differs among diatoms : Possible consequences on the spatial distribution of diatoms related to fluctuations in the underwater light climate. Limnol. Oceanogr. **52**: 1188–1194.

Laviale, M., A. Barnett, J. Ezequiel, B. Lepetit, S. Frankenbach, V. Méléder, J. Serôdio, and J. Lavaud. 2015. Response of intertidal benthic microalgal biofilms to a coupled light-temperature stress: evidence for latitudinal adaptation along the Atlantic coast of Southern Europe. Environ. Microbiol. **17**: 3662–3677. doi:10.1111/1462-2920.12728

Laviale, M., S. Frankenbach, and J. Serôdio. 2016. The importance of being fast: comparative kinetics of vertical migration and non-photochemical quenching of benthic diatoms under light stress. Mar. Biol. **163**: 10. doi:10.1007/s00227-015-2793-7

van Leeuwe, M., V. Brotas, M. Consalvey, R. Forster, D. Gillespie, B. Jesus, J. Roggeveld, and W. Gieskes. 2008. Photoacclimation in microphytobenthos and the role of xanthophyll pigments. Eur. J. Phycol. **43**: 123–132. doi:10.1080/09670260701726119

Lepetit, B., S. Sturm, A. Rogato, A. Gruber, M. Sachse, A. Falciatore, P. G. Kroth, and J. Lavaud. 2013. High light acclimation in the secondary plastids containing diatom *Phaeodactylum tricornutum* is triggered by the redox state of the plastoquinone pool. Plant Physiol. **161**: 853–865. doi:10.1104/pp.112.207811

Lohr, M., and C. Wilhelm. 1999. Algae displaying the diadinoxanthin cycle also possess the violaxanthin cycle. Proc. Natl. Acad. Sci. **96**: 8784–8789. doi:10.1073/pnas.96.15.8784

Lohr, M., and C. Wilhelm. 2001. Xanthophyll synthesis in diatoms: quantification of putative intermediates and comparison of pigment conversion kinetics with rate constants derived

from a model. Planta **212**: 382–391. doi:10.1007/s004250000403

Lyu, H., and D. Lazár. 2017. Modeling the light-induced electric potential difference (ΔΨ), the pH difference (ΔpH) and the proton motive force across the thylakoid membrane in C3 leaves. J. Theor. Biol. **413**: 11–23. doi:10.1016/j.jtbi.2016.10.017

MacIntyre, H. L., T. M. Kana, T. Anning, and R. J. Geider. 2002. Photoacclimation of photosynthesis irradiance response curves and photosynthetic pigments in macroalgae and cyanobacteria. J. Phycol. **38**: 17–38. doi:10.1046/j.1529-8817.2002.00094.x

Méléder, V., Y. Rincé, L. Barillé, P. Gaudin, and P. Rosa. 2007. Spatiotemporal changes in microphytobenthos assemblages in a macrotidal flat (Bourgneuf Bay, France). J. Phycol. **43**: 1177–1190. doi:10.1111/j.1529-8817.2007.00423.x

Mewes, H., and M. Richter. 2002. Supplementary ultraviolet-B radiation induces a rapid reversal of the diadinoxanthin cycle in the strong light-exposed diatom *Phaeodactylum tricornutum*. Plant Physiol. **130**: 1527–35. doi:10.1104/pp.006775

Middelburg, J. J., C. Barranguet, H. T. S. Boschker, P. M. J. Herman, T. Moens, and C. H. R. Heip. 2000. The fate of intertidal microphytobenthos carbon: An in situ 13C-labeling study. Limnol. Oceanogr. **45**: 1224–1234. doi:10.4319/lo.2000.45.6.1224

Migné, A., G. Delebecq, D. Davoult, N. Spilmont, D. Menu, and F. Gévaert. 2015. Photosynthetic activity and productivity of intertidal macroalgae: In situ measurements, from thallus to community scale. Aquat. Bot. **123**: 6–12. doi:10.1016/j.aquabot.2015.01.005

Miller, A. R., R. L. L. Lowe, and J. T. T. Rotenberry. 1987. Succession of diatom communities on sand Grains. J. Ecol. **75**: 693–709. doi:10.2307/2260200

Mitchell, P. 1961. Coupling of Phosphorylation to Electron and Hydrogen Transfer by a Chemi-Osmotic type of Mechanism. Nature **191**: 144–148. doi:10.1038/191144a0

Morosinotto, T., and R. Bassi. 2014. Molecular Mechanisms for Activation of Non-Photochemical Fluorescence Quenching: From Unicellular Algae to Mosses and Higher Plants, p. 315–331. *In* B. Demmig-Adams, G. Garab, W. Adams III, and Govindjee [eds.], Non-Photochemical Quenching and Energy Dissipation in Plants, Algae and Cyanobacteria. Springer Netherlands.

Niyogi, K. K. 1999. Photoprotection revisited: Genetic and Molecular Approaches. Annu. Rev. Plant Physiol. Plant Mol. Biol. **50**: 333–359. doi:10.1146/annurev.arplant.50.1.333

Niyogi, K. K., and T. B. Truong. 2013. Evolution of flexible non-photochemical quenching mechanisms that regulate light harvesting in oxygenic photosynthesis. Curr. Opin. Plant Biol. **16**: 307–14. doi:10.1016/j.pbi.2013.03.011

Nymark, M., K. C. Valle, T. Brembu, K. Hancke, P. Winge, K. Andresen, G. Johnsen, and A. M. Bones. 2009. An integrated analysis of molecular acclimation to high light in the marine diatom *Phaeodactylum tricornutum*. PLoS One **4**: e7743. doi:10.1371/journal.pone.0007743

Oeltjen, A., W. E. Krumbein, and E. Rhiel. 2002. Investigations on transcript sizes, steady state mRNA concentrations and diurnal expression of genes encoding fucoxanthin chlorophyll a/c light harvesting polypeptides in the centric diatom *Cyclotella cryptica*. Plant Biol. **4**: 250–257. doi:10.1055/s-2002-25737

Onno Feikema, W., M. A. Marosvölgyi, J. Lavaud, and H. J. van Gorkom. 2006. Cyclic electron transfer in photosystem II in the marine diatom *Phaeodactylum tricornutum*. Biochim. Biophys. Acta **1757**: 829–34. doi:10.1016/j.bbabio.2006.06.003

Palmer, J. D., and F. E. Round. 1967. Persistent, vertical migration rhythms in benthic microflora. VI. The tidal and diurnal nature of the rhythms in the diatom *Hantzschia virgata*. Biol. Bull. **132**: 44–55. doi:10.2307/1539877

Park, S., G. Jung, Y. Hwang, and E. Jin. 2010. Dynamic response of the transcriptome of a psychrophilic diatom, *Chaetoceros neogracile*, to high irradiance. Planta **231**: 349–60. doi:10.1007/s00425-009-1044-x

Parker, M. S., and E. V. Armbrust. 2005. Synergistic Effects of Light, Temperature, and Nitrogen Source on Transcription of Genes for Carbon and Nitrogen Metabolism in the Centric Diatom *Thalassiosira Pseudonana* (Bacillariophyceae). J. Phycol. **41**: 1142–1153. doi:10.1111/j.1529-8817.2005.00139.x

Parker, M. S., E. V Armbrust, J. Piovia-Scott, and R. G. Keil. 2004. Induction of photorespiration by light in the centric diatom *Thalassiosira wiessflogii* (Bacillariophyceae): Molecular characterization and physiological consequences. J. Phycol. **40**: 557–567. doi:10.1111/j.1529-8817.2004.03184.x

Passarelli, C., F. Olivier, D. M. Paterson, T. Meziane, and C. Hubas. 2014. Organisms as cooperative ecosystem engineers in intertidal flats. J. Sea Res. **92**: 92–101. doi:10.1016/j.seares.2013.07.010

Paterson, D. M. 1986. The migratory behaviour of diatom assemblages in a laboratory tidal micro-ecosystem examined by low temperature scanning electron microscopy. Diatom Res. **1**: 227–239. doi:10.1080/0269249X.1986.9704971

Paterson, D. M., and S. E. Hagerthey. 2001. Microphytobenthos in Constrasting Coastal Ecosystems: Biology and Dynamics, p. 105–125. *In* Ecological Comparisons of Sedimentary Shores. Springer Berlin Heidelberg.

Peers, G., T. B. Truong, E. Ostendorf, A. Busch, D. Elrad, A. R. Grossman, M. Hippler, and K. K. Niyogi. 2009. An ancient light-harvesting protein is critical for the regulation of algal photosynthesis. Nature **462**: 518–521. doi:10.1038/nature08587

Perkins, E. J. 1960. The Diurnal Rhythm of the Littoral Diatoms of the River Eden Estuary, Fife. J. Ecol. **48**: 725. doi:10.2307/2257345

Perkins, R. G., J. Lavaud, J. Serôdio, and others. 2010. Vertical cell movement is a primary response of intertidal benthic biofilms to increasing light dose. Mar. Ecol. Prog. Ser. **416**: 93–103. doi:10.3354/meps08787

Petrou, K., M. A. Doblin, and P. J. Ralph. 2011. Heterogeneity in the photoprotective capacity of three Antarctic diatoms during short-term changes in salinity and temperature. Mar. Biol. **158**: 1029–1041. doi:10.1007/s00227-011-1628-4

Pinckney, J., K. Carman, S. Lumsden, and S. Hymel. 2003. Microalgal-meiofaunal trophic relationships in muddy intertidal estuarine sediments. Aquat. Microb. Ecol. **31**.

Pniewski, F. F., P. Biskup, I. Bubak, P. Richard, A. Latała, and G. Blanchard. 2015. Photo-regulation in microphytobenthos from intertidal mudflats and non-tidal coastal shallows. Estuar. Coast. Shelf Sci. **152**: 153–161. doi:10.1016/j.ecss.2014.11.022

Raven, J. A. 2011. The cost of photoinhibition. Physiol. Plant. **142**: 87–104. doi:10.1111/j.1399-3054.2011.01465.x

Ribeiro, L., V. Brotas, Y. Rincé, and B. Jesus. 2013. Structure and diversity of intertidal benthic diatom assemblages in contrasting shores: a case study from the Tagus estuary. J. Phycol. **49**: 258–270. doi:10.1111/jpy.12031

Riera, P. 1998. δ15N of organic matter sources and benthic invertebrates along an estuarine gradient in Marennes-Oléron Bay (France):implications for the study of trophic structure. Mar. Ecol. Prog. Ser. **166**: 143–150. doi:10.3354/meps166143

Round, F. E., R. M. Crawford, and D. G. Mann. 1990. The Diatoms - Biology & Morphology of the genera., Cambridge University Press.

Round, F. E., and J. D. Palmer. 1966. Persistent vertical-migration rhythms in benthic microflora: II. field and laboratory studies on diatoms from banks of river Avon. J. Mar. Biol. Assoc. United Kingdom **46**: 191–214.

Ruban, A. V. 2016. Nonphotochemical Chlorophyll Fluorescence Quenching: Mechanism and Effectiveness in Protecting Plants from Photodamage. Plant Physiol. **170**: 1903–16. doi:10.1104/pp.15.01935

Sabbe, K. 1993. Short-term fluctuations in benthic diatom numbers on an intertidal sandflat in the Westerschelde estuary (Zeeland, The Netherlands). Hydrobiologia **269–270**: 275–284. doi:10.1007/BF00028026

Sabbe, K. 1997. Systematics and ecology of intertidal benthic diatoms of the Westerschelde estuary (The Netherlands). Ghent University.

Sabbe, K., and W. Vyverman. 1991. Distribution of benthic diatom assemblages in the Westerschelde (Zeeland, The Netherlands). Belgian J. Bot. **124**: 91–101. doi:10.2307/1934940

Schumann, A., R. Goss, T. Jakob, and C. Wilhelm. 2007. Investigation of the quenching efficiency of diatoxanthin in cells of *Phaeodactylum tricornutum* (Bacillariophyceae) with different pool sizes of xanthophyll cycle pigments. Phycologia **46**: 113–117. doi:10.2216/06-30.1

Serôdio, J. 2004. Analysis of variable chlorophyll fluorescence in microphytobenthos assemblages: implications of the use of depth-integrated measurements. Aquat. Microb. Ecol. **36**: 137–152. doi:10.3354/ame036137

Serôdio, J., J. Ezequiel, A. Barnett, J.-L. Mouget, V. Méléder, M. Laviale, and J. Lavaud. 2012. Efficiency of photoprotection in microphytobenthos: role of vertical migration and the xanthophyll cycle against photoinhibition. Aquat. Microb. Ecol. **67**: 161–175. doi:10.3354/ame01591

Serôdio, J., J. Marques da Silva, and F. Catarino. 2001. Use of in vivo chlorophyll a fluorescence to quantify short-term variations in the productive biomass of intertidal microphytobenthos. Mar. Ecol. Prog. Ser. **218**: 45–61. doi:10.3354/meps218045

Serôdio, J., J. M. Da Silva, and F. Catarino. 1997. Nondestructive tracing of migratory rhytms of intertidal benthic microalgea using in vivo chlorophyll a fluorescence. J. Phycol. **33**: 542–553. doi:10.1111/j.0022-3646.1997.00542.x

Serôdio, J., S. Vieira, S. Cruz, and H. Coelho. 2006. Rapid light-response curves of chlorophyll

fluorescence in microalgae: relationship to steady-state light curves and non-photochemical quenching in benthic diatom-dominated assemblages. Photosynth. Res. **90**: 29–43. doi:10.1007/s11120-006-9105-5

Stal, L. J. 2010. Microphytobenthos as a biogeomorphological force in intertidal sediment stabilization. Ecol. Eng. **36**: 236–245. doi:10.1016/j.ecoleng.2008.12.032

Taddei, L., G. R. Stella, A. Rogato, and others. 2016. Multisignal control of expression of the LHCX protein family in the marine diatom *Phaeodactylum tricornutum*. J. Exp. Bot. **67**: 3939–3951. doi:10.1093/jxb/erw198

Takahashi, S., and M. R. Badger. 2011. Photoprotection in plants: a new light on photosystem II damage. Trends Plant Sci. **16**: 53–60. doi:10.1016/j.tplants.2010.10.001

Thornton, D. C. O., L. F. Dong, G. J. C. Underwood, and D. B. Nedwell. 2007. Sediment-water inorganic nutrient exchange and nitrogen budgets in the Colne Estuary, UK. Mar. Ecol. Prog. Ser. **337**: 63–77. doi:10.3354/meps337063

Underwood, G. J. C., and M. Barnett. 2006. What determines species composition in microphytobenthic biofilms, p. 123–140. *In* J.C. Kromkamp, J.F.C. De Brouwer, G.F. Blanchard, R.M. Forster, and V. Créach [eds.], Functioning of microphytobenthos in estuaries. Royal Netherlands Academy of Arts and Sciences, Amsterdam, The Netherlands.

Underwood, G. J. C., and J. Kromkamp. 1999. Primary production by phytoplankton and microphytobenthos in estuaries estuaries. Adv. Ecol. Res. **29**: 93–153. doi:10.1016/S0065-2504(08)60192-0

Underwood, G. J. C., R. G. Perkins, M. C. Consalvey, A. R. M. Hanlon, K. Oxborough, N. R. Baker, and D. M. Paterson. 2005. Patterns in microphytobenthic primary productivity: Species-specific variation in migratory rhythms and photosynthesis in mixed-species biofilms. Limnol. Oceanogr. **50**: 755–767. doi:10.4319/lo.2005.50.3.0755

Waring, J., M. Klenell, U. Bechtold, G. J. C. Underwood, and N. R. Baker. 2010. Light-induced responses of oxygen photoreduction, reactive oxygen species production and scavenging in two diatom species. J. Phycol. **46**: 1206–1217. doi:10.1111/j.1529-8817.2010.00919.x

Wilhelm, C., A. Jungandreas, T. Jakob, and R. Goss. 2014. Light acclimation in diatoms: From phenomenology to mechanisms. Mar. Genomics **16**: 5–15. doi:10.1016/j.margen.2013.12.003

Wilson, A., G. Ajlani, J.-M. Verbavatz, I. Vass, C. A. Kerfeld, and D. Kirilovsky. 2006. A soluble carotenoid protein involved in phycobilisome-related energy dissipation in cyanobacteria. Plant Cell **18**: 992–1007. doi:10.1105/tpc.105.040121

Wingler, A., P. J. Lea, W. P. Quick, and R. C. Leegood. 2000. Photorespiration: metabolic pathways and their role in stress protection. Philos. Trans. R. Soc. Lond. B. Biol. Sci. **355**: 1517–29. doi:10.1098/rstb.2000.0712

Yallop, M. L., B. de Winder, D. M. Paterson, and L. J. Stal. 1994. Comparative structure, primary production and biogenic stabilization of cohesive and non-cohesive marine sediments inhabited by microphytobenthos. Estuar. Coast. Shelf Sci. **39**: 565–582. doi:10.1016/S0272-7714(06)80010-7

Zhu, S.-H., and B. R. Green. 2010. Photoprotection in the diatom *Thalassiosira pseudonana*: role of LI818-like proteins in response to high light stress. Biochim. Biophys. Acta **1797**: 1449–

1457. doi:10.1016/j.bbabio.2010.04.003

Chapter 2: Growth form defines physiological photoprotective capacity in intertidal benthic diatoms

Alexandre Barnett[1], Vona Méléder[1,2], Lander Blommaert[1,3], Bernard Lepetit[1#], Pierre Gaudin[1,2$], Wim Vyverman[3], Koen Sabbe[3], Christine Dupuy[1] & Johann Lavaud[1]

1. UMR7266 LIENSs 'Littoral, Environnement et Sociétés', CNRS/Université de La Rochelle, Institut du Littoral et de l'Environnement, 2 rue Olympe de Gouges, 17000 La Rochelle, France.
2. UPRES EA 2160 MMS 'Mer, Molécules, Santé', Université de Nantes, Faculté des Sciences et Techniques, 2 rue de la Houssinière, BP 92208, 44322 Nantes cedex 3, France.
3. Laboratory of Protistology & Aquatic Ecology, Department of Biology, Ghent University,
   Krijgslaan 281-S8, B-9000 Ghent, Belgium.

Current address: Group of Plant Ecophysiology, Department of Biology, University of Konstanz, Universitätsstraße 10, 78457 Konstanz, Germany
$ Current address: UMR6112 'LPGN', CNRS / Université de Nantes, Faculté des Sciences et Techniques, 2 rue de la Houssinière, BP 92208, 44322 Nantes cedex 3, France.

Adapted from:

Barnett, A., V. Méléder, L. Blommaert, and others. 2015. Growth form defines physiological photoprotective capacity in intertidal benthic diatoms. ISME J. 9: 32–45. doi:10.1038/ismej.2014.105

My contribution comprises isolating diatoms, conducting all experiments on *Seminavis robusta* and *Opephora guenter-grasssii*, data analysis and writing.

Abstract

In intertidal marine sediments, characterized by rapidly fluctuating and often extreme light conditions, primary production is frequently dominated by diatoms. We performed a comparative analysis of photophysiological traits in 15 marine benthic diatom species belonging to the four major morphological growth forms (epipelon (EPL), motile epipsammon (EPM-M) and non-motile epipsammon (EPM-NM) and tychoplankton (TYCHO)) found in these sediments. Our analyses revealed a clear relationship between growth form and photoprotective capacity, and identified fast regulatory physiological photoprotective traits (that is, non-photochemical quenching (NPQ) and the xanthophyll cycle (XC)) as key traits defining the functional light response of these diatoms. EPM-NM and motile EPL showed the highest and lowest NPQ, respectively, with EPM-M showing intermediate values. Like EPL, TYCHO had low NPQ, irrespective of whether they were grown in benthic or planktonic conditions, reflecting an adaptation to a low light environment. Our results thus provide the first experimental evidence for the existence of a trade-off between behavioural (motility) and physiological photoprotective mechanisms (NPQ and the XC) in the four major intertidal benthic diatoms growth forms using unialgal cultures. Remarkably, although motility is restricted to the raphid pennate diatom clade, raphid pennate species, which have adopted a non-motile epipsammic or a tychoplanktonic life style, display the physiological photoprotective response typical of these growth forms. This observation underscores the importance of growth form and not phylogenetic relatedness as the prime determinant shaping the physiological photoprotective capacity of benthic diatoms.

Introduction

Functional trait-based approaches are increasingly adopted to explain and understand the distribution and diversity of phytoplankton communities (Litchman and Klausmeier, 2008; Barton et al. 2013; Edwards et al. 2013). Various morphological and physiological traits have been shown to define the ecological niches of phytoplankton species, including size, temperature response and resource acquisition and utilization traits. For example, in planktonic diatoms, which play a key role in marine primary production and biogeochemical cycling (Armbrust, 2009), pronounced species-specific differences in photosynthetic architecture and photophysiological strategies have been documented (e.g. Dimier et al. 2007; Key et al. 2010; Schwaderer et al. 2011; Wu et al. 2012) and related to their in situ light environment (Strzepek and Harrison, 2004; Lavaud et al. 2007; Dimier et al. 2009; Petrou et al. 2011). A high capacity for physiological photoprotection is generally observed in highly fluctuating light climates and/or under on average high irradiances. This suggests that photoprotective capacity is an adaptive trait that shapes the distribution of planktonic diatoms in the environment (Lavaud et al. 2007; Dimier et al. 2009; Bailleul et al. 2010; Petrou et al. 2011; Lavaud and Lepetit, 2013).

Benthic marine environments, and especially intertidal environments, are characterized by even more changeable and extreme light climates resulting from the interplay of weather conditions, tides, water column turbidity and sediment composition (and hence light penetration) (Admiraal, 1984; Underwood and Kromkamp, 1999; Paterson and Hagerthey, 2001). Nevertheless, intertidal sediments rank amongst the most productive ecosystems on Earth, largely owing to the primary production of highly diverse assemblages of benthic diatoms (Underwood and Kromkamp, 1999). To date however, little is known about the role of functional traits, and especially photophysiological traits, in shaping the structure, dynamics and function of benthic diatom assemblages. In most studies, diatom functional groups are defined on the basis of morphological growth form (e.g. Gottschalk and Kahlert, 2012; Larson and Passy, 2012) and not physiological traits. In addition, photoprotective ability (limited to the measurement of the 'xanthophyll cycle', XC) and its relationship with ecology has only been studied in natural communities with mixed assemblages of functional groups (e.g. Jesus et al. 2009; van Leeuwe et al. 2009; Cartaxana et al. 2011).

In temperate seas, intertidal benthic communities are largely dominated by diatoms (Méléder et al. 2007; Ribeiro et al. 2013), which display a high degree of taxonomic, phylogenetic and functional diversity (Kooistra et al. 2007). Several growth forms can be distinguished, which mainly differ in their attachment mode and degree of motility (see Ribeiro et al. (2013) for a detailed description): (1) the epipelon (EPL) comprises larger (usually > 10 µm) motile diatoms which can move freely in between sediment particles

and typically form biofilms (cf. (Herlory et al. 2004); (2) the epipsammon (EPM) groups smaller (usually < 10 µm) diatoms which live in close association with individual sand grains; and (3) the tychoplankton (TYCHO), which is an ill-defined and rather enigmatic group of largely non-motile diatoms which presumably have an amphibious life style (both sediment and water column) (e.g. Sabbe et al. (2010)). Within the epipsammic group, non-motile (EPM-NM) species are firmly attached (either stalked or adnate) to sand particles, while motile forms (EPM-M) can move within the sphere of individual sand grains. From a phylogenetic perspective, motile forms (i.e. all epipelon and motile epipsammon) exclusively belong to the pennate raphid clade (Kooistra et al. 2007), possessing a raphe allowing motility. Most non-motile epipsammon belongs to the pennate araphid lineage, but also includes some raphid pennates, such as *Biremis lucens*, which firmly attaches to sand grains (Sabbe et al. 1995). Tychoplankton includes both centric and pennate raphid forms. Intertidal benthic diatom species, but also growth forms, show distinct distribution patterns in time and space, suggesting pronounced (micro)niche differentiation (Sabbe, 1993; Méléder et al. 2007, Ribeiro et al. 2013). For example, epipsammon dominates non-cohesive sandy sediments (Méléder et al. 2007), while epipelon dominates cohesive muddy sediments (Haubois et al. 2005). Epipelon typically display vertical 'micromigration' in the sediment following endogenous tidal/dial rhythms and environmental stimuli (Saburova and Polikarpov, 2003; Consalvey et al. 2004; Coelho et al. 2011): during daylight emersion, they migrate to the sediment surface, while during immersion they migrate to deeper sediment layers.

To prevent photoinhibition (Serôdio et al. 2008), benthic diatoms utilize behavioural and physiological responses (Mouget et al. 2008; van Leeuwe et al. 2009; Perkins et al. 2010b; Cartaxana et al. 2011; Serôdio et al. 2012). Behavioural photoprotection involves motility, allowing cells to position themselves in light gradients and escape from prolonged exposure to excess light (Admiraal, 1984; Kromkamp et al. 1998; Consalvey et al. 2004; Serôdio et al. 2006). In addition, both motile and non-motile species employ fast regulatory physiological processes for photoprotection (i.e. 'physiological photoprotection'; Lavaud, 2007; Goss and Jakob, 2010; Depauw et al. 2012; Lepetit et al. 2012). In diatoms, two processes are important in field situations (Lavaud, 2007): photosystem II cyclic electron transfer (PSII CET) and non-photochemical quenching of chlorophyll (Chl) fluorescence (NPQ) (Depauw et al. 2012; Lepetit et al. 2012; Lavaud and Lepetit, 2013). NPQ is controlled by several regulatory partners including the light-dependent conversion of diadinoxanthin (Ddx) to diatoxanthin (Dtx) by the Ddx de-epoxidase (i.e. the XC) (Brunet and Lavaud, 2010; Goss and Jakob, 2010). In benthic diatoms however, XC-NPQ has only rarely been studied, and mostly in situ: it has been shown to vary with diurnal and tidal cycles, season, latitude (Serôdio et al. 2005; van Leeuwe et al. 2009; Chevalier et al. 2010), and to the organisms' position within the sediments and along the intertidal elevation gradient (Jesus et al. 2009; Cartaxana et al.

2011). On the basis of their in situ measurements, the latter authors hypothesized the existence of a trade-off between behavioural and physiological photoprotection mechanisms in benthic diatoms, as a stronger XC was shown to occur in sandy vs. muddy sediments. However, at least the sandy sediments contained a mix of both epipsammic and epipelic forms (Jesus et al. 2009; Cartaxana et al. 2011), and even when the latter are not numerically dominant, they can still make a substantial contribution to biomass because of their much larger biovolumes (see for example, Hamels et al. 1998).

Our study represents a comprehensive characterization of fast regulatory physiological photoprotection capacity in typical representatives of the major diatom growth forms occurring in intertidal marine sediments. Given the highly dynamic and often extreme intertidal light climate, we hypothesize that photoprotective features are key traits shaping niche differentiation between benthic growth forms, as has been proposed before for phytoplankton (Huisman et al. 2001; Litchman and Klausmeier, 2008; Dimier et al. 2009; Petrou et al. 2011; Lavaud and Lepetit, 2013). In this respect, we predict that the largely immotile epipsammic life forms are better able to cope with pronounced and rapid changes in light intensity at the physiological level than the motile epipelic forms which can actively position themselves in the sediment light gradient.

Materials and methods

Diatom culturing and harvesting

Fifteen benthic diatom strains were used (Table 1). All species were assigned to their respective growth form on the basis of microscopical observations on natural assemblages. They were grown in batch cultures at 20°C in sterile artificial F/2 seawater medium enriched with $NaHCO_3$ (80 mg L^{-1} final concentration). Tychoplankton species were also grown in continuously flushed airlift (i.e. with air bubbling) to mimic 'planktonic' growth conditions. Two light intensities (E, 20 and 75 µmol photons m^{-2} s^{-1}) were used with a 16 h light:8 h dark photoperiod white fluorescent tubes, L58W/840, OSRAM, Munich, Germany. Cultures were photoacclimated to the above conditions at least 2 weeks before measurements and experiments (see below). Diatom suspensions for the experiments were prepared to a final concentration of 10 µg chlorophyll *a* (Chl *a*) mL^{-1}. For this purpose, Chl *a* concentration was determined according to the Jeffrey and Humphrey (1975) spectrophotometric method. Diatom suspensions were continuously stirred at 20°C under the growth E (i.e. 20 or 75 µmol photons m^{-2} s^{-1}) at least 1 h before the start of the experiments and all along the course of the experiments (Lavaud et al. 2007). This kept the photosynthetic machinery in an oxidized state and prevented NPQ.

Growth rates and biovolumes

Specific growth rates, µ (day^{-1}), were calculated from regression of the natural logarithm of the number of diatom cells during their exponential growth phase as microscopically determined in a Malassez's counting chamber. Biovolumes (μm^3) were calculated using the formula of Hillebrand et al. (1999) based on measurements performed on fifteen specimens per species.

HPLC pigment analyses

Chl *a*, Chlorophyll *c* (Chl *c*), fucoxanthin (Fx), Ddx, Dtx and β-carotene (β-car) content, all normalized to Chl *a* (i.e. expressed as mol. 100 mol Chl a^{-1}), were measured using high-performance liquid chromatography as described in Jakob et al. (1999). One milliliter of diatom suspension was rapidly filtered (Isopore 1.2 µm RTTP filters, Merck Millipore, Darmstadt, Germany) and immediately frozen in liquid nitrogen before extraction in a cold (4°C) mixture of 90% methanol/0.2 M ammonium acetate (90/10 vol/vol) and 10% ethyl acetate. The pigment extraction was improved by the use of glass beads (diameter 0.25-0.5 mm, Roth, Karlsruhe, Germany) and included several short (20 s) vortexing steps. Supernatants were collected after centrifugation (5 min, 10 000 g, 4°C) and immediately injected into an HPLC system (Hitachi Lachrom Elite, Tokyo, Japan) equipped with a cooled auto-sampler and a photodiode array detector (L-2455). Chromatographic separation was carried out using a Nucleosil 120-5 C18 column (125 mm long, 4 mm internal diameter, 5 µm particles, Macherey-Nagel, Germany) equipped with a pre-column (CC 8/4 Nucleosil, Macherey-Nagel, Düren, Germany) for reverse

phase chromatography during a 25 min elution program. The solvent gradient followed Jakob et al. (1999) with an injection volume of 50 µL and a flow rate of 1.5 mL min^{-1}. Pigments were identified from absorbance spectra (400-800 nm) and retention times (Roy et al. 2011), and their concentrations were obtained from the signals in the photodiode array detector at 440 nm. The de-epoxidation state (DES in %) was calculated as [(Dtx / Ddx + Dtx) x 100], where Ddx is the epoxidized form and Dtx is the de-epoxidized form. Chl *a* concentration per cell was determined during exponential growth based on cell counts (see above) and the Chl *a* measurements.

Chl fluorescence yield and light curves (Table 2)

For a complete overview of the definition and measurement of the photophysiological parameters, see Table 2. Chl fluorescence yield was monitored with a Diving-PAM fluorometer (Walz, Effeltrich, Germany) on a 2.5 mL stirred and 20°C controlled diatom suspension (Lavaud et al. 2004). Before measurement, the cells were dark-adapted for 15 min, and a saturating pulse (3600 µmol photons m^{-2} s^{-1}, duration 0.4 ms) was fired to measure F_0, F_m and F_v/F_m. Two types of light curves were performed: Non Sequential and Rapid Light Curves (NSLCs and RLCs) (Perkins et al. 2010a). For NSLCs, continuous light (KL-2500 lamp, Schott, Mainz, Germany) was applied for 5 min at different Es (48-1950 µmol photons $m^{-2}s^{-1}$); a new diatom suspension was used for each E. At the end of each exposure, F_m' and NPQ were measured. For RLCs, one diatom suspension was exposed to 8 successive, incrementally increasing Es (29-1042 µmol photons m^{-2} s^{-1}) of 30 s each (Perkins et al. 2006) (Supplementary Table S1). RLCs allow constructing relative electron transport rate (rETR) vs. E and NPQ vs. E curves. The NPQ vs. E curve is based on the Hill equation model and it is described by the equation $NPQ(E) = NPQ_m \times [E^{nNPQ}/(E50_{NPQ}{}^{nNPQ} + E^{nNPQ'})]$ (Serôdio and Lavaud, 2011). From the fitted rETR-E curves (Eilers and Peeters, 1988) and NPQ-E curves (Serôdio and Lavaud, 2011), $rETR_m$, α, E_k, and NPQ_m, $E50_{NPQ}$, n_{NPQ} can be derived, respectively. All parameters are described in the Table 2. n_{NPQ} is the Hill coefficient or the sigmoidicity coefficient of the NPQ-E curve (Serôdio and Lavaud, 2011). It informs on the onset of NPQ at moderate Es, i.e. when the Dtx molecules are being 'activated' with increasing Es to effectively participate to NPQ: Dtx 'activation' depends on its enzymatic conversion and its binding to the PSII light-harvesting antenna complex in order to promote the antenna switch to a dissipative state of excess energy which is measurable by NPQ (see Lavaud and Lepetit, 2013). When n_{NPQ} is < 1, the NPQ-E curve shows an asymptotic saturation-like increase towards NPQ_m, while when n_{NPQ} is > 1, the NPQ-E curve shows a sigmoidal shape. In the latter case, the Hill reaction (i.e. NPQ onset) is allosteric (as proposed for the NPQ mechanism, see Lavaud and Lepetit, 2013), n_{NPQ} thus informing on the degree of allostery of the NPQ-E curve. The higher n_{NPQ}, the more positively cooperative the Hill reaction is; n_{NPQ} around 2 being the highest values reported so far (Serôdio and Lavaud, 2011). The same fitting procedure can obviously be used for the Dtx-E and the DES-E curves, thereby extracting analogous parameters as from the fitted NPQ E curves.

O2 yield and the PSII CET

The relative O2 yield produced during a sequence of single-turnover saturating flashes at a frequency of 2 Hz was measured with a home-made rate electrode (Lavaud et al. 2002). The steady-state O_2 yield per flash (YSS) was attained for the last 4 flashes of a sequence of 20 when the S-state cycle oscillations were fully damped (Lavaud et al. 2002). Y_{SS} of 15 min dark-adapted ($_D$) and illuminated ($_L$, samples taken at the end of each NSLC) cells was used to calculate the PSII CET (Lavaud et al. 2002; Lavaud et al. 2007) as follows:

$$[\{(20xY_{SS\,L})-(\Sigma\,(Y_{1\ldots20})_L)\} - \{(20xY_{SS\,D})-(\,\Sigma\,(Y_{1\ldots20})_D)\}] \,/\, Y_{SS\,D}.$$

Statistics

Statistical analyses were conducted using the statistical software package SAS 9.3 (Cary, NC, USA). Species were compared using the general linear model PROC GLM. Growth forms (groups) were compared using the mixed linear model PROC MIXED. Groups were regarded as fixed effects. Data were log transformed or square root transformed when needed to allow the best possible fit. Where necessary, estimated least squares means (lsmeans) and standard errors (SE) were back-transformed as in Jørgensen and Pedersen (1998).

Species	Growth form	Collection n°	Sampling location
Craspedostauros britannicus C.b.	Epipelon (EPL)	NCC195-06-2	Pouliguen, Atlantic, France
Entomoneis paludosa E.p.		NCC18-1	Bay of Bourgneuf, Atlantic, France
Halamphora coffeaeformis H.c.		UTCC58	Victoria, British Columbia, Pacific, Canada
Navicula phyllepta N.p.		CCY9804	Westerschelde estuary, North sea, The Netherlands
Seminavis robusta S.r.		DCG 0105	Progeny of strains from Veerse Meer, The Netherlands

Amphora sp. A. sp.	Epipsammon (EPM)	motile (EPM-M)	DCG 0493	Rammekenshoek, North sea, The Netherlands
Nitzschia cf. *frustulum* N.f.			DCG 0494	Rammekenshoek, North Sea, The Netherlands
Planothidium delicatulum P.d.			NCC363	Bay of Bourgneuf, Atlantic, France
Biremis lucens B.l.		non-motile (EPM-NM)	NCC360.2	Bay of Bourgneuf, Atlantic, France
Fragilaria cf. *subsalina* F.s.			DCG 0492	Rammekenshoek, North sea, The Netherlands
Opephora guenter-grassii O.g.			DCG 0448	Rammekenshoek, North Sea, The Netherlands
Plagiogramma staurophorum P.s.			DCG 0495	Rammekenshoek, North sea, The Netherlands
Brockmanniella brockmannii B.b.	Tychoplankton (TYCHO)		NCC161	Bay of Bourgneuf, Atlantic, France
Cylindrotheca closterium C.c.			Collection Univ. Aveiro	Ria de Aveiro, Atlantic, Portugal
Plagiogrammopsis vanheurckii P.v.			NCC186-2	Bay of Bourgneuf, Atlantic, France

Table 1: List of the fifteen diatom species used in this study with their growth form classification, collection number, origin and average biovolume. Abbreviations: NCC, Nantes Culture Collection-France ; UTCC, University of Toronto Culture Collection of Algae and Cyanobacteria-Canada (now the Canadian Phycological Culture Collection-CPCC); CCY, Culture Collection Yerseke-The Netherlands; DCG: BCCM (Belgian Coordinated Collections of Microorganisms) Diatom Culture Collection hosted by Laboratory for Protistology & Aquatic Ecology, Ghent University, Belgium ; n.d. not determined.

Parameter	Unit	Definition	Photophysiological meaning	Measurement conditions
F_0	No units	Minimum PSII Chl fluorescence yield	Used to calculate F_v/F_m (see below)	Measured with NSLCs after 15 min of dark acclimation
F_m	No units	Maximum PSII Chl fluorescence yield	Used to calculate F_v/F_m and NPQ (see below)	Measured with NSLCs during a saturating pulse after 15 min of dark acclimation
F_v/F_m	No units	Maximum photosynthetic efficiency of PSII; $F_v = F_m - F_0$	Maximum quantum efficiency of PSII photochemistry	See the above measurement conditions for F_0 and F_m
F_m'	No units	F_m for illuminated cells	Used to measure NPQ and rETR	Measured with NSLCs during a saturating pulse after 5 min of illumination at specific E
NPQ	No units	Non-photochemical quenching of Chl fluorescence; $NPQ = F_m / F_m' - 1$	Estimates the photoprotective dissipation of excess energy	Measured with NSLCs
rETR	µmol electrons m^{-2} s^{-1}	Relative electron transport rate of PSII; $rETR = \phi PSII \times E$ where $\phi PSII = F_m'-F/F_m'$	Effective quantum yield of photochemistry *vs*. E	Measured with RLCs; F is the steady-state of Chl fluorescence measured after 30 s illumination at a given E)
α	Relative units	rETR-E curve initial slope	Maximum light efficiency use	Derived from fitted rETR-E curves measured with RLCs (Eilers and Peeters, 1988)
$rETR_m$	µmol electrons m^{-2} s^{-1}	rETR-E curve asymptote	Maximum relative photosynthetic electron transport rate	Derived from fitted rETR-E curves measured with RLCs (Eilers and Peeters, 1988)
E_k	µmol photons. m^{-2}. s^{-1}	$E_k = rETR_m / \alpha$	Light saturation coefficient	Derived from fitted rETR-E curves measured with RLCs (Eilers and Peeters, 1988)
NPQ_m	No units	NPQ-E curve asymptote	Maximum NPQ	Measured with NSLCs
$E50_{NPQ}$	µmol photons. m^{-2}. s^{-1}	E for reaching 50% of NPQ_m	Pattern of NPQ induction *vs.* E	Derived from fitted NPQ-E curves (Serôdio and Lavaud, 2011) measured with NSLCs
n_{NPQ}	No units	NPQ-E curve sigmoidicity coefficient	Onset of NPQ induction for moderate Es (< $E50_{NPQ}$)	Derived from fitted NPQ-E curves (Serôdio and Lavaud, 2011) measured with NSLCs
Dtx_m	mol . 100 mol Chl a^{-1}	Dtx-E curve asymptote	Maximum Dtx concentration	Measured with NSLCs
$E50_{DT}$	µmol photons . m^{-2}. s^{-1}	E for reaching 50% of DT_{max}	Pattern of Dtx synthesis *vs.* E	Derived from fitted Dtx-E curves (Serôdio and Lavaud, 2011) measured with NSLCs
nDtx	No units	Dtx-E curve sigmoidicity coefficient	Onset of Dtx synthesis for moderate Es (< $E50_{NPQ}$)	Derived from fitted Dtx-E curves (Serôdio and Lavaud, 2011) measured with NSLCs
DES_m	%	DES-E curve asymptote; DES = [Dtx / (Ddx + Dtx) x 100]	Maximum de-epoxidation state	Measured with NSLCs
NPQ / Dtx	No units	NPQ-Dtx curve slope	Effective involvement of Dtx in NPQ for all Es (Lavaud et Lepetit, 2013)	Measured with NSLCs

Table 2: Photophysiological parameters used in this study, their photophysiological meaning and measurement method and conditions. Abbreviations: Chl, chlorophyll; Ddx, diadinoxanthin; Dtx, diatoxanthin; E, light intensity; NSLCs, Non-Sequential Light Curves; PSII, photosystem II; RLCs, Rapid Light Curves. See the Materials and Methods section for further details.

Results

Growth rate and photosynthetic properties

Growth Form		Pigments						Photosynthetic parameters				
	μ	Chl *a* cell^{-1}	Chl *c*	Fx	β-car	Ddx+Dtx	DES	F_v/F_m	α	$rETR_m$	E_k	PSII CET_m
EPL	1.66 ± 0.12	12.55 ± 12.91	18.91 ± 3.05	65.99 ± 7.90	3.91 ± 0.39	6.39 ± 0.61	0.75 ± 0.93	0.72 ± 0.01	0.68 ± 0.03	52.41 ± 5.90	78.93 ± 9.79	2.09 ± 0.23
EPM-M	1.56 ± 0.14	1.45 ± 0.78	16.05 ± 3.34	64.29 ± 10.21	2.76 ± 0.43	10.34 ± 1.17	4.25 ± 1.79	0.68 ± 0.02	0.65 ± 0.04	51.50 ± 7.36	80.41 ± 12.89	2.86 ± 0.33
EPM-NM	1.45 ± 0.12	2.13 ± 1.63	20.12 ± 3.63	70.52 ± 8.83	2.11 ± 0.43	11.52 ± 1.13	2.30 ± 1.33	0.67 ± 0.02	0.63 ± 0.04	39.20 ± 4.88	61.01 ± 8.52	2.82 ± 0.23
TYCHO	1.61 ± 0.14	1.72 ± 2.45	24.81 ± 5.17	79.36 ± 10.12	3.04 ± 0.51	9.25 ± 1.09	4.29 ± 1.83	0.73 ± 0.02	0.71 ± 0.04	58.32 ± 8.44	82.79 ± 13.40	2.03 ± 0.26

Table 3: Growth rate, pigment content and photosynthetic properties of the four growth forms of benthic diatoms. All parameters were measured on cells in exponential growth phase sampled 2 h after the onset of light. Growth conditions were 20 µmol photons m^{-2} s^{-1}, 16 h light:8 h dark, 20°C. Abbreviations: EPL, epipelon; EPM-M, motile epipsammon; EPM NM, non-motile epipsammon; TYCHO, tychoplankton. µ, growth rate (day^{-1}); pigments are expressed in mol 100 mol Chl a^{-1}: Chl, chlorophyll; Fx, fucoxanthin; β-car, β-carotene; Ddx, diadinoxanthin; Dtx, diatoxanthin. Definitions and conditions of measurement of all parameters are listed in Table 2. The values for the individual species can be found in Table S3. Values are least squares means estimates and estimated standard errors (PROC MIXED procedure).

The Chl *a* concentration per cell showed an exponential relationship with biovolume with relatively small changes at the smaller cell volumes (Supplementary Figure S1). The average diatom biovolumes were independent of growth form (Table 3, Supplementary Figure S1). Growth rate did not differ significantly between the growth forms at growth E = 20 µmol photons m^{-2} s^{-1} (Table 3, Supplementary Table S2). Relative concentrations of the light-harvesting pigments Chl *c* and Fucoxanthin were comparable among growth forms. β-carotene, which is mainly associated with the photosystem cores, was only slightly but significantly higher in epipelon than in non-motile epipsammon. Ddx + Dtx content was significantly lower in epipelon than in the other growth forms. Because the cells were grown

at low E, DES was generally low, with no significant differences between the growth forms (Table 3, Supplementary Table S3). The highest Ddx + Dtx (16.95 ± 2.56 mol 100 mol Chl a^{-1}) and DES (16.4 ± 6.2 %) values were observed in *Plagiogramma staurophorum* (non-motile epipsammon) (Table 3, Supplementary Table S2). There were no significant differences in F_v/F_m, α, $rETR_m$, E_k and PSII CET_{max} between the growth forms. E_k was on average 3 to 4 times the growth E in all growth forms. PSII CET_m was close to 3 (its maximum, Lavaud et al. 2002) for the two epipsammon growth forms, and about 2 in epipelon and tychoplankton (Table 3).

NPQ properties

At E values ≥ 230 µmol photons m^{-2} s^{-1}, NPQ was significantly higher in non-motile epipsammon than in both epipelon and tychoplankton; the same holds true for motile epipsammon vs. epipelon and tychoplankton at E values ≥ 1050 µmol photons m^{-2} s^{-1} (Figure 1, Supplementary Table S4). NPQ was also significantly higher in non-motile epipsammon than in motile epipsammon except at the lowest and highest E values. Likewise, NPQ_m was significantly higher (x 3.5 and x 2.4, respectively) in non-motile epipsammon and motile epipsammon than in epipelon and tychoplankton (Figure 1, Table 4 and Supplementary Tables S5 and S6). In epipelon and tychoplankton, the NPQ-E curves showed a lower variability than in the two epipsammon growth forms (Supplementary Figure S2). Non-motile epipsammon had the lowest $E50_{NPQ}$, significantly lower than all other groups (Table 4, Supplementary Tables S5 and S6). In contrast, tychoplankton $E50_{NPQ}$ was significantly higher than in the other groups. Epipelic and motile epipsammic $E50_{NPQ}$ did not differ significantly from each other. In contrast, n_{NPQ} was not significantly different and varied around its optimum (i.e. 2, Serôdio and Lavaud, 2011) in most species except the tychoplanktonic ones (which is significantly lower than in epipsammon non-motile) (Table 4, Supplementary Tables S5 and S6).

Growth form	NPQ_m	$E50_{NPQ}$	n_{NPQ}	DES_m	Dtx_m	$E50_{Dtx}$	n_{Dtx}	NPQ/Dtx
EPL	0.69 ± 0.09	866.45 ± 200.24	1.88 ± 0.26	21.20 ± 3.38	1.34 ± 0.52	714.73 ± 128.29	2.39 ± 0.20	0.46 ± 0.10
EPM-M	1.71 ± 0.28	1061.25 ± 310.20	2.04 ± 0.34	28.68 ± 4.37	3.08 ± 1.36	809.41 ± 164.71	1.38 ± 0.20	0.52 ± 0.14
EPM-NM	2.41 ± 0.34	360.61 ± 91.42	2.27 ± 0.29	29.43 ± 3.79	3.45 ± 2.21	465.91 ± 80.04	2.30 ± 0.21	0.67 ± 0.16
TYCHO	0.66 ± 0.11	3887.42 1105.58	1.12 ± 0.34	22.73 ± 4.39	1.78 ± 0.61	1099.82 ± 341.05	1.42 ± 0.19	0.36 ± 0.10

Table 4: Non-photochemical quenching (NPQ) and xanthophyll cycle (XC) properties of the four growth forms of benthic diatoms. Abbreviations: EPL, epipelon; EPM-M, motile epipsammon; EPM-NM, non-motile epipsammon; TYCHO, tychoplankton. Definitions and conditions of measurement of all parameters are listed in Table 2. The values for the individual species can be found in Tables S4. Values are least squares means estimates and estimated standard errors (PROC MIXED procedure).

XC properties

DES was only significantly different between epipelon and both tychoplankton and motile epipsammon at 105 µmol photons $m^{-2}s^{-1}$ and between epipelon and both epipsammic forms at 230 µmol photons m^{-2} s^{-1} (Figure 1, Supplementary Table S7). DES_m varied between 21.2 ± 3.4 for epipelon, 22.7 ± 4.4 for tychoplankton, 28.7 ± 4.4 for motile epipsammon-M and 29.4 ± 3.8 for non-motile epipsammon (lsmeans ± SE) (Figure 1, Table 4 and Supplementary Tables S5 and S6). The slight difference between epipelon and the epipsammon growth forms, although not significant, in combination with the significantly higher Ddx + Dtx in the latter, generated a significantly lower Dtx_m in epipelon than in the epipsammon growth forms (Tables 3 and 4). $E50_{Dtx}$ was close to the $E50_{NPQ}$ in all growth forms except in tychoplankton where it was lower; no significant differences between the epipsammon and epipelon were observed, only non-motile epipsammon and tychoplankton $E50_{Dtx}$ differed significantly (Table 4, Supplementary Tables S5 and S6). n_{Dtx} was significantly lower in motile epipsammon and tychoplankton than in epipelon and non-motile epipsammon. NPQ/Dtx

was about half its optimum (= 1 under these experimental conditions) in all groups except non-motile epipsammon (Table 4, Supplementary Tables S5 and S6). It roughly followed the same order as observed for NPQ_m, i.e. non-motile epipsammon > motile epipsammon > epipelon ≅ tychoplankton, with a 2x higher value in non-motile epipsammon (Table 4). The difference between non-motile epipsammon and the other growth forms, however, was not significant due to the low NPQ/Dtx value in *Plagiogramma staurophorum* (Supplementary Table S5). Figure 2 shows that in all growth forms except motile epipsammon there were species (*Seminavis robusta*, *Fragilaria.* cf. *subsalina*, *P. staurophorum*, *Brockmanniella brockmannii*) for which a low NPQ developed without Dtx synthesis, while two motile epipsammon species (*Amphora* sp. and *Planothidium delicatulum*) showed Dtx synthesis (0.17 ± 0.03 mol 100 mol Chl a^{-1}) without NPQ (See also supplementary Table S5). All other species showed a NPQ/Dtx relationship with an origin close to 0, as expected.

Effect of high light acclimation on the NPQ and XC properties

All species were grown under an E (75 µmol photons m^{-2} s^{-1}) roughly corresponding to the mean E_k for the low E acclimated cells (20 µmol photons m^{-2} s^{-1}, Table 3); (Figure 3, Supplementary Table S8). Only epipelon had significantly higher growth rates at 75 µmol photons m^{-2} s^{-1}. Ddx + Dtx significantly increased with a factor 1.6-1.7 in epipelon and epipsammon, and 2.3 in tychoplankton. There was a significant increase in DES at 75 µmol photons $m^{-2}s^{-1}$ in all growth forms except in motile epipsammon. The increase in Ddx +Dtx and DES at the higher light intensity was most pronounced in tychoplankton and resulted in a pronounced, significant difference in both parameters between tychoplankton and epipelon at this light intensity. The comparison of Chl fluorescence yield and light curve parameters could only be performed for a selection of six species (covering all growth forms) and is summarized in Figure 4 (See also Supplementary Table S9). As expected, the Chl *a* content per cell decreased, roughly with a factor of 2 in all species (except *Navicula phyllepta*). There was only a slight (up to about 10 %) decrease in F_v/F_m in all species, illustrating the unstressed state of the cells (note that in *Seminavis robusta* and *Planothidium delicatulum* this decrease was slightly significant). DES_m significantly increased in *S. robusta* only. Together with the overall increase in Ddx + Dtx, this resulted in a significant increase in Dtx_m (by a factor of 4) in this species, but also in *P. delicatulum* and *Plagiogrammopsis vanheurckii*. The corresponding NPQ_m did not follow the same trend: it significantly increased in all species (except for *P. delicatulum* and *Opephora* sp.) but only by a factor of maximally 2. NPQ/Dtx remained low (0.2 to 0.5) in all species (and significantly decreased in *Opephora* sp.). $E50_{NPQ}$ was significantly higher only in the non-motile epipsammic species *Plagiogramma staurophorum*.

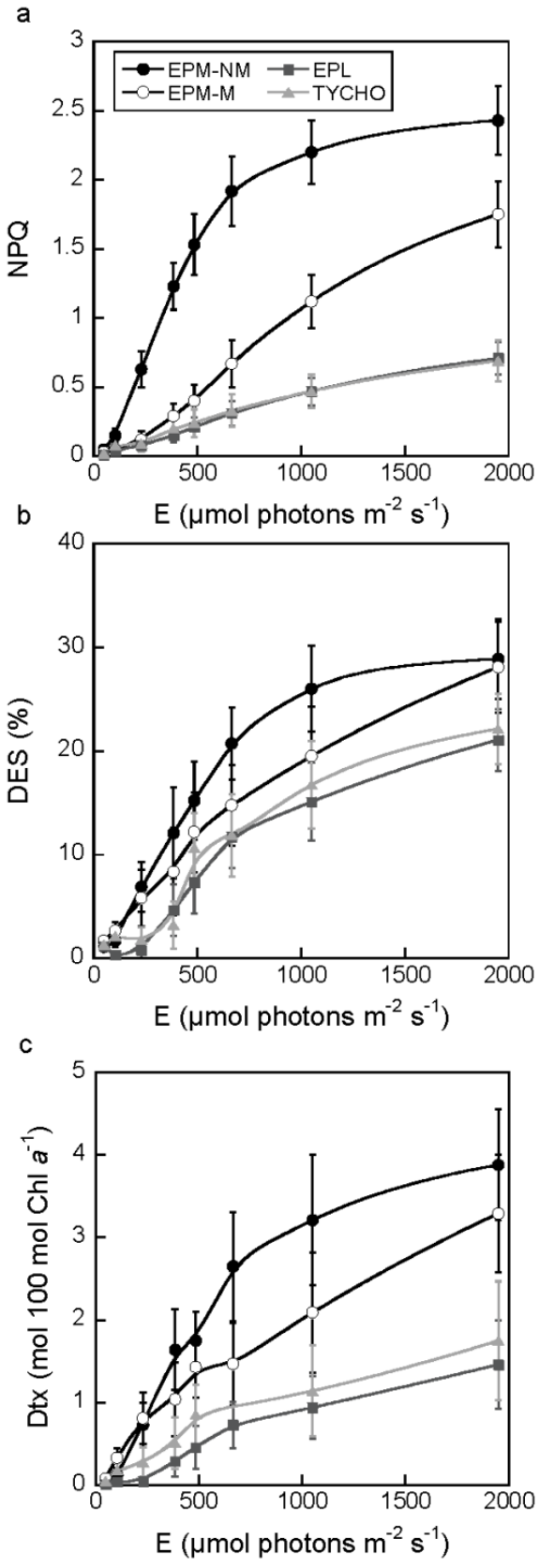

Figure 1. Non-photochemical quenching of Chl fluorescence (NPQ) (a), de-epoxidation state of the diadinoxanthin (Ddx) to diatoxanthin (Dtx) [DES = Dtx / (Ddx + Dtx) x 100] (b), and Dtx content (c) as a function of light intensity (E from darkness to 1950 µmol photons m^{-2} s^{-1} which is equivalent to full sunlight in the field) measured during Non-Sequential Light Curves (NSLCs) in the four benthic diatom growth forms (EPM-NM, epipsammon non-motile, EPM-M, epipsammon motile; EPL, epipelon; TYCHO, thychoplankton). Cells were grown at 20 µmol photons m^{-2} s^{-1}. The NPQ-E curves for the individual species can be found in Supplementary Figure S3. Values are estimated least squares means ± estimated standard errors (PROC MIXED procedure).

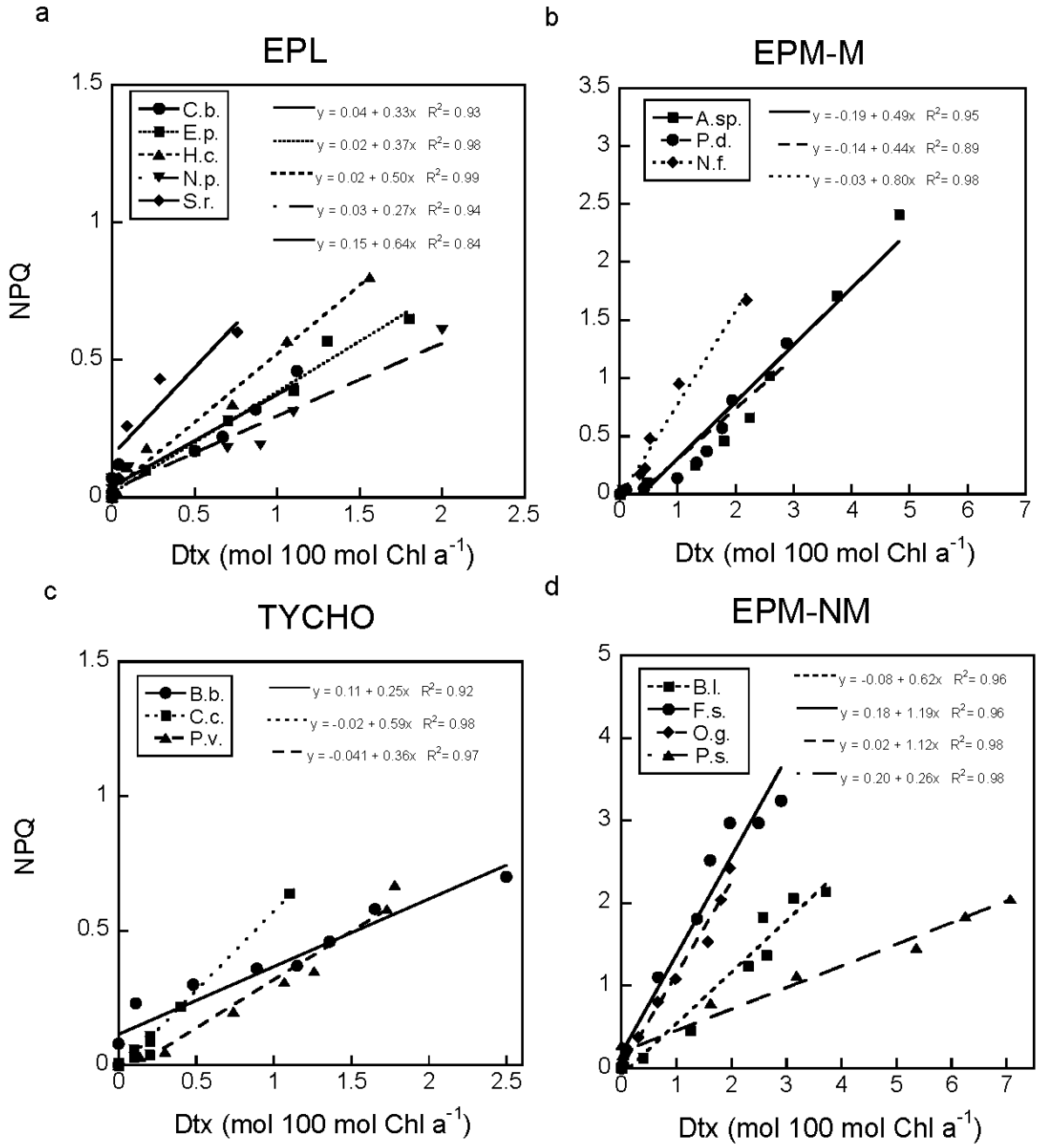

Figure 2. Non-photochemical quenching of Chl fluorescence (NPQ) as a function of the amount of diatoxanthin (Dtx) measured during Non-Sequential Light Curves (NSLCs) in the five species of epipelon (EPL) (a), the four species of motile epipsammon (EPM-M) (b), the three species of tychoplankton (TYCHO) (c), and the three species of non-motile epipsammon (EPM-NM) (d). Cells were grown at 20 µmol photons m^{-2} s^{-1}. The full names and classification of all species is listed in Table 1.

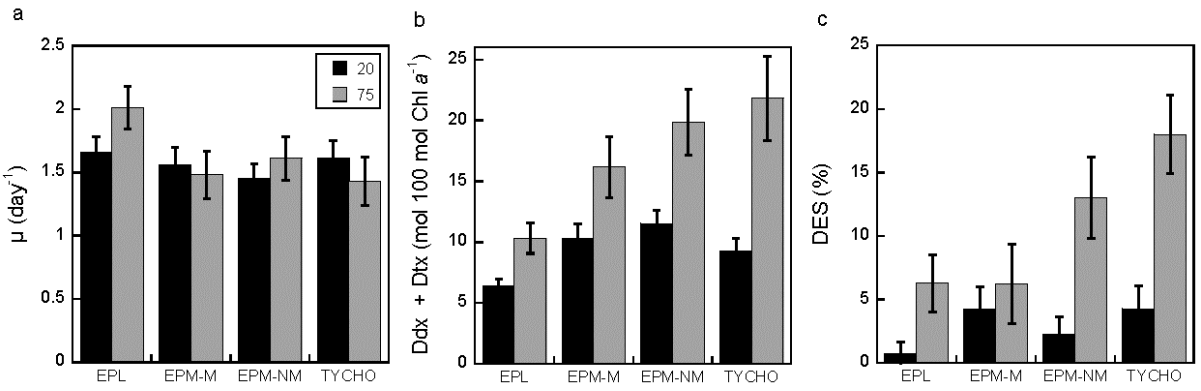

Figure 3. Growth rate (μ) (a), diadinoxanthin (Ddx) + diatoxanthin (Dtx) content (b) and de-epoxidation state of Ddx to Dtx [DES = (Dtx / Ddx + Dtx x 100] (c) in the four benthic diatom growth forms (EPM-NM, epipsammon non-motile, EPM-M, epipsammon motile; EPL, epipelon motile; TYCHO, thychoplankton) for cells grown at light intensities of 20 and 75 μmol photons m^{-2} s^{-1} respectively. All parameters were measured on cells in exponential growth and sampled 2 h after the onset of light; growth conditions were 16 h light:8 h dark, 20°C. The values for all species in 20 and 75 μmol photons m^{-2} s^{-1} conditions are found in Supplementary Tables S3 and S8, respectively. Values are estimated least squares means ± estimated standard errors (PROC MIXED procedure).

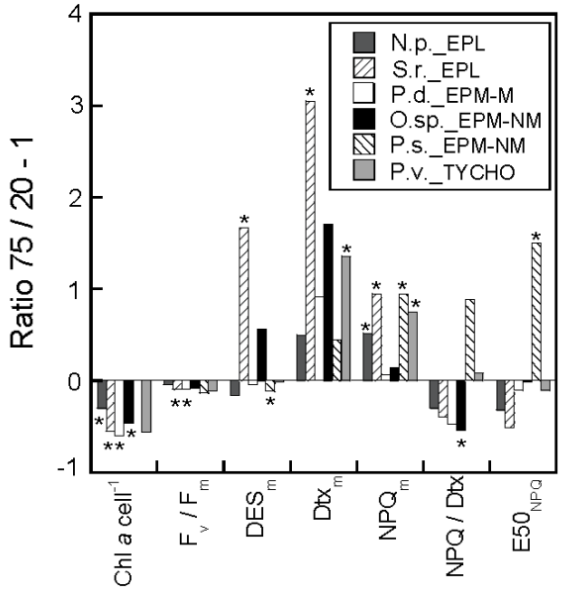

Figure 4. Comparison of photosynthetic, non-photochemical quenching of Chl fluorescence (NPQ) and xanthophyll cycle (XC) parameters measured in diatom species representative of the four benthic diatom growth forms grown at light intensities of 20 and 75 μmol photons m^{-2} s^{-1} respectively. For each parameter the ratio of the values obtained at 75 and 20 μmol photons m^{-2} s^{-1} – 1 was calculated (i.e. the 0 line is equal to a 75/20 ratio = 1 which is equivalent to no change of values between light intensities). Significant changes between both light intensities are indicated with an asterisk. The values used for the 20 and the 75 μmol photons m^{-2} s^{-1} conditions can be found in Supplementary Tables S3 and S8 respectively.

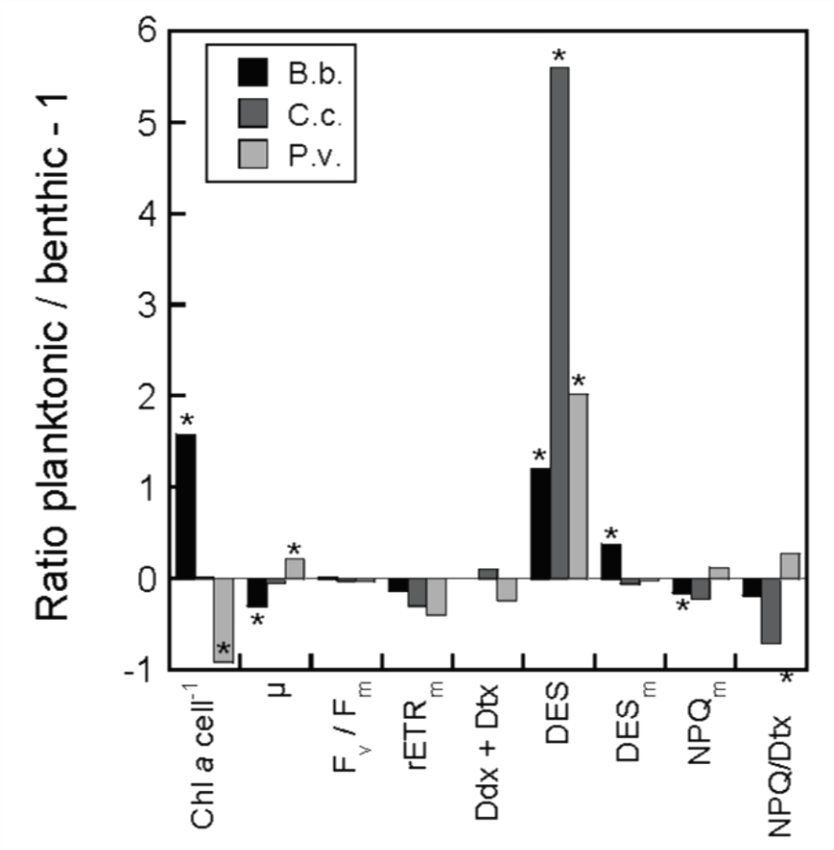

Figure 5. Comparison of growth, photosynthetic, pigment, non-photochemical quenching of Chl fluorescence (NPQ) and xanthophyll cycle (XC) parameters measured in the three tychoplankton diatom species in 'benthic' and 'planktonic' conditions. For each parameter the ratio of the values obtained under benthic and planktonic conditions – 1 was calculated (i.e. the 0 line is equal to a planktonic/benthic ratio = 1 which is equivalent to no change of values between 'benthic' and 'planktonic' conditions). Chl *a* per cell (in pg cell^{-1}) and growth rates (in day^{-1}) were measured on cells in exponential growth phase sampled 2 h after the onset of light; growth conditions were 20 µmol photons m^{-2} s^{-1}, 16 h light:8 h dark, 20°C. Significant changes between both light intensities are indicated with an asterisk. The values used for the 'benthic' and 'planktonic' growth conditions can be found in Supplementary Tables S3/S5 and S10, respectively.

Effect of 'planktonic' growth on the NPQ and XC properties of tychoplankton

The three tychoplanktonic species were grown under 'planktonic' conditions (at 20 µmol photons m^{-2} s^{-1}) for a comparison with growth under 'benthic' conditions (Figure 5, Supplementary Table s10). *Brockmaniella brockmannii* responded most strongly to a switch from 'benthic' to 'planktonic' growth: it showed a significantly lower growth rate and a higher DES and DES_m but a lower NPQ_m, suggesting photosynthetic stress and investment of additional Dtx in other processes than NPQ. *Plagiogrammopsis vanheurckii* and *Cylindrotheca closterium* showed very little change, apart from a significantly higher growth rate during planktonic growth in *P. vanheurckii*, a slight decrease in NPQ/Dtx in *C. closterium*, and an increase in DES in both species. The most pronounced and consistent change in tychoplankton thus concerned an increase in DES when grown in suspension. Note that there is also an overall decrease in $rETR_m$, but this decrease was just not significant (p=0.08).

Discussion

The present work constitutes the first comparative experimental study, using unialgal cultures in standardized conditions, of fast regulatory photoprotective mechanisms in the four main benthic diatom growth forms present in intertidal marine sediments (epipelon, motile and non-motile epipsammon and tychoplankton). Because no sediment was added in our experiments, motile diatoms were not able to position themselves in a light gradient, hence effectively incapacitating their behavioural response. As the growth rate and photosynthetic characteristics (main pigments, F_v/F_m, α, E_k, $rETR_m$) of the studied species were comparable between the growth forms at 20 µmol photons m^{-2} s^{-1}, we were able to compare their purely physiological light response.

Our study revealed a highly significant and pronounced difference in NPQ between the four growth forms. NPQ was significantly lower in epipelic and tychoplanktonic than in epipsammic species; differences in DES were only observed between epipelic and other forms at lower light intensities. Within the epipsammon, NPQ capacity was significantly higher in the non-motile than in the motile forms. As all growth forms included both small and large species, the functional light response (NPQ capacity) apparently did not depend on biovolume or the Chl *a* concentration per cell, as has also been observed in situ (Jesus et al. 2009). The absence of significant differences in PSII CET between growth forms underscores the importance of NPQ as the main fast photoprotective process in intertidal benthic diatoms, confirming earlier results for these organisms (Lavaud et al. 2002) but in contrast with planktonic diatoms (Lavaud e et al. 2002; Lavaud et al. 2007). By analogy with previous studies on planktonic diatoms (Dimier et al. 2009; Lavaud et al. 2007; Lavaud and

Lepetit, 2013; Petrou et al. 2011; Strzepek and Harrison, 2004), our data suggest that epipelic and tychoplanktonic diatoms are adapted to a less fluctuating light climate and/or to a lower average irradiance, and vice versa for epipsammic diatoms. This result fits well with the ecology of these growth forms. Large motile diatoms are not only more abundant in muddy cohesive sediments where light penetration is more restricted than in sandy sediments (Paterson and Hagerthey 2001; Cartaxana et al. 2011), but, more importantly, their (micro-)migratory behaviour allows positioning at the optimal irradiance in the vertical light gradient and rapid escape from periodic excess light (Kromkamp et al. 1998; Conn et al. 2004; Consalvey et al. 2004; Serôdio et al. 2006). This alleviates the need to invest in a strong physiological capacity to respond to light stress as previously proposed (Jesus et al. 2009; Cartaxana et al. 2011), although the right balance between motility and physiology still remains essential (van Leeuwe et al. 2009; Perkins et al. 2010b; Cartaxana et al. 2011; Serôdio et al. 2012). Such balance is more crucial in the motile epipsammic species, which can move but have only limited control over their immediate light environment as movement is restricted, usually within the sphere of individual sand grains. As expected, they showed a significantly lower NPQ and a higher $E50_{NPQ}$ than non-motile epipsammon, which have no behavioural control over their light environment. An alternative, but not exclusive, explanation could be related to the difference in exopolysaccharide (EPS) secretion between motile and non-motile growth forms. EPS secretion could work as an alternative electron sink under stressful conditions (i.e. high light, nutrient limitation, etc.) in order to limit the over-reduction of the photosynthetic machinery ('overflow' hypothesis; Staats et al. 2000), alleviating the need for a strong NPQ. However, EPS secretion is not as fast as NPQ (minutes/hours vs. seconds/minutes) and may not be useful to the cells for responding to rapid light changes but only to cope with prolonged high light exposure. Additionally, while the 'overflow' hypothesis is often proposed (Underwood and Paterson, 2003; Stal, 2009), it was never clearly proven. A few studies have shown a positive relationship between light intensity and EPS production (Underwood, 2002; Wolfstein and Stal, 2002) but other studies have reported a negative relation with light intensity and no relationship with nutrient limitation (Hanlon et al. 2001; Perkins et al. 2006). To date there is no information on EPS production in different benthic diatom growth forms, and only epipelic species have been compared (Underwood and Paterson, 2003), showing no clear relationship between light response and EPS secretion. To our knowledge, there are no reports on a relationship between NPQ-XC capacity and EPS production. Finally, tychoplankton typically alternates between resuspension in a highly turbid shallow water column at high tide and deposition and burial in the upper sediment layers of muddy sediments at low tide (deposition in sandy sediments does not occur due to the intense hydrodynamic disturbance in these sediments). As such, the tychoplankton resembles planktonic diatoms adapted to subtle light fluctuations and/or on average low irradiance

(Bailleul et al. 2010; Lavaud and Lepetit, 2013). The reason for the NPQ differences between epipelon and epipsammon can be explained by its main control: the XC dynamics. Previous in situ studies reported a consistently stronger DES under light stress in epipsammic than in epipelic diatom communities (that is, in sandy vs. muddy sediments) and related growth form with differential (behavioural vs. physiological) photoregulatory strategies (Jesus et al. 2009; Cartaxana et al. 2011). As recently shown, high NPQ is supported by the strong effective involvement of Dtx which first depends both on a high Ddx + Dtx content and a high DES (Lavaud and Lepetit, 2013). The slope of the NPQ/Dtx relationship has been proposed as a good indicator of light climate adaptation: the higher the NPQ/Dtx slope, the better the adaptation to a highly fluctuating and/or on average high light climate (Dimier et al. 2009; Lavaud and Lepetit, 2013). All epipsammic species, and especially the non-motile ones, showed XC parameter values which are characteristic for a high NPQ capacity, viz. a higher Ddx + Dtx content and Dtx_m which was 2x higher than in epipelon. Non-motile epipsammon also tended to show a higher efficiency in promoting NPQ (NPQ/Dtx), but this difference was not significant due to high intra-group variability.

Within the epipsammon, NPQ is clearly more efficient in non-motile than in motile epipsammic species. In motile epipsammon, the discrepancy between $E50_{NPQ}$ and E_k is more pronounced than in non-motile forms: while there is no significant difference in E_k between both growth forms, $E50_{NPQ}$ is significantly higher in the motile growth forms. This suggests a weaker relationship between NPQ development and photochemistry in the latter group, with slower NPQ development with increasing E. Remarkably, $E50_{Dtx}$ does not significantly differ between both growth forms, and the significantly higher initial induction of Dtx synthesis (n_{Dtx}) but not NPQ (n_{NPQ}) in the motile group, together with the fact that some representatives of this group show Dtx synthesis without NPQ, suggests that either Dtx is less or not involved in NPQ development, or that the light-dependent built-up of the transthylakoidal proton gradient (which is involved in both the activation of the Ddx de-epoxidase and the molecular control of NPQ) and the onset of NPQ are uncoupled (Lavaud et al. 2012; Lavaud and Lepetit, 2013). Our observations thus suggest that in contrast to the non-motile group, motile epipsammic species rely more on a behavioural response (motility) and/or involve Dtx in other photoprotective processes such as the prevention of lipid peroxidation by reactive oxygen species (ROS) (Lepetit et al. 2010). The increase in $E50_{NPQ}$ in the non-motile epipsammic species *Plagiogramma staurophorum* during a shift to higher light illustrates the ability to physiologically modulate the NPQ vs. E development kinetics to its light environment in contrast to motile epipsammon, epipelon and tychoplankton.

The influence of Dtx on the inter-group/species NPQ differences was further investigated by the acclimation to higher light (75 µmol photons m^{-2} s^{-1}, close to the mean E_k for cells acclimated to 20 µmol photons m^{-2} s^{-1}). High light exposure is known to induce constitutive Dtx synthesis (Schumann et al. 2007) and in field conditions, Dtx is usually even present in significant amounts in cells adapted to low/moderate light (Jesus et al. 2009; van Leeuwe et al. 2009; Chevalier et al. 2010; Cartaxana 423 et al. 2011). Acclimation to higher light resulted in a significant increase in XC pigments (Ddx + Dtx) and DES in most growth forms, suggesting that although epipelon uses behavioural photoprotection, the XC is still important (cf. above). NPQ_m increased in most of the species examined, mainly due to a higher Dtx_m resulting from a higher Ddx + Dtx rather than a higher DES_m. The discrepancy between DES_m and NPQ_m as well as the low NPQ/Dtx may be due to the fact that the additional Dtx primarily served in the prevention of lipid peroxidation rather than in NPQ as previously reported in high light acclimated diatoms (see also above).

While under low light conditions, the growth, photosynthetic and steady-state light-response features of tychoplankton were similar to those of epipelic diatoms (i.e. low NPQ, NPQ_m and Dtx_m), their dynamic light response was significantly different, i.e. higher $E50_{NPQ}$. Surprisingly, $E50_{NPQ}$ was beyond the natural light maximum (2000-2500 µmol photons m^{-2} s^{-1}) illustrating the inability of tychoplankton to strongly and/or continuously develop NPQ in the environmental high light range (a situation also encountered in one epipelic species: *Navicula phyllepta*). In contrast, its low n_{NPQ} supported a relatively strong onset of NPQ at low Es. Both $E50_{Dtx}$ and nDtx were correspondingly high and low, respectively (and significantly different from epipelon for n_{Dtx}), although $E50_{Dtx}$ was much lower than $E50_{NPQ}$ suggesting a discrepancy between Dtx synthesis and NPQ development (cf. above). The response of tychoplankton to higher light was much more pronounced, with the strongest increase in XC pigments and DES of all growth forms (Fig. 3). However, the NPQ_m and Dtx_m data (only available however for one representative species, *Plagiogrammopsis vanheurckii*) did not show a similar response, with Dtx_m showing a more pronounced increase than NPQ_m, suggesting that NPQ development was low and that Dtx may have mainly been involved in other processes than NPQ. For most parameters, the response of the tychoplankton species to growth in suspension ('planktonic' growth) was limited and largely species-specific, except for a general increase in DES and a decrease (albeit just non-significant) in $rETR_m$. These data suggest that representatives of the tychoplanktonic growth form are well-adapted to their amphibious life style, which is characterized by an on average low irradiance (MacIntyre et al. 1996). In contrast, epipelic species do not grow well in suspended, turbulent conditions (J. Lavaud, pers. observation).

Our study for the first time shows that intertidal benthic diatoms display growth form specific variation in fast regulatory physiological mechanisms for photoprotective capacity (NPQ and the XC), which mirrors their behavioural light response. In epipelic motile diatoms, exclusively belonging to the raphid pennate clade, the physiological response is not well developed, as these diatoms appear to largely rely on motility to control their immediate light environment. In the motile epipsammon however the physiological response remains essential because their movement is restricted to the sphere of individual sand grains. The evolution of the raphe system, the hallmark synapomorphy of the raphid pennate diatom clade which enables locomotion, has therefore been essential for the colonization of intertidal sediments by not only migratory epipelic biofilms but also motile epipsammon. In contrast, NPQ and XC capacity is high in non-motile araphid pennate diatoms which passively have to abide often pronounced variations in the intertidal light climate. Tychoplanktonic diatoms, which alternate between high tide resuspension in a turbulent and turbid water column, and low tide deposition in muddy sediments, appear to be adapted to an on average low light environment, with low NPQ and XC capacity.

Although we made no formal analysis of the relationship between functional and phylogenetic diversity, it is obvious that despite the fact that a behavioural photoprotective response (motility) is restricted to the raphid pennate diatom clade, differences in the studied physiological traits are more strongly driven by growth form than phylogenetic relatedness. For example, the epipsammic species *Biremis lucens*, despite being a raphid pennate species, has a non-motile growth form, and shows a NPQ capacity which is more similar to non-motile epipsammon than to the (phylogenetically more closely related) motile epipsammon and epipelon. Likewise, photophysiological features of pennate raphid (*Cylindrotheca closterium*) and centric (*Plagiogrammopsis vanheurckii* and *Brockmanniella brockmannii*) tychoplankton

species were similar as reported before in planktonic centric/pennate species (Lavaud et al. 2004). Raphid pennate diatoms which have colonized an epipsammic or tychoplanktonic niche thus display a reverse evolutionary trade-off switch towards a much more performant physiological response. Our observations thus suggest that photoprotective capacity in diatoms is a highly adaptive trait which is to a certain degree constrained by clade-specific evolutionary innovations (the evolution of the raphe system and hence a behavioural response) but also, and more importantly, by growth form, which ultimately defines the balance between the physiological and behavioural photoprotective response in these organisms. Such differential adaptation is of primary importance for the regulation of the photosynthetic productivity vs. light, as has been demonstrated before in planktonic diatoms, where the photochemical vs. the photoprotective energy allocation as a function of light is drastically different in species adapted to a fluctuating vs. a more stable light environment (Wagner et al. 2006; Lavaud et al. 2007; Petrou et al. 2011; Lavaud and

Lepetit, 2013). However, unlike in planktonic environments, the trade-off between a physiological and behavioural response in benthic diatoms allows local co-existence of different growth forms under the same overall light environment.

Acknowledgements

The authors acknowledge the Centre National de la Recherche Scientifique-CNRS, the University of La Rochelle-ULR, the Contrat Plant Etat Région-CPER 'Littoral', the Region Poitou-Charentes, the Deutscher Akademischer Austausch Dienst-DAAD, the Research Foundation Flanders (FWO project G.0222.09N), Ghent University (BOF-GOA 01G01911) and the Egide/Campus France-PHC Tournesol (n°28992UA) exchange program for their financial support.

References

Admiraal, W. 1984. The ecology of estuarine sediment-inhabiting diatoms. Prog. Phycol. Res. **3**: 269–322.

Armbrust, E. V. 2009. The life of diatoms in the world's oceans. Nature **459**: 185–92. doi:10.1038/nature08057

Bailleul, B., A. Rogato, A. De Martino, S. Coesel, P. Cardol, C. Bowler, A. Falciatore, and G. Finazzi. 2010. An atypical member of the light-harvesting complex stress-related protein family modulates diatom responses to light. Proc. Natl. Acad. Sci. **107**: 18214–18219. doi:10.1073/pnas.1007703107

Barton, A. D., A. J. Pershing, E. Litchman, N. R. Record, K. F. Edwards, Z. V. Finkel, T. Kiørboe, and B. A. Ward. 2013. The biogeography of marine plankton traits J. Elser [ed.]. Ecol. Lett. **16**: 522–534. doi:10.1111/ele.12063

Brunet, C., and J. Lavaud. 2010. Can the xanthophyll cycle help extract the essence of the microalgal functional response to a variable light environment? J. Plankton Res. **32**: 1609–1617. doi:10.1093/plankt/fbq104

Cartaxana, P., M. Ruivo, C. Hubas, I. Davidson, J. Serôdio, and B. Jesus. 2011. Physiological versus behavioral photoprotection in intertidal epipelic and epipsammic benthic diatom communities. J. Exp. Mar. Bio. Ecol. **405**: 120–127. doi:10.1016/j.jembe.2011.05.027

Chevalier, E. M., F. Gévaert, and A. Créach. 2010. In situ photosynthetic activity and xanthophylls cycle development of undisturbed microphytobenthos in an intertidal mudflat. J. Exp. Mar. Bio. Ecol. **385**: 44–49. doi:10.1016/j.jembe.2010.02.002

Coelho, H., S. Vieira, and J. Serôdio. 2011. Endogenous versus environmental control of vertical migration by intertidal benthic microalgae. Eur. J. Phycol. **46**: 271–281. doi:10.1080/09670262.2011.598242

Conn, S. A., M. Bahena, J. T. Davis, R. L. Ragland, C. D. Rauschenberg, and B. J. Smith. 2004. Characterisation of the diatom photophobic response to high irradiance. Diatom Res. **19**: 167–179. doi:10.1080/0269249X.2004.9705869

Consalvey, M., D. M. Paterson, and G. J. C. Underwood. 2004. The ups and downs of life in a benthic biofilm: Migration of benthic diatoms. Diatom Res. **19**: 181–202.

Depauw, F. A., A. Rogato, M. Ribera d'Alcalá, and A. Falciatore. 2012. Exploring the molecular basis of responses to light in marine diatoms. J. Exp. Bot. **63**: 1575–91. doi:10.1093/jxb/ers005

Dimier, C., F. Corato, F. Tramontano, and C. Brunet. 2007. Photoprotection and xanthophyll cycle activity in three marine diatoms. J. Phycol. **43**: 937–947. doi:10.1111/j.1529-8817.2007.00381.x

Dimier, C., S. Giovanni, T. Ferdinando, and C. Brunet. 2009. Comparative ecophysiology of the xanthophyll cycle in six marine phytoplanktonic species. Protist **160**: 397–411. doi:10.1016/j.protis.2009.03.001

Edwards, K. F., E. Litchman, and C. A. Klausmeier. 2013. Functional traits explain phytoplankton

community structure and seasonal dynamics in a marine ecosystem J. Elser [ed.]. Ecol. Lett. **16**: 56–63. doi:10.1111/ele.12012

Eilers, P. H. C., and J. C. H. Peeters. 1988. A model for the relationship between light intensity and the rate of photosynthesis in phytoplankton. Ecol. Modell. **42**: 199–215. doi:10.1016/0304-3800(88)90057-9

Goss, R., and T. Jakob. 2010. Regulation and function of xanthophyll cycle-dependent photoprotection in algae. Photosynth. Res. **106**: 103–122. doi:10.1007/s11120-010-9536-x

Gottschalk, S., and M. Kahlert. 2012. Shifts in taxonomical and guild composition of littoral diatom assemblages along environmental gradients. Hydrobiologia **694**: 41–56. doi:10.1007/s10750-012-1128-7

Hamels, I., K. Sabbe, K. Muylaert, C. Barranguet, C. Lucas, P. Herman, and W. Vyverman. 1998. Organisation of microbenthic communities in intertidal estuarine flats, a case study from the molenplaat (Westerschelde estuary, The Netherlands). Eur. J. Protistol. **34**: 308–320. doi:10.1016/S0932-4739(98)80058-8

Hanlon, A. R. M., B. Bellinger, K. Haynes, and others. 2006. Dynamics of extracellular polymeric substance (EPS) production and loss in an estuarine, diatom-dominated, microalgal biofilm over a tidal emersion-immersion period. Limnol. Oceanogr. **51**: 79–93. doi:10.4319/lo.2006.51.1.0079

Haubois, A. G., F. Sylvestre, J. M. Guarini, P. Richard, and G. F. Blanchard. 2005. Spatio-temporal structure of the epipelic diatom assemblage from an intertidal mudflat in Marennes-Oléron Bay, France. Estuar. Coast. Shelf Sci. **64**: 385–394. doi:10.1016/j.ecss.2005.03.004

Herlory, O., J. M. Guarini, P. Richard, and G. F. Blanchard. 2004. Microstructure of microphytobenthic biofilm and its spatio-temporal dynamics in an intertidal mudflat (Aiguillon Bay, France). Mar. Ecol. Prog. Ser. **282**: 33–44. doi:10.3354/meps282033

Hillebrand, H., C.-D. Dürselen, D. Kirschtel, U. Pollingher, and T. Zohary. 1999. Biovolume calculation for pelagic and benthic microalgae. J. Phycol. **35**: 403–424. doi:10.1046/j.1529-8817.1999.3520403.x

Huisman, J., A. M. Johansson, E. O. Folmer, and F. J. Weissing. 2001. Towards a solution of the plankton paradox: The importance of physiology and life history. Ecol. Lett. **4**: 408–411. doi:10.1046/j.1461-0248.2001.00256.x

Jakob, T., R. Goss, and C. Wilhelm. 1999. Activation of diadinoxanthin de-epoxidase due to a chlororespiratory proton gradient in the dark in the diatom *Phaeodactylum tricornutum*. Plant Biol. **1**: 76–82. doi:10.1111/j.1438-8677.1999.tb00711.x

Jeffrey, S. W., and G. S. Humphrey. 1975. New spectrophotometric equations for determining chlorophylls *a*, *b*, *c*1 and *c*2 in higher plants, algae and natural phytoplankton. Biochem. Physiol. Pflanz. Bd **167**: 191–194.

Jesus, B., V. Brotas, L. Ribeiro, C. R. Mendes, P. Cartaxana, and D. M. Paterson. 2009. Adaptations of microphytobenthos assemblages to sediment type and tidal position. Cont. Shelf Res. **29**: 1624–1634. doi:10.1016/j.csr.2009.05.006

Jørgensen, E., and Pedersen, A. R. 1997. How to obtain those nasty standard errors from transformed data- and why they should not be used: international report. Vol. 7; Aarhus Universitet, Det Jordbrugsvidenskabelige Fakultet.

Key, T., A. McCarthy, D. A. Campbell, C. Six, S. Roy, and Z. V Finkel. 2010. Cell size trade-offs govern light exploitation strategies in marine phytoplankton. Environ. Microbiol. **12**: 95–104. doi:10.1111/j.1462-2920.2009.02046.x

Kooistra, W. H. C. F., R. Gersonde, L. K. Medlin and D. G. Mann. 2007. The origin and the evolution of the diatoms: their adaptation to a planktonic existence, p. 207-249. *In* P. G. Falkowski, and A. H. Knoll [eds.], Evolution of Primary Producers in the Sea. Elsevier Academic Press, Burlington.

Kromkamp, J. C., C. Barranguet, and J. Peene. 1998. Determination of microphytobenthos PSII quantum efficiency and photosynthetic activity by means of variable chlorophyll fluorescence. Mar. Ecol. Prog. Ser. **162**: 45–55. doi:10.3354/meps162045

Larson, C. A., and S. I. Passy. 2012. Taxonomic and functional composition of the algal benthos exhibits similar successional trends in response to nutrient supply and current velocity R. Laanbroek [ed.]. FEMS Microbiol. Ecol. **80**: 352–362. doi:10.1111/j.1574-6941.2012.01302.x

Lavaud, J. 2007. Fast regulation of photosynthesis in diatoms: mechanisms, evolution and ecophysiology. Funct. Plant Sci. Biotechonology **1**: 267–287. doi:http://dx.doi.org/

Lavaud, J., H. J. van Gorkom, and A.-L. Etienne. 2002. Photosystem II electron transfer cycle and chlororespiration in planktonic diatoms. Photosynth. Res. **74**: 51–59. doi:10.1023/A:1020890625141

Lavaud, J., and B. Lepetit. 2013. An explanation for the inter-species variability of the photoprotective non-photochemical chlorophyll fluorescence quenching in diatoms. Biochim. Biophys. Acta **1827**: 294–302. doi:10.1016/j.bbabio.2012.11.012

Lavaud, J., A. C. Materna, S. Sturm, S. Vugrinec, and P. G. Kroth. 2012. Silencing of the violaxanthin de-epoxidase gene in the diatom *Phaeodactylum tricornutum* reduces diatoxanthin synthesis and non-photochemical quenching. PLoS One **7**: e36806. doi:10.1371/journal.pone.0036806

Lavaud, J., B. Rousseau, and A.-L. Etienne. 2004. General features of photoprotection by energy dissipation in planktonic diatoms (Bacillariophyceae). J. Phycol. **40**: 130–137. doi:10.1046/j.1529-8817.2004.03026.x

Lavaud, J., R. F. Strzepek, and P. G. Kroth. 2007. Photoprotection capacity differs among diatoms : Possible consequences on the spatial distribution of diatoms related to fluctuations in the underwater light climate. Limnol. Oceanogr. **52**: 1188–1194.

van Leeuwe, M., V. Brotas, M. Consalvey, R. Forster, D. Gillespie, B. Jesus, J. Roggeveld, and W. Gieskes. 2008. Photoacclimation in microphytobenthos and the role of xanthophyll pigments. Eur. J. Phycol. **43**: 123–132. doi:10.1080/09670260701726119

Lepetit, B., R. Goss, T. Jakob, and C. Wilhelm. 2012. Molecular dynamics of the diatom thylakoid membrane under different light conditions. Photosynth. Res. **111**: 245–57.

doi:10.1007/s11120-011-9633-5

Lepetit, B., D. Volke, M. Gilbert, C. Wilhelm, and R. Goss. 2010. Evidence for the existence of one antenna-associated, lipid-dissolved and two protein-bound pools of diadinoxanthin cycle pigments in diatoms. Plant Physiol. **154**: 1905–1920. doi:10.1104/pp.110.166454

Litchman, E., and C. A. Klausmeier. 2008. Trait-Based Community Ecology of Phytoplankton. Annu. Rev. Ecol. Evol. Syst. **39**: 615–639. doi:10.1146/annurev.ecolsys.39.110707.173549

MacIntyre, H. L., R. J. Geider, and D. C. Miller. 1996. Microphytobenthos: The ecological role of the "Secret Garden" of unvegetated, shallow-water marine habitats. I. Distribution, abundance and primary production. Estuaries **19**: 186. doi:10.2307/1352224

Méléder, V., Y. Rincé, L. Barillé, P. Gaudin, and P. Rosa. 2007. Spatiotemporal changes in microphytobenthos assemblages in a macrotidal flat (Bourgneuf Bay, France). J. Phycol. **43**: 1177–1190. doi:10.1111/j.1529-8817.2007.00423.x

Mouget, J., R. G. Perkins, M. Consalvey, and S. Lefebvre. 2008. Migration or photoacclimation to prevent high irradiance and UV-B damage in marine microphytobenthic communities. Aquat. Microb. Ecol. **52**: 223–232. doi:10.3354/ame01218

Paterson, D. M., and S. E. Hagerthey. 2001. Microphytobenthos in Constrasting Coastal Ecosystems: Biology and Dynamics, p. 105–125. *In* Ecological Comparisons of Sedimentary Shores. Springer Berlin Heidelberg.

Perkins, R. G., J. C. Kromkamp, J. Serôdio, J. Lavaud, B. Jesus, J.-L. Mouget, S. Lefebvre, and R. M. Forster. 2010a. Chlorophyll *a* Fluorescence in Aquatic Sciences: Methods and Applications, D.J. Suggett, O. Prášil, and M.A. Borowitzka [eds.]. Springer Netherlands.

Perkins, R. G., J. Lavaud, J. Serôdio, and others. 2010b. Vertical cell movement is a primary response of intertidal benthic biofilms to increasing light dose. Mar. Ecol. Prog. Ser. **416**: 93–103. doi:10.3354/meps08787

Perkins, R. G., J.-L. Mouget, S. Lefebvre, and J. Lavaud. 2006. Light response curve methodology and possible implications in the application of chlorophyll fluorescence to benthic diatoms. Mar. Biol. **149**: 703–712. doi:10.1007/s00227-005-0222-z

Petrou, K., M. A. Doblin, and P. J. Ralph. 2011. Heterogeneity in the photoprotective capacity of three Antarctic diatoms during short-term changes in salinity and temperature. Mar. Biol. **158**: 1029–1041. doi:10.1007/s00227-011-1628-4

Roy S., C. A. Llewellyn, E. Skarstad Egeland and G. Johnsen. 2011. Phytoplankton Pigments-Characterization, Chemotaxonomy and Applications in Oceanography, Cambridge Environmental Chemistry Series. Cambridge University Press: Cambridge, UK.

Ribeiro, L., V. Brotas, Y. Rincé, and B. Jesus. 2013. Structure and diversity of intertidal benthic diatom assemblages in contrasting shores: a case study from the Tagus estuary. J. Phycol. **49**: 258–270. doi:10.1111/jpy.12031

Sabbe, K. 1993. Short-term fluctuations in benthic diatom numbers on an intertidal sandflat in the Westerschelde estuary (Zeeland, The Netherlands). Hydrobiologia **269–270**: 275–284.

doi:10.1007/BF00028026

Sabbe, K., A. Witkowski, and W. Vyverman. 1995. Taxonomy, morphology and ecology of Biremis lucens comb. nov. (Bacillariophyta): A brackish-marine, benthic diatom species comprising different morphological types. Bot. Mar. **38**: 379–391. doi:10.1515/botm.1995.38.1-6.379

Saburova, M., and I. Polikarpov. 2003. Diatom activity within soft sediments: behavioural and physiological processes. Mar. Ecol. Prog. Ser. **251**: 115–126. doi:10.3354/meps251115

Schumann, A., R. Goss, T. Jakob, and C. Wilhelm. 2007. Investigation of the quenching efficiency of diatoxanthin in cells of *Phaeodactylum tricornutum* (Bacillariophyceae) with different pool sizes of xanthophyll cycle pigments. Phycologia **46**: 113–117. doi:10.2216/06-30.1

Schwaderer, A. S., K. Yoshiyama, P. de Tezanos Pinto, N. G. Swenson, C. A. Klausmeier, and E. Litchman. 2011. Eco-evolutionary differences in light utilization traits and distributions of freshwater phytoplankton. Limnol. Oceanogr. **56**: 589–598. doi:10.4319/lo.2011.56.2.0589

Serôdio, J., S. Cruz, S. Vieira, and V. Brotas. 2005. Non-photochemical quenching of chlorophyll fluorescence and operation of the xanthophyll cycle in estuarine microphytobenthos. J. Exp. Mar. Bio. Ecol. **326**: 157–169. doi:10.1016/j.jembe.2005.05.011

Serôdio, J., J. Ezequiel, A. Barnett, J.-L. Mouget, V. Méléder, M. Laviale, and J. Lavaud. 2012. Efficiency of photoprotection in microphytobenthos: role of vertical migration and the xanthophyll cycle against photoinhibition. Aquat. Microb. Ecol. **67**: 161–175. doi:10.3354/ame01591

Serôdio, J., and J. Lavaud. 2011. A model for describing the light response of the nonphotochemical quenching of chlorophyll fluorescence. Photosynth. Res. 61–76. doi:10.1007/s11120-011-9654-0

Serôdio, J., S. Vieira, and S. Cruz. 2008. Photosynthetic activity, photoprotection and photoinhibition in intertidal microphytobenthos as studied in situ using variable chlorophyll fluorescence. Cont. Shelf Res. **28**: 1363–1375. doi:10.1016/j.csr.2008.03.019

Serôdio, J., S. Vieira, S. Cruz, and H. Coelho. 2006. Rapid light-response curves of chlorophyll fluorescence in microalgae: relationship to steady-state light curves and non-photochemical quenching in benthic diatom-dominated assemblages. Photosynth. Res. **90**: 29–43. doi:10.1007/s11120-006-9105-5

Sabbe K. 1993. Short-term fluctuations in benthic diatom numbers on an intertidal sandflat in the Westerschelde estuary (Zeeland, The Netherlands). Hydrobiologia. **269-270:** 275–284.

Sabbe, K., B. Vanelslander, L. Ribeiro, A. Witkowski, K. Muylaert and W. Vyverman. 2010. A new genus, *Pierrecomperia* gen. nov., a new species and two new combinations in the marine diatom family Cymatosiraceae. Vie et Milieu **60:** 243–256.

Sabbe K., A. Witkowski and W. Vyverman. 1995. Taxonomy, morphology and ecology of *Biremis lucens* comb. nov. (Bacillariophyta): a brackish-marine, benthic diatom species comprising different morphological types.. Bot. Mar. **38:** 379–391.

Staats, N., L. J. Stal, B. de Winder, and L. R. Mur. 2000. Oxygenic photosynthesis as driving porcess in exopolysaccharide production of benthic diatoms. Mar. Ecol. Prog. Ser. **193**: 261–269. doi:http://dx.doi.org/10.3354/meps193261

Stal, L. J. 2010. Microphytobenthos as a biogeomorphological force in intertidal sediment stabilization. Ecol. Eng. **36**: 236–245. doi:10.1016/j.ecoleng.2008.12.032

Strzepek, R. F., and P. J. Harrison. 2004. Photosynthetic architecture differs in coastal and oceanic diatoms. Nature **431**: 689–692. doi:10.1038/nature02954

Underwood, G. J. C. 2002. Adaptations of tropical marine microphytobenthic assemblages along a gradient of light and nutrient availability in Suva Lagoon, Fiji. Eur. J. Phycol. **37**: 449–462. doi:10.1017/S0967026202003785

Underwood, G. J. C., and J. Kromkamp. 1999. Primary production by phytoplankton and microphytobenthos in estuaries estuaries. Adv. Ecol. Res. **29**: 93–153. doi:10.1016/S0065-2504(08)60192-0

Underwood, G. J. C., and D. M. Paterson. 2003. The importance of extracellular carbohydrate production by marine epipelic diatoms. Adv. Bot. Res. **40**: 183–240. doi:10.1016/S0065-2296(05)40005-1

Wagner, H., T. Jakob, and C. Wilhelm. 2006. Balancing the energy flow from captured light to biomass under fluctuating light conditions. New Phytol. **169**: 95–108. doi:10.1111/j.1469-8137.2005.01550.x

Wolfstein, K., and L. J. Stal. 2002. Production of extracellular polymeric substances (EPS) by benthic diatoms: Effect of irradiance and temperature. Mar. Ecol. Prog. Ser. **236**: 13–22. doi:10.3354/meps236013

Wu, H., S. Roy, M. Alami, B. R. Green, and D. A. Campbell. 2012. Photosystem II photoinactivation, repair, and protection in marine centric diatoms. Plant Physiol. **160**: 464–76. doi:10.1104/pp.112.203067

Supplementary Table S1

Light intensity (E in µmol photons m^{-2} s^{-1}) provided by the internal halogen lamp of the Diving-PAM as measured by a quantameter Li-250A (Li-Cor, Biosciences, USA) immediately and 30 s after the onset of light, respectively. The light measurement was performed at 1.5 cm from the optic guide which corresponded to the centre of the 2.5 mL algal suspension in the DW2/2 O_2 electrode vial (see the Materials and methods section). The decrease of E during the 30 s illumination is unavoidable and is due to the heating of the halogen lamp of the Diving-PAM. E values measured after 30 s were preferred in order to optimize the building of relative electron transport rate (rETR) *vs*. E curves.

Diving-PAM light steps	Instantaneous E	E after 30 s illumination
1	5	5
2	15	15.5
3	31	29
4	55	52
5	81	76
6	111	105
7	164	152
8	222	208
9	333	310
10	478	445
11	698	649
12	1117	1042

Supplementary Table S2

Growth rate, pigment content and photosynthetic parameters of the fifteen diatom species. All parameters were measured on cells in exponential growth phase sampled 2 h after the onset of light. Growth conditions were 20 µmol photons m^{-2} s^{-1}, 16 h light:8 h dark, 20°C. µ, growth rate (day^{-1}), Chl *a* $cell^{-1}$, content of chlorophyll *a* (in pg) per diatom cell; other pigments are expressed in mol 100 mol. Chl a^{-1}: Chl, chlorophyll; Fx, fucoxanthin; β-car, β-carotene; Ddx, diadinoxanthin; Dtx, diatoxanthin; DES: de-epoxidation state of Ddx into Dtx (in %); n.d.: not determined. The full names of the species are listed in Table 1. Abbreviations, definitions and conditions of measurement of the photosynthetic parameters are listed in Table 2. Values are averages per species ± standard deviation.

			Pigments					Photosynthetic parameters					
Species	Growth form	µ	Chl *a* $cell^{-1}$	Chl *c*	CET_m	β-car	Ddx+Dtx	DES	F_v/F_m	α	$rETR_m$	E_k	PSII CET_m
C.b.		1.62 ± 0.12	32.10 ± 9.19	24.58 ± 0.90	68.68 ± 1.96	4.55 ± 0.12	5.98 ± 1.78	0.98 ± 0.11	0.74 ± 0.00	0.70 ± 0.05	86.35 ± 6.02	128.28 ± 21.39	n.d.
E.p.		1.71 ± 0.02	2.74 ± 0.21	19.13 ± 0.08	72.92 ± 1.81	3.57 ± 0.21	5.66 ± 0.46	0.70 ± 0.99	0.73 ± 0.01	0.73 ± 0.03	31.92 ± 1.85	44.36 ± 3.54	2.48 ± 0.51
H.c.		2.05 ± 0.02	7.98 ± 1.00	15.29 ± 0.63	60.96 ± 3.77	3.68 ± 0.01	7.76 ± 1.42	2.87 ± 1.55	0.69 ± 0.04	0.67 ± 0.07	42.26 ± 6.54	63.71 ± 10.20	2.32 ± 0.59
N.p.		1.33 ± 0.21	1.19 ± 0.09	15.99 ± 1.22	56.89 ± 2.02	4.31 ± 0.53	7.53 ± 0.78	0.00 ± 0.00	0.71 ± 0.03	0.61 ± 0.09	53.72 ± 11.12	86.04 ±17.92	2.01 ± 0.57
S.r.	EPL	1.77 ± 0.13	18.73 ± 4.69	21.18 ± 2.13	70.52 ± 4.73	3.54 ± 1.23	5.78 ± 2.12	1.19 ± 0.33	0.72 ± 0.02	0.69 ± 0.06	63.09 ± 10.87	98.77 ± 6.36	1.60 ± 0.37
A. sp.		1.38 ± 0.15	1.08 ± 0.07	11.87 ± 0.21	50.30 ± 2.46	3.09 ± 1.05	10.01 ± 1.41	4.52 ± 2.20	0.70 ± 0.02	0.67 ± 0.02	51.27 ± 3.73	75.32 ± 3.53	3.24 ± 0.81
N.f.		1.37 ± 0.02	0.92 ± 0.02	17.53 ± 0.32	64.02 ± 2.40	2.98 ± 0.46	11.06 ± 0.90	8.66 ± 1.72	0.69 ± 0.01	0.69 ± 0.12	62.30 ± 3.77	92.31 ± 14.16	n.d.
P.d.	EPM-M	1.98 ± 0.20	2.35 ± 1.09	19.98 ± 2.22	78.64 ± 0.10	2.22 ± 1.23	10.32 ± 1.75	2.56 ± 3.13	0.66 ± 0.01	0.58 ± 0.06	43.16 ± 3.72	76.41 ± 11.26	2.48 ± 0.25

B.l.	EPM-NM	1.30 ± 0.07	3.94 ± 1.45	15.13 ± 0.37	56.83 ± 0.43	1.26 ± 0.12	8.88 ± 0.96	1.77 ± 1.57	0.72 ± 0.01	0.74 ± 0.07	34.29 ± 3.72	46.53 ± 2.06	2.85 ± 0.11
F.s.		1.43 ± 0.11	0.80 ± 0.12	24.49 ± 2.39	74.16 ± 3.75	1.70 ± 0.48	13.01 ± 5.23	0.91 ± 1.31	0.70 ± 0.01	0.58 ± 0.03	45.35 ± 11.79	82.08 ± 20.41	2.54 ± 0.30
O.g.		1.65 ± 0.06	1.64 ± 0.07	10.43 ± 0.85	41.82 ± 1.78	3.62 ± 0.48	9.81 ± 0.66	0.68 ± 0.96	0.71 ± 0.01	0.71 ± 0.05	37.22 ± 2.64	54.11 ± 5.29	3.59 ± 0.27
P.s.		1.43 ± 0.02	n.d.	42.95 ± 4.24	109.54 ± 4.51	1.70 ± 0.48	16.95 ± 2.58	16.41 ± 6.23	0.59 ± 0.09	0.51 ± 0.05	44.12 ± 14.84	71.44 ± 21.20	2.29 ± 0.47
B.b.	TYCHO	1.92 ± 0.08	0.24 ± 0.05	25.63 ± 0.95	86.37 ± 4.82	2.59 ± 0.28	11.23 ± 0.58	9.56 ± 1.31	0.69 ± 0.04	0.70 ± 0.08	44.82 ± 2.36	67.77 ± 5.38	2.08 ± 0.38
C.c.		1.53 ± 0.26	0.37 ± 0.13	23.82 ± 0.22	64.98 ± 0.54	4.50 ± 0.34	7.10 ± 0.73	2.62 ± 4.54	0.77 ± 0.01	0.74 ± 0.02	68.41 ± 3.36	92.87 ± 7.35	1.66 ± 0.33
P.v.		1.45 ± 0.02	4.55 ± 0.61	25.04 ± 0.99	86.76 ± 3.48	1.93 ± 0.34	11.04 ± 3.71	5.37 ± 1.19	0.73 ± 0.01	0.67 ± 0.02	62.95 ± 9.58	90.59 ± 10.71	2.36 ± 0.22

Supplementary Table S3

Results of the PROC MIXED procedure for the comparison of the parameters of Table 3 between the different growth forms. Red: $p > 0.05$; orange: $p < 0.05$; light green: $p < 0.01$; dark green: $p < 0.001$. Abbreviations: EPL, epipelon; EPM-M, motile epipsammon; EPM-NM, non-motile epipsammon; TYCHO, tychoplankton; μ, growth rate (day^{-1}); Chl, chlorophyll; Fx, fucoxanthin; β-car, β-carotene; Ddx, diadinoxanthin; Dtx, diatoxanthin. Abbreviations, definitions and conditions of measurement of the photosynthetic parameters are listed in Table 2.

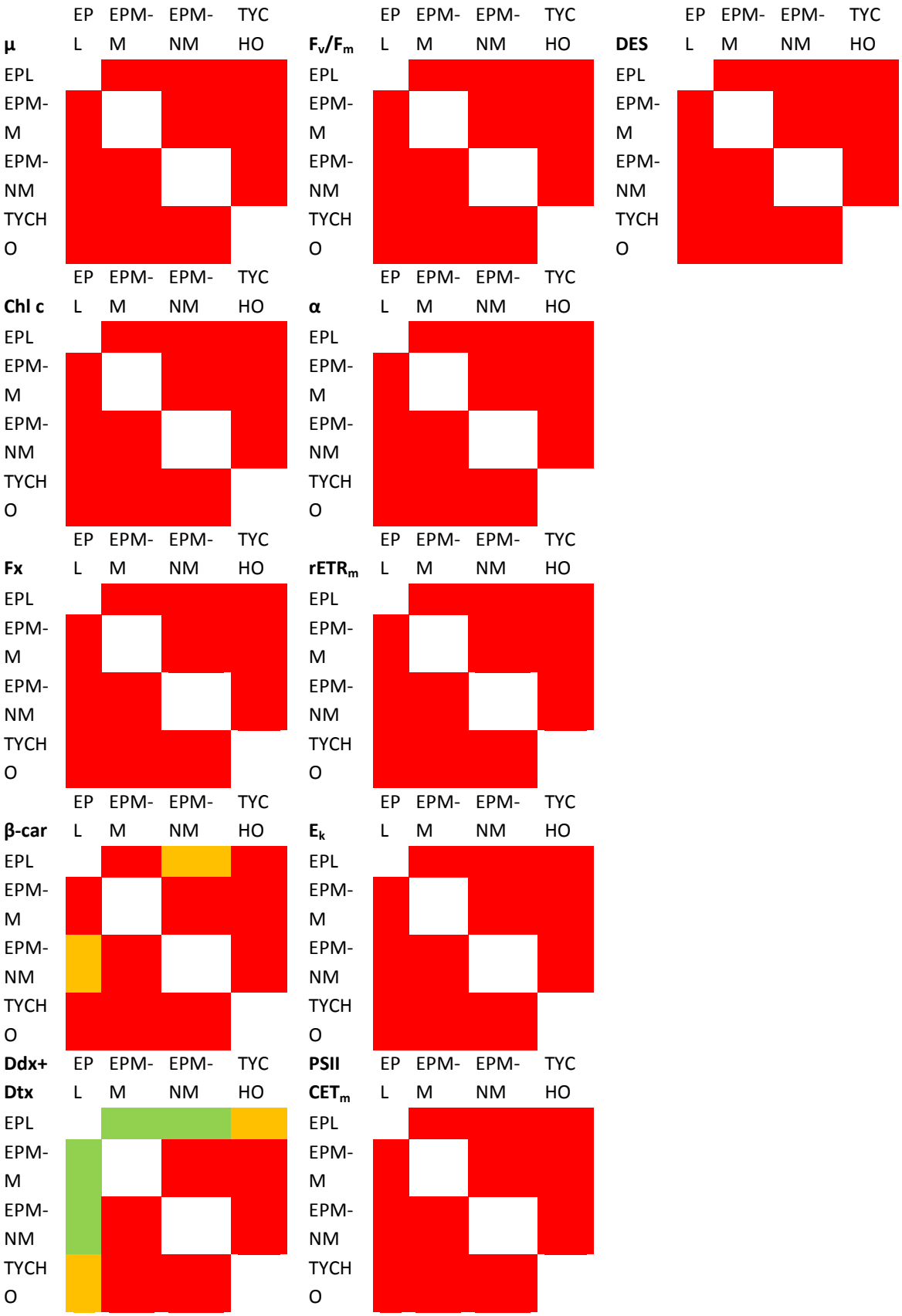
μ
Fv/Fm
DES
Chl c
α
Fx
rETRm
β-car
Ek
Ddx+ Dtx
PSII CETm
EPL
EPM-M
EPM-NM
TYCHO

Supplementary Table S4

Non-photochemical quenching (NPQ) and xanthophyll cycle (XC) properties of the fifteen diatom species. The full names of the species are found in Table 1. Definitions and conditions of measurement of all parameters are listed in Table 2. For some S.r., the fitting procedure of Dtx synthesis yielded unsatisfactory results: these have been indicated as n.d. and were excluded from further statistical analyses. Values represent averages per species ± standard deviation.

Species	Growth form	NPQ_m	$E50_{NPQ}$	n_{NPQ}	DES_m	DT_m	$E50_{DT}$	n_{Dtx}	NPQ/Dtx
C.b.	EPL	0.46 ± 0.08	1054.33 ± 179.86	1.55 ± 0.35	16.57 ± 3.51	1.12 ± 0.16	528.00 ± 127.18	2.63 ± 0.81	0.33 ± 0.07
E.p.		0.65 ± 0.14	399.50 ± 184.55	1.97 ± 0.51	28.00 ± 2.72	1.81 ± 0.06	682.67 ± 278.75	2.18 ± 0.70	0.35 ± 0.08
H.c.		0.80 ± 0.16	821.33 ± 222.83	2.88 ± 0.52	19.48 ± 1.34	1.56 ± 0.33	974.00 ± 93.98	2.80 ± 0.45	0.47 ± 0.11
N.p.		1.14 ± 0.08	2540.33 ± 428.27	1.30 ± 0.29	28.88 ± 2.14	2.05 ± 0.06	796.60 ± 236.56	2.20 ± 0.40	0.60 ± 0.22
S.r.		0.60 ± 0.06	587.67 ± 173.08	1.44 ± 0.39	12.45 ± 3.61	0.76 ± 0.27	n.d.	n.d.	0.74 ± 0.10
A.sp.	EPM-M	2.41 ± 0.30	997.00 ± 198.03	1.85 ± 0.31	34.48 ± 4.46	4.82 ± 0.46	950.50 ± 58.69	1.16 ± 0.01	0.46 ± 0.09
N.f.		1.67 ± 0.04	1230.00 ± 319.61	2.49 ± 0.88	17.78 ± 0.08	2.19 ± 0.69	946.50 ± 57.28	1.99 ± 0.01	0.79 ± 0.18
P.d.		1.30 ± 0.48	1007.50 ± 57.28	1.81 ± 0.21	33.70 ± 1.93	2.88 ± 0.04	623.00 ± 193.38	1.20 ± 0.49	0.42 ± 0.16
B.l.	EPM-NM	2.14 ± 0.32	348.67 ± 41.04	2.56 ± 0.27	35.25 ± 0.86	3.71 ± 0.23	313.50 ± 79.90	1.99 ± 0.63	0.67 ± 0.03
F.s.		3.24 ± 0.19	297.50 ± 98.29	2.80 ± 0.78	23.36 ± 1.61	2.90 ± 0.74	790.33 ± 198.90	2.23 ± 0.70	1.09 ± 0.47
O.sp.		2.42 ± 0.21	598.67 ± 48.23	2.13 ± 0.23	20.54 ± 2.69	1.97 ± 0.21	412.33 ± 45.00	2.77 ± 0.48	1.07 ± 0.17
P.s.		2.05 ± 0.01	288.00 ± 84.18	1.65 ± 0.31	38.40 ± 4.48	7.07 ± 1.51	472.50 ± 67.18	2.33 ± 1.24	0.26 ± 0.04

B.b.		0.70 ± 0.03	6387.00 ± 171.12	0.56 ± 0.05	27.45 ± 0.48	2.50 ± 0.42	1069.00 ± 140.00	1.17 ± 0.09	0.21 ± 0.03
C.c.		0.64 ± 0.18	3829.33 ± 332.06	1.82 ± 0.11	18.44 ± 4.29	1.05 ± 0.53	3281.50 ± 1402.19	2.06 ± 0.67	0.62 ± 0.62
P.v.	TYCHO	0.67 ± 0.08	2414.50 ± 238.29	0.92 ± 0.09	22.28 ± 2.96	1.78 ± 0.19	656.00 ± 370.26	1.29 ± 0.40	0.37 ± 0.02

Supplementary Table S5

Results of the PROC MIXED procedure for the comparison of the non-photochemical quenching (NPQ) values at different light intensities (cf. Fig 1) between the different growth forms. Red: $p > 0.05$; orange: $p < 0.05$; light green: $p < 0.01$; dark green: $p < 0.001$. Abbreviations: EPL, epipelon; EPM-M, motile epipsammon; EPM-NM, non-motile epipsammon; TYCHO, tychoplankton; E, light intensity (in µmol photons. m^{-2}. s^{-1}).

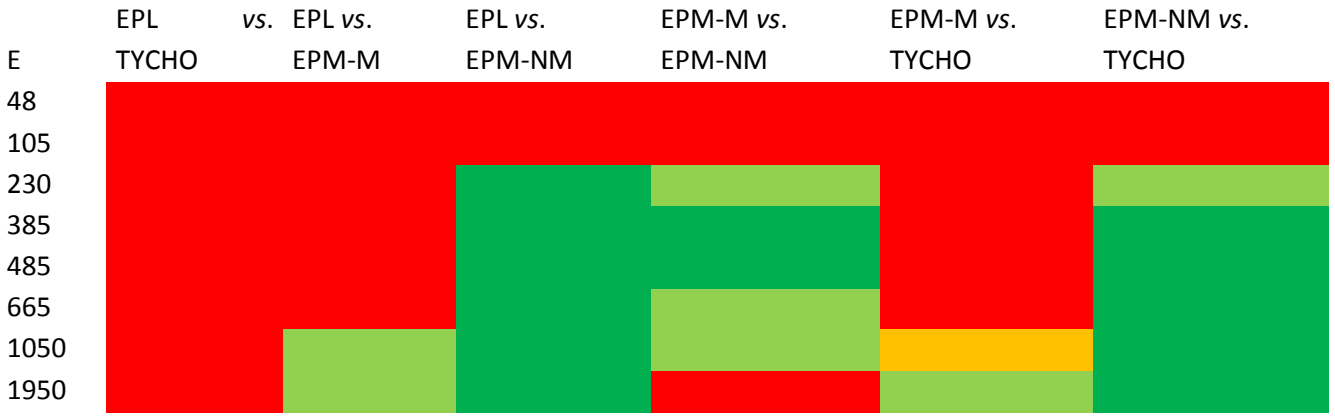

Supplementary Table S6

Results of the PROC MIXED procedure for the comparison of the diadinoxanthin (Ddx) de-epoxidation (DES) values at different light intensities (cf. Fig 1) between the different growth forms. Red: p > 0.05; orange: p < 0.05; light green: p < 0.01; dark green: p < 0.001. Abbreviations: EPL, epipelon; EPM-M, motile epipsammon; EPM-NM, non-motile epipsammon; TYCHO, tychoplankton; E, light intensity (in µmol photons. m^{-2}. s^{-1}).

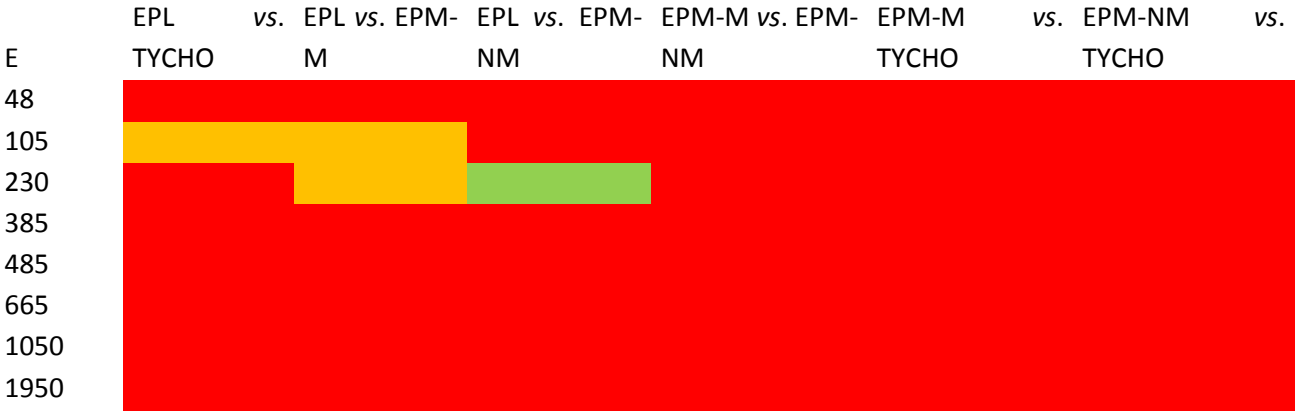

Supplementary Table S7

Results of PROC MIXED procedure for the comparison of the parameters of Table 4 between the different growth forms. Red: $p > 0.05$; orange: $p < 0.05$; light green: $p < 0.01$; dark green: $p < 0.001$. Abbreviations: EPL, epipelon; EPM-M, motile epipsammon; EPM-NM, non-motile epipsammon; TYCHO, tychoplankton. Abbreviations, definitions and conditions of measurement of all parameters are listed in Table 2. Species whose parameter values were not determined (see Table S4) were not included in the PROC MIXED analysis for that specific parameter.

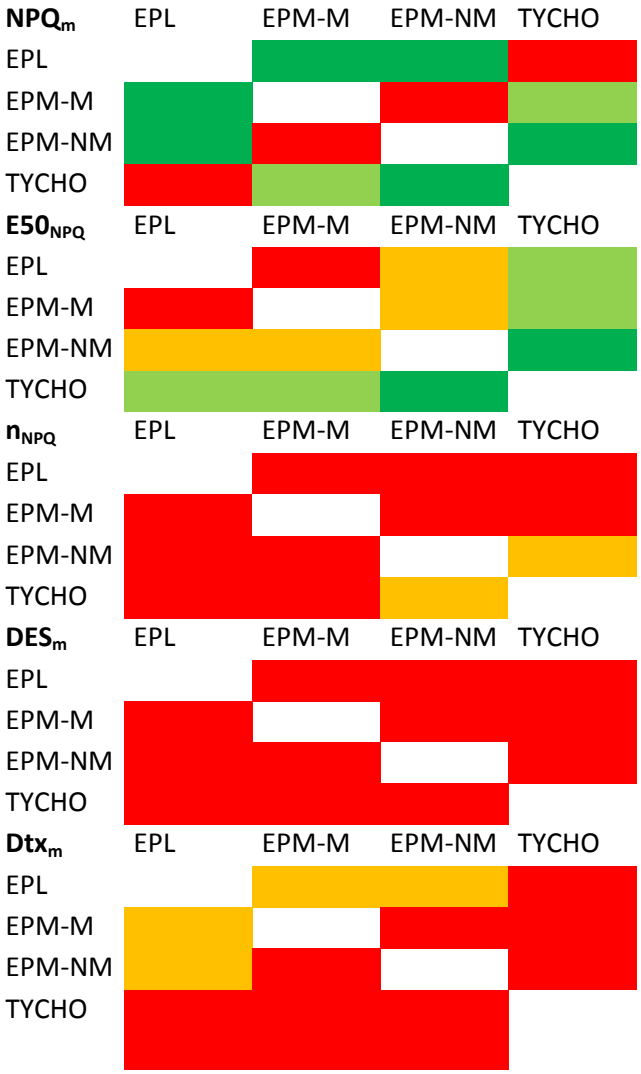
NPQm EPL EPM-M EPM-NM TYCHO
EPL
EPM-M
EPM-NM
TYCHO
E50NPQ EPL EPM-M EPM-NM TYCHO
EPL
EPM-M
EPM-NM
TYCHO
nNPQ EPL EPM-M EPM-NM TYCHO
EPL
EPM-M
EPM-NM
TYCHO
DESm EPL EPM-M EPM-NM TYCHO
EPL
EPM-M
EPM-NM
TYCHO
Dtxm EPL EPM-M EPM-NM TYCHO
EPL
EPM-M
EPM-NM
TYCHO

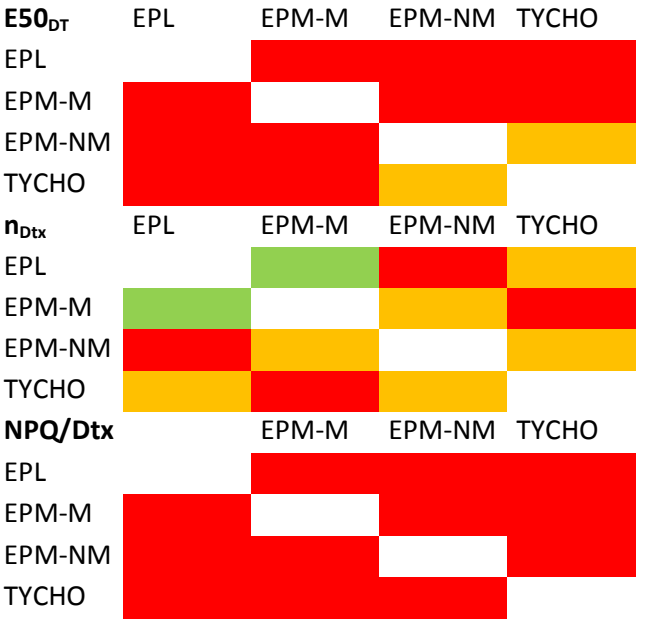
E50DT EPL EPM-M EPM-NM TYCHO
EPL
EPM-M
EPM-NM
TYCHO
nDtx EPL EPM-M EPM-NM TYCHO
EPL
EPM-M
EPM-NM
TYCHO
NPQ/Dtx EPM-M EPM-NM TYCHO
EPL
EPM-M
EPM-NM
TYCHO

Supplementary Tables S8

S8A. Growth rate and xanthophyll cycle properties of the fifteen diatom species and of the four growth forms of benthic diatoms grown under 75 µmol photons m^{-2} s^{-1}. For each parameter, the ratio of the values obtained under 75 µmol photons m^{-2} s^{-1} (this table, left side) and 20 µmol photons m^{-2} s^{-1} (see Table S2) growth conditions was calculated (this table, right side). The full names of all species can be found in Table 1. Abbreviations: EPL, epipelon; EPM-M, motile epipsammon; EPM-NM, non-motile epipsammon; TYCHO, tychoplankton; µ, growth rate (in day^{-1}); Ddx + Dtx, diadinoxanthin + diatoxanthin in mol 100 mol Chl a^{-1}; DES, de-epoxidation state of Ddx into Dtx (in %). Values are averages ± standard deviation for species and estimated least-square means from the PROC MIXED procedure ± estimated standard error for the growth forms.

Species	Growth form	Parameters 75 µmol photons m^{-1} s^{-2}			Ratio 75/20		
		µ	Ddx+Dtx	DES	µ	Ddx+Dtx	DES
C.b.	EPL	1.69 ± 0.10	9.27 ± 0.20	3.09 ± 0.08	1.04	1.55	3.15
E.p.	EPL	1.81 ± 0.02	11.38 ± 0.39	6.53 ± 0.53	1.06	2.01	9.37
H.c.	EPL	2.52 ± 0.03	13.32 ± 1.03	4.16 ± 0.38	1.23	1.72	1.45
N.p.	EPL	1.64 ± 0.06	10.41 ± 1.72	10.68 ± 6.99	1.23	1.38	n.d.
S.r.	EPL	2.53 ± 0.18	8.12 ± 1.24	6.69 ± 2.25	1.43	1.40	5.62
A.sp.	EPM-M	1.94 ± 0.22	17.42 ± 0.59	7.32 ± 1.10	1.40	1.74	1.62
N.f.	EPM-M	1.34 ± 0.07	12.30 ± 2.07	9.22 ± 2.64	0.98	1.11	1.07
P.d.	EPM-M	1.23 ± 0.08	19.88 ± 0.51	2.56 ± 3.13	0.62	1.93	1.00
B.l.	EPM-NM	1.46 ± 0.09	19.86 ± 2.12	18.49 ± 1.52	1.13	2.24	10.47
F.s.	EPM-NM	1.57 ± 0.21	16.45 ± 1.87	13.65 ± 7.63	1.10	1.26	14.92
O.g.	EPM-NM	2.12 ± 0.02	14.14 ± 1.58	6.98 ± 1.67	1.28	1.44	10.29
P.s.	EPM-NM	1.34 ± 0.05	34.00 ± 5.38	23.09 ± 2.94	0.93	2.01	1.41
B.b.	TYCHO	1.50 ± 0.03	26.63 ± 4.83	27.16 ± 4.70	0.78	2.37	2.84
C.c.	TYCHO	1.57 ± 0.02	17.09 ± 0.71	10.13 ± 2.30	1.03	2.41	3.86
P.v.	TYCHO	1.25 ± 0.17	23.13 ± 3.03	16.17 ± 1.88	0.86	2.10	3.01
	EPL	2.01 ± 0.17	10.33 ± 1.24	6.31 ± 2.24	1.21	1.62	8.41
	EPM-M	1.48 ± 0.19	16.17 ± 2.52	6.26 ± 3.14	0.95	1.56	1.47
	EPM-NM	1.61 ± 0.17	19.85 ± 2.72	13.04 ± 3.19	1.11	1.72	5.67
	TYCHO	1.43 ± 0.19	21.81 ± 3.43	18.00 ± 3.08	0.89	2.36	4.20

S8B. Results of the PROC MIXED procedure for the comparison of the parameters measured at 75 µmol photons m^{-2} s^{-1} (see Table S8A) between the growth forms (left) and for the comparison of the same parameters at 20 *vs* 75 µmol photons m^{-2} s^{-1} (cf. Tables 3 and S8A) for all growth forms (right). Red: $p > 0.05$; orange: $p < 0.05$; light green: $p < 0.01$; dark green: $p < 0.001$. Arrows indicate an increase or decrease in the parameter from 20 to 75 µmol photons m^{-2} s^{-1}.

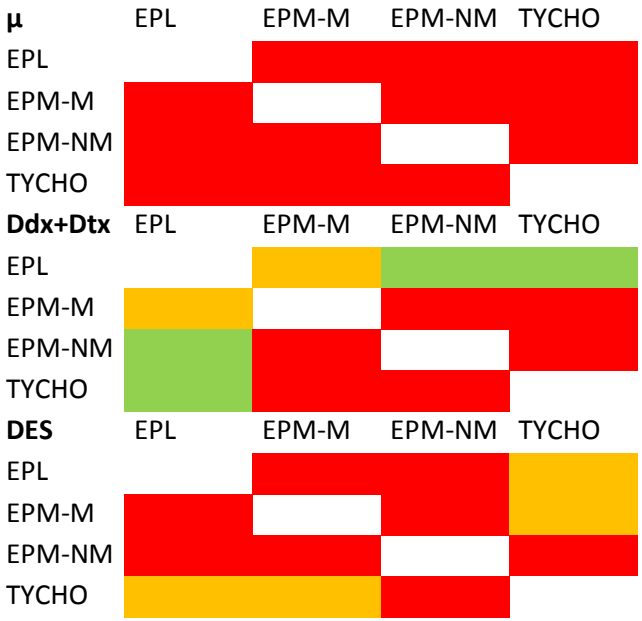

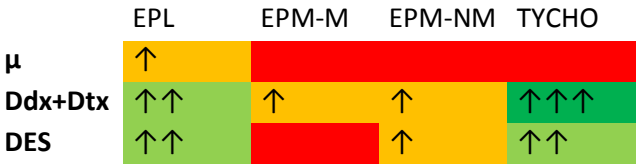

Supplementary Tables S9

S9A. Photosynthetic, xanthophyll cycle and non-photochemical quenching (NPQ) properties of six diatom species representative of the four benthic growth forms grown under 75 µmol photons m^{-2} s^{-1}. The full names of all species can be found in Table 1. Abbreviations, definitions and conditions of measurement of all parameters are listed in Table 2, Chl *a* $cell^{-1}$, content of chlorophyll *a* (in pg) per diatom cell. Abbreviations: EPL, epipelon; EPM-M, motile epipsammon; EPM-NM, non-motile epipsammon; TYCHO, tychoplankton. n.d. = not determined. Values are averages ± standard deviation for each species.

Species	Growth form	Chl *a* $cell^{-1}$	F_v/F_m	DES_m	Dtx_m	NPQ_m	NPQ/Dtx	$E50_{NPQ}$
N.p.	EPL	0.83 ± 0.02	0.68 ± 0.04	24.28 ± 2.79	3.07 ± 1.26	1.73 ± 0.24	0.42 ± 0.16	1730.00 ± 861.26
S.r.		8.41 ± 0.68	0.65 ± 0.05	33.21 ± 1.29	3.08 ± 0.98	1.17 ± 0.03	0.45 ± 0.08	287.00 ± 84.12
P.d.	EPM-M	0.93 ± 0.10	0.60 ± 0.01	32.19 ± 6.45	5.52 ± 0.65	1.38 ± 0.45	0.22 ± 0.04	900.50 ± 259.51
O.g.	EPM-NM	0.89 ± 0.30	0.65 ± 0.03	32.13 ± 5.89	5.33 ± 1.92	2.76 ± 0.46	0.49 ± 0.10	584.00 ± 65.78
P.s.		n.d.	0.51 ± 0.06	33.98 ± 1.02	10.23 ± 0.49	3.99 ± 0.06	0.49 ± 0.10	720.50 ± 67.18
P.v.	TYCHO	2.01 ± 0.41	0.65 ± 0.05	22.01 ± 8.66	4.20 ± 0.60	1.17 ± 0.20	0.40 ± 0.24	2156.00 ± 985.44

S9B. Results of the PROC GLM procedure for the comparison of the parameters of Table S9A at 20 *vs* 75 µmol photons m^{-2} s^{-1} (cf. Tables S3, S4 and S9A) for all growth forms. Red: p > 0.05; orange: p < 0.05; light green: p < 0.01; dark green: p < 0.001. n.d. = not determined. The full names of all species can be found in Table 1. Abbreviations, definitions and conditions of measurement of all parameters are listed in Table 2. Arrows indicate an increase or decrease in the parameter from 20 to 75 µmol photons m^{-2} s^{-1}.

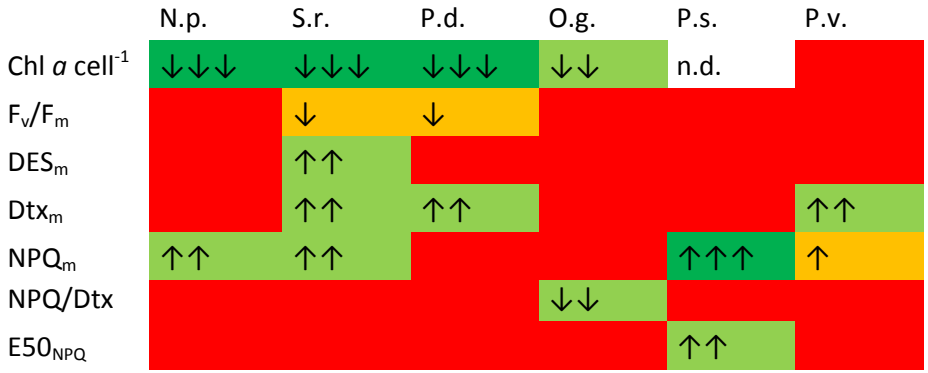

Supplementary Tables S10

S10A. Growth rate, photosynthetic, xanthophyll cycle and non-photochemical quenching (NPQ) properties of the three tychoplankton diatom species grown under 'planktonic' conditions. The full names of the species can be found in Table 1. Abbreviations, definitions and conditions of measurement of all parameters are listed in Table 2. μ, growth rate (day^{-1}), Chl *a* $cell^{-1}$, content of chlorophyll *a* (in pg) per diatom cell. Values are averages ± standard deviation per species.

Species	μ	Chl *a* $cell^{-1}$	F_v/F_m	$rETR_m$	Ddx+Dtx	DES	NPQ_m	DES_m	NPQ/Dtx
B.b.	1.34 ± 0.13	0.62 ± 0.05	0.70 ± 0.00	38.9 ± 0.41	11.19 ± 2.19	21.02 ± 3.03	0.59 ± 0.03	37.87 ± 2.79	0.17 ± 0.04
C.c.	1.46 ± 0.03	0.37 ± 0.17	0.75 ± 0.02	47.72 ± 16.56	7.82 ± 1.20	17.29 ± 3.32	0.50 ± 0.02	17.29 ± 3.32	0.18 ± 0.11
P.v.	1.76 ± 0.06	0.36 ± 0.19	0.71 ± 0.03	37.64 ± 6.72	8.43 ± 2.68	16.18 ± 5.51	0.75 ± 0.09	21.74 ± 7.29	0.47 ± 0.12

S10B. Results of the PROC MIXED procedure (group effect) and PROC GLM procedure (species difference) for the comparison of the parameters of Table S10A measured under 'benthic' *vs* 'planktonic' conditions (cf. Tables S3, S4 and S10A). Red: $p > 0.05$; orange: $p < 0.05$; light green: $p < 0.01$; dark green: $p < 0.001$. The full names of the species can be found in Table 1. Abbreviations, definitions and conditions of measurement of all parameters are listed in Table 2. Arrows indicate an increase or decrease in the parameter from benthic to planktonic growth condition.

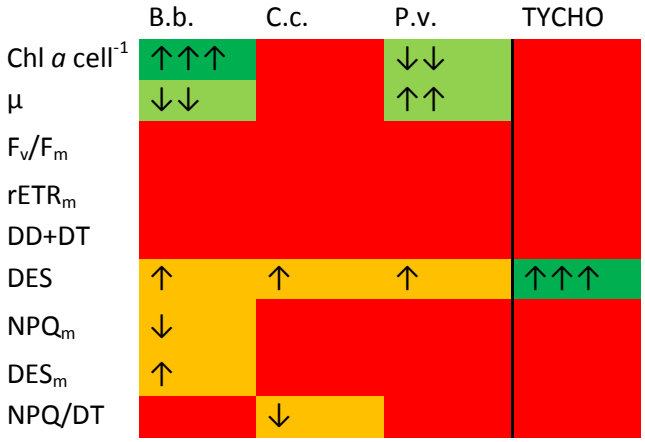

Supplementary Figure S1

Relationship between the average biovolume of diatom cells and their chlorophyll *a* (Chl *a*) content (in pg cell^{-1}). Cells were grown at 20 µmol photons m^{-2} s^{-1} and sampled in their exponential phase of growth. The full names and functional classification of all species are listed in Table 1. Data are from Table 1 and Table S2.

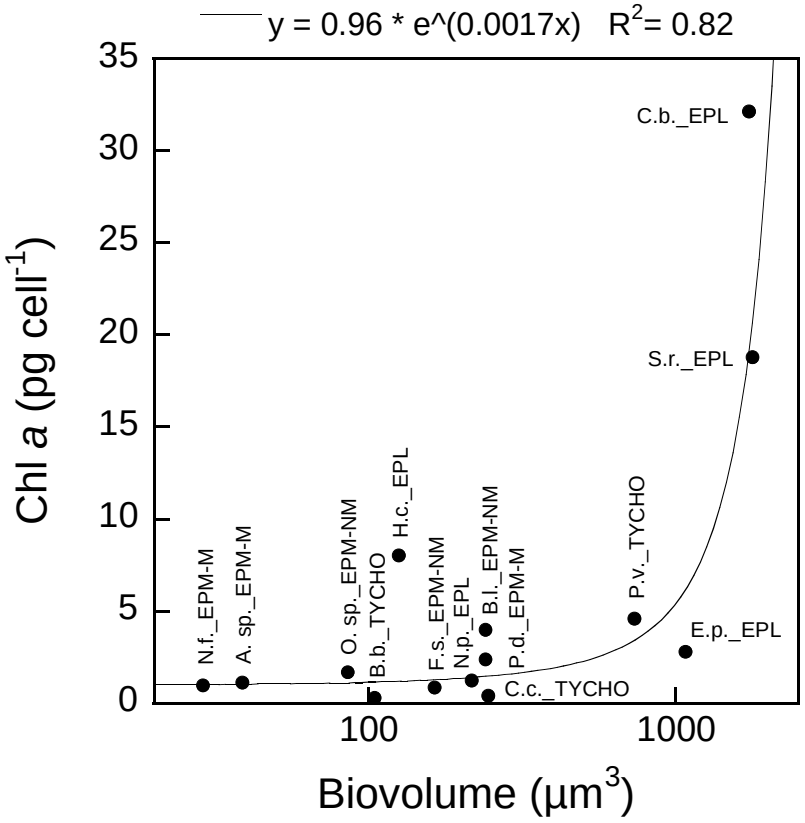

Supplementary Figure S2

Non-photochemical quenching of Chl fluorescence (NPQ) as a function of light intensity (E from darkness to 1950 µmol photons m^{-2} s^{-1} which is equivalent to full sunlight in the field) measured during Non-Sequential Light Curves (NSLCs) **in the five species of epipelon (EPL) (A), the seven species of motile (EPM-M, open symbols) (B) and non-motile epipsammon (EPM-NM, closed symbols), and in the three species of tychoplankton (TYCHO) (C)**. Cells were grown at 20 µmol photons m^{-2} s^{-1}. The full names and functional classification of all species are listed in Table 1. Values are averages ± standard deviation.

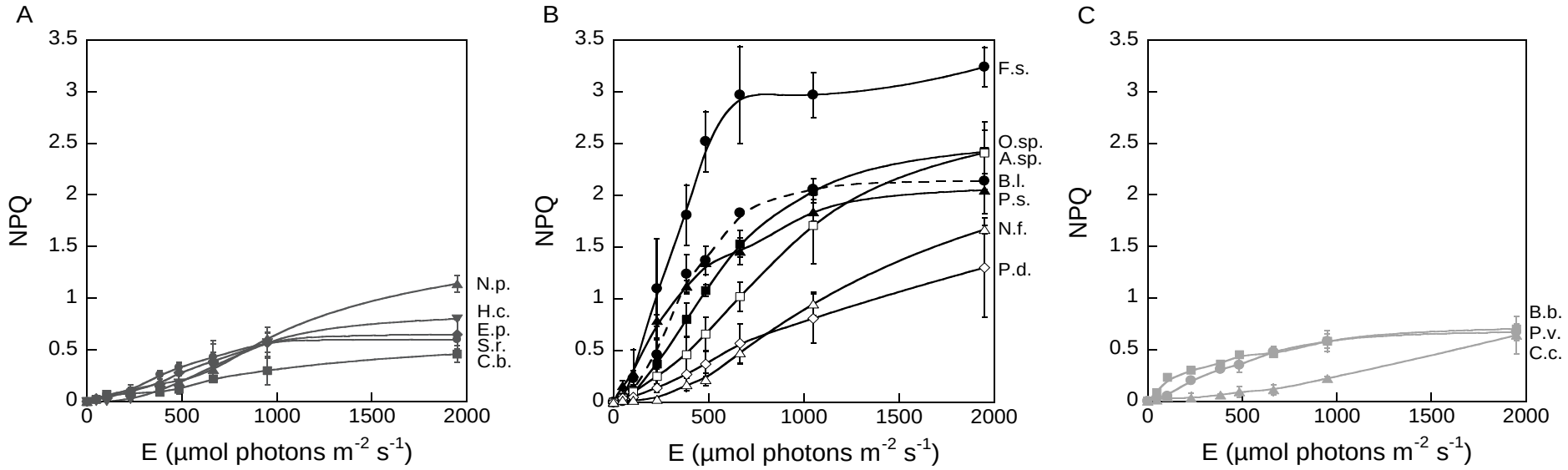

Chapter 3: Contrasting NPQ dynamics and xanthophyll cycling in a motile and a non-motile intertidal benthic diatom

Lander Blommaert[1,4], Marie J. J. Huysman[1,2,3], Wim Vyverman[1], Johann Lavaud[4,5] & Koen Sabbe[1]

1 Ghent University, Lab. Protistology & Aquatic Ecology, B-9000 Ghent, Belgium

2 VIB, Department of Plant Systems Biology, B-9052 Ghent, Belgium

3 Ghent University, Department of Plant Biotechnology and Bioinformatics, B-9052 Ghent, Belgium

4 CNRS/Université de La Rochelle, UMR7266 LIENSs, Institut du Littoral et de l'Environnement, 17000 La Rochelle, France

5 Current address : CNRS/Université Laval, UMI3376 Takuvik Joint International Laboratory, Département de Biologie, Pavillon Alexandre Vachon, Université Laval, 1045 avenue de la Médecine, Québec, Qc, G1V 0A6, Canada

Adapted from:

Blommaert, L., M. J. J. Huysman, W. Vyverman, J. Lavaud, and K. Sabbe. 2017. Contrasting NPQ dynamics and xanthophyll cycling in a motile and a non-motile intertidal benthic diatom. Limnol. Oceanogr. doi:10.1002/lno.10511

Abstract

Diatoms living in intertidal sediments have to be able to rapidly adjust photosynthesis in response to often pronounced changes in light intensity during tidal cycles and changes in weather conditions. Strategies to deal with oversaturating light conditions, however, differ between growth forms. Motile epipelic diatoms can migrate to more optimal light conditions. In contrast, non-motile epipsammic diatoms appear to mainly rely on higher Non-Photochemical Quenching (NPQ) of chlorophyll *a* fluorescence to dissipate excess light energy, and this has been related to a larger pool of xanthophyll cycle (XC) pigments. We studied the effect of 1 h high Photosynthetically Available Radiation (PAR) (2000 µmol photons $m^{-2} s^{-1}$) on the kinetics of the xanthophyll cycle and NPQ in both a motile diatom (*Seminavis robusta*) and a non-motile diatom (*Opephora guenter-grassii*) in an experimental set-up which did not allow for vertical migration. *O. guenter-grassii* could rapidly switch NPQ on and off by relying on fast XC kinetics. This species also demonstrated high de novo synthesis of xanthophylls within a relatively short period of time (1 h), including significant amounts of zeaxanthin, a feature not observed before in other diatoms. In contrast, *S. robusta* showed slower NPQ and associated XC kinetics, partly relying on NPQ conferred by de novo synthetized diatoxanthin molecules and synthesis of Light-Harvesting Complex X (LHCX) isoforms. Part of this observed NPQ increase, however, is sustained quenching (NPQs). Our data illustrate the high and diverse adaptive capacity of microalgal growth forms to maximize photosynthesis in dynamic light environments.

Introduction

Diatoms are dominant primary producers in areas characterized by pronounced fluctuations in light conditions (Armbrust 2009; Lavaud and Goss 2014). Rapid changes in light climate in well mixed waters or on intertidal flats challenge planktonic and benthic diatoms, respectively, to adjust light harvesting to what can be safely used for photosynthesis. As periods of high light conditions can result in oxidative damage to, in particular, the photosystem II (PSII) core, diatoms possess various mechanisms to deal with high light stress: (1) avoid excess light energy absorption by decreasing cell pigment content (MacIntyre et al. 2002); (2) dissipate excess excitation energy as heat in a process called Non-Photochemical Quenching of chlorophyll *a* (Chl *a*) fluorescence (NPQ) (Lavaud and Goss 2014; Goss and Lepetit 2015), and/or by engaging alternative electron cycling pathways (Wagner et al. 2016); (3) scavenge reactive oxygen species (ROS) (Janknegt et al. 2008, 2009a; b; Waring et al. 2010); (4) repair damaged PSII cores, mainly by replacing the D1 protein of the PSII reaction centre (Wu et al. 2011; Lavaud et al. 2016); (5) behavioural down regulation through vertical cell movement (microcycling and bulk migration) (Kromkamp et al. 1998; Serôdio 2004). Of the above mechanisms, especially NPQ is able to track fast light fluctuations experienced in the natural habitat (Brunet and Lavaud 2010; Lavaud and Goss 2014).

In land plants, three NPQ components have been distinguished, based on the relaxation kinetics after high light exposure: the rapidly relaxing component qE (seconds to minutes), the slower state transitions qT (tens of minutes), and the so-called 'photoinhibitory' quenching qI, which relaxes in the range of hours (Horton and Hague 1988). In diatoms, however, only two of these have been observed (Owens 1986). Energy dependent quenching (qE) is the main component and is controlled by (1) the build-up of a proton gradient (ΔpH) across the thylakoid membrane, (2) the (reversible) de-epoxidation of diadinoxanthin (Ddx) to diatoxanthin (Dtx) in the xanthophyll cycle (XC) and (3) the presence of Light-Harvesting Complex X (LHCX) proteins, homologs of the Light-Harvesting Complex Stress-Related (LHCSR) proteins found in green algae (Lavaud and Goss 2014; Goss and Lepetit 2015). The origin of the second component (qI), however, is less clear. Besides PSII photoinactivation and damage, Dtx and some LHCX isoforms might be involved in this sustained quenching mechanism (Zhu and Green 2010; Lavaud and Lepetit 2013). It is increasingly referred to as NPQs (for sustained NPQ) or 'dark NPQ' as it persists even under prolonged dark acclimation, particularly in intertidal benthic diatoms (Perkins et al. 2011; Lavaud and Goss 2014).

A molecular mechanism of qE in diatoms has been recently proposed (Lavaud and Goss 2014; Goss and Lepetit 2015). qE is hypothesized to be based on two quenching sites within the LHC antenna of PSII: (1) Q2 which is localized in a part of the LHC that remains attached to the PSII and which directly depends on the synthesis and activation of Dtx, and (2) Q1 which is localized in a part of the LHC that detaches from PSII upon Dtx

activation at Q2 and which forms an energy sink that amplifies Q2 quenching. It is believed that the persistence of Dtx, even in the dark, is responsible for keeping both quenching sites active and especially Q1, i.e. as long as Dtx is present at Q2 site, FCP (Fucoxanthin Chlorophyll *a*/*c* binding Protein) oligomers cannot reconnect to PSII which generates part of the sustained qI/NPQs (Lavaud and Goss 2014).

Marked differences in NPQ capacity and kinetics were discovered between planktonic diatom species and even between ecotypes isolated from habitats experiencing different degrees of average irradiances and/or light fluctuations. These differences have been attributed either to variation in XC kinetics and/or the amount of LHCX proteins (Lavaud et al. 2007; Dimier et al. 2007; Bailleul et al. 2010; Petrou et al. 2011; Lavaud and Lepetit 2013; Lepetit et al. 2017). The emerging picture from these reports is that a higher/faster Dtx synthesis supports a faster NPQ induction and a higher NPQ capacity in species/ecotypes adapted to habitats characterized by strong light fluctuations and/or average higher irradiance (Lavaud and Goss 2014). One of the specificities is the de novo Dtx synthesis, which in case of prolonged stress light conditions helps to amplify photoprotection via enhanced NPQ and/or ROS scavenging (Lepetit et al. 2010). Species thriving in fluctuating light conditions, for example, exhibit high de novo synthesis of Dtx molecules which correlates well with NPQ development during strong light conditions. Species experiencing a more stable light climate in their natural habitat also synthetize Dtx molecules de novo when shifted to high light conditions but these are probably not involved in NPQ but may rather have an antioxidant function (Lavaud and Lepetit 2013). In addition to a high NPQ capacity and fast Dtx production during oversaturating light conditions, fast relaxation of NPQ in low light conditions is key to track changes in irradiance (Lavaud et al. 2007). As Dtx molecules have to be epoxidized back to Ddx to switch the antenna system from an energy dissipating to a light harvesting mode, diatoms with a high Dtx epoxidation rate dissipate NPQ faster compared to diatoms with a lower epoxidation rate (Goss et al. 2006a; Lavaud and Lepetit 2013). A difference in NPQ capacity can also be attributed to differences in LHCX protein content. The low amount of LHCX1 protein, for instance, explains limited NPQ capacity in a high latitude *Phaeodactylum tricornutum* ecotype isolated from a supralitoral rockpool (P.t.4) which experiences lower average light intensity, and less drastically fluctuating light conditions, compared to other ecotypes (Bailleul et al. 2010). Whereas the *LHCX1* gene is already maximally expressed in low light conditions, several other *LHCX* family members of both centric and pennate diatoms are highly and rapidly upregulated when exposed to high light (Nymark et al. 2009; Park et al. 2010; Zhu and Green 2010; Lepetit et al. 2013) and other stressful environmental conditions that impair photosynthetic capacity (Taddei et al. 2016). These proteins might either confer higher NPQ capacity by binding newly synthetized Dtx molecules and/or be involved in NPQs after prolonged high light exposure (Zhu and Green 2010; Lepetit et al. 2013, 2017).

While our knowledge of NPQ regulation is mostly based on studies of planktonic diatoms, whose light climate is mostly governed by water column turbulence, far less attention has been paid to NPQ regulation in benthic diatoms thriving in, and on, the sediments of intertidal flats (Jesus et al. 2009; Perkins et al. 2010; Cartaxana et al. 2011, 2016b; a; Serôdio et al. 2012; Lavaud and Goss 2014; Ezequiel et al. 2015; Pniewski et al. 2015; Laviale et al. 2015). Like terrestrial plants, these diatoms can experience fast light fluctuations, not buffered by a water column, during low tide. The tidal rhythm, furthermore, can change the light climate drastically as no or very little light reaches the sediments in turbid estuaries when submerged (Underwood and Kromkamp 1999).

NPQ capacity of intertidal benthic diatoms is mainly defined by their ability or inability to avoid excess light energy (Jesus et al. 2009; Cartaxana et al. 2011; Barnett et al. 2015). Diatoms belonging to the raphid clade possess a raphe system that allows movement by secreting extracellular polymer substances (EPS) through the raphe slit. Raphid diatoms can thus migrate vertically into the sediment matrix to a more optimal light climate (Consalvey et al. 2004). In addition, microcycling of motile diatoms within the top layers of the sediments was proposed with algae migrating down to avoid photoinhibition being replaced by others (Kromkamp et al. 1998; Serôdio 2004). Such sequential turnover at the species level was indeed observed in laboratory mesocosms (Paterson 1986) and during an in situ emersion period (Underwood et al. 2005).

In contrast, diatoms living attached or in close association with single sand grains (epipsammic diatoms) are immotile or only capable of limited movement and therefore need to rely on physiological photoprotection (Cartaxana et al. 2011). This can explain a higher de-epoxidation of the Ddx-Dtx cycle pigments in epipsammic communities (Jesus et al. 2009). Barnett et al. (2015) experimentally demonstrated higher NPQ values, coupled with higher Dtx content, in epipsammic diatoms. A more comprehensive comparison between the regulation and kinetics of the NPQ mechanism of both motile and non-motile diatoms, however, has so far not been made.

In this study we demonstrate fast irradiance tuning of NPQ, coupled with fast XC kinetics in the immotile epipsammic diatom species *Opephora guenter-grassii*. We show that this species, in addition to Dtx, also accumulates considerable amounts of the de-epoxidized xanthophyll zeaxanthin (Zx) during a short period (1 h) of high light exposure, a feature so far only observed in planktonic diatoms after prolonged (up to 6 h) periods of oversaturating light conditions (Lohr and Wilhelm 1999). As the high de novo synthesis of de-epoxidized xanthophylls in this species is not paralleled by an equal increase in NPQ, these xanthophylls are not expected to be directly involved in the NPQ mechanism. In contrast, an epipelic species, *Seminavis robusta*, shows a less dynamic NPQ, despite concerted de novo synthesis of both Dtx molecules and LHCX proteins. Our findings add to the physiological underpinning of the differential response of motile and non-motile diatom species (Juneau et al. 2015; Barnett et al. 2015) and of benthic

diatom communities in sediment (Pniewski et al. 2015; Laviale et al. 2015; Cartaxana et al. 2016b) to their environment.

Materials & methods

Culture conditions

Strains were obtained from the diatom culture collection (BCCM/DCG) of the Belgian Coordinated Collection of Micro-organisms (http://bccm.belspo.be), accession numbers *Seminavis robusta* (DCG 0105) and *Opephora guenter-grassii* (DCG 0448), and grown in semi-continuous batch culture in 1.8 L glass Fernbach flasks (Schott) in a day/night rhythm of 16/8 h with a Photosynthetically Available Radiation (PAR) of 20 µmol photons m^{-2} s^{-1}. Cells were cultured in Provasoli's enriched f/2 seawater medium using Tropic Marin artificial sea salt (34.5 g L^{-1}) enriched with $NaHCO_3$ (80 mg L^{-1} final concentration). Cultures were acclimated to these culturing conditions for at least 2 weeks. Chlorophyll *a* (Chl *a*) was measured daily according to Jeffrey and Humphrey (1975) to monitor growth.

High light exposure

Cultures in exponential growth were concentrated to 10 mg Chl *a* L^{-1} by centrifugation (Eppendorf 5810 R) at 4000 RCF for 5 min in 50 mL falcons. The cultures were again acclimated to their growth conditions for 2 h before exposure to high light. Immediately before the experiment started $NaHCO_3$ (4 mM, final concentration) was added from a 2 M stock to prevent carbon limitation during the experiment. Four 65 W white light energy-saving lamps (Lexman) were used to provide high light (HL) conditions (2000 µmol photons m^{-2} s^{-1}) for 1 h. Cells were then allowed to recover for 1 h in low light (LL, 20 µmol photons m^{-2} s^{-1}), provided by one 20 W Lexman energy saving lamp. All light conditions were measured as PAR with a spherical micro quantum sensor (Walz) submerged in the centre of a 10 mg Chl *a* L^{-1} diatom suspension, thus corresponding to the concentrations used during the experiments. Cells were continuously stirred in a glass test tube to obtain a homogenous cell suspension. This glass test tube was cooled in a custom-made glass cooler by a water bath at 20°C.

LHCX protein detection

Sampling was conducted as described by Lepetit et al. (2013). Samples were taken immediately before light exposure (T0), after 1 h HL and after one subsequent h of LL recovery. Protein extraction, SDS-PAGE, Western-blot and ECL immunodetection were carried out as published by Laviale et al. (2015). Both an FCP6 antibody (dilution 1/10,000), anti-FCP6 (LHCX1) from *Cyclotella cryptica* (Westermann and Rhiel 2005), and an anti-LHCSR3 (dilution 1/20,000) from *Chlamydomonas reinhardtii* (Bonente et al. 2011) were tested. Anti-PsbB (CP47, Agrisera) was used as a loading control. Anti-LHCX6 from *T. pseudonana* (Zhu and Green 2010) was not usable for the two investigated species. *Phaeodactylum tricornutum* CCAP 1055/1 (P.t.) samples exposed to HL for 3 h were analysed at the same time as a control.

Pigment analyses

Diatom suspensions were rapidly filtered onto Isopore 1.2 µm RTTP filters (Merck Millipore), immediately frozen in liquid nitrogen and stored at -80°C. Samples were freeze-dried before adding -20°C cold 1.4 mL extraction buffer (90% methanol/0.2 M ammonium acetate (90/10 vol/vol) and 10% ethyl acetate). Pigment extraction was enhanced by adding glass beads (diameter 0.25–0.5 mm, Roth) and vortexing for 30 s. The extracts were sonicated for 30 s on ice at 40% amplitude with 2 s pulse, 1 s rest and filtered over a 0.2 µm filter. One hundred microliters were immediately injected into the HPLC system (Agilent). Samples were analysed according to Van Heukelem and Thomas (2001). As buffered extraction medium was used, no additional TBAA buffer was injected. All pigment concentrations (chlorophyll *c* (Chl *c*), fucoxanthin (Fx), diadinoxanthin (Ddx), diatoxanthin (Dtx), violaxanthin (Vx), antheraxanthin (Ax), zeaxanthin (Zx), chlorophyll *a* (Chl *a*) and β-carotene (β-car)) were calculated by comparison with pigment standards. All standards were obtained from DHI, with exception of Chl *a*, which was obtained from Sigma-Aldrich.

Pulse Amplitude Modulated (PAM) Fluorometry

Chlorophyll fluorescence was measured using a Diving PAM fluorometer (Walz). Saturating flashes (0.4 s, 3600 µmol photons $m^{-2}s^{-1}$) were provided by the internal halogen lamp to measure photosynthetic parameters (see Barnett et al. 2015 for a complete overview of parameters). The duration of 0.4 s for saturating pulses was tested as the best setting for measurement of the maximum photosynthetic efficiency of PSII (F_v/F_m) and effective quantum efficiency of PSII photochemistry ($\Delta F/F_m'$). When applied longer, the maximal fluorescence yield (F_m) is under-estimated which artificially lowers F_v/F_m and $\Delta F/F_m'$. This is most probably due to the high energy delivered by the halogen lamp of the Diving-PAM fluorometer (different from the LEDs used for most other PAM fluorometers). We have applied these settings before (see Barnett et al. 2015) and it provided reliable results. To avoid interference from the HL setup, the lights were switched off immediately before firing a saturating pulse (see Lepetit et al. 2013). The photosynthetic efficiency of PSII ($\Delta F/F_m'$) was calculated as $(F_m'-F')/F_m'$ and expressed as a percentage, taking the maximal photosynthetic efficiency (F_v/F_m), measured immediately before HL onset as 100%. Non-Photochemical Quenching (NPQ) was calculated as $(F_m-F_m')/F_m'$.

Rate estimation and statistics

The $\Delta F/F_m'$ recovery rate constant (k) was calculated by fitting an exponential decay function:

$$\Delta F/F_m'(t) = \Delta F/F_m'rec + [\Delta F/F_m'(0) - \Delta F/F_m'rec]e^{-kt}$$

where t represents time (in min) during recovery and $\Delta F/F_m'(0)$ and $\Delta F/F_m'rec$ represents $\Delta F/F_m'$ (expressed in percentage from the $\Delta F/F_m'$ before HL onset) at the start of the recovery period and after 30 min of recovery in LL respectively (Serôdio et al. 2012). Ddx de-epoxidation, Dtx and Zx epoxidation and the XC de novo synthesis rates were calculated as in Lavaud et al. (2004) using exponential decay functions for epoxidation and de-epoxidation rate constants (k). The Ddx epoxidation, for instance, was fitted as the decrease of Ddx with the exponential decay function:

$$Ddx\ (t) = Ddx_{minimal} + (Ddx_{initial} - Ddx_{minimal})e^{-kt}$$

where t represents time (in min), and $Ddx_{initial}$ and $Ddx_{minimal}$ represent the highest and lowest observed concentrations, respectively. Linear functions were fitted for xanthophyll de novo synthesis rates. Statistical analyses were conducted using the statistical software package SAS 9.4. Species parameters (3 biological replicates per species) were compared using the general linear model PROC GLM. In case of unequal variances, a Welch's t-test was performed.

Results

General characteristics

The epipelic diatom *Seminavis robusta* and epipsammic diatom *Opephora guenter-grassii* were grown under low light (LL) conditions; resulting in a XC pigment pool (Ddx + Dtx) of 4.94 ± 0.45 mol (100 mol Chl *a*)$^{-1}$ for *S. robusta* and 9.88 ± 0.59 mol (100 mol Chl *a*)$^{-1}$ for *O. guenter-grassii*. The maximal PSII quantum yield $\Delta F/F_{m,}$ measured immediately before HL exposure and without dark adaptation, was 0.685 ± 0.031 for *S. robusta* and 0.665 ± 0.017 for *O. guenter-grassii* and did not differ significantly (p = 0.099) between the two species. This indicates that the cells were in an unstressed condition prior to HL exposure, which is also supported by the absence or negligible concentrations of diatoxanthin (Dtx).

PSII quantum yield and NPQ

Both *O. guenter-grassii* and *S. robusta* were exposed to HL for 1 h, after which they were allowed to recover in LL conditions. The quantum yield of PSII ($\Delta F/F_m'$) of both species dropped during HL (Fig. 1a), but was significantly higher for *O. guenter-grassii* at the end of the HL period in comparison with *S. robusta* (p = 0.049, Welch's t-test). During the subsequent low light conditions $\Delta F/F_m'$ of *O. guenter-grassii* recovered about 90 % of its value before HL exposure whereas *S. robusta* recovered less than 75 %. The $\Delta F/F_m'$ recovery rate constant was more than double the rate constant for the epipsammic species (0.096 min^{-1} ± 0.009 compared to 0.040 min^{-1} ± 0.004 for *S. robusta*). At each time point during HL, NPQ was higher in *O. guenter-grassii,* compared to *S. robusta* (Fig. 1b). During the start of the LL period, *O. guenter-grassii* showed very rapid NPQ relaxation, with about half of its NPQ relaxing within 2.5 minutes. Both fast NPQ relaxation and recovery of $\Delta F/F_m'$ slowed down when *O. guenter-grassii* was placed in darkness instead of LL (Fig. 2a&b). NPQ dissipation in *S. robusta* occurred more gradually and was incomplete after 1 h of LL, with a remaining NPQ of 0.504 ± 0.07 compared to 0.188 ± 0.002 for *O. guenter-grassii*.

	S. robusta	*O. guenter-grassii*
Ddx + Dtx content [mol (100 Chl *a*)$^{-1}$]	**4.942** ±0.479	**9.880** ±0.594
Dtx after 60 min HL [mol (100 Chl *a*)$^{-1}$]	**3.146** ±0.424	**5.685** ±1.413
Ddx de-epoxidaton rate [min^{-1}]	**0.081** ±0.017	**0.164** ±0.0521
De novo synthetized Dtx [mol (100 Chl *a*)$^{-1}$]	**1.976** ±0.422	**2.138** ±0.612
Dtx de novo synthesis rate [mmol (mol Chl *a*)$^{-1}$ min^{-1}]	**0.341** ±0.035	**0.444** ±0.065
De novo synthetized Vx cycle pigments [mol (100 Chl *a*)$^{-1}$]	**0.131** ±0.010	**2.043** ±0.216
De novo synthesis rate Vx cycle pigments [mmol (mol Chl *a*)$^{-1}$ min^{-1}]	**0.0185** ±0.009	**0.35** ±0.025
Dtx epoxidation rate in LL [min^{-1}]	**0.08** ±0.01	**0.406** ±0.144
Zx epoxidation rate in LL [min^{-1}]	**n.d.**	**0.311** ±0.060

Table 1: Xanthophyll cycle characteristics. Abbreviations: Chl *a*, Chlorophyll *a*; Ddx, diadinoxanthin; Dtx, diatoxanthin; Vx, violaxanthin; Zx, zeaxanthin. All pigments are expressed as mol (100 mol chlorophyll *a*)$^{-1}$. Epoxidation and de-epoxidation rates are calculated by fitting exponential decay functions. De novo synthesis rates were fitted with linear functions. Values represent averages of three independent measurements ± standard deviations.

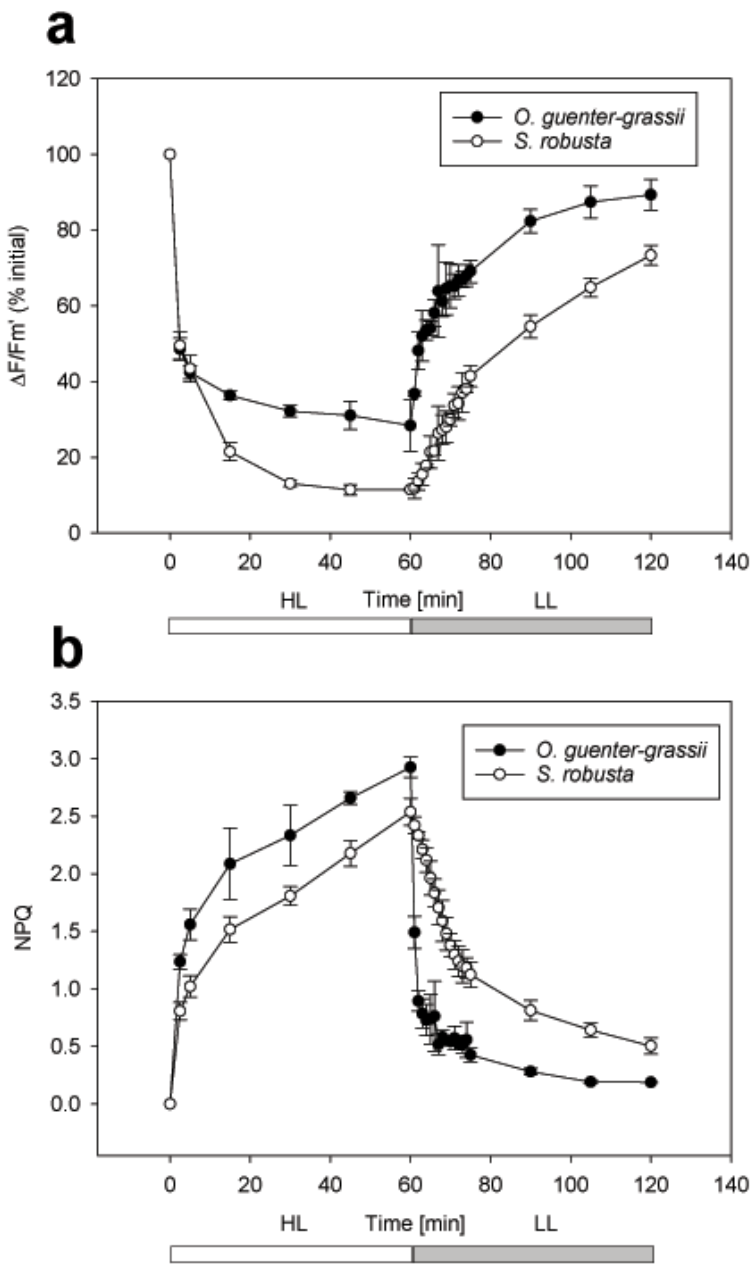

Figure 1a&b: Photophysiological measurements. *O. guenter-grassii* (filled circles) and *S. robusta* (open circles) were exposed to one h of HL (2000 µmol photons m^{-2} s^{-1}) and one subsequent h of recovery in low light (LL, 20 µmol photons m^{-2} s^{-1}). The quantum yield of PSII ($\Delta F/F_m'$) (a), expressed in percentage of the maximal photosynthetic efficiency of PSII (F_v/F_m) before HL exposure and (b) Non-photochemical quenching (NPQ). Values represent averages of three independent measurements ± standard deviations.

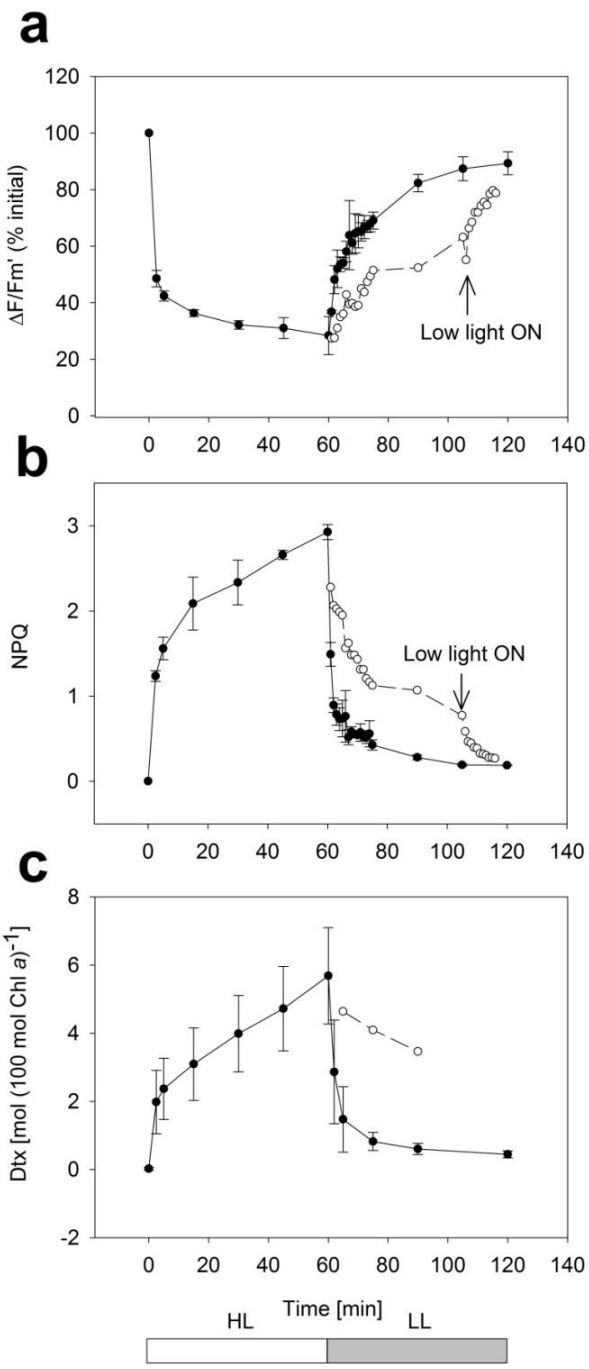

Figure 2: Dark recovery of *O. guenter-grassii* after HL exposure. *O. guenter-grassii* was exposed to 1 h of HL (2000 µmol photons m^{-2} s^{-1}) and one subsequent h of recovery in low light (LL, 20 µmol photons m^{-2} s^{-1})(filled circles) or in dark recovery (open circles) with LL onset at 105 min (indicated by an arrow). (a) Photosynthetic efficiency of PSII $\Delta F/F_m'$ is expressed in percentage of the maximal photosynthetic efficiency of PSII (F_v/F_m) measured before high light onset. (b) Non-photochemical quenching (NPQ) and (c) Dtx, expressed in mol (100 mol Chl *a*)$^{-1}$. Values represent averages of three independent measurements ± standard deviations for the low light recovery treatment. For the dark recovery treatment, only one replicate is plotted.

Xanthophyll cycle characteristics

The higher Ddx-Dtx pool of *O. guenter-grassii* (p = 0.000) resulted in higher Dtx concentrations after 5 minutes of HL (p = 0.0447) (Fig. 3a&b, Table 1). The de-epoxidation state (DES, calculated as Dtx/(Ddx + Dtx)), however, was not significantly different between the species during the HL period (Fig. 4). From 15 minutes onwards the total Ddx + Dtx pool increased (due to de novo synthesis of xanthophylls) with similar rates in both species (Fig. 3a&b, Table 1). During 1 h of HL treatment each species synthetized an additional 2 mol Ddx + Dtx (100 mol Chl a)$^{-1}$. At the end of the HL period *O. guenter-grassii* contained significantly (p = 0.040) more Dtx (5.69 ± 1.41 mol (100 mol Chl a)$^{-1}$) than *S. robusta* (3.15 ± 0.42 mol (100 mol Chl a)$^{-1}$) (Table 1). Due to the lower amount of Dtx originating from de-epoxidation of Ddx in *S. robusta* and similar de novo Dtx synthesis as *O. guenter-grassii*, the relative contribution of de novo synthetized Dtx was about two-thirds of the accumulated Dtx in *S. robusta*, whereas the de novo contribution was only one third in the case of *O. guenter-grassii*.

During the LL recovery period, Dtx was rapidly epoxidized by *O. guenter-grassii*. Its Dtx epoxidation rate constant in LL was about 5 times higher than in *S. robusta* (p = 0.003) (see Table 1), with most Dtx being epoxidized to Ddx within the first 5 min of LL recovery. Epoxidation occurred more gradually in *S. robusta* (Fig. 3a&b). Differences in epoxidation rate resulted in significant differences in de-epoxidation state at 5 (p = 0.022) and 15 min (p = 0.019) during the LL recovery period (Fig. 4). At the end of the recovery period however, nearly all Dtx had disappeared in both species (Fig. 3a&b, Table 1). The fast Dtx epoxidation by *O. guenter-grassii* in LL was not observed in darkness (Fig. 2c). In both species, an increase in the Ddx + Dtx pool was recorded during LL treatment. *O. guenter-grassii* gained 2.26 ± 0.21 mol Ddx + Dtx (100 mol Chl a)$^{-1}$, whereas in *S. robusta* the increase was 1.84 ± 1.10 mol Ddx + Dtx (100 mol Chl a)$^{-1}$ (Table 1).

Besides the Dtx cycle pigments, pigments of the violaxanthin (Vx) cycle were detected in both species during HL (Fig. 3c&d, Table 1). *O. guenter-grassii* accumulated about 2 mol (100 mol Chl a)$^{-1}$ Vx cycle pigments during the HL period (Table 1). At the end of the HL treatment, 1.34 ± 0.19 mol (100 mol Chl a)$^{-1}$ of the de-epoxidized pigment Zeaxanthin (Zx) was detected in *O. guenter-grassii*. The intermediate between Zx and Vx, antheraxanthin (Ax), was also detected during HL (Fig. 3c). In comparison, *S. robusta* accumulated significantly less (p = 0.001) Vx cycle pigments (Fig. 3d) and both Zx and Ax were only present in trace amounts. During the LL recovery period epoxidation of Zx started immediately in *O. guenter-grassii*, resulting in a short peak of Ax (at time point 2.5-5 min) and an increase in Vx. The total Vx cycle pool (Vx + Ax + Zx) decreased markedly for both species during LL with a decrease of 1.62 ± 0.48 mol (100 mol Chl a)$^{-1}$ for *O. guenter-grassii* and a smaller decrease of 0.07 ± 0.02 mol (100 mol Chl a)$^{-1}$ for *S. robusta*. Notably, in *O. guenter-grassii*, Vx cycle pigments decreased as fast during the LL

period as new Ddx cycle pigments were synthetized (0.28 mmol (mol Chl *a*)$^{-1}$ min^{-1} ± 0.08 and 0.36 mmol (mol Chl *a*)$^{-1}$ min^{-1} ± 0.05, respectively). During the course of the experiment no notable changes in Fx, Chl *c* and β-car were observed (Data not shown).

Correlation between Dtx accumulation and NPQ

NPQ correlated well with Dtx mol (100 mol Chl *a*)$^{-1}$ for both species (Fig. 5). They showed similar slopes (0.7-0.8) until about 3 Dtx mol (100 mol Chl *a*)$^{-1}$, after which less NPQ was developed per mol Dtx for *O. guenter-grassii*. The relationship remained true for *S. robusta* during the course of the experiment. Its Dtx content, nevertheless, did not exceed the threshold at which the curve slope changed in *O. guenter-grassii*. The y-axis intercept differed from zero for *S. robusta*, as was reported earlier (Barnett et al. 2015).

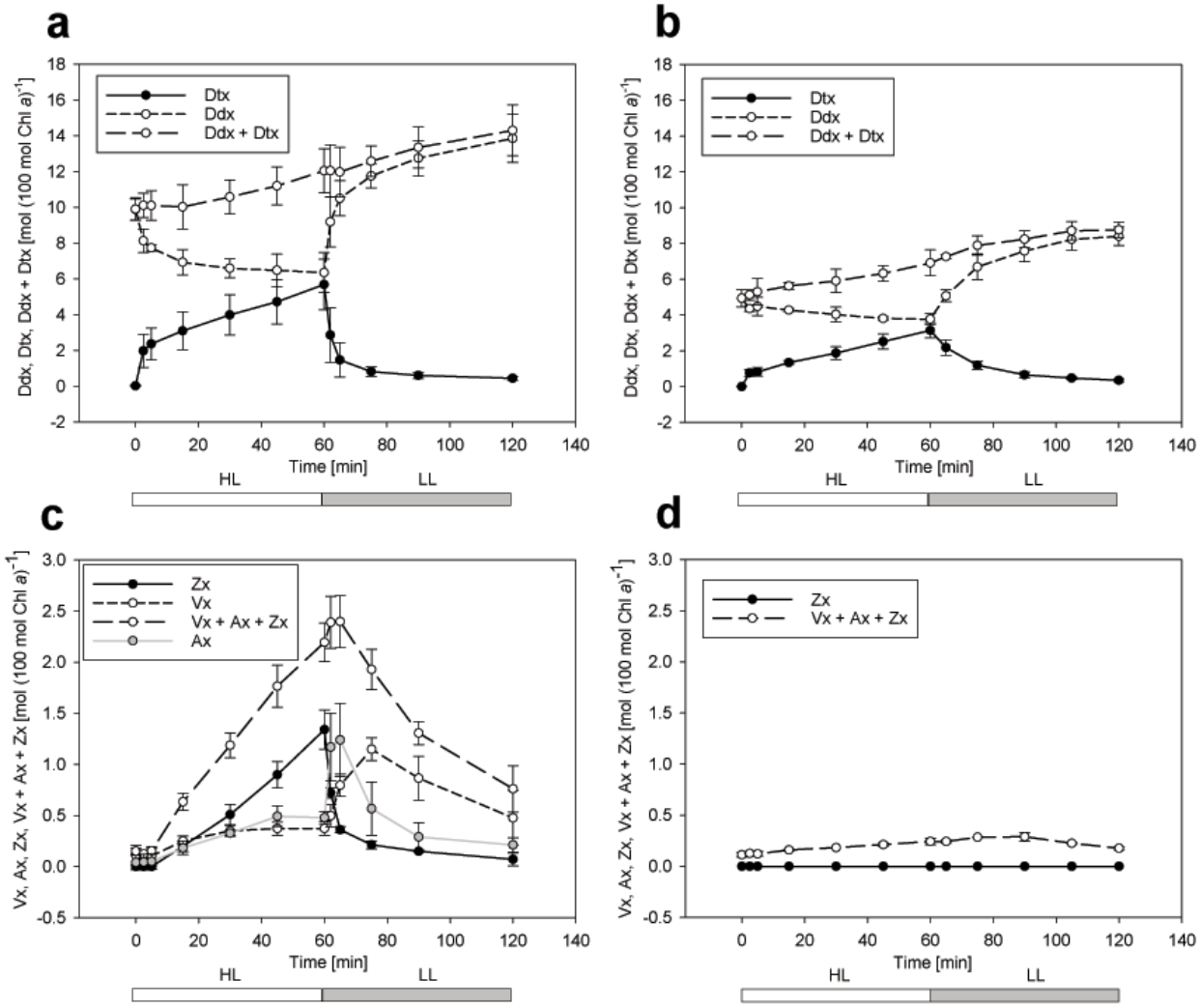

Figure 3a,b,c&d: Xanthophyll cycle kinetics. *O. guenter-grassii* and *S. robusta* were exposed to 1 h of HL (2000 µmol photons m^{-2} s^{-1}) and one subsequent h of recovery in low light (LL, 20 µmol photons m^{-2} s^{-1}). (a) Ddx cycle kinetics of *O. guenter-grassii;* (b) Ddx cycle kinetics of *S. robusta*; (c) Vx cycle kinetics of *O. guenter-grassii*; (d) Vx cycle kinetics of *S. robusta*. Short dashed lines represent the epoxidized pigment (Ddx or Vx) whereas solid lines represent the fully de-epoxidized pigment (Dtx of Zx). The grey line represents the intermediate Ax. Long dashed lines represent the sum of all xanthophylls per cycle. Values represent averages of three independent measurements ± standard deviations.

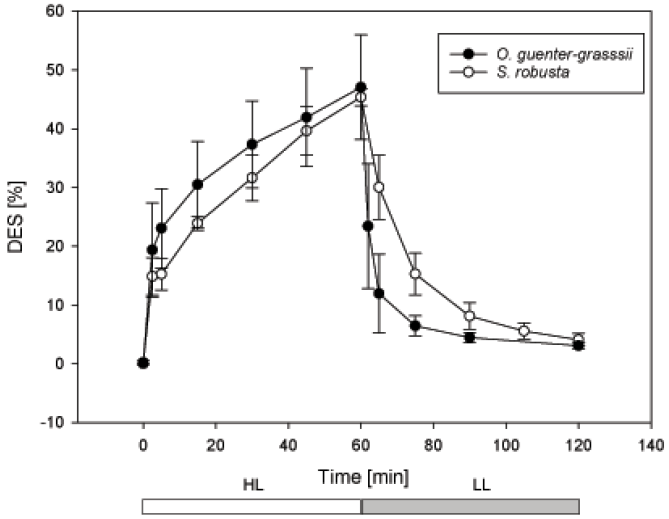

Figure 4: De-epoxidation state of *O. guenter-grassii* and *S. robusta*. *O. guenter-grassii* (filled circles) and *S. robusta* (open circles) were exposed to 1 h of HL (2000 µmol photons m^{-2} s^{-1}) and one subsequent h of recovery in low light (LL, 20 µmol photons m^{-2} s^{-1}). De-epoxidation state (DES) was calculated as 100[Dtx/(Ddx + Dtx)]. Values represent averages of three independent measurements ± standard deviations.

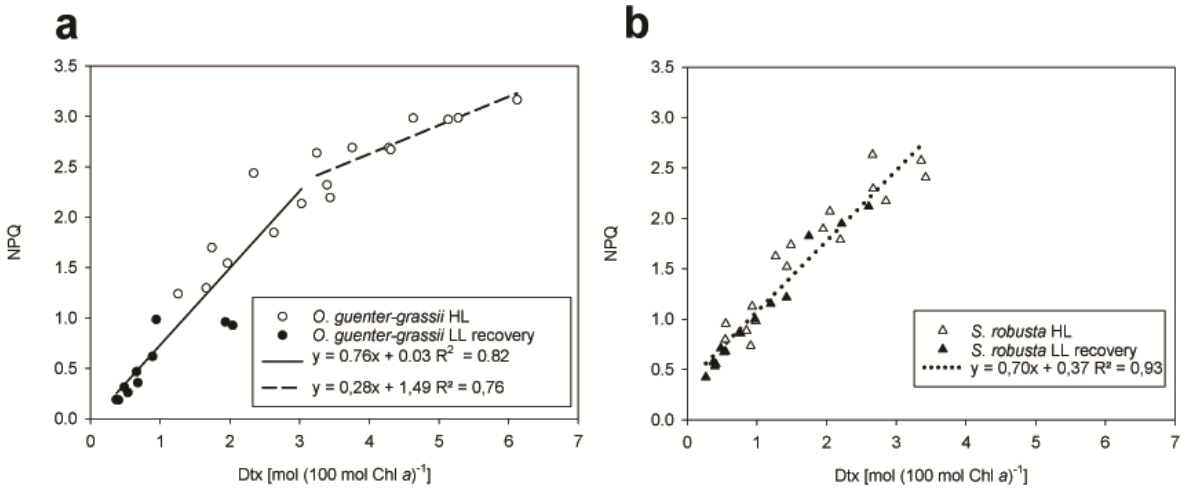

Fig. 5a&b: Relationship between NPQ and Dtx. NPQ is plotted in function of Dtx, sampled at the same timepoints for *O. guenter-grassii* (a, circles) and *S. robusta* (b, triangles), exposed to 1 h of HL (2000 µmol photons m^{-2} s^{-1}) and one subsesquent h of recovery in low light (LL, 20 µmol photons m^{-2} s^{-1}). White symbols represent data points sampled during HL, whereas black symbols represent data points sampled during LL recovery. For *O. guenter-grassii* a distinction is made in the relationship below (solid line, slope $p < 0.001$) and above 3 mol Dtx (100 mol Chl *a*)$^{-1}$ (dashed line, slope $p < 0.001$). The NPQ/Dtx relationship for *S. robusta* is represented by a dotted line (slope $p < 0.001$, intercept $p < 0.001$).

LHCX presence during HL

For immunodetection of LHCX-isoforms, we tested an anti-FCP6 (LHCX1) antibody from *Cyclotella cryptica* (Westermann and Rhiel 2005), and an anti-LHCSR3 antibody from *Chlamydomonas reinhardtii* (Bonente et al. 2011). In *O. guenter-grassii* (Fig. 6a) the best results were obtained using the anti-FCP6 antibody, as less a-specific binding occurred in comparison with the LHCSR3 antibody. Only one LHCX isoform could be detected with a molecular weight close to that of *P. tricornutum* LHCX3 (22.24 KDa). This isoform was apparent in LL acclimated cells and increased in abundance during the 1 h of HL and the subsequent h of recovery in LL.

In *S. robusta* (Fig. 6b) only the anti-LHCSR3 antibody revealed LHCX isoforms. One isoform, with a molecular weight equal to *P. tricornutum* LHCX3 (22.24 KDa) and another more faint band with an equal size to *P. tricornutum* LHCX2 (24.73 KDa) were present in LL acclimated cells. The former increased in abundance during HL and subsequent recovery in LL. After 1 h of HL, moreover, two additional LHCX isoforms could be detected. An LHCX isoform of about 23 KDa was clearly present after 1 h of HL and after the additional recovery period. The second one, about the size of LHCX1 in *P. tricornutum* (21.95 KDa), became visible after 1 h of HL.

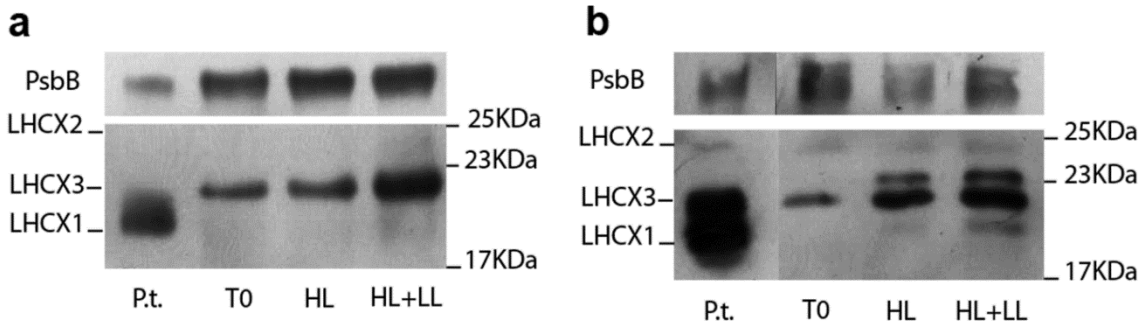

Figure 6a&b: Western blot of LHCX proteins. Western blot of (a) *O. guenter-grassii* using an FCP6 antibody and (b) *S. robusta* using anti-LHCSR3 sampled before (T0) exposure to HL (2000 µM photons m^{-2} s^{-1}), after 1 h of HL (HL) and after 1 h of recovery in LL (20 µM photons m^{-2} s^{-1}) (HL + LL). An antibody against the plastid encoded PsbB (CP47) protein was used as a loading control. *Phaeodactylum tricornutum* (P.t.) samples which were exposed to HL for 3 h were analysed at the same time as a control. *Phaeodactylum* samples showed three LHCX bands using the LHCSR3 antibody which were previously identified as LHCX1, LHCX2 and LHCX3 (Lepetit et al., 2013). Identification of P.t. LHCX2&3 was less clear using the FCP6 antibody in (a).

Discussion

In this study we demonstrate marked differences in irradiance tuning of NPQ and associated XC pigment and LHCX protein dynamics between a motile and a non-motile marine benthic diatom. The non-motile species (*O. guenter-grassii*) exhibits a dynamic and strong high-energy quenching (qE), coupled to fast XC kinetics and pronounced synthesis of de-epoxidized xanthophylls, including zeaxanthin. In this species, strong physiological photoprotection may compensate for its lack of motility as a way to avoid oversaturating light conditions. The motile species (*S. robusta*) on the other hand exhibited an overall lower qE capacity, even though NPQ increased during the light period, possibly due to de novo synthesis of both Dtx and LHCX proteins.

Prior to the experiments, both species were acclimated to low light conditions, to avoid the presence of Dtx and NPQ in cultures, as much as possible, which could bias the measurement of F_m. These growth conditions resulted in similar XC content as observed by Barnett et al. (2015) under identical light conditions for the same benthic species used in this study, and also as observed for a range of planktonic species grown in a PAR of 40 µmol photons $m^{-2}s^{-1}$ (Lavaud et al. 2004). The non-motile epipsammic species *O. guenter-grassii* showed higher NPQ during high light exposure, compared to the epipelic diatom *S. robusta*. As reported by Barnett et al. (2015), higher NPQ values coincided with a higher overall Dtx content de-epoxidized from a larger initial Ddx pool, rather than a higher de-epoxidation state (DES) or a higher involvement of Dtx molecules in the NPQ mechanism (Lavaud and Lepetit 2013). Indeed, we did not observe a difference in DES between *O. guenter-grassii* and *S. robusta*, nor a difference in the slopes of the NPQ/Dtx plots. Note that Jesus et al. (2009), working on natural epipelic and epipsammic communities, did observe a difference in DES between both, but this may have been due to high light avoidance by vertical migration and/or microcycling in the epipelic communities, which was impeded in our study.

Accumulation of Dtx, independent from Ddx de-epoxidation, was observed for both species during high light exposure as reported for planktonic diatoms (Lavaud et al. 2004; Lavaud and Lepetit 2013) and natural epipelic communities (Laviale et al. 2015). The rate constant of this de novo Dtx synthesis was similar for both species and in the range of planktonic diatoms exposed to the same HL conditions (Lavaud et al. 2004), resulting in the same increase of the Ddx + Dtx pool. The XC pool at the end of the HL period, nonetheless, was still relatively low for both species, as up to 26 mol Ddx + Dtx (100 mol Chl *a*)$^{-1}$ were observed by Lohr and Wilhelm (1999) in *Cyclotella meneghiniana* and even up to 30-40 Ddx + Dtx (100 mol Chl *a*)$^{-1}$ in *Chaetoceros socialis* (Dimier et al. 2007). These large XC pools, however, required a prolonged exposure (i.e., several h) to high irradiances, whereas in this study the HL period was relatively short (1 h). In the diatoms *Plagiogramma staurophorum* and *Brockmanniella brockmannii*, nonetheless,

acclimation to a PAR of 75 µmol photons $m^{-2}s^{-1}$ resulted in XC pools higher than 25 Ddx + Dtx (100 mol Chl *a*)$^{-1}$ (Barnett et al. 2015).

The involvement of de novo synthetized Dtx differed between both species. Whereas the NPQ-Dtx relationship remained true for *S. robusta*, de novo synthetized Dtx in *O. guenter-grassii* did not contribute equally to the NPQ mechanism, as shown by a decline in the NPQ-Dtx relationship. Part of this additionally synthetized Dtx is possibly present in the lipid matrix of the thylakoid membrane (Schumann et al. 2007) to prevent lipid peroxidation (Lepetit et al. 2010). It should be noted, however, that the total Dtx values observed for *S. robusta* during our experiments remained rather low compared to values recorded for other species using a similar setup (Lavaud et al. 2004; Lepetit et al. 2013; Lavaud and Lepetit 2013) and might be due to a small Ddx pool before HL onset (Lavaud et al. 2004). A stable NPQ/Dtx slope during de novo synthesis of Dtx, as observed in *S. robusta*, nonetheless, may indicate synthesis of new Dtx-binding proteins such as LHCXs (Lepetit et al. 2013).

As fast epoxidation of Dtx is crucial to switch the light harvesting system from an energy dissipation state to a light harvesting state, we monitored NPQ relaxation and Dtx epoxidation during low light following high light exposure. *O. guenter-grassii* displayed very rapid Dtx epoxidation coupled with an equally fast NPQ relaxation, but not during dark recovery, as previously reported (Goss et al. 2006b). This is also demonstrated by the fast recovery of PSII quantum yield in low light, which is severely restricted in darkness as the epoxidation reaction is possibly slowed down by NADPH depletion (Goss et al. 2006b). The fast reversal of NPQ and nearly complete recovery of PSII quantum yield, moreover, indicate that the observed high NPQ values comprise mostly qE while qI/NPQs is virtually absent.

A fast switch from energy dissipation to light harvesting after high light exposure was not observed in the epipelic diatom *S. robusta*, where Dtx epoxidation and coupled NPQ relaxation occurred more gradually. Together with an incomplete and slower recovery of PSII quantum yield our data demonstrate a higher susceptibility to photoinhibition during prolonged high light as has been shown for species isolated from habitats lacking strong light fluctuations (Goss et al. 2006b; Su et al. 2012; Lavaud and Lepetit 2013). The observed NPQ values, increasing during the high light treatment, therefore comprise not only qE but also a significant fraction of qI due to PSII photoinactivation and damage (since Dtx is almost fully converted back to Ddx).

Even though both *S. robusta* and *O. guenter-grassii* accumulated similar amounts of newly synthetized Dtx within 1 h of high light, the latter synthetized the same amount of Vx cycle and Dtx cycle pigments, including Zx. The presence of a parallel Vx-Ax-Zx cycle has been demonstrated in several algae possessing the Ddx-Dtx cycle, including the diatom species *C. meneghiniana* and *P. tricornutum* (Lohr & Wilhelm, 1999). Zx accumulation in these species, however, required prolonged (up to 6 h) high light

exposure (Lohr and Wilhelm 1999, 2001) and has never been reported in studies on *P. tricornutum* using similar PAR and exposure time (i.e. within 1 h, 2000 µmol photons $m^{-2}s^{-1}$) as used in this study (Lavaud et al. 2004; Domingues et al. 2012; Lepetit et al. 2013; Lavaud and Lepetit 2013). Epoxidation of Zx in low light was as fast as Dtx epoxidation, while the second epoxidation step occurred more slowly, resulting in a transient peak in the intermediate Ax. This transient peak in Ax has been reported before for the green alga *Chlorella* (Goss et al. 2006a). The Vx cycle pool of *O. guenter-grassii* declined during the 1 h recovery period and to a lesser degree also in *S. robusta*, whereas a similar Vx cycle pool decline in *P. tricornutum* was not observed within 1 h of low light recovery (Lohr & Wilhelm, 1999). The high amount of Vx cycle pigments synthetized by *O. guenter-grassii* in high light may have been converted to Ddx during the recovery period, as the decline in Vx cycle pigments was paralleled by an equal increase in Ddx + Dtx. A pathway from Vx to Ddx through the intermediate neoxanthin has been proposed by Dambek et al. (2012). In *S. robusta*, however, more Ddx + Dtx accumulated during the LL period than was lost from the Vx cycle pool. This might be due to additional synthesis of Ddx cycle pigments during low light, even though additional de novo synthesis in low light conditions is considered to be low (Lohr & Wilhelm, 1999). According to Lohr and Wilhelm (1999, 2001), the primary role of Vx cycle pigments in diatoms is not photoprotection as they mainly serve as intermediates in Ddx and fucoxanthin production. Increasing the light intensity, nonetheless, changes the allocation of newly synthesized xanthophylls to the Vx-Ax-Zx pool in *P. tricornutum* (Lohr and Wilhelm 1999). Moreover, Vx cycle pigments are mostly detected in algae displaying high de novo xanthophyll synthesis combined with high de-epoxidase activity. This fits with our observations of *O. guenter-grassii*, de novo synthetizing substantially more xanthophylls (considering both Ddx and Zx cycle pigments) and de-epoxidising more Ddx to Dtx during HL than *S. robusta*. We do not expect Zx to be directly involved in the NPQ mechanism of *O. guenter-grassii* as the NPQ/Dtx relationship decreased during de novo synthesis of both xanthophylls. In higher plants, Zx can dissolve in the thylakoid membrane lipids instead of being protein bound (Jahns et al. 2009), scavenging reactive oxygen species with a higher capacity than other xanthophylls found in higher plants (Havaux et al. 2007), or possibly regulating membrane fluidity (Havaux and Gruszecki 1993).

As LHCX proteins play a central role in the NPQ mechanism of diatoms (Bailleul et al. 2010; Zhu and Green 2010; Lepetit et al. 2013), we compared LHCX synthesis for the first time between an epipsammic and an epipelic diatom. We could detect only one LHCX isoform (~22 kDa) in the epipsammic model *O. guenter-grassii* using the FCP6 antibody. It did not strongly react to a shift to high light and was more abundant in subsequent low light. The epipelic diatom *S. robusta*, however, revealed two out of four isoforms which strongly reacted to HL: one isoform with MW ~23 kDa and a second one with MW ~19 kDa. However, aspecific binding of the used antibody or MW differences due to post-translational modifications (e.g. phosphorylation, see Bonente et al. 2011) could

not be excluded. Interestingly, in epipelic communities, a 23 kDa isoform was shown to positively reacts to high light, high temperature and motility inhibition (Laviale et al. 2015). The two isoforms already present in low light might provide benthic diatoms with a basic NPQ to rapidly cope with sudden changes in light climate, as has been demonstrated for LHCX1 of *P. tricornutum* (Bailleul et al., 2010). However, the *S. robusta* genome does not contain a close homolog to the *P. tricornutum LHCX1* gene at the sequence level (L. Blommaert et al., data not shown). LHCXs which are strongly upregulated during high light have been suspected to either bind de novo synthetized Dtx, conferring higher NPQ and/or participate in a sustained component of NPQ (NPQs) after prolonged high light exposure (Zhu and Green 2010; Lepetit et al. 2013, 2017). As *S. robusta* accumulates novel Dtx during HL while its NPQ increases, the two observed light-responsive LHCX isoforms may be responsible for Dtx binding, as suggested by Zhu and Green (2010), and (Lepetit et al. 2013, 2017). However, other FCP proteins may be responsible as for instance the *LHCR6* and *LHCR8* (Light-Harvesting Complex Red lineage) genes are strongly upregulated in *P. tricornutum*, upon a shift to high light (Nymark et al. 2009).

Ecological implications

A fast and strong irradiance-tuning of NPQ is to be expected in immotile epipsammic diatoms as they live attached to sand grains (Ribeiro et al. 2013) and are unable to move away from oversaturating light conditions. Furthermore, sandy sediments are characterized by strong light scattering in the uppermost layers, thereby increasing the average incident irradiance to which these diatoms are exposed (Kuhl et al. 1994; Cartaxana et al. 2016b). Even though our epipsammic species was acclimated to low PAR (20 µmol photons $m^{-2}s^{-1}$) it was able to cope with a sudden change to a light intensity similar to full sunlight. Similar transitions from low to full sunlight (and vice versa) can be common in sandy sediments during low tide (Hamels et al. 1998). Given the prolonged harsh light conditions in these sediments, epipsammic diatoms probably demonstrate a high de novo synthesis of photoprotective xanthophylls in situ, including Zx. This can also explain the previously observed discrepancy between high Zx content and absence of colonial cyanobacteria (containing Zx) in sandy sediments, as reported in Hamels et al. (1998). Taken together, our results suggest that epipsammic diatoms use a combination of distinct photoprotective strategies described by Lavaud and Lepetit (2013) to cope with the light climate of sandy intertidal sediments: (1) a strong and fast reversible qE to track light fluctuations, combined with (2) high de novo synthesis of de-epoxidized xanthophylls, probably unbound to the LHC antenna system, which may fulfil an anti-oxidant function during prolonged light conditions. Even though our study was performed on only one epipsammic representative, a strong qE and a relatively higher XC pool (compared to epipelic species) seem to be general for epipsammic species (Barnett et al. 2015).

The epipelic model *S. robusta* displayed a lower NPQ consisting partly of photoinhibition (qI). This is expected as epipelic diatoms use vertical migration and/or microcycling as their primary photoprotection mechanism when motility is allowed (Kromkamp et al. 1998; Serôdio 2004; Perkins et al. 2010; Cartaxana et al. 2011; Serôdio et al. 2012; Laviale et al. 2015). Furthermore, vertical migration is fast enough to reduce the amount of absorbed photons and can operate simultaneously with NPQ induction (Laviale et al. 2016). Both synthesis of new Dtx pigments and LHCX proteins, nonetheless, have been shown in epipelic communities under high light conditions (Laviale et al. 2015), which is in line with our findings. Furthermore, our data suggests the involvement of light-regulated LHCX proteins during harsh light conditions, allowing epipelic species to acclimate to prolonged higher light conditions (Ezequiel et al. 2015; Barnett et al. 2015). Hence, although adapted to a habitat with more cohesive sediments, characterized by a strongly attenuated photic zone (Cartaxana et al. 2016b), epipelic diatoms still possess the ability to increase their low basal photoprotective ability. The fact that epipelic species have been shown to emerge at the sediment surface at different times during tidal emersion suggests that they have different species-specific light niches (Paterson 1986; Underwood et al. 2005). As a result, their capacity for physiological photoprotection is also expected to differ between species. Future studies, therefore, should focus on the interspecific differences in the balance between behavioural and physiological photoprotection.

Acknowledgements

The authors would like to thank the Research Foundation Flanders (FWO project G.0222.09N), Ghent University (BOF-GOA 01G01911) and the Egide/Campus France-PHC Tournesol (n128992UA) exchange program for their financial support. JL also thanks the CNRS and the French consortium CPER Littoral for their financial support. M.J.J.H. acknowledges a Postdoctoral Fellowship of the Research Foundation Flanders.

References

Armbrust, E. V. 2009. The life of diatoms in the world's oceans. Nature **459**: 185–92. doi:10.1038/nature08057

Bailleul, B., A. Rogato, A. De Martino, S. Coesel, P. Cardol, C. Bowler, A. Falciatore, and G. Finazzi. 2010. An atypical member of the light-harvesting complex stress-related protein family modulates diatom responses to light. Proc. Natl. Acad. Sci. **107**: 18214–18219. doi:10.1073/pnas.1007703107

Barnett, A., V. Méléder, L. Blommaert, and others. 2015. Growth form defines physiological photoprotective capacity in intertidal benthic diatoms. ISME J. **9**: 32–45. doi:10.1038/ismej.2014.105

Bonente, G., M. Ballottari, T. B. Truong, T. Morosinotto, T. K. Ahn, G. R. Fleming, K. K. Niyogi, and R. Bassi. 2011. Analysis of LhcSR3, a protein essential for feedback de-excitation in the green alga *Chlamydomonas reinhardtii*. T. Shikanai [ed.]. PLoS Biol. **9**: e1000577. doi:10.1371/journal.pbio.1000577

Brunet, C., and J. Lavaud. 2010. Can the xanthophyll cycle help extract the essence of the microalgal functional response to a variable light environment? J. Plankton Res. **32**: 1609–1617. doi:10.1093/plankt/fbq104

Cartaxana, P., S. Cruz, C. Gameiro, and M. Kühl. 2016a. Regulation of intertidal microphytobenthos photosynthesis over a diel emersion period is strongly affected by diatom migration patterns. Front. Microbiol. **7**: 872. doi:10.3389/fmicb.2016.00872

Cartaxana, P., L. Ribeiro, J. Goessling, S. Cruz, and M. Kühl. 2016b. Light and O_2 microenvironments in two contrasting diatom-dominated coastal sediments. Mar. Ecol. Prog. Ser. **545**: 35–47. doi:10.3354/meps11630

Cartaxana, P., M. Ruivo, C. Hubas, I. Davidson, J. Serôdio, and B. Jesus. 2011. Physiological versus behavioral photoprotection in intertidal epipelic and epipsammic benthic diatom communities. J. Exp. Mar. Bio. Ecol. **405**: 120–127. doi:10.1016/j.jembe.2011.05.027

Consalvey, M., D. M. Paterson, and G. J. C. Underwood. 2004. The ups and downs of life in a benthic biofilm: Migration of benthic diatoms. Diatom Res. **19**: 181–202.

Dambek, M., U. Eilers, J. Breitenbach, S. Steiger, C. Büchel, and G. Sandmann. 2012. Biosynthesis of fucoxanthin and diadinoxanthin and function of initial pathway genes in *Phaeodactylum tricornutum*. J. Exp. Bot. **63**: 5607–5612. doi:10.1093/jxb/ers211

Dimier, C., F. Corato, F. Tramontano, and C. Brunet. 2007. Photoprotection and xanthophyll cycle activity in three marine diatoms. J. Phycol. **43**: 937–947. doi:10.1111/j.1529-8817.2007.00381.x

Domingues, N., A. R. Matos, J. Marques da Silva, and P. Cartaxana. 2012. Response of the diatom *Phaeodactylum tricornutum* to photooxidative stress resulting from high light exposure. PLoS One **7**: e38162. doi:10.1371/journal.pone.0038162

Ezequiel, J., M. Laviale, S. Frankenbach, P. Cartaxana, and J. Serôdio. 2015. Photoacclimation state determines the photobehaviour of motile microalgae: The case of a benthic diatom. J. Exp. Mar. Bio. Ecol. **468**: 11–20. doi:10.1016/j.jembe.2015.03.004

Goss, R., and B. Lepetit. 2015. Biodiversity of NPQ. J. Plant Physiol. **172**: 13–32. doi:10.1016/j.jplph.2014.03.004

Goss, R., B. Lepetit, and C. Wilhelm. 2006a. Evidence for a rebinding of antheraxanthin to the light-harvesting complex during the epoxidation reaction of the violaxanthin cycle. J. Plant Physiol. **163**: 585–590. doi:10.1016/j.jplph.2005.07.009

Goss, R., E. A. Pinto, C. Wilhelm, and M. Richter. 2006b. The importance of a highly active and ΔpH-regulated diatoxanthin epoxidase for the regulation of the PS II antenna function in diadinoxanthin cycle containing algae. J. Plant Physiol. **163**: 1008–1021. doi:10.1016/j.jplph.2005.09.008

Hamels, I., K. Sabbe, K. Muylaert, C. Barranguet, C. Lucas, P. Herman, and W. Vyverman. 1998. Organisation of microbenthic communities in intertidal estuarine flats, a case study from the molenplaat (Westerschelde estuary, The Netherlands). Eur. J. Protistol. **34**: 308–320. doi:10.1016/S0932-4739(98)80058-8

Havaux, M., L. Dall'osto, and R. Bassi. 2007. Zeaxanthin has enhanced antioxidant capacity with respect to all other xanthophylls in Arabidopsis leaves and functions independent of binding to PSII antennae. Plant Physiol. **145**: 1506–1520. doi:10.1104/pp.107.108480

Havaux, M., and W. I. Gruszecki. 1993. Heat and light induced chlorophull a fluorescence changes in potato leaves containign high or low levels of the carotenoid zeaxanthin: indications of a regulatory effect of zeaxanthin on thylakoid fluidity. Photochem. Photobiol. **58**: 607–614. doi:10.1111/j.1751-1097.1993.tb04940.x

Van Heukelem, L., and C. S. Thomas. 2001. Computer-assisted high-performance liquid chromatography method development with applications to the isolation and analysis of phytoplankton pigments. J. Chromatogr. A **910**: 31–49. doi:10.1016/S0378-4347(00)00603-4

Horton, P., and A. Hague. 1988. Studies on the induction of chlorophyll fluorescence in isolated barley protoplasts. IV. Resolution of non - photochemical quenching. Biochim. Biophys. Acta **932**: 107–115.

Jahns, P., D. Latowski, and K. Strzalka. 2009. Mechanism and regulation of the violaxanthin cycle: the role of antenna proteins and membrane lipids. Biochim. Biophys. Acta **1787**: 3–14. doi:10.1016/j.bbabio.2008.09.013

Janknegt, P. J., C. M. De Graaff, W. H. Van De Poll, R. J. W. Visser, E. W. Helbling, and A. G. J. Buma. 2009a. Antioxidative responses of two marine microalgae during acclimation to static and fluctuating natural uv radiation. Photochem. Photobiol. **85**: 1336–1345. doi:10.1111/j.1751-1097.2009.00603.x

Janknegt, P. J., C. M. De Graaff, W. H. Van De Poll, R. J. W. Visser, J. W. Rijstenbil, and A. G. J. Buma. 2009b. Short-term antioxidative responses of 15 microalgae exposed to excessive irradiance including ultraviolet radiation. Eur. J. Phycol. **44**: 525–539. doi:10.1080/09670260902943273

Janknegt, P. J., W. H. van de Poll, R. J. W. Visser, J. W. Rijstenbil, and A. G. J. Buma. 2008. Oxidative stress responses in the marine antarctic diatom *Chaetoceros Brevis* (Bacillariophyceae) during photoacclimation. J. Phycol. **44**: 957–966. doi:10.1111/j.1529-8817.2008.00553.x

Jeffrey, S. W., and G. S. Humphrey. 1975. New spectrophotometric equations for determining

chlorophylls *a*, *b*, *c*1 and *c*2 in higher plants, algae and natural phytoplankton. Biochem. Physiol. Pflanz. Bd. **167**: 191–194.

Jesus, B., V. Brotas, L. Ribeiro, C. R. Mendes, P. Cartaxana, and D. M. Paterson. 2009. Adaptations of microphytobenthos assemblages to sediment type and tidal position. Cont. Shelf Res. **29**: 1624–1634. doi:10.1016/j.csr.2009.05.006

Juneau, P., A. Barnett, V. Méléder, C. Dupuy, and J. Lavaud. 2015. Combined effect of high light and high salinity on the regulation of photosynthesis in three diatom species belonging to the main growth forms of intertidal flat inhabiting microphytobenthos. J. Exp. Mar. Bio. Ecol. **463**: 95–104. doi:10.1016/j.jembe.2014.11.003

Kromkamp, J. C., C. Barranguet, and J. Peene. 1998. Determination of microphytobenthos PSII quantum efficiency and photosynthetic activity by means of variable chlorophyll fluorescence. Mar. Ecol. Prog. Ser. **162**: 45–55. doi:10.3354/meps162045

Kuhl, M., C. Lassen, and B. B. Jorgensen. 1994. Light penetration and light intensity in sandy marine sediments measured with irradiance and scalar irradiance fiber-optic microprobes. Mar. Ecol. Prog. Ser. **105**: 139–148. doi:10.3354/meps105139

Lavaud, J., and R. Goss. 2014. The peculiar features of the non-photochemical fluorescence quenching in diatoms and brown algae, p. 421–443. *In* B. Demmig-Adams, G. Garab, W. Adams III, and Govindjee [eds.], Non-Photochemical Quenching and Energy Dissipation in Plants, Algae and Cyanobacteria. Springer.

Lavaud, J., and B. Lepetit. 2013. An explanation for the inter-species variability of the photoprotective non-photochemical chlorophyll fluorescence quenching in diatoms. Biochim. Biophys. Acta **1827**: 294–302. doi:10.1016/j.bbabio.2012.11.012

Lavaud, J., B. Rousseau, and A.-L. Etienne. 2004. General features of photoprotection by energy dissipation in planktonic diatoms (Bacillariophyceae). J. Phycol. **40**: 130–137. doi:10.1046/j.1529-8817.2004.03026.x

Lavaud, J., C. Six, and D. A. Campbell. 2016. Photosystem II repair in marine diatoms with contrasting photophysiologies. Photosynth. Res. **127**: 189–199. doi:10.1007/s11120-015-0172-3

Lavaud, J., R. F. Strzepek, and P. G. Kroth. 2007. Photoprotection capacity differs among diatoms : Possible consequences on the spatial distribution of diatoms related to fluctuations in the underwater light climate. Limnol. Oceanogr. **52**: 1188–1194.

Laviale, M., A. Barnett, J. Ezequiel, B. Lepetit, S. Frankenbach, V. Méléder, J. Serôdio, and J. Lavaud. 2015. Response of intertidal benthic microalgal biofilms to a coupled light-temperature stress: evidence for latitudinal adaptation along the Atlantic coast of Southern Europe. Environ. Microbiol. **17**: 3662–3677. doi:10.1111/1462-2920.12728

Laviale, M., S. Frankenbach, and J. Serôdio. 2016. The importance of being fast: comparative kinetics of vertical migration and non-photochemical quenching of benthic diatoms under light stress. Mar. Biol. **163**: 10. doi:10.1007/s00227-015-2793-7

Lepetit, B., G. Gélin, M. Lepetit, and others. 2017. The diatom *Phaeodactylum tricornutum* adjusts nonphotochemical fluorescence quenching capacity in response to dynamic light via fine-tuned Lhcx and xanthophyll cycle pigment synthesis. New Phytol. **214**: 205–218. doi:10.1111/nph.14337

Lepetit, B., S. Sturm, A. Rogato, A. Gruber, M. Sachse, A. Falciatore, P. G. Kroth, and J. Lavaud. 2013. High light acclimation in the secondary plastids containing diatom *Phaeodactylum tricornutum* is triggered by the redox state of the plastoquinone pool. Plant Physiol. **161**: 853–865. doi:10.1104/pp.112.207811

Lepetit, B., D. Volke, M. Gilbert, C. Wilhelm, and R. Goss. 2010. Evidence for the existence of one antenna-associated, lipid-dissolved and two protein-bound pools of diadinoxanthin cycle pigments in diatoms. Plant Physiol. **154**: 1905–1920. doi:10.1104/pp.110.166454

Lohr, M., and C. Wilhelm. 1999. Algae displaying the diadinoxanthin cycle also possess the violaxanthin cycle. Proc. Natl. Acad. Sci. **96**: 8784–8789. doi:10.1073/pnas.96.15.8784

Lohr, M., and C. Wilhelm. 2001. Xanthophyll synthesis in diatoms: quantification of putative intermediates and comparison of pigment conversion kinetics with rate constants derived from a model. Planta **212**: 382–391. doi:10.1007/s004250000403

MacIntyre, H. L., T. M. Kana, T. Anning, and R. J. Geider. 2002. Photoacclimation of photosynthesis irradiance response curves and photosynthetic pigments in macroalgae and cyanobacteria. J. Phycol. **38**: 17–38. doi:10.1046/j.1529-8817.2002.00094.x

Nymark, M., K. C. Valle, T. Brembu, K. Hancke, P. Winge, K. Andresen, G. Johnsen, and A. M. Bones. 2009. An integrated analysis of molecular acclimation to high light in the marine diatom *Phaeodactylum tricornutum*. PLoS One **4**: e7743. doi:10.1371/journal.pone.0007743

Owens, T. G. 1986. Light-harvesting function in the diatom *Phaeodactylum tricornutum* II. distribution of excitation energy between photosystems. **80**: 739–746.

Park, S., G. Jung, Y. Hwang, and E. Jin. 2010. Dynamic response of the transcriptome of a psychrophilic diatom, *Chaetoceros neogracile*, to high irradiance. Planta **231**: 349–60. doi:10.1007/s00425-009-1044-x

Paterson, D. M. 1986. The migratory behaviour of diatom assemblages in a laboratory tidal micro-ecosystem examined by low temperature scanning electron microscopy. Diatom Res. **1**: 227–239. doi:10.1080/0269249X.1986.9704971

Perkins, R. G., J. C. Kromkamp, J. Serôdio, J. Lavaud, B. Jesus, J.-L. Mouget, S. Lefebvre, and R. M. Forster. 2011. The application of variable chlorophyll fluorescence to microphytobenthic biofilms, p. 237–275. *In* D.J. Suggett, M.A. Borowitzka, and O. Prášil [eds.], Chlorophyll *a* Fluorescence in Aquatic Sciences: Methods and Applications. Springer Netherlands.

Perkins, R. G., J. Lavaud, J. Serôdio, and others. 2010. Vertical cell movement is a primary response of intertidal benthic biofilms to increasing light dose. Mar. Ecol. Prog. Ser. **416**: 93–103. doi:10.3354/meps08787

Petrou, K., M. A. Doblin, and P. J. Ralph. 2011. Heterogeneity in the photoprotective capacity of three Antarctic diatoms during short-term changes in salinity and temperature. Mar. Biol. **158**: 1029–1041. doi:10.1007/s00227-011-1628-4

Pniewski, F. F., P. Biskup, I. Bubak, P. Richard, A. Latała, and G. Blanchard. 2015. Photo-regulation in microphytobenthos from intertidal mudflats and non-tidal coastal shallows. Estuar. Coast. Shelf Sci. **152**: 153–161. doi:10.1016/j.ecss.2014.11.022

Ribeiro, L., V. Brotas, Y. Rincé, and B. Jesus. 2013. Structure and diversity of intertidal benthic diatom assemblages in contrasting shores: a case study from the Tagus estuary. J. Phycol.

49: 258–270. doi:10.1111/jpy.12031

Schumann, A., R. Goss, T. Jakob, and C. Wilhelm. 2007. Investigation of the quenching efficiency of diatoxanthin in cells of *Phaeodactylum tricornutum* (Bacillariophyceae) with different pool sizes of xanthophyll cycle pigments. Phycologia **46**: 113–117. doi:10.2216/06-30.1

Serôdio, J. 2004. Analysis of variable chlorophyll fluorescence in microphytobenthos assemblages: implications of the use of depth-integrated measurements. Aquat. Microb. Ecol. **36**: 137–152. doi:10.3354/ame036137

Serôdio, J., J. Ezequiel, A. Barnett, J.-L. Mouget, V. Méléder, M. Laviale, and J. Lavaud. 2012. Efficiency of photoprotection in microphytobenthos: role of vertical migration and the xanthophyll cycle against photoinhibition. Aquat. Microb. Ecol. **67**: 161–175. doi:10.3354/ame01591

Su, W., T. Jakob, and C. Wilhelm. 2012. the Impact of non-photochemical quenching of fluorescence on the photon balance in diatoms Under dynamic light conditions. J. Phycol. **48**: 336–346. doi:10.1111/j.1529-8817.2012.01128.x

Taddei, L., G. R. Stella, A. Rogato, and others. 2016. Multisignal control of expression of the LHCX protein family in the marine diatom *Phaeodactylum tricornutum*. J. Exp. Bot. **67**: 3939–3951. doi:10.1093/jxb/erw198

Underwood, G. J. C., and J. Kromkamp. 1999. Primary production by phytoplankton and microphytobenthos in estuaries estuaries. Adv. Ecol. Res. **29**: 93–153. doi:10.1016/S0065-2504(08)60192-0

Underwood, G. J. C., R. G. Perkins, M. C. Consalvey, A. R. M. Hanlon, K. Oxborough, N. R. Baker, and D. M. Paterson. 2005. Patterns in microphytobenthic primary productivity: Species-specific variation in migratory rhythms and photosynthesis in mixed-species biofilms. Limnol. Oceanogr. **50**: 755–767. doi:10.4319/lo.2005.50.3.0755

Wagner, H., T. Jakob, J. Lavaud, and C. Wilhelm. 2016. Photosystem II cycle activity and alternative electron transport in the diatom *Phaeodactylum tricornutum* under dynamic light conditions and nitrogen limitation. Photosynth. Res. **128**: 151–161.

Waring, J., M. Klenell, U. Bechtold, G. J. C. Underwood, and N. R. Baker. 2010. Light-induced responses of oxygen photoreduction, reactive oxygen species production and scavenging in two diatom species. J. Phycol. **46**: 1206–1217. doi:10.1111/j.1529-8817.2010.00919.x

Westermann, M., and E. Rhiel. 2005. Localisation of fucoxanthin chlorophyll *a*/*c*-binding polypeptides of the centric diatom *Cyclotella cryptica* by immuno-electron microscopy. Protoplasma **225**: 217–223. doi:10.1007/s00709-005-0083-9

Wu, H., A. M. Cockshutt, A. McCarthy, and D. A. Campbell. 2011. Distinctive photosystem II photoinactivation and protein dynamics in marine diatoms. Plant Physiol. **156**: 2184–2195. doi:10.1104/pp.111.178772

Zhu, S.-H., and B. R. Green. 2010. Photoprotection in the diatom *Thalassiosira pseudonana*: role of LI818-like proteins in response to high light stress. Biochim. Biophys. Acta **1797**: 1449–1457. doi:10.1016/j.bbabio.2010.04.003

Chapter 4: Behavioural versus physiological photoprotection in epipelic and epipsammic benthic diatoms

Lander Blommaert[1], Johann Lavaud[2], Wim Vyverman[1] & Koen Sabbe[1]

1. Ghent University, Laboratory of Protistology and Aquatic Ecology, B-9000 Ghent, Belgium
2. CNRS/Université Laval, UMI3376 Takuvik Joint International Laboratory, Département de Biologie, Pavillon Alexandre Vachon, Université Laval, 1045 avenue de la Médecine, Québec, Qc, G1V 0A6, Canada

Abstract

Benthic diatoms are dominant primary producers in intertidal marine sediments, which are characterized by widely fluctuating and often extreme light conditions. To cope with sudden increases in light intensity, benthic diatoms display both behavioural and physiological photoprotection mechanisms. Behavioural photoprotection is restricted to raphid pennate diatoms, which possess a raphe system that enables motility and hence positioning in sediment light gradients (e.g. via vertical migration into the sediment). The main physiological photoprotection mechanism is to dissipate excess light energy as heat, measured as Non-Photochemical Quenching (NPQ) of chlorophyll fluorescence. A trade-off between vertical migration and physiological photoprotection (NPQ) in benthic diatoms has been hypothesized before, but this has never been formally tested. We exposed five epipelic diatom species (which move in between sediment particles) and four epipsammic diatom species (which live in close association with individual sand grains) to high light conditions, and characterized both NPQ and the relative magnitude of the migratory response to high light. Our results reveal the absence of a significant downward migratory response in the araphid diatom (*Opephora guenter-grasssii*), but also in several raphid epipsammic diatoms, while all epipelic species showed a significant migratory response (20-40 % decrease in surface biomass in 30 min) upon high light exposure. In all epipsammic species the upregulation of NPQ was rapid and pronounced (NPQ ~3 after 5 min); NPQ relaxation in low light conditions, however, occurred faster in the araphid diatom (*Opephora guenter-grasssii*), compared to the raphid epipsammic species. In contrast, all epipelic species lacked a strong and flexible NPQ response (NPQ ~1.5 after 5 min of high light) and showed higher susceptibility to photodamage when not able to migrate, with the exception of *Navicula arenaria* that relaxed its NPQ to the same extent as epipsammic diatoms. While overall our results support the vertical migration-NPQ trade-off, the lack of strong relationships between the capacity for vertical migration and NPQ within the epipsammic and epipelic groups suggests that other factors as well, such as cell size, substrate type and photoacclimation, may influence photoprotective strategies.

Introduction

Light is an indispensable but often highly variable resource for microalgae. While traits associated with light utilization are plastic, they can also differ between taxa, often in relation to the specific light climate in their respective habitats (Litchman and Klausmeier 2008). For example, rapid physiological photoprotection mechanisms, such as excess energy dissipation as heat through Non-Photochemical Quenching of chlorophyll fluorescence [NPQ, related to de-epoxidation of xanthophyll pigments in the so-called xanthophyll cycle (XC), (Lavaud and Goss 2014)] are more strongly developed in diatom species which inhabit strongly mixed and turbid coastal environments than in those inhabiting open ocean environments with a more stable light climate (Lavaud et al. 2007; Dimier et al. 2009; Bailleul et al. 2010).

At low tide, benthic diatoms living in intertidal sediments experience a light climate similar to the terrestrial environment, with often fast and unpredictable fluctuations in light (Lavaud and Goss 2014), and display a high NPQ capacity (Perkins et al. 2010a). Large differences in NPQ capacity have been observed between benthic growth forms (Jesus et al. 2009, Cartaxana et al. 2011, Barnett et al. 2015, Pniewski et al. 2015, Cartaxana et al. 2016b). Dense biofilms composed of epipelic diatoms are formed on fine-grained sediments (Sabbe 1993; Ribeiro et al. 2013). Epipelic diatoms live freely on and in sediments and possess a raphe structure through which mucilage is secreted allowing movement (Round et al. 1990; Aumeier and Menzel 2012). In addition to endogenous vertical migration rhythms in response to diurnal and tidal cycles (Consalvey et al. 2004), epipelic diatoms can also actively position themselves within sediment light gradients in order to maximize photosynthesis and/or avoid overexposure (Admiraal 1984; Serôdio et al. 2006; Cartaxana et al. 2016a). While in situ epipelic diatom communities also activate the XC as a response to high light (Chevalier et al. 2010), downward vertical migration (VM) into the sediment is considered to be their prime response to high light stress (Perkins et al. 2010b). This behavioural response could as such minimize the need for physiological photoprotection (Serôdio et al. 2001; Raven, 2011).

In more sandy sediments, epipelic communities are largely replaced by communities of epipsammic diatoms. These diatoms are either araphid (and hence non-motile) and firmly attached to sand grains (either adnate or via a mucilage stalk), or raphid. In the latter case, it is hypothesized that their movement is largely restricted to the sphere of individual sand grains (Sabbe 1997; Ribeiro et al. 2013). As in situ communities living on sandy sediments showed no migratory behaviour and exhibited higher diatoxanthin/diadinoxanthin (Dtx/Ddx) ratios than communities living on silt, a trade-off between behavioural (VM) and physiological photoprotection (NPQ) was proposed (van Leeuwe et al. 2008; Jesus et al. 2009). Exposing both silt- and sand-inhabiting

communities to high light in controlled laboratory conditions supported this hypothesis as the sand-inhabiting communities showed higher Dtx/Ddx ratios while not migrating downward in response to high light (Cartaxana et al. 2011). These observations were confirmed by Barnett et al. (2015) who used unialgal cultures to show that epipsammic diatoms indeed have a higher capacity for NPQ and XC than epipelic species. In addition, non-motile epipsammic species show a stronger coupling between NPQ development and the light saturation point (E_k) than motile epipsammic species. Finally, Laviale et al. (2016) showed that in epipelic communities light induction of VM occurs at a similar rate as NPQ induction, an essential condition for a migration-physiology trade-off.

While all above studies support a trade-off between NPQ and VM, combined measurements of both traits are limited to natural communities (Perkins et al. 2010b; Serôdio et al. 2012; Laviale et al. 2015, 2016). Natural communities however usually contain a mix of growth forms and species (Hamels et al. 1998), which can hamper the interpretation of NPQ and XC measurements as both growth form and species responses can be quite specific (Underwood et al. 2005; Barnett et al. 2015; Cohn et al. 2015). Photoprotection capacity of raphid and araphid epipsammic growth forms has rarely been investigated in unialgal cultures (Barnett et al. 2015; Blommaert et al. 2017), while the capacity for vertical migration in epipsammic species has to our knowledge never been investigated in cultures.

Here we investigated the relationship between NPQ activation and relaxation and the vertical migration capacity, measured as a decrease in surface biomass, expressed as Normalized Difference Vegetation Index (NDVI) (as used by Serôdio et al. 2006; Laviale et al. 2016), for a set of common epipelic (5) and epipsammic (4) diatom species. As it is important that trade-offs are studied with all else being equal (Litchman and Klausmeier 2008), we quantified both traits under identical conditions, with all strains acclimated to the same light climate.

Materials and Methods

Epipelic and epipsammic diatom strains were obtained from the diatom culture collection (BCCM/DCG) of the Belgian Coordinated Collection of Micro-organisms (http:/BCCM.belspo.be) and the Nantes Culture Collection-France (NCC), (http://ncc.univ-nantes.fr/). Accession numbers are given in Table 1. Photographs of all species were taken with an Axiophot2 microscope (Carl Zeiss AG, Oberkochen, Germany), equipped with a monochrome digital camera, AxioCam MRm (Carl Zeiss AG, Oberkochen, Germany) (Fig. 1). Species were grown at 20°C in batch cultures in a day/night regime of 16/8 h with a light intensity of 20 µmol photons m^{-2} s^{-1} using two L58W/840 Lumilux cool white tubes and one L58W/865 cool daylight fluorescent tube (Osram, Munich, Germany). Cells were cultured in Provasoli's enriched f/2 seawater medium using Tropic Marin artificial sea salt (Dr. Beiner GmbH, Wartenberg, Germany) (34.5 g l^{-1}) enriched with $NaHCO_3$ (80 mg l^{-1} final concentration). Cultures were acclimated to these culturing conditions for at least 2 weeks prior to the experiments.

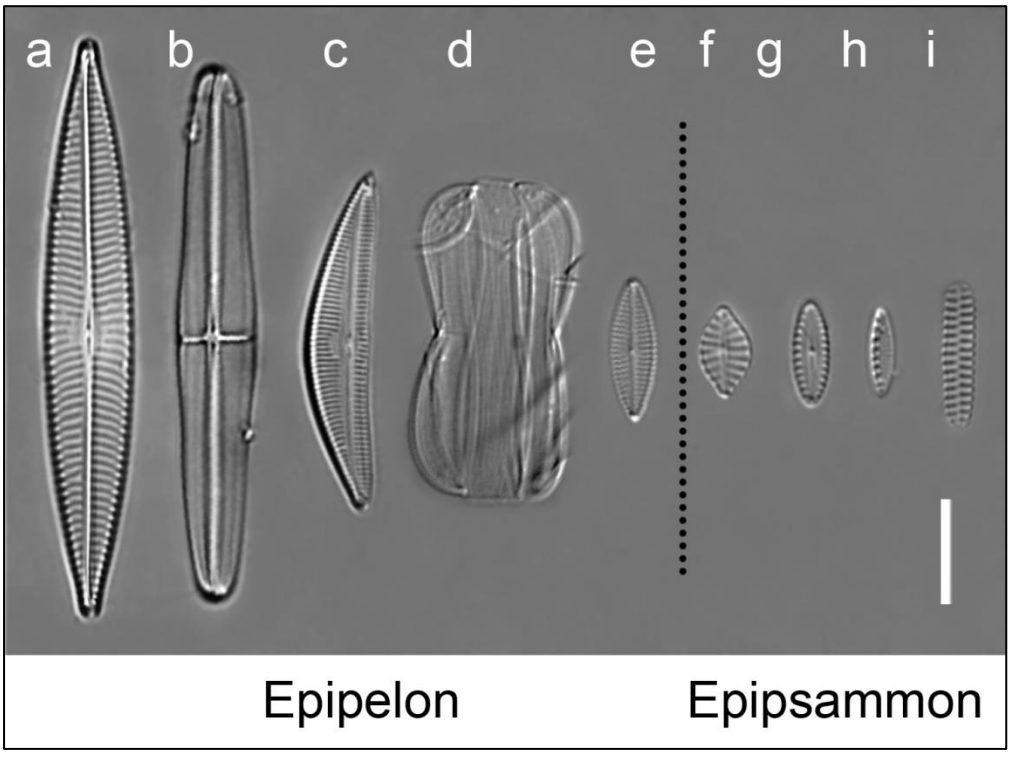

Fig. 1: Light microscopy photographs of the species used in this study. a: *Navicula arenaria var. rostellata*, b: *Craspedostauros britannicus*, c: *Seminavis robusta*, d: *Entomoneis paludosa*, e: *Navicula phyllepta*, f: *Planothidium delicatulum*, g: *Biremis lucens*, h: *Nitzschia cf. frustulum*, i: *Opephora guenter-grassii*. Scale bar = 10 µm.

Table1: Species information

Species	*Abbreviation*	*Growth form*	*Collection n°*	*Sampling location*
Craspedostauros britannicus E.J. Cox	C.b.	Epipelon	NCC195-06-02	Pouliguen, Atlantic, France
Entomoneis paludosa (W. Smith) C.W. Reimer	E.p.	Epipelon	NCC18-1	Bay of Bourgneuf, Atlantic, France
Navicula phyllepta F.T. Kützing	N.p.	Epipelon	DCG 0486	Paulina Schor, The Netherlands
Navicula arenaria var. rostellata H. Lange-Bertalot	N.a.	Epipelon	DCG 0489	Paulina Schor, The Netherlands
Seminavis robusta D.B. Danielidis & D.G. Mann	S.r.	Epipelon	DCG 0105	Progeny of strains from Veerse Meer, The Netherlands
Nitzschia cf. frustulum (F.T. Kützing) A. Grunow	N.f.	Epipsammon (raphid)	DCG 0494	Rammekenshoek, North Sea, The Netherlands
Planothidium delicatulum (F.T. Kützing) F.E. Round & L. Bukthiyarova,	P.d.	Epipsammon (raphid)	NCC363	Bay of Bourgneuf, Atlantic, France
Biremis lucens (F.R. Hustedt) K. Sabbe A. Witkowski & W. Vyverman	B.l.	Epipsammon (raphid)	NCC360.2	Bay of Bourgneuf, Atlantic, France
Opephora guenter-grassii (A. Witkowski & H. Lange-Bertalot) K. Sabbe & W. Vyverman	O.g.	Epipsammon (araphid)	DCG 0448	Rammekenshoek, North Sea, The Netherlands

Preparation of monospecific biofilms

Light brown kaolin (Carl Roth GmbH, Karlsruhe, Germany) was used as a standard test substrate for diatom motility as it has similar properties as mudflat sediment (Hay et al. 1993) and is commercially available. Differences in sediment light climate between natural sediments and kaolin, however, could not be excluded. A schematic overview of artificial biofilm preparation is shown in Fig. 2. 24-well plates were filled with 0.75 g kaolin in each well and mixed with one ml of medium to obtain a homogenous suspension. The sediment was pelleted by centrifugation at 1000 RCF for 5 min. For epipelic diatoms, monospecific suspensions (0.5 ml, 6-10 µg Chl *a*/ml) were mixed with 0.1 g kaolin, pipetted on top of the kaolin within the wells and centrifuged at 50 RCF for 1 min. The diatom suspensions were mixed with kaolin because centrifugation without kaolin resulted in an uneven distribution of the diatom layer on the sediment. For epipelic species 10 µg Chl *a*/ml suspensions were used, except for both *Navicula* species (6 µg Chl *a*/ml). After a second centrifugation step (to conform with the epipsammic treatment, see below), the supernatant medium was removed and diatoms were allowed to migrate to the surface for 6 h in 20 µmol photons m^{-2} s^{-1} at 20°C. Higher light intensities were not used for upward migration to avoid a photophobic response or a change in photophysiology. For epipsammic diatoms, 0.1 g kaolin, mixed with 0.5 ml artificial seawater but without diatoms, was first added to the wells already containing 0.75 g centrifuged kaolin, as described above, and then centrifuged at 50 RCF for 1 min. Afterwards, 1 ml suspension of epipsammic diatoms (2 µg Chl *a*/ml) was added and centrifuged at 50 RCF for 1 min after which the supernatant medium was removed. The epipsammic treatment was slightly different from the epipelic one because the cells were either non-motile or did not migrate to the sediment surface within the same time frame used for the epipelic diatoms. By analogy with the epipelic treatment, the epipsammic species were then placed in 20 µmol photons m^{-2} s^{-1} at 20°C for 6 h before high light exposure. Surface biomass (expressed as Normalized Difference Vegetation Index (NDVI), see further), measured before the start of the experiments, ranged between 0.1 and 0.25 for all species. To quantify the extent of vertical migration, relative values were calculated, thus standardizing for differences in initial surface biomass.

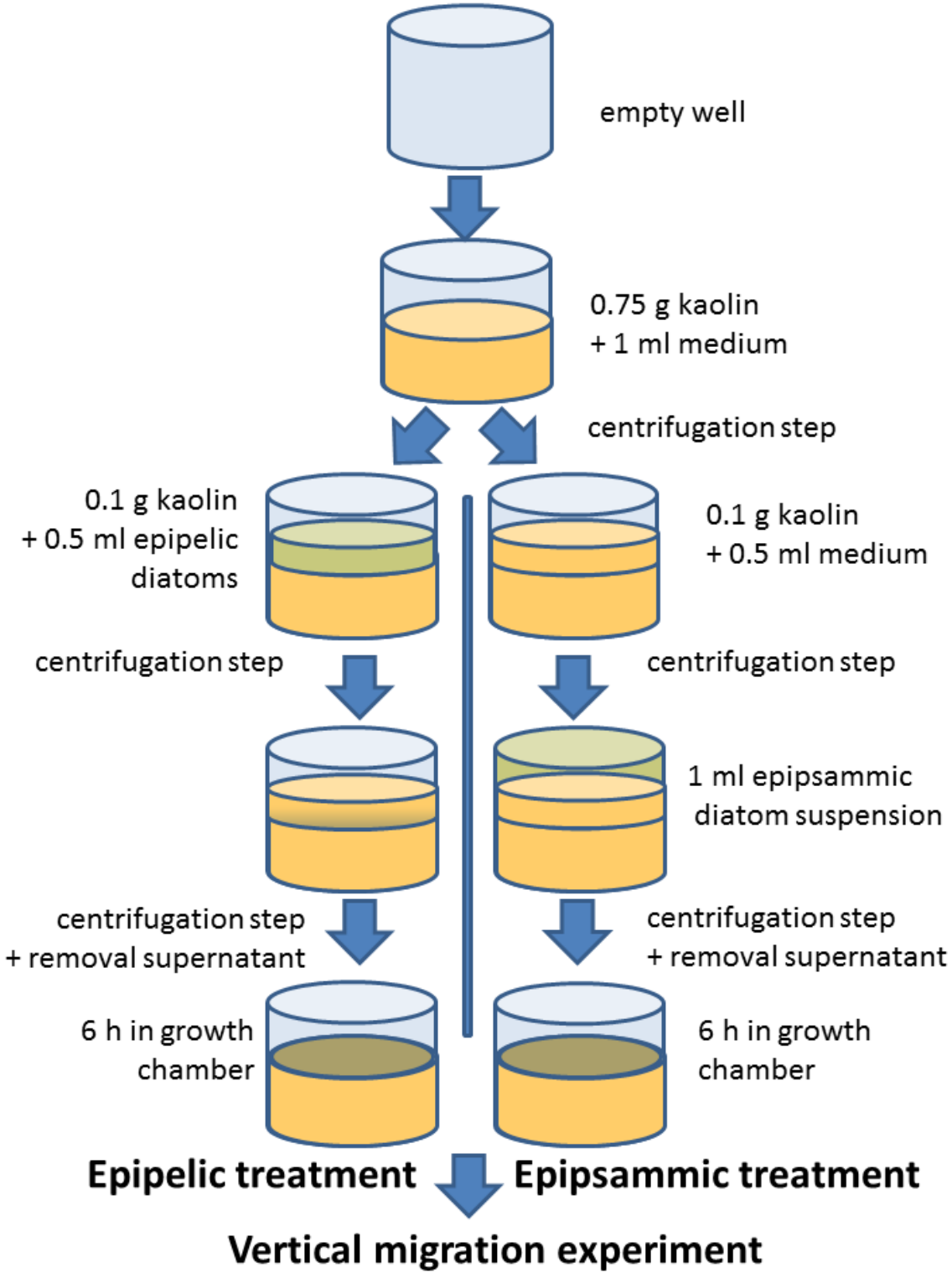

Fig. 2: A schematic overview of artificial biofilm preparation.

NDVI and chlorophyll fluorescence measurements

Both pulse amplitude modulated (PAM) fluorescence imaging and NDVI were measured with a standard MAXI Imaging PAM *M-series* (Heinz Walz GmbH, Effeltrich, Germany), equipped with an IMAG-K4 camera and mounted with an IMAG-MAX/F filter. The illumination unit of the imaging system contains red (660 nm) and near-infrared (NIR, 780 nm) LEDs providing monochromatic pulse modulated light. The reflectance images of the monochromatically illuminated samples were captured by the same CCD-chip that captures chlorophyll fluorescence.

In two separate experiments, NPQ and VM (see below) were measured immediately before (0 min) and after 2.5, 5, 10, 15, 20, 25 and 30 min HL illumination (1900 µmol photons m^{-2} s^{-1}, photosynthetically available radiation), provided by the MAXI Imaging PAM Blue LED-panel. The outer wells of the 24-well plates were not included to avoid inhomogeneity in light intensity.

The intensities of both red and NIR illumination sources were calibrated with a 18% grey standard (Neutral Grey Card 4963, FOTOWAND-Technic Dietmar Meisel, Sudwalde, Germany), placed in the middle of the camera field of view as during HL exposure the NIR reflectance decreased while red reflectance increased. Red and NIR reflectance images were captured automatically using the script function in the ImagingWin software. Areas of interest (AOI) were placed in the middle of each well to avoid edge-effects using the ImagingWin (v2.41a) software (Heinz Walz GmbH, Effeltrich, Germany). Sediment temperature was maintained at 20°C by working in an air-conditioned room, removing the Perspex eye-protection hood and providing additional cooling by a fan, and keeping the 24-well plate, which was perforated in between the wells, in a water bath on a stirring plate.

For NDVI measurements, a saturating pulse (0.8 s, INT 8) was fired at the end of each HL interval to create a new file in which only one red and NIR image could be saved. Red and NIR were captured after 10 s of darkness after this saturating pulse to avoid interference. NDVI was calculated as (R780 – R660)/(R780 + R660) using the AOI averages (Rouse et al. 1974). An NDVI vs. chlorophyll *a* (Chl *a*) calibration curve was constructed by creating artificial biofilms by centrifuging (cf. epipsammic treatment above) suspensions of known Chl *a* content (determined spectrophotometrically, Jeffrey and Humphrey, 1975) of the diatom *Phaeodactylum tricornutum* K. Bohlin (Fig. 3). The extent of vertical migration was calculated as the relative (percentage) decline in initial NDVI values (Laviale et al. 2016) after subtraction of the NDVI value of kaolin without diatoms, which was recorded simultaneously. Even though we controlled for changes in red and NIR illumination, we observed a decline in recorded NDVI of a sheet of green paper (absorbing in the red spectrum) under the same light conditions, possibly due to a shift in LED-spectrum resulting from the heating up of the LED panel during HL illumination. We corrected for this artifact (see Supplemental Fig. S1) by adding the

average decline of 15 observations (3 independent measurements of 5 AIOs in the green sheet) to the recorded data for diatoms.

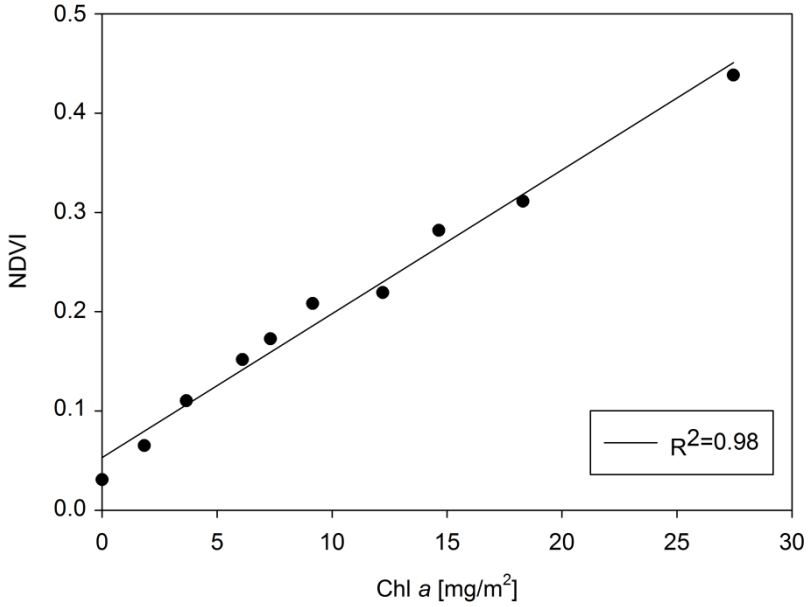

Fig. 3: Correlation of Normalized Difference Vegetation Index (NDVI) with Chlorophyll *a* content, determined photospectrometrically, on a *Phaeodactylum tricornutum* dilution series centrifuged on kaolin.

NPQ was measured on diatom suspensions in 24-well plates (1 ml containing 1 µg Chl *a*, measured as above) using the same light conditions as the vertical migration essay. As no sediment was present, a behavioural photoprotection response was not possible. NPQ reversal was measured during an additional 30 min low light (LL) recovery period (15 µmol photons m^{-2} s^{-1}). Saturating pulses (0.8 s, INT 8) were fired automatically each 5 min. A fluorescence standard (Heinz Walz GmbH, Effeltrich, Germany) was measured simultaneously to correct for deviations in measuring light intensity during HL. NPQ was calculated as $(F_m\text{-}F_m')/F_m'$, where F_m is the Maximum PSII chlorophyll fluorescence yield and F_m' is maximum PSII Chl fluorescence yield (F_m) during illumination. As F_m' values recorded during HL were lower than the minimum PSII Chl fluorescence yield F_0 (as observed in diatoms by Lavaud et al. 2002), qN (as used by Laviale et al. 2016) was not determined. Photosynthetic efficiency of PSII ($\Delta F/F_m'$) was calculated as $(F_m'\text{-}F')/F_m'$ and expressed as a percentage, taking the maximal photosynthetic efficiency (F_v/F_m), measured immediately before HL onset as 100%.

The NPQ induction (1) and recovery (2) rates (k) were calculated by fitting an exponential decay function (nonlinear regression), derived from Olaizola and Yamamoto (1994):

(1) $NPQ(t) = NPQ_{max} + [NPQ_0 - NPQ_{max}]e^{-kt}$

where t represents time during HL and NPQ_{max} and NPQ_0 represent NPQ after 30 min HL and before HL onset, respectively.

(2) $NPQ(t) = NPQ_r + [NPQ_{max} - NPQ_r]e^{-kt}$

where t represents time during recovery and NPQ_{max} and NPQ_r represent NPQ at the start of the recovery period and after 30 min of recovery in LL, respectively. Statistical analyses were conducted using the statistical software package SAS 9.4. Exponential decay functions were fitted using the nonlinear regression procedure (PROC NLIN). Measured and fitted parameters (3 biological replicates per species) were compared between species using ANOVA, followed by a Tukey's test, using the General Linear Model procedure (PROC GLM) in the statistical software package SAS 9.4 (SAS Institute Inc., Cary, NC, USA). *P*-values of 0.05 or less were considered statistically significant. A decrease in surface biomass was evaluated as a one-sided t-test (only a decrease was considered).

Results

NDVI measured with the MAXI Imaging PAM *M-series*

A dilution series of *Phaeodactylum tricornutum* suspensions of known Chl *a* content was centrifuged on kaolin sediment to create artificial biofilms. NDVI of these biofilms correlated very well (R^2=0.98, $p < 0.0001$) with Chl *a* content (Fig. 3). As the y-intercept was larger than zero ($p = 0.0002$), a blank with bare sediment was included and its NDVI measurement subtracted from all samples in all VM experiments.

Behavioural photoprotection - vertical migration (VM)

All epipelic species showed a significant (one-sided t-test, $p < 0.05$) decrease in surface biomass (20-40%) by the end of the HL illumination period (VM_{30})(Fig. 4a, b; significant *p*-values listed in Table S1). As only two replicates were included for *Entomoneis paludosa*, this species was excluded from statistical analysis. None of the epipsammic species, including the motile ones, showed a significant surface biomass decline during the HL period (Fig. 4a, b; *p*-values listed in Table S1). Of the epipelic species, only *Craspedostauros britannicus* showed a small but significant decrease in surface biomass after 2.5 min ($p = 0.001$). After 15 min of HL, *C. britannicus*, *Navicula phyllepta* and *N. arenaria* had significantly lower surface biomass than at the start of the experiment (one-sided t-test). The smallest epipelic species *N. phyllepta* exhibited the most pronounced vertical migration (Fig. 4a); decreasing its surface biomass significantly more than any other tested epipelic species within the 30 min HL exposure period (ANOVA and Tukey's post hoc pairwise comparison, *p*-values reported in Table S2). No significant differences in surface biomass decrease were found between the other epipelic diatoms after 30 min of HL (Table S2). A control experiment, using only the largest (*N. arenaria*) and smallest (*N. phyllepta*) epipelic diatoms (2 technical replicates each), showed no VM in growth light conditions (20 µmol photons m^{-2} s^{-1}, Supplemental Fig. S2).

Physiological photoprotection - NPQ

All investigated epipsammic species displayed a strong NPQ induction, resulting in significantly higher NPQ values than epipelic species after 5 min HL (Fig. 4c, d) (ANOVA and Tukey's post hoc pairwise comparison, *p*-values reported in Table S3). No significant differences in NPQ were observed between diatoms of the same growth form at this time point (Table S3). The NPQ induction rate was lowest in *C. britannicus* (rate constant k = 0.08 min^{-1}; SD = 0.02), which was significantly lower than in *B. lucens*, *E. paludosa*, *O. guenter-grassii* and *P. delicatulum* (ANOVA and Tukey's post hoc pairwise comparison, *p*-values reported in Table S4). The epipsammic species showed a comparable but lower further increase in NPQ during the rest of the HL period. In the epipelic species, NPQ diverged by the end of the HL exposure period. Both *C. britannicus* and *E. paludosa*

showed a strong NPQ increase during the HL period, resulting in significantly higher NPQ values than the other tested epipelic species (except for the difference between *E. paludosa* and *N. phyllepta* which was not significant, ANOVA and Tukey's post hoc pairwise comparison, *p*-values reported in Table S5).

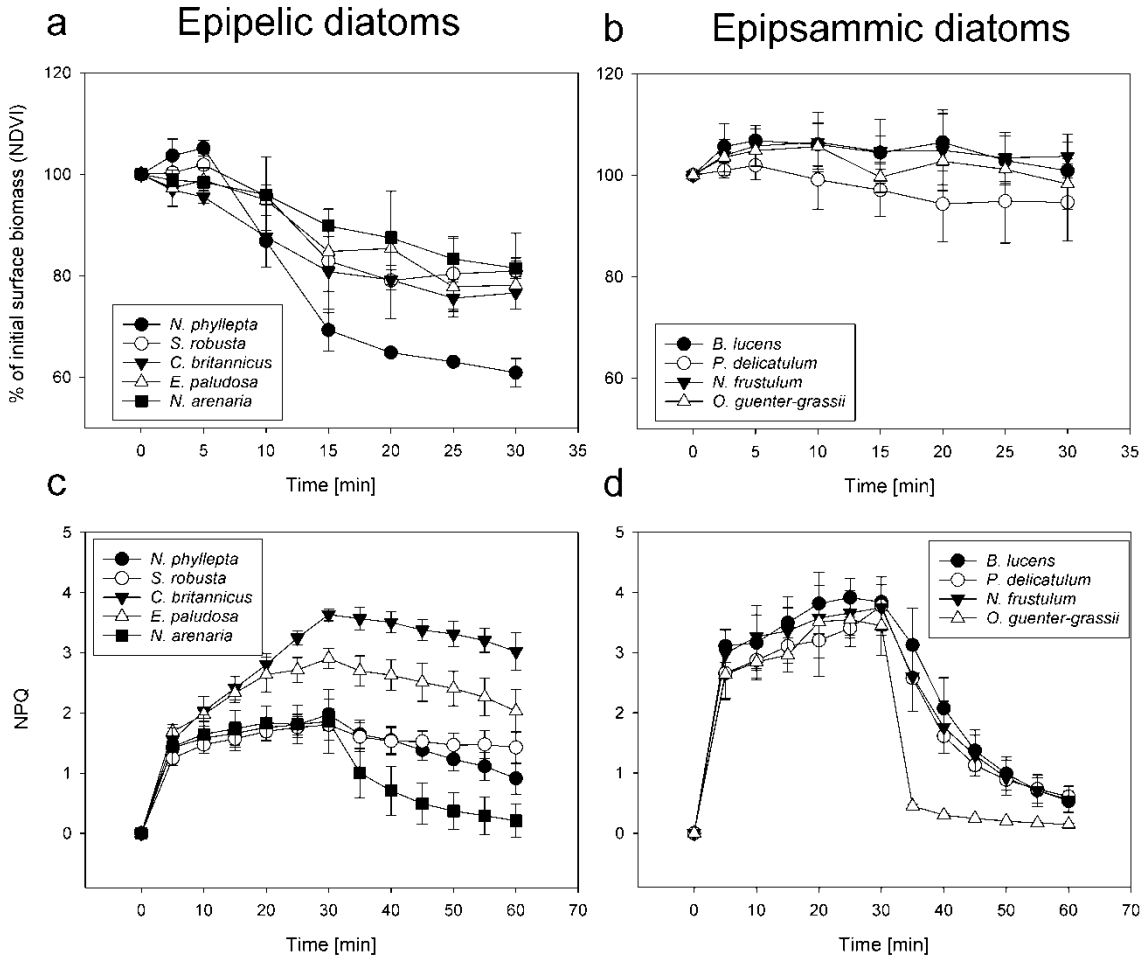

Fig. 4a, b, c, d: The decrease in surface biomass, measured as NDVI, of epipelic diatoms (a) and epipsammic diatoms (b) on kaolin during 30 min of HL. Note that the y-axis in these plots starts at 50%. Non-photochemical quenching (NPQ) for epipelic diatoms (d) and epipsammic diatoms (c), measured during 30 min HL and 30 min LL recovery. Values represent averages of three independent measurements ± standard deviations.

During the 30 min low light recovery period NPQ relaxed rapidly in all epipsammic species, whereas only one epipelic species, *N. arenaria*, showed clear NPQ relaxation. Sustained quenching (NPQs) after 30 min recovery was highest for *C. britannicus*, followed by *E. paludosa*. Fitting NPQ relaxation with exponential decay functions revealed significantly faster NPQ relaxation in the araphid epipsammic diatom *Opephora guenter-grassii* (rate constant k = 0.52 min^{-1}; SD = 0.03), whereas no significant differences were observed between the raphid epipsammic diatoms and *N. arenaria* (rate constant k = 0.13 min^{-1}; SD = 0.06) (ANOVA and Tukey's post hoc pairwise comparison, *p*-values reported in Table S4). The recovery of the quantum yield of PSII ($\Delta F/F_m'$) after 30 min of LL (Fig. 5) was higher in all epipsammic species compared to the investigated epipelic species, with the notable exception of the epipelic species *N. arenaria* which showed an equally high recovery (ANOVA and Tukey's post hoc pairwise comparison, *p*-values reported in Table S6).

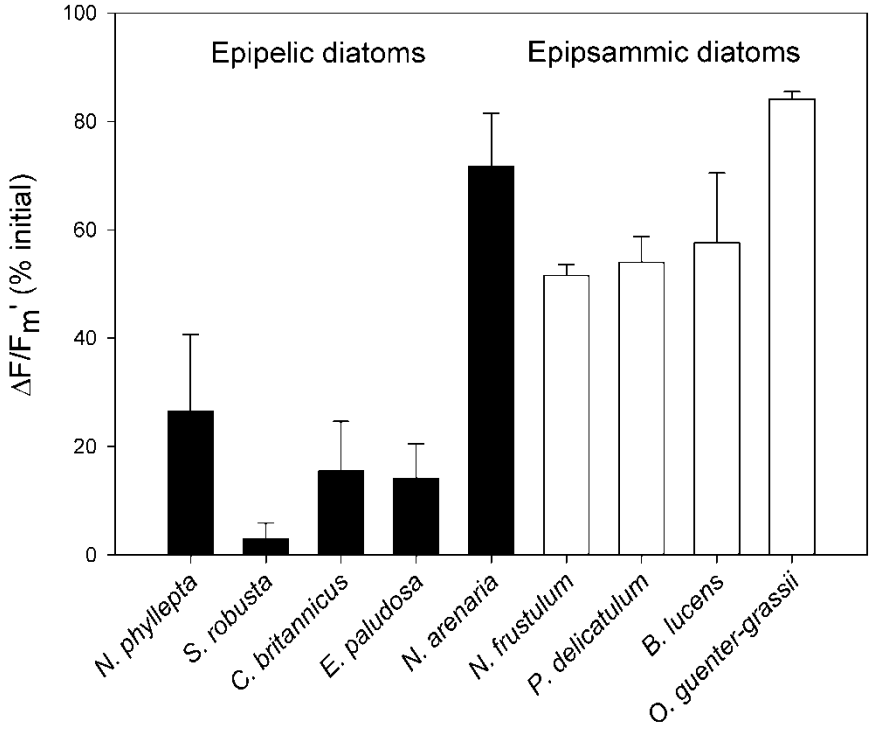

Fig. 5: The quantum yield of PSII ($\Delta F/F_m'$), after 30 min of HL and 30 min of LL recovery, expressed in percentage of the maximal photosynthetic efficiency of PSII (F_v/F_m) before HL exposure for epipelic (black bars) and epipsammic diatoms (white bars). Values represent averages of three independent measurements ± standard deviations.

Plotting the NPQ values after 5 min HL versus VM_{30} (% NDVI decrease after 30 min) (Fig. 6) revealed a clear VM-NPQ trade-off between the epipelic and epipsammic diatom groups, with epipelic diatoms displaying high VM_{30} and low NPQ, and epipsammic diatoms showing no clear VM and high NPQ. No VM_{30}/NPQ trade-offs, however, were observed within both functional groups.

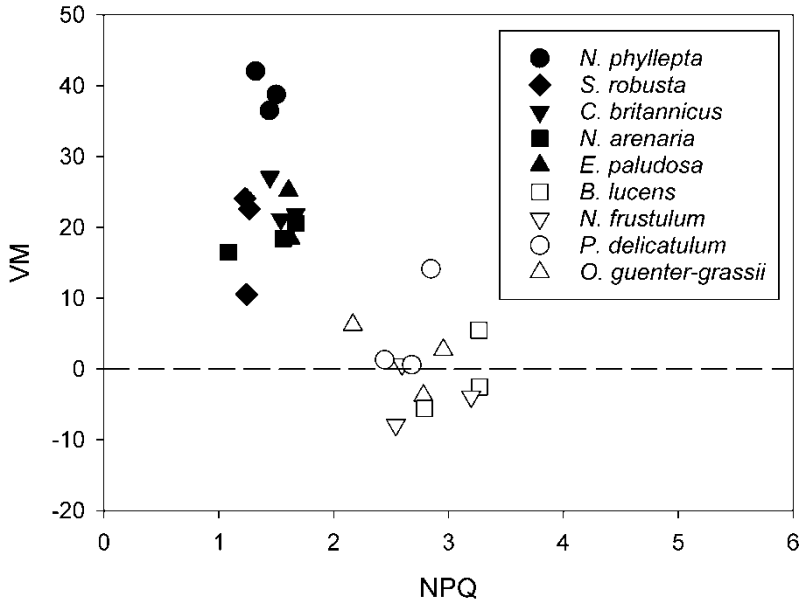

Fig. 6: The extent of vertical migration (measured as the decrease in surface biomass in percentage, cf. Fig. 4a, b), measured after 30 min of HL in function of the NPQ capacity, measured after 5 min of HL to avoid the effect of photoinhibition for epipelic (black symbols) and epipsammic diatoms (white symbols). Three replicates per species are plotted (with exception of *E. paludosa*, n = 2).

Discussion

As the ability to vertically migrate (VM) away from high light to avoid photoinhibition might minimize the costs associated with high and flexible NPQ (Raven 2011), we compared NPQ and VM capacity as photoprotection mechanisms in a set of five epipelic and four epipsammic species and confirm a general NPQ-VM trade-off between both functional groups.

The fact that no vertical movement was observed in the epipsammic species shows that the migration observed in the epipelic species was not caused by a passive process such as water percolation. To further test whether the response was indeed caused by high light, we performed a control experiment with the largest (*N. arenaria*) and smallest (*N. phyllepta*) epipelic diatoms in which we exposed them to growth light conditions (i.e. low light) instead of high light conditions. No migratory response was observed (see supplemental Fig. S2), clearly demonstrating that the migratory response was caused by high light. Even though diatom motility response changes according to the spectral quality of light at relatively low light intensities (McLachlan et al. 2009; Cohn et al. 2015), high light intensities evoke photophobic responses (Cohn et al. 2015). In our experiments, the used blue light induced a high level of photoinhibition in all epipelic diatoms (with the exception of *N. arenaria*), indicating we were mainly observing photophobic responses, while positive phototaxis (motility towards light) could be considered to be low.

While all epipelic species showed significant VM, they migrated less fast compared to natural epipelic communities, where surface biomass decreased up to 30% within the first 2.5 min of high light (Laviale et al. 2016). In our experiments, where VM was prevented under HL conditions, NPQ was initially low for all epipelic species, but for some species, it increased considerably during the course of the HL exposure. Most of this NPQ, however, coincided with high sustained NPQ (NPQs, see below). Epipsammic species compensated for the absence of significant VM with a strong NPQ response during HL onset. Consistent differences in NPQ induction rate between epipelic and epipsammic diatoms were not observed, possibly due to the fact that we have no data for the first five minutes of high light, during which most of the NPQ induction, due to Ddx de-epoxidation, takes place (Serôdio et al. 2005).

Besides a strong NPQ after HL onset, epipsammic diatoms were also able to relax NPQ rapidly during low light conditions. Within both growth forms, trade-offs between both photoprotective strategies were not observed. However, the only araphid (and hence by definition non-motile) epipsammic diatom included here showed considerably faster relaxation of NPQ after high light exposure than the raphid epipsammic diatoms and is therefore able to more efficiently track rapid changes in irradiance intensity (Lavaud et al. 2007; Lavaud and Lepetit 2013). Taken together, our results confirm that epipelic and

epipsammic growth forms can be seen as different functional groups exhibiting contrasting primary photoprotection strategies.

NPQ differences between epipelic and epipsammic growth forms were studied by Barnett et al. (2015), and agree with our observations after 5 min HL. Higher NPQ values in epipsammic diatoms were attributed to higher Dtx production, originating from a larger Ddx + Dtx pool rather than a higher Ddx de-epoxidation state. The measured NPQ values in two epipelic species (*C. britannicus* and *E. paludosa*), however, increased to similar levels as in the epipsammic diatoms after 30 min HL, a feature not observed by Barnett et al. (2015) as only 5 min illumination periods were used. During the low light recovery period, however, all epipelic species except *N. arenaria* showed high NPQs and a low recovery of PSII quantum yield. High NPQs has been observed after exposure to high light conditions or a combination of high light and elevated temperatures (Zhu et al. 2010; Lavaud and Lepetit 2013; Laviale et al. 2015), and has been attributed to a slow epoxidation of Dtx back to Ddx (Lavaud and Lepetit 2013; Lavaud and Goss 2014; Blommaert et al. 2017) and/or photoinhibition (qI). In contrast with our observations, epipelic communities freshly obtained from the field are able to withstand high light doses (up to 1200 µmol photons $m^{-2}s^{-1}$) for up to three hours, even when VM is inhibited (Serôdio et al. 2012; Laviale et al. 2015). Moreover, they show higher NPQ values, while relaxing their NPQ more in low light conditions (Serôdio et al. 2005, 2008, 2012), suggesting that these field communities are less sensitive to photoinhibition than monospecific epipelic cultures. This could be due to the fact that the diatom cultures used in our study were acclimated to rather low light intensities (20 µmol photons $m^{-2}s^{-1}$) and exposed to relatively high light intensities. Acclimation to higher irradiances increased the NPQ capacity of epipelic diatoms (Cruz and Serôdio 2008; Ezequiel et al. 2015; Barnett et al. 2015) and caused them to accumulate at higher light intensities in a light gradient (Ezequiel et al. 2015). As a result, the VM/NPQ trade-off between epipsammic and epipelic diatoms observed in the field may not be as pronounced as observed in our experiments.

Alternatively, the high NPQs/qI in epipelic species, as observed in this study, could be related by the origin of the strains. Diatom communities originating from Portuguese mudflats, as used in the above studies, tend to have overall higher NPQ and less NPQs and/or photoinhibition after high light exposure than communities sampled at higher latitudes along the Atlantic Coast (Laviale et al. 2015). Pniewski et al. (2015) also observed photoinhibition (measured as a decline in oxygen evolution-irradiance curves) in epipelic communities from Aiguillon Bay (Atlantic coast, France). The observed absence or low amount of NPQs/qI and in general higher recovery of PSII quantum yield in epipsammic diatoms in this study confirms that the energy dissipating mechanisms of these diatoms are capable of tracking light fluctuations (cf. Blommaert et al. 2017) and optimizing photosynthesis in rapidly fluctuating and high light conditions, as photosynthesis can be forgone if energy dissipating mechanisms fail to relax in light-

limiting conditions (Raven 2011). Finally, sustained NPQ in MPB diatoms may be advantageous to keep the antenna system in a basal dissipative state, allowing the cells to cope with a sudden increase in light intensity after a long dark period as may happen during immersion and night emersion (Lavaud and Goss 2014).

Differences in motility of epipelic diatoms (here mainly between *N. phyllepta* and larger species) were not reflected in NPQ capacity and thus do not point to a VM-NPQ trade-off within the epipelic group. *N. phyllepta* is much smaller (~13 µm long) than the other studied epipelic species (>30 µm long) but exhibited the strongest migratory response, whereas no differences in VM were observed between the larger species. The difference in VM between *N. phyllepta* and the larger species may be due to the fact that because of its smaller size (and assuming comparable pigment concentration per unit biovolume) pigment self-shading may be lower, rendering the cells more vulnerable to photoinactivation (Key et al. 2010) and therefore requiring higher photoprotection (i.c. VM). In this respect it is interesting to note that in a field study small naviculoid diatoms were mainly observed at the sediment surface in early morning when light intensity was still relatively low whereas larger species dominated the intertidal surface biofilm at noon (Underwood et al. 2005). It should also be noted that while VM was observed in all epipelic species, most diatom biomass stayed at the sediment surface as observed by Laviale et al. (2015, 2016). Therefore, epipelic diatoms might have used alternative photoprotection strategies or displayed within-population cyclical micromigration at the sediment surface (Kromkamp et al. 1998), as such obscuring differences in VM as a photoprotection strategy.

An NPQ-VM capacity trade-off was also not observed within the epipsammic group: no significant NPQ differences were detected during the high light period and no significant VM was observed. However, all epipsammic species we tested, with the exception of *O. guenter-grasssii,* were raphid and therefore in principle capable of movement. However, despite the fact that some of them were in the same size range (see Fig. 1) as *N. phyllepta* (which displayed the strongest migratory response), they did not migrate down in response to high light. The absence of vertical migration is in accordance with the lack of endogenous migratory rhythms in epipsammic communities (Jesus et al. 2009) and the observation that epipsammic diatoms in the field do not seem to migrate down in response to high light (Cartaxana et al. 2011). Barnett et al. (2015) did observe differences in NPQ capacity between motile and non-motile epipsammic species but not at the highest light intensity (2000 µmol photons $m^{-2}s^{-1}$). The most notable difference between the epipsammic species in our study was the faster NPQ relaxation in the araphid species *O. guenter-grassii*, which is due to fast Dtx epoxidation in low light conditions (Blommaert et al. 2017). The slower relaxation in raphid epipsammic species may suggest that they do use motility, not to perform VM but to move to slightly more shaded areas on the sand grain surface, such as depressions, where epipsammic diatoms are often seen to aggregate (Miller et al. 1987; Jewson et al. 2006; Sabbe, unpubl. obs.).

While it has been hypothesized that cell accumulations in depressions can represent a strategy to protect against abrasion (Miller et al. 1987), it could also be a way to reduce high light stress through increased cell shading caused by cell accumulation and the microtopography of the sand grain. This may slightly reduce the need for the very rapid NPQ relaxation observed in the araphid species. An alternative explanation for the absence of significant VM in raphid epipsammic species in sandy sediments is that because light is scattered and penetrates deeper than in silty sediments (Kuhl et al. 1994; Cartaxana et al. 2016b), downward VM would probably not drastically change the experienced light climate (Cartaxana et al. 2016b). A third potential explanation for the observed difference in NPQ relaxation between the araphid and raphid epipsammic species could be that slower NPQ relaxation represents a phylogenetic signal typical for raphid, motile diatoms which was retained in raphid taxa which adopted an epipsammic growth form.

Finally, it needs to be pointed out that the distinction between araphid and raphid epipsammon does not necessarily coincide with a difference in motility. Some raphid species, such as *Biremis lucens* are usually observed as small colonies which are attached to the sand grain surface via their girdle side (Sabbe et al. 1995). For this reason, this species was classified as non-motile in Barnett et al. (2015). In the present study, we focused on the distinction between araphid and raphid, as raphid diatoms are at least potentially motile as they possess a raphe. Motility in most of these forms, however, has not yet been properly characterized.

Acknowledgements

The authors would like to thank the Research Foundation Flanders (FWO project G.0222.09N), Ghent University (BOF-GOA 01G01911) and the Egide/Campus France-PHC Tournesol (n128992UA) exchange program for their financial support. JL also thanks the CNRS for their financial support.

References

Admiraal, W. 1984. The ecology of estuarine sediment-inhabiting diatoms. Prog. Phycol. Res. **3**: 269–322.

Aumeier, C., and D. Menzel. 2012. Secretion in the Diatoms, p. 221–250. *In* J.M. Vivanco and F. Baluška [eds.], Secretions and Exudates in Biological Systems. Springer Berlin Heidelberg.

Bailleul, B., A. Rogato, A. De Martino, S. Coesel, P. Cardol, C. Bowler, A. Falciatore, and G. Finazzi. 2010. An atypical member of the light-harvesting complex stress-related protein family modulates diatom responses to light. Proc. Natl. Acad. Sci. **107**: 18214–18219. doi:10.1073/pnas.1007703107

Barnett, A., V. Méléder, L. Blommaert, and others. 2015. Growth form defines physiological photoprotective capacity in intertidal benthic diatoms. ISME J. **9**: 32–45. doi:10.1038/ismej.2014.105

Blommaert, L., M. J. J. Huysman, W. Vyverman, J. Lavaud, and K. Sabbe. 2017. Contrasting NPQ dynamics and xanthophyll cycling in a motile and a non-motile intertidal benthic diatom. Limnol. Oceanogr. doi:10.1002/lno.10511

Cartaxana, P., S. Cruz, C. Gameiro, and M. Kuhl. 2016a. Regulation of intertidal microphytobenthos photosynthesis over a diel emersion period is strongly affected by diatom migration patterns. Front. Microbiol. **7**: 872. doi:10.3389/fmicb.2016.00872

Cartaxana, P., L. Ribeiro, J. Goessling, S. Cruz, and M. Kühl. 2016b. Light and O2 microenvironments in two contrasting diatom-dominated coastal sediments. Mar. Ecol. Prog. Ser. **545**: 35–47. doi:10.3354/meps11630

Cartaxana, P., M. Ruivo, C. Hubas, I. Davidson, J. Serôdio, and B. Jesus. 2011. Physiological versus behavioral photoprotection in intertidal epipelic and epipsammic benthic diatom communities. J. Exp. Mar. Bio. Ecol. **405**: 120–127. doi:10.1016/j.jembe.2011.05.027

Chevalier, E. M., F. Gévaert, and A. Créach. 2010. In situ photosynthetic activity and xanthophylls cycle development of undisturbed microphytobenthos in an intertidal mudflat. J. Exp. Mar. Bio. Ecol. **385**: 44–49. doi:10.1016/j.jembe.2010.02.002

Cohn, S. A., D. Halpin, N. Hawley, and others. 2015. Comparative analysis of light-stimulated motility responses in three diatom species. Diatom Res. **30**: 213–225. doi:10.1080/0269249X.2015.1058295

Consalvey, M., D. M. Paterson, and G. J. C. Underwood. 2004. The ups and downs of life in a benthic biofilm: Migration of benthic diatoms. Diatom Res. **19**: 181–202.

Cruz, S., and J. Serôdio. 2008. Relationship of rapid light curves of variable fluorescence to photoacclimation and non-photochemical quenching in a benthic diatom. Aquat. Bot. **88**: 256–264. doi:10.1016/j.aquabot.2007.11.001

Dimier, C., S. Giovanni, T. Ferdinando, and C. Brunet. 2009. Comparative ecophysiology of the xanthophyll cycle in six marine phytoplanktonic species. Protist **160**: 397–411. doi:10.1016/j.protis.2009.03.001

Ezequiel, J., M. Laviale, S. Frankenbach, P. Cartaxana, and J. Serôdio. 2015. Photoacclimation

state determines the photobehaviour of motile microalgae: The case of a benthic diatom. J. Exp. Mar. Bio. Ecol. **468**: 11–20. doi:10.1016/j.jembe.2015.03.004

Hamels, I., K. Sabbe, K. Muylaert, C. Barranguet, C. Lucas, P. Herman, and W. Vyverman. 1998. Organisation of microbenthic communities in intertidal estuarine flats, a case study from the molenplaat (Westerschelde estuary, The Netherlands). Eur. J. Protistol. **34**: 308–320. doi:10.1016/S0932-4739(98)80058-8

Hay, S. I., T. C. Maitland, and D. M. Paterson. 1993. The speed of diatom migration through natural and artificial substrata. Diatom Res. **8**: 371–384.

Jeffrey, S. W., and G. S. Humphrey. 1975. New spectrophotometric equations for determining chlorophylls *a*, *b*, *c*1 and *c*2 in higher plants, algae and natural phytoplankton. Biochem. Physiol. Pflanz. Bd. **167**: 191–194.

Jesus, B., V. Brotas, L. Ribeiro, C. R. Mendes, P. Cartaxana, and D. M. Paterson. 2009. Adaptations of microphytobenthos assemblages to sediment type and tidal position. Cont. Shelf Res. **29**: 1624–1634. doi:10.1016/j.csr.2009.05.006

Jewson, D. H., S. F. Lowry, and R. Bowen. 2006. Co-existence and survival of diatoms on sand grains. Eur. J. Phycol. **41**: 131–146. doi:10.1080/09670260600652903

Key, T., A. McCarthy, D. A. Campbell, C. Six, S. Roy, and Z. V Finkel. 2010. Cell size trade-offs govern light exploitation strategies in marine phytoplankton. Environ. Microbiol. **12**: 95–104. doi:10.1111/j.1462-2920.2009.02046.x

Kromkamp, J. C., C. Barranguet, and J. Peene. 1998. Determination of microphytobenthos PSII quantum efficiency and photosynthetic activity by means of variable chlorophyll fluorescence. Mar. Ecol. Prog. Ser. **162**: 45–55. doi:10.3354/meps162045

Kuhl, M., C. Lassen, and B. B. Jorgensen. 1994. Light penetration and light intensity in sandy marine sediments measured with irradiance and scalar irradiance fiber-optic microprobes. Mar. Ecol. Prog. Ser. **105**: 139–148. doi:10.3354/meps105139

Lavaud, J., and R. Goss. 2014. The peculiar features of the non-photochemical fluorescence quenching in diatoms and brown algae, p. 421–443. *In* B. Demmig-Adams, G. Garab, W. Adams III, and Govindjee [eds.], Non-Photochemical Quenching and Energy Dissipation in Plants, Algae and Cyanobacteria. Springer.

Lavaud, J., and B. Lepetit. 2013. An explanation for the inter-species variability of the photoprotective non-photochemical chlorophyll fluorescence quenching in diatoms. Biochim. Biophys. Acta **1827**: 294–302. doi:10.1016/j.bbabio.2012.11.012

Lavaud, J., B. Rousseau, H. J. Van Gorkom, and A.-L. Etienne. 2002. Influence of the diadinoxanthin pool size on photoprotection in the marine planktonic diatom *Phaeodactylum tricornutum*. Plant Physiol. **129**: 1398–1406. doi:10.1104/pp.002014.dissipation

Lavaud, J., R. F. Strzepek, and P. G. Kroth. 2007. Photoprotection capacity differs among diatoms : Possible consequences on the spatial distribution of diatoms related to fluctuations in the underwater light climate. Limnol. Oceanogr. **52**: 1188–1194.

Laviale, M., A. Barnett, J. Ezequiel, B. Lepetit, S. Frankenbach, V. Méléder, J. Serôdio, and J. Lavaud. 2015. Response of intertidal benthic microalgal biofilms to a coupled light-temperature stress: evidence for latitudinal adaptation along the Atlantic coast of Southern

Europe. Environ. Microbiol. **17**: 3662–3677. doi:10.1111/1462-2920.12728

Laviale, M., S. Frankenbach, and J. Serôdio. 2016. The importance of being fast: comparative kinetics of vertical migration and non-photochemical quenching of benthic diatoms under light stress. Mar. Biol. **163**: 10. doi:10.1007/s00227-015-2793-7

van Leeuwe, M., V. Brotas, M. Consalvey, R. Forster, D. Gillespie, B. Jesus, J. Roggeveld, and W. Gieskes. 2008. Photoacclimation in microphytobenthos and the role of xanthophyll pigments. Eur. J. Phycol. **43**: 123–132. doi:10.1080/09670260701726119

Litchman, E., and C. A. Klausmeier. 2008. Trait-Based Community Ecology of Phytoplankton. Annu. Rev. Ecol. Evol. Syst. **39**: 615–639. doi:10.1146/annurev.ecolsys.39.110707.173549

McLachlan, D. H., C. Brownlee, A. R. Taylor, R. J. Geider, and G. J. C. Underwood. 2009. Light-Induced motile responses of the estuarine benthic diatoms *Navicula Perminuta* and *Cylindrotheca Closterium* (Bacillariophyceae). J. Phycol. **45**: 592–599. doi:10.1111/j.1529-8817.2009.00681.x

Miller, A. R., R. L. L. Lowe, and J. T. T. Rotenberry. 1987. Succession of diatom communities on sand Grains. J. Ecol. **75**: 693–709. doi:10.2307/2260200

Olaizola, M., and H. Y. Yamamoto. 1994. Short-term response of the diadinoxanthin cycle and fluorescence yield to high irradiance in Chaeotoceros muelleri (Bacillariophyceae). J. Phycol. **30**: 606–612. doi:10.1111/j.0022-3646.1994.00606.x

Perkins, R. G., J. C. Kromkamp, J. Serôdio, J. Lavaud, B. Jesus, J.-L. Mouget, S. Lefebvre, and R. M. Forster. 2010a. Chlorophyll a Fluorescence in Aquatic Sciences: Methods and Applications, D.J. Suggett, O. Prášil, and M.A. Borowitzka [eds.]. Springer Netherlands.

Perkins, R. G., J. Lavaud, J. Serôdio, and others. 2010b. Vertical cell movement is a primary response of intertidal benthic biofilms to increasing light dose. Mar. Ecol. Prog. Ser. **416**: 93–103. doi:10.3354/meps08787

Pniewski, F. F., P. Biskup, I. Bubak, P. Richard, A. Latała, and G. Blanchard. 2015. Photo-regulation in microphytobenthos from intertidal mudflats and non-tidal coastal shallows. Estuar. Coast. Shelf Sci. **152**: 153–161. doi:10.1016/j.ecss.2014.11.022

Raven, J. A. 2011. The cost of photoinhibition. Physiol. Plant. **142**: 87–104. doi:10.1111/j.1399-3054.2011.01465.x

Ribeiro, L., V. Brotas, Y. Rincé, and B. Jesus. 2013. Structure and diversity of intertidal benthic diatom assemblages in contrasting shores: a case study from the Tagus estuary. J. Phycol. **49**: 258–270. doi:10.1111/jpy.12031

Round, F. E., R. M. Crawford, and D. G. Mann. 1990. The Diatoms - Biology & Morphology of the genera., Cambridge University Press.

Rouse, J. W., R. H. Hass, J. A. Shell, and D. W. Deering. 1974. Monitoring vegetation systems in the Great Plains with ERTS-1. *Third Earth Resources Technologhy Satellite Symposium*. 309–317.

Sabbe, K. 1993. Short-term fluctuations in benthic diatom numbers on an intertidal sandflat in the Westerschelde estuary (Zeeland, The Netherlands). Hydrobiologia **269–270**: 275–284. doi:10.1007/BF00028026

Sabbe, K. 1997. Systematics and ecology of intertidal benthic diatoms of the Westerschelde estuary (The Netherlands). Ghent University.

Sabbe, K., A. Witkowski, and W. Vyverman. 1995. Taxonomy, morphology and ecology of *Biremis lucens* comb. nov. (Bacillariophyta): A brackish-marine, benthic diatom species comprising different morphological types. Bot. Mar. **38**: 379–391. doi:10.1515/botm.1995.38.1-6.379

Serôdio, J., S. Cruz, S. Vieira, and V. Brotas. 2005. Non-photochemical quenching of chlorophyll fluorescence and operation of the xanthophyll cycle in estuarine microphytobenthos. J. Exp. Mar. Bio. Ecol. **326**: 157–169. doi:10.1016/j.jembe.2005.05.011

Serôdio, J., J. Ezequiel, A. Barnett, J.-L. Mouget, V. Méléder, M. Laviale, and J. Lavaud. 2012. Efficiency of photoprotection in microphytobenthos: role of vertical migration and the xanthophyll cycle against photoinhibition. Aquat. Microb. Ecol. **67**: 161–175. doi:10.3354/ame01591

Serôdio, J., J. Marques da Silva, and F. Catarino. 2001. Use of in vivo chlorophyll a fluorescence to quantify short-term variations in the productive biomass of intertidal microphytobenthos. Mar. Ecol. Prog. Ser. **218**: 45–61. doi:10.3354/meps218045

Serôdio, J., S. Vieira, and S. Cruz. 2008. Photosynthetic activity, photoprotection and photoinhibition in intertidal microphytobenthos as studied in situ using variable chlorophyll fluorescence. Cont. Shelf Res. **28**: 1363–1375. doi:10.1016/j.csr.2008.03.019

Serôdio, J., S. Vieira, S. Cruz, and H. Coelho. 2006. Rapid light-response curves of chlorophyll fluorescence in microalgae: relationship to steady-state light curves and non-photochemical quenching in benthic diatom-dominated assemblages. Photosynth. Res. **90**: 29–43. doi:10.1007/s11120-006-9105-5

Underwood, G. J. C., R. G. Perkins, M. C. Consalvey, A. R. M. Hanlon, K. Oxborough, N. R. Baker, and D. M. Paterson. 2005. Patterns in microphytobenthic primary productivity: Species-specific variation in migratory rhythms and photosynthesis in mixed-species biofilms. Limnol. Oceanogr. **50**: 755–767. doi:10.4319/lo.2005.50.3.0755

Zhu, S.-H., J. Guo, M. T. Maldonado, and B. R. Green. 2010. Effects of iron and copper deficiency on the expression of members of the light-harvesting family in the diatom *Thalassiosira pseudonana* (Bacillariophyceae). J. Phycol. **46**: 974–981. doi:10.1111/j.1529-8817.2010.00884.x

Supplemental information

Supplemental Figure S1. Decline in NDVI, expressed in percentage, during the HL period, measured on green paper.

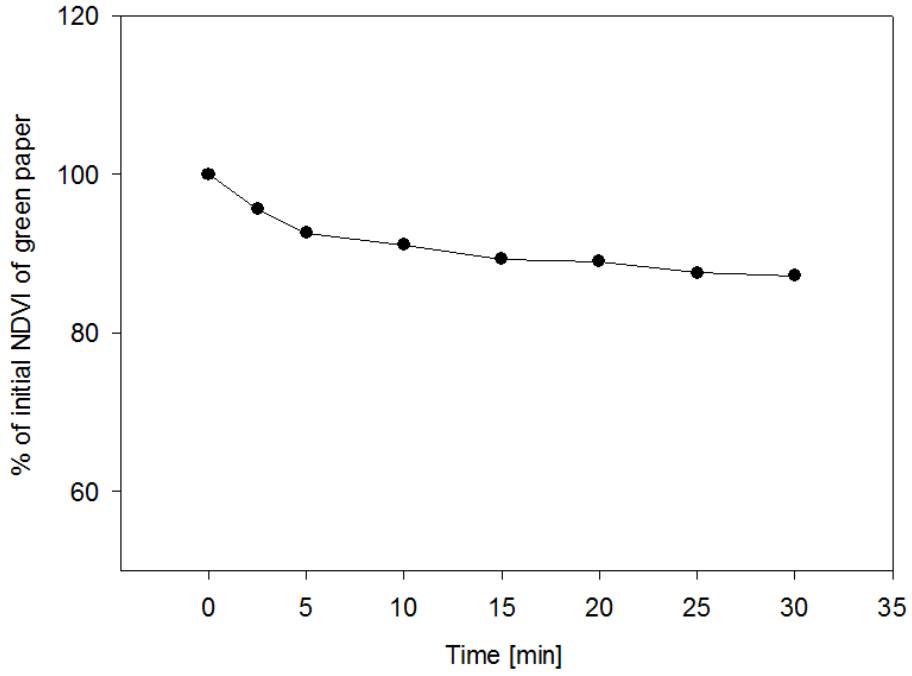

Supplemental Figure S2: Absence in vertical migration in the epipelic species *Navicula phyllepta* and *N. arenaria* at 20 µmol photons m^{-2} s^{-1}.

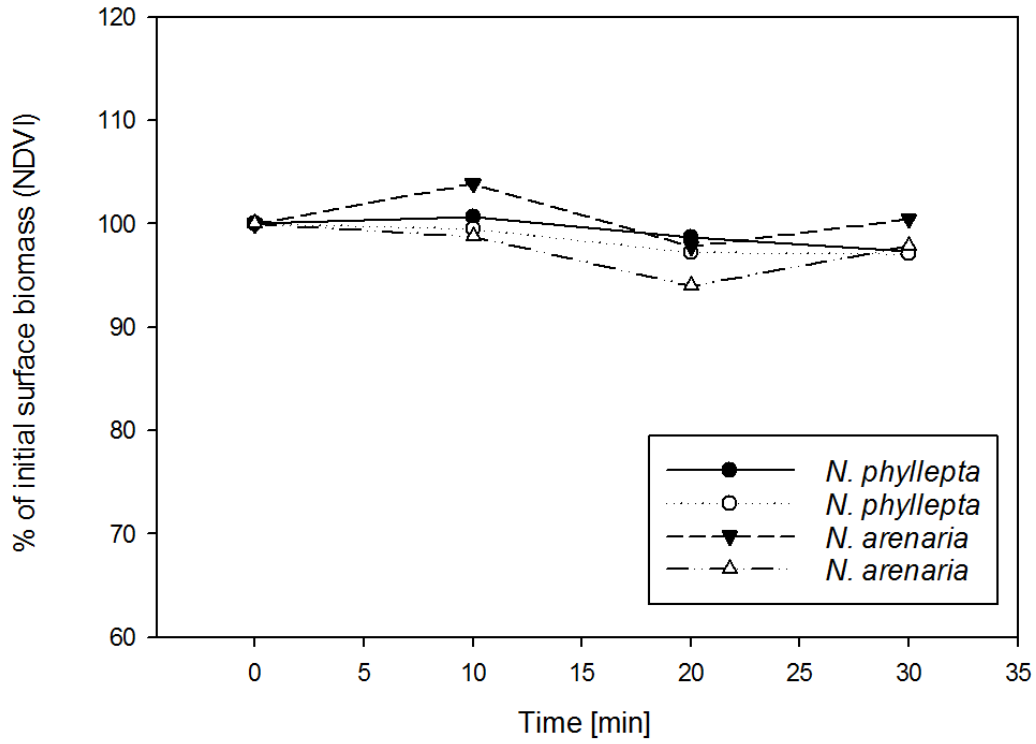

The absence of a VM response in epipsammic diatoms and in the largest (*N. arenaria*) and smallest (*N. phyllepta*) epipelic diatoms (2 technical replicates) in growth light conditions (20 µmol photons m^{-2} s-1) confirms that the observed VM in Fig. 4a occurred in response to the HL conditions.

Supplemental Table S1: significance of surface biomass (NDVI) decline

		NDVI decline 15 min. One sided t-test significances at the 0.05 level are indicated by *	NDVI decline 30 min. One sided t-test significances at the 0.05 level are indicated by *
Navicula phyllepta	epipelic	0.003	0.0008
Seminavis robusta	epipelic	/	0.02
Craspedostauros britannicus	epipelic	0.0068	0.0037
Navicula arenaria	epipelic	0.0003	0.002
Biremis lucens	epipsammic	/	/
Opephora guenter-grasssii	epipsammic	/	/
Nitzschia cf. frustulum	epipsammic	/	/
Planothidium delicatulum	epipsammic	/	/

Supplemental Table S2: Comparison of surface biomass differences between species after 30 min of HL.

Comparisons significant at the 0.05 level are indicated by *.				
species Comparison	**Difference Between Means**	**Simultaneous 95% Confidence Limits**		
N.f. - B.l.	2.847	-11.940	17.634	
N.f. - O.g.	5.464	-9.323	20.251	
N.f. - P.d.	9.068	-5.719	23.855	
N.f. - N.a.	22.218	7.431	37.005	*
N.f. - S.r.	22.793	8.006	37.580	*
N.f. - E.p.	25.555	9.023	42.087	*
N.f. - C.b.	27.102	12.315	41.889	*
N.f. - N.p.	42.818	28.031	57.605	*
B.l. - N.f.	-2.847	-17.634	11.940	
B.l. - O.g.	2.617	-12.170	17.404	
B.l. - P.d.	6.221	-8.566	21.008	
B.l. - N.a.	19.371	4.584	34.158	*
B.l. - S.r.	19.946	5.159	34.733	*
B.l. - E.p.	22.708	6.175	39.240	*
B.l. - C.b.	24.255	9.468	39.042	*
B.l. - N.p.	39.971	25.184	54.758	*
O.g. - N.f.	-5.464	-20.251	9.323	
O.g. - B.l.	-2.617	-17.404	12.170	
O.g. - P.d.	3.604	-11.183	18.391	
O.g. - N.a.	16.754	1.967	31.541	*
O.g. - S.r.	17.329	2.542	32.116	*
O.g. - E.p.	20.091	3.558	36.623	*

O.g. - C.b.	21.638	6.851	36.425	*
O.g. - N.p.	37.354	22.567	52.141	*
P.d. - N.f.	-9.068	-23.855	5.719	
P.d. - B.l.	-6.221	-21.008	8.566	
P.d. - O.g.	-3.604	-18.391	11.183	
P.d. - N.a.	13.150	-1.637	27.937	
P.d. - S.r.	13.725	-1.062	28.512	
P.d. - E.p.	16.487	-0.046	33.019	
P.d. - C.b.	18.034	3.247	32.821	*
P.d. - N.p.	33.750	18.963	48.536	*
N.a. - N.f.	-22.218	-37.005	-7.431	*
N.a. - B.l.	-19.371	-34.158	-4.584	*
N.a. - O.g.	-16.754	-31.541	-1.967	*
N.a. - P.d.	-13.150	-27.937	1.637	
N.a. - S.r.	0.575	-14.212	15.362	
N.a. - E.p.	3.337	-13.196	19.869	
N.a. - C.b.	4.884	-9.903	19.671	
N.a. - N.p.	20.600	5.813	35.386	*
S.r. - N.f.	-22.793	-37.580	-8.006	*
S.r. - B.l.	-19.946	-34.733	-5.159	*
S.r. - O.g.	-17.329	-32.116	-2.542	*
S.r. - P.d.	-13.725	-28.512	1.062	
S.r. - N.a.	-0.575	-15.362	14.212	
S.r. - E.p.	2.762	-13.770	19.294	
S.r. - C.b.	4.309	-10.477	19.096	
S.r. - N.p.	20.025	5.238	34.812	*
E.p. - N.f.	-25.555	-42.087	-9.023	*
E.p. - B.l.	-22.708	-39.240	-6.175	*

E.p. - O.g.	-20.091	-36.623	-3.558	*
E.p. - P.d.	-16.487	-33.019	0.046	
E.p. - N.a.	-3.337	-19.869	13.196	
E.p. - S.r.	-2.762	-19.294	13.770	
E.p. - C.b.	1.548	-14.985	18.080	
E.p. - N.p.	17.263	0.731	33.795	*
C.b. - N.f.	-27.102	-41.889	-12.315	*
C.b. - B.l.	-24.255	-39.042	-9.468	*
C.b. - O.g.	-21.638	-36.425	-6.851	*
C.b. - P.d.	-18.034	-32.821	-3.247	*
C.b. - N.a.	-4.884	-19.671	9.903	
C.b. - S.r.	-4.309	-19.096	10.477	
C.b. - E.p.	-1.548	-18.080	14.985	
C.b. - N.p.	15.715	0.929	30.502	*
N.p. - N.f.	-42.818	-57.605	-28.031	*
N.p. - B.l.	-39.971	-54.758	-25.184	*
N.p. - O.g.	-37.354	-52.141	-22.567	*
N.p. - P.d.	-33.750	-48.536	-18.963	*
N.p. - N.a.	-20.600	-35.386	-5.813	*
N.p. - S.r.	-20.025	-34.812	-5.238	*
N.p. - E.p.	-17.263	-33.795	-0.731	*
N.p. - C.b.	-15.715	-30.502	-0.929	*

Supplemental Table S3: Comparison of NPQ, measured after 5 min HL, between species.

Means with the same letter are not significantly different.			
Tukey Grouping	**Mean**	**N**	**species**
A	3.1085	3	B.l.
A			
A	2.9853	3	N.f.
A			
A	2.6575	3	P.d.
A			
A	2.6343	3	O.g.
B	1.6879	3	E.p.
B			
B	1.5507	3	C.b.
B			
B	1.4392	3	N.a.
B			
B	1.4205	3	N.p.
B			
B	1.2458	3	S.r.

Supplemental Table S4: Values (a) and comparison of the NPQ induction rate k per species (b).

a

Least Squares Means						
Effect	**species**	**Estimate**	**Standard Error**	**DF**	**t Value**	**Pr > |t|**
species	**B.l.**	0.3083	0.001733	2	177.85	<.0001
species	**C.b.**	0.07573	0.009312	2	8.13	0.0148
species	**E.p.**	0.1457	0.007279	2	20.02	0.0025
species	**N.a.**	0.4308	0.09057	2	4.76	0.0415
species	**N.f.**	0.3386	0.04592	2	7.37	0.0179
species	**N.p.**	0.2797	0.04184	2	6.69	0.0216
species	**O.g.**	0.2592	0.02730	2	9.50	0.0109
species	**P.d.**	0.2640	0.01303	2	20.26	0.0024
species	**S.r.**	0.2382	0.03472	2	6.86	0.0206

b

Differences of Least Squares Means									
Effect	**species**	**_species**	**Estimate**	**Standard Error**	**DF**	**t Value**	**Pr > |t|**	**Adjustment**	**Adj P**
species	**B.l.**	**C.b.**	0.2325	0.009472	2.14	24.55	0.0012	Tukey-Kramer	0.0004
species	**B.l.**	**E.p.**	0.1626	0.007482	2.23	21.73	0.0012	Tukey-Kramer	0.0006
species	**B.l.**	**N.a.**	-0.1225	0.09058	2	-1.35	0.3088	Tukey-Kramer	0.8696
species	**B.l.**	**N.f.**	-0.03033	0.04595	2.01	-0.66	0.5769	Tukey-Kramer	0.9964
species	**B.l.**	**N.p.**	0.02853	0.04187	2.0	0.68	0.5657	Tukey-	0.995

					1			Kramer	6
species	**B.l.**	**O.g.**	0.04903	0.02735	2.02	1.79	0.2139	Tukey-Kramer	0.6946
species	**B.l.**	**P.d.**	0.04423	0.01315	2.07	3.36	0.0745	Tukey-Kramer	0.2273
species	**B.l.**	**S.r.**	0.07007	0.03476	2.01	2.02	0.1808	Tukey-Kramer	0.6026
species	**C.b.**	**E.p.**	-0.06996	0.01182	3.78	-5.92	0.0049	Tukey-Kramer	0.0465
species	**C.b.**	**N.a.**	-0.3550	0.09105	2.04	-3.90	0.0579	Tukey-Kramer	0.1563
species	**C.b.**	**N.f.**	-0.2629	0.04685	2.16	-5.61	0.0253	Tukey-Kramer	0.0549
species	**C.b.**	**N.p.**	-0.2040	0.04286	2.2	-4.76	0.0343	Tukey-Kramer	0.0897
species	**C.b.**	**O.g.**	-0.1835	0.02884	2.46	-6.36	0.0139	Tukey-Kramer	0.0371
species	**C.b.**	**P.d.**	-0.1883	0.01602	3.62	-11.75	0.0005	Tukey-Kramer	0.0048
species	**C.b.**	**S.r.**	-0.1625	0.03595	2.29	-4.52	0.0354	Tukey-Kramer	0.1041
species	**E.p.**	**N.a.**	-0.2851	0.09086	2.03	-3.14	0.0869	Tukey-Kramer	0.2678
species	**E.p.**	**N.f.**	-0.1929	0.04649	2.1	-4.15	0.0491	Tukey-Kramer	0.1322
species	**E.p.**	**N.p.**	-0.1340	0.04246	2.12	-3.16	0.0810	Tukey-Kramer	0.2641
species	**E.p.**	**O.g.**	-0.1135	0.02825	2.28	-4.02	0.0453	Tukey-Kramer	0.1442
species	**E.p.**	**P.d.**	-0.1183	0.01493	3.14	-7.93	0.0036	Tukey-Kramer	0.0182
species	**E.p.**	**S.r.**	-0.09251	0.03548	2.18	-2.61	0.1111	Tukey-Kramer	0.3956
species	**N.a.**	**N.f.**	0.09217	0.1015	2.96	0.91	0.4317	Tukey-Kramer	0.9775
species	**N.a.**	**N.p.**	0.1510	0.09976	2.8	1.51	0.2330	Tukey-	0.809

					2			Kramer	5
species	**N.a.**	**O.g.**	0.1715	0.09459	2.36	1.81	0.1918	Tukey-Kramer	0.6859
species	**N.a.**	**P.d.**	0.1667	0.09150	2.08	1.82	0.2050	Tukey-Kramer	0.6822
species	**N.a.**	**S.r.**	0.1926	0.09699	2.58	1.99	0.1563	Tukey-Kramer	0.6148
species	**N.f.**	**N.p.**	0.05887	0.06212	3.97	0.95	0.3974	Tukey-Kramer	0.9720
species	**N.f.**	**O.g.**	0.07937	0.05342	3.26	1.49	0.2271	Tukey-Kramer	0.8205
species	**N.f.**	**P.d.**	0.07457	0.04773	2.32	1.56	0.2416	Tukey-Kramer	0.7902
species	**N.f.**	**S.r.**	0.1004	0.05757	3.72	1.74	0.1614	Tukey-Kramer	0.7150
species	**N.p.**	**O.g.**	0.02050	0.04995	3.44	0.41	0.7058	Tukey-Kramer	0.9999
species	**N.p.**	**P.d.**	0.01570	0.04382	2.38	0.36	0.7494	Tukey-Kramer	0.9999
species	**N.p.**	**S.r.**	0.04153	0.05437	3.87	0.76	0.4888	Tukey-Kramer	0.9913
species	**O.g.**	**P.d.**	-0.00480	0.03025	2.87	-0.16	0.8844	Tukey-Kramer	1.0000
species	**O.g.**	**S.r.**	0.02103	0.04417	3.79	0.48	0.6601	Tukey-Kramer	0.9996
species	**P.d.**	**S.r.**	0.02583	0.03709	2.55	0.70	0.5441	Tukey-Kramer	0.9949

Supplemental Table S5: Comparison of NPQ, measured after 30 min HL, between species.

Means with the same letter are not significantly different.				
Tukey Grouping		**Mean**	**N**	**species**
	A	3.8379	3	B.l.
	A			
	A	3.7760	3	P.d.
	A			
	A	3.7466	3	N.f.
	A			
	A	3.6312	3	C.b.
	A			
	A	3.4449	3	O.g.
	A			
B	A	2.9071	3	E.p.
B				
B	C	1.9736	3	N.p.
	C			
	C	1.8584	3	N.a.
	C			
	C	1.8016	3	S.r.

Supplemental Table S6: Comparison of $\Delta F/F_m'$, measured after 30 min LL recovery, between species.

Means with the same letter are not significantly different.				
Tukey Grouping		**Mean**	**N**	**species**
	A	84.151	3	O.g.
	A			
B	A	71.693	3	N.a.
B	A			
B	A	70.904	3	B.l.
B	A			
B		53.999	3	P.d.
B				
B		51.608	3	N.f.
	C	26.461	3	N.p.
	C			
	C	15.451	3	C.p.
	C			
	C	14.089	3	E.p.
	C			
	C	2.950	3	S.r.

Chapter 5: LHCX proteins in *Seminavis robusta*

Lander Blommaert[1], Emmelien Vancaester[2,3], Marie Huysman[2,3], Sofie D'hondt[1], Tore Brembu[4], Per Winge[4], Atle Bones[4], Bernard Lepetit[5], Johann Lavaud[6], Klaas Vandepoele[2,3], Wim Vyverman[1] & Koen Sabbe[1]

1. Ghent University, Lab. Protistology & Aquatic Ecology, B-9000 Ghent, Belgium
2. VIB, Department of Plant Systems Biology, B-9052 Ghent, Belgium
3. Ghent University, Department of Plant Biotechnology and Bioinformatics, B-9052 Ghent, Belgium
4. Department of Biology, Norwegian University of Science and Technology, Trondheim, Norway
5. Zukunftskolleg, Pflanzliche Ökophysiologie, Universität Konstanz 78457, Germany
6. CNRS/Université Laval, UMI3376 Takuvik Joint International Laboratory, Département de Biologie, Pavillon Alexandre Vachon, Université Laval, 1045 avenue de la Médecine, Québec, Qc, G1V 0A6, Canada

Abstract

Intertidal benthic diatoms experience a highly variable light regime, which especially challenges these organisms to cope with excess light energy during low tide. Non-photochemical quenching of chlorophyll fluorescence (NPQ) is one of the most rapid mechanisms diatoms possess to dissipate excess energy. Its capacity is mainly defined by the xanthophyll cycle (XC) and Light-Harvesting Complex X (LHCX) proteins. Whereas the XC and its relation to NPQ has been well-studied in both planktonic and benthic diatoms, our current knowledge about LHCX proteins and their potential involvement in NPQ regulation is mostly based on planktonic diatoms. While recent studies using immuno-localization have revealed the presence of light-regulated LHCX proteins in benthic diatom communities and isolates, nothing is as yet known about the diversity, identity and transcriptional regulation of these LHCX proteins. We identified LHCX genes in the *Seminavis robusta* and followed their transcriptional regulation during a day/night cycle and during exposure to high light conditions. The *S. robusta* genome contains 14 LHCX sequences, which is much more than in the sequenced planktonic model diatoms (4-5), but similar to the sea ice associated diatom *Fragilariopsis cylindrus*. *LHCX* diversification in both species, however, seems to have occurred independently. Our data suggest that the involvement of several light regulated *LHCX* genes in the photophysiology of *S. robusta* may represent an adaptation to the complex and highly changeable light environment in this benthic diatom species.

Introduction

Due to the complex interplay of diurnal and tidal cycles and weather conditions, the surface sediments of tidal flats experience highly variable light conditions. Nevertheless, they are very productive ecosystems thanks to the presence of biofilms, called microphytobenthos (MPB), which is dominated by benthic diatoms (Underwood and Kromkamp 1999). The fluctuating light conditions challenge these diatoms to maximize light harvesting under low light conditions while avoiding oxidative damage to their photosynthetic apparatus under high light, either by minimizing light absorbance or by the dissipation of excess light energy. Benthic diatoms possess two main strategies which are fast enough to track rapid fluctuations in light intensity, namely, vertical migration and excess energy dissipation as heat (Lavaud and Goss 2014; Laviale et al. 2016). Raphid pennate diatoms possess a raphe structure which allows for motility by the secretion of mucilage. These diatoms, often referred to as epipelic diatoms, can form dense biofilms on fine-grained sediments (Sabbe 1993; Ribeiro et al. 2013) and are able to position themselves within the sediment light gradient via vertical migration (Admiraal 1984; Consalvey et al. 2004; Serôdio et al. 2006; Cartaxana et al. 2016). In addition, they can dissipate excess light energy as heat, measured as Non-Photochemical Quenching of chlorophyll *a* fluorescence (NPQ). NPQ comprises a quickly and a slowly reversible component, referred to as 'qE' and NPQs (Lavaud and Goss 2014) respectively. The capacity for this fast physiological photoprotection mechanism is mainly defined by the xanthophyll cycle (XC) pigments diatoxanthin (Dtx) and its de-epoxidized form diadinoxanthin (Ddx) (Barnett et al. 2015; Blommaert et al. 2017) and the presence of Light-Harvesting Complex X (LHCX) proteins (Bailleul et al. 2010; Taddei et al. 2016; Ghazaryan et al. 2016; Lepetit et al. 2017). While the XC in benthic diatoms has been well-studied using natural communities (van Leeuwe et al. 2008; Jesus et al. 2009; Serôdio et al. 2012; Laviale et al. 2015) and more recently also unialgal isolates (Barnett et al. 2015; Blommaert et al. 2017), our current knowledge about LHCX proteins as an NPQ regulator is mostly based on studies on planktonic diatoms (Büchel 2014; Lavaud and Goss 2014; Goss and Lepetit 2015; Ghazaryan et al. 2016). The latter includes studies on the pennate model diatom *Phaeodactylum tricornutum* (Bowler et al. 2008) whose ecological life style to date remains obscure but which has mainly been isolated from coastal plankton samples (De Martino et al. 2007).

LHCX proteins are closely related to the Light-Harvesting Complex Stress-Related (LHCSR) proteins that are present in most eukaryotic algae and mosses but absent in plants (Niyogi and Truong 2013; Goss and Lepetit 2015). Even though LHCX/LHCSR proteins are Light Harvesting Proteins, they have an energy dissipating rather than a light harvesting function (Niyogi and Truong 2013). LHCSR proteins appear to function both as excess light sensors and quenching sites (Bonente et al. 2011b; Ballottari et al. 2016). A similar function as NPQ regulators has been proposed for LHCX proteins in

planktonic diatoms as high light induces LHCX transcription and augments LHCX protein content (Oeltjen et al. 2002; Nymark et al. 2009; Bailleul et al. 2010; Park et al. 2010; Zhu and Green 2010; Lepetit et al. 2013; Taddei et al. 2016). However, the precise function of LHCX proteins in NPQ and their location in the thylakoid membrane is as yet not known. They are hypothesized to bind the XC pigments Ddx and Dtx (Beer et al. 2006; Lepetit et al. 2013) and change the supramolecular organization of antenna complexes (Ghazaryan et al. 2016), a crucial feature in a recent mechanistic model for NPQ formation (Lavaud and Goss 2014; Goss and Lepetit 2015).

LHCX function and transcriptional regulation has been intensively studied in *Phaeodactylum tricornutum* (Nymark et al. 2009, 2013; Bailleul et al. 2010; Lepetit et al. 2013, 2017; Taddei et al. 2016). Its genome contains four *LHCX* genes (*LHCX*1-4). Of these four genes, *LHCX1* is highly expressed in non-stressful light conditions; additional expression upon high light exposure is low (Nymark et al. 2009; Lepetit et al. 2013; Taddei et al. 2016). Its corresponding protein consequently is present in low light conditions where it might provide the diatom with a basal level of NPQ when exposed to sudden changes in light climate. In addition, the different content in LHCX1 between different *P. tricornutum* ecotypes has been related to their natural variability in NPQ capacity. In strong light conditions, both *LHCX*2 and *LHCX*3 transcription is strongly induced (Nymark et al. 2009; Lepetit et al. 2013, 2017; Taddei et al. 2016). As both proteins accumulate in concert with de novo synthesis of Ddx + Dtx, they may provide additional Ddx/Dtx binding sites to enhance the basal NPQ provided by LHCX1 (Lepetit et al. 2013). Overexpresssion of both *LHCX*2&3, indeed, has been shown to rescue NPQ in a low-NPQ ecotype of *P. tricornutum* (Pt4) (Taddei et al. 2016). *LHCX4* gene expression is inhibited by light, whereas its transcript accumulates in prolonged darkness, questioning its role in photoprotection (Nymark et al. 2013; Lepetit et al. 2013; Taddei et al. 2016). As overexpresssion of this gene can (partly) rescue the low-NPQ phenotype of Pt4, it seems to be able to contribute to NPQ and could together with an enhanced Ddx + Dtx pool play a role in the high NPQ levels observed in cultures exposed to long dark periods interrupted by short light periods (Lavaud et al. 2002; Ruban et al. 2004; Lepetit et al. 2017). Interestingly, in the LHCX4 protein only one of the three amino-acid residues responsible for luminal pH (ΔpH) sensing (as a NPQ trigger) in the LHCSR3 protein in *Chlamydomonas reinhardtii* is conserved, whereas in the LHCX1,2&3 proteins two out of the three protonable residues are conserved (Ballottari et al. 2016; Taddei et al. 2016).

Recent studies using immuno-localization revealed the presence of several light-regulated LHCX-isoforms in natural communities and isolates of MPB diatoms (Laviale et al. 2015; Blommaert et al. 2017). Up to date, however, nothing is known about the sequence identity and transcriptional regulation of these LHCX proteins in truly benthic diatoms. Several studies, moreover, indicate that the findings for the *P. tricornutum* may not be directly transferable to other pennate diatoms and benthic epipelic diatoms in

particular. This is corroborated by the recent discovery of 11 *LHCX* genes in the genome of the sea ice diatom *Fragilariopsis cylindrus*, none of which could readily be related to the four *LHCX* genes in *P. tricornutum* (Mock et al. 2017). In addition, the *F. cylindrus* genome contains an LHCX gene that is closely related to the LHCX6 in *Thalassiosira pseudonana*, whereas a similar sequence is absent in the *P. tricornutum* genome. The *T. pseudonana* LHCX6 protein could be associated with Dtx binding and may play a direct role in excess energy dissipation via sustained quenching NPQs during acclimation to prolonged HL stress (Zhu & Green 2010). Interestingly, an LHCX isoform of slightly larger size was detected with an anti-LHCX6 antibody in the intertidal benthic diatom *Navicula phyllepta* (Laviale et al. 2015). Recently, we studied the presence and high light responsiveness of LHCX isoforms in the intertidal benthic diatom *Seminavis robusta* and revealed an isoform, present in low light, and two isoforms that were only observed after high light exposure (Blommaert et al. 2017), one of which did not correspond in size to any isoform in *P. tricornutum*. In the present study, therefore, we identified *LHCX* genes in the *S. robusta* draft genome and followed their transcriptional regulation during a day/night cycle and during exposure to high light conditions.

Materials and methods

Culture conditions

Seminavis robusta was obtained from the diatom culture collection (BCCM/DCG) of the Belgian Coordinated Collection of Micro-organisms (http://bccm.belspo.be/about-us/bccm-dcg), accession number (DCG 0105). Diatom cultures were grown in semi-continuous batch culture in 1.8 l glass Fernbach flasks (Schott) under a day/night rhythm of 16/8 hour with a light intensity of 20 µmol photons m^{-2} s^{-1}. Cells were cultured in Provasoli's enriched f/2 seawater medium (Guillard, 1975) using Tropic Marin artificial sea salt (34.5 gL^{-1}) enriched with $NaHCO_3$ (80 mg L^{-1} final concentration) Cultures were acclimated to these culturing conditions for at least 2 weeks. *S. robusta* was then grown in 650 mL culture flasks (Greiner bio-one) to monitor *LHCX* expression during a 24 hour 16/8 hour day/night and extended dark cycle (where cultures were kept in the dark during the normal light period, after the normal night period). Three biological replicates were sampled independently. Gene expression was compared to the samples at the end of the first light period.

High light exposure

High light exposure was identical to the conditions described in Blommaert et al. (2017). Cultures in exponential growth were concentrated to 10 mg/L Chl *a* (determined spectrophotometrically, Jeffrey and Humphrey 1975) by centrifugation at 4000 RCF for 5 min. The cultures were again acclimated to their standard growth conditions for 2 h before exposure to high light. Immediately before the start of the experiment, $NaHCO_3$ (4 mM) was added from a 2M stock to prevent carbon limitation during the experiment. Four 65 W white light energy-saving lamps (Lexman) were used to provide high light (HL) conditions (2000 µmol photons/$m^{-2}s^{-1}$) as used by (Lepetit et al. 2013). Cells were continuously stirred in a glass test tube to obtain a homogenous cell suspension. This glass test tube was continuously cooled in a custom-made glass cooler by a water bath at 20°C. Three biological replicates were sampled immediately before the onset of 2000 µmol photons $m^{-2}s^{-1}$ and after 15, 30 and 60 min of HL. Gene expression of treated samples was compared to the samples before HL.

RNA extraction and cDNA synthesis

Samples for RNA were taken before high light exposure (T0) and during 15, 30 and 60 min of high light exposure. Four mL of cell culture was sampled each time on 3 µm Versapore filters (PALL corporation), washed with ice-cooled phosphate buffered saline (PBS) and immediately frozen in liquid nitrogen. Samples were stored at -80°C before

RNA extraction. RNA extraction was based on (Le Bail et al. 2008). Frozen samples were immediately incubated in 500 µL extraction buffer (100 mM Tris-HCl pH 7.5, 2% CTAB, 1.5 M NaCl, 50 mM EDTA, and 10% β-mercaptoethanol) and subsequently beaten with carbid beads for 30 min in a bead-beater at 30 Hz. One hundred µl of 10% Chelex-100 was added before the samples were incubated for 15 minutes at 56°C with occasional vortexing. One volume of chloroform:isoamyl alcohol (24:1, Vol/Vol) was subsequently added before shaking the samples for 25 min at 5 Hz. After centrifugation, the upper phase was transferred to a new tube and mixed with 0.3 volume of absolute ethanol to precipitate polysaccharides. One volume of chloroform was added and after centrifugation the upper phase was transferred to a fresh tube. RNA was precipitated overnight at -20°C, by adding 0.25 volumes of 12M LiCl and 1% (of final volume) β-mercapto-ethanol. The next day, the RNA was pelleted, dried and washed with 70% ethanol. Residual DNA was eliminated with DNAse I (Turbo DNAse, Ambion) according to the manufacturer's instructions. Extraction was performed with 1 volume Phenol-Chlorophorm (1:1, Vol/Vol). After centrifugation the upper phase was transferred to a fresh tube, extracted with one volume of chlorophorm:isoamylic alcohol (24:1, Vol/Vol) and centrifuged again. The upper phase was precipitated with 0.3 M NaOAc (pH 5.5) and 100% ice cold ethanol by incubating for 1 hour at -80°C. After the samples were centrifuged for 20 minutes at 4°C, the supernatant was discarded and the pellet washed with 70% ethanol. The pellet was finally resuspended in RNAse-free water. The samples were reverse transcribed using Bio-Rad iScript cDNA kit.

Identification LHCX genes in *S. robusta* draft genome

A HMMER search (Biosequence analysis using profile Hidden Markov Models) for LHCX homologs was conducted using an in-house draft genome of the D6 strain of *S. robusta* (DCG 0489). A non-redundant set of *LHCX* genes, containing only one copy of each *LHCX* gene, was obtained according to Mock et al. (2017): contigs containing putative *LHCX* genes were aligned with NCBI BLASTn (Basic Local Alignment Search Tool for nucleotides) using as thresholds at least 50% coverage and at least 90% sequence identity (in contrast to 95% as in Mock et al. 2017). *LHCX* genes on these contigs were considered as alleles if they had best bi-directional hits on the corresponding contig and had at least 90% nucleotide identity with one another. Tandem repeats were identified with Tandem Repeats Finder (Benson 1999).

A maximum likelihood tree was constructed, based on amino-acid sequences with RaxML, after sequence alignment with MUSCLE and manual editing with Jalview. 1000 bootstrap iterations were run. LHCX sequences from *Thalassiosira pseudonana*, *Phaeodactylum tricornutum*, *Fragilariopsis cylindrus* and *Pseudo-nitzschia multiseries* (with kind permission of E. V. Armbrust) were obtained from the JGI database (http://genome.jgi.doe.gov/).

qPCR

RT-qPCR was performed with a Light Cycler ® 480II (ROCHE). Primers were designed using Primer3 (Supplementary table S1b). Primer specificity was tested in silico with FastPCR (PrimerDigital). Single nucleotide polymorphisms (SNPs) between the whole genome sequenced strain (D6) and the strain used in the experiments (85A) were identified using in-house RNAseq data (Bilcke et al. unpublished data) using Integrative Genomics Viewer (IGV, Broad Institute) and did not affect primer specificity.

CDKA1, V4 and V1 (Moeys et al. 2016) were used for normalization as these were most stably expressed (Qbase+ software). Log_2 expression ratios were compared with REST2013 software. The RT-qPCR program contained the following steps:

Pre-incubation: 95°C – 5 min
Amplification: 95°C – 10 s
58°C – 10 S
72°C – 20 s (40 cycli)
Melting curve: 95°C – 5 min
65°C – 1 min
97°C – continuous

Results

LHCX presence in the genome of *S. robusta*

A HMMER search, with a profile based on the four *P. tricornutum* LHCX sequences, yielded 21 putative *LHCX* sequences in the draft *S. robusta* genome, (Sr*LHCX*) (Table 1, Fig. 1). We removed six sequences (highlighted in grey in Table 1), present on redundant contigs, from the total set of *LHCX* loci. From the remaining sequences, 11 showed complete LHCX sequences (see alignment Fig. 2). The automatically annotated SrLHCX3h sequence contained two introns, but was adjusted to contain only one intron, changing the N-terminal part based on in-house RNAseq data and corresponding to other LHCXs. Four sequences (including one possible allele) were incomplete and lacked the N-terminal part (indicated with a red font color in Table 1). Based on homology with other SrLHCX sequences, they were extended to a plausible start codon. The automatically annotated sequence on Sr-Backbone_263_11.1 contained multiple introns, possibly introduced by the software due the high amount of stop codons in all reading frames. In addition, the in-house RNA seq data did not support transcription of this sequence. It might therefore be a pseudogene and was not given an LHCX name or included in the gene tree (Fig. 1). For both alleles of SrLHCX3g (Sr-Backbone_377_4.1 and Sr-Backbone_757_9.1) a complete open reading frame (ORF) could not be determined. However, Sr-Backbone_757_9.1 contained 9 consecutive guanine (G) nucleotides, which might be an incorrect homopolymer due to a sequencing error. Removing two, five of seven guanine nucleotides, however, yielded a complete ORF. The deletion of several guanine nucleotides, moreover, is supported by a gap at this position (Fig. S1) in the mapped PACBIO reads. However, due to lack of RNA seq support for the sequence in general, the complete transcript sequence could not be determined. Its potential allele Sr-Backbone_377_4.1, contains a tandem repeat (Fig. S2a) (Benson 1999) from which the first repeat does not result in an LHCX amino acid sequence (Fig. S2b) and is not strongly supported by in-house PACBIO reads. The second repeat however does correspond to an LHCX sequence.

The maximum likelihood LHCX tree (Fig. 1) shows that the SrLHCX sequences do not show a clear one on one relationship with sequences from *P. tricornutum* or the other included diatom species. Most SrLHCX sequences, however, seem to cluster with PtLHCX3, but this is not well supported by the bootstrap values. High bootstrap values, nonetheless, support the clustering of SrLHCX1a and SrLHCX1b, of SrLHCX4a and SrLHCX4b and of SrLHCX3b and the other SrLHCX3 sequences. SrLHCX6 seems rather unrelated to the other SrLHCX sequences and is found in a cluster containing TpLHCX6 and FcLHCX6, however, again with low bootstrap support. The long branches for SrLHCX3f and 3g, probably reflect uncertainties in their respective gene models, see above.

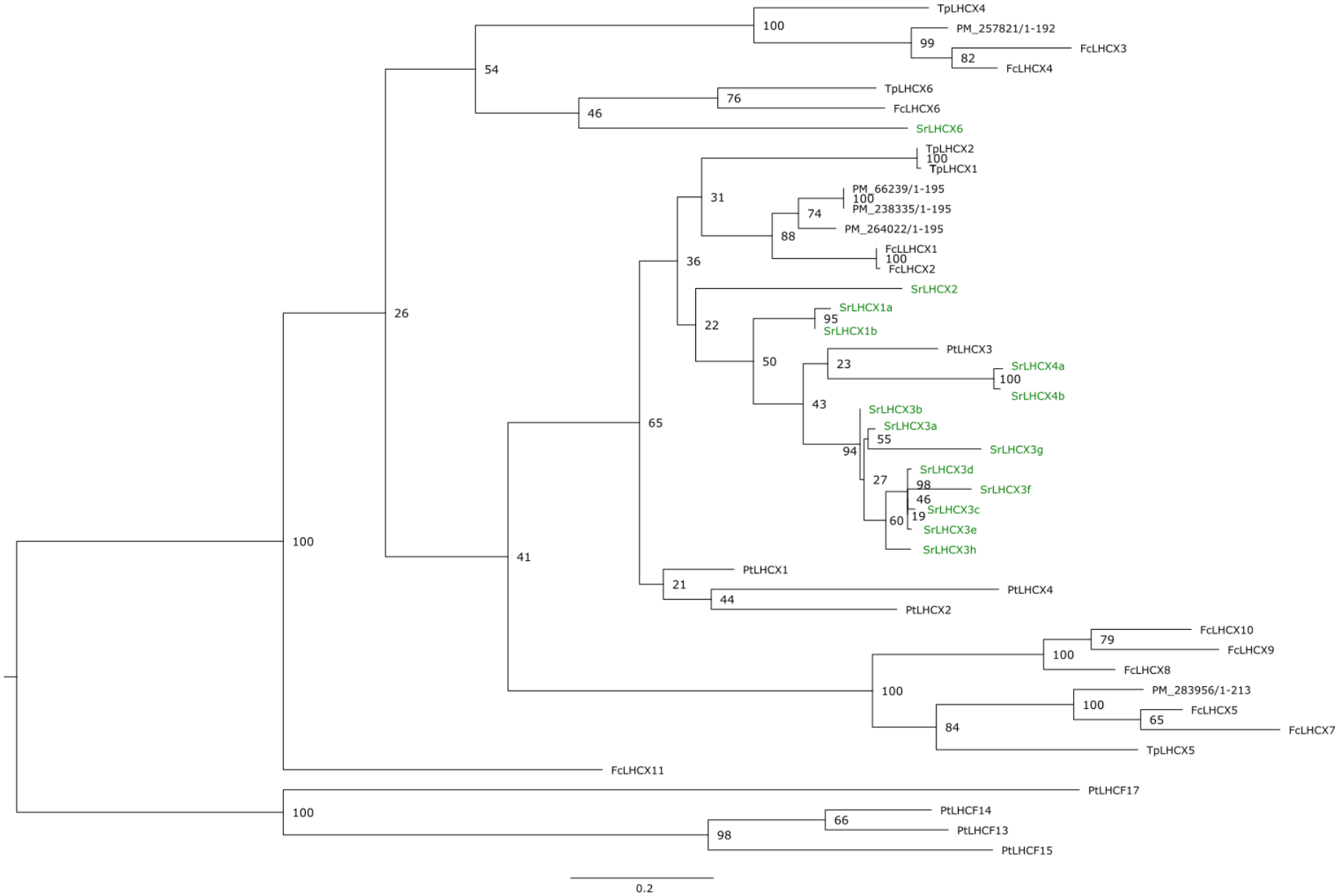

Figure 1: Maximum likelihood tree of LHCX genes in *Seminavis robusta* (Sr, green), constructed, based on amino-acid sequences with RaxML, after sequence alignment with MUSCLE and manual editing with Jalview. 1000 bootstrap iterations were run (values are shown at the nodes. LHCX sequences from *Thalassiosira pseudonana* (Tp), *Phaeodactylum tricornutum* (Pt), *Fragilariopsis cylindrus* (Fc) and *Pseudo-nitzschia multiseries* (PM, with kind permission of E. V. Armbrust) were obtained from the JGI database (http://genome.jgi.doe.gov/).

Gene ID	Name	MW[KDa]	query cover	contig seq id	gene seq id	location
Sr-Backbone_1106_30.1	**SrLHCX1a**	20.86				87110..87610,87690..87779
Sr-Backbone_38_3.1	**SrLHCX1b**	20.87				41589..42089,42164..42253
Sr-Backbone_1106_29.1	**SrLHCX2**	21.60				85759..85851,85961..86467
Sr-Backbone_478_55.1	**SrLHCX3a**	22.38				131757..132398
Sr-Backbone_785_13.1			58%	94%	100%	25569..26210
Sr-Backbone_392_6.1	**SrLHCX3b**	22.33				32258..32899
Sr-Backbone_440_61.1	**SrLHCX3c**	22.43				175336..175878,175963..176061
Sr-Backbone_1330_26.1	**SrLHCX3d**	22.42				49819..49914,50012..50554
Sr-Backbone_514_62.1	**SrLHCX3e**	22.38				155822..155917,156001..156543
Sr-Backbone_413_8.1			66%	100%		19435..19530,19614..19903
Sr-Backbone_1430_6.1			82%	92%		22330..22872,22960..23055
Sr-Backbone_335_3.1	**SrLHCX3f**					10678..11342
Sr-Backbone_377_4.1	**SrLHCX3g**					2109..2881
Sr-Backbone_757_9.1			52%	97%	97%	15478..16136
Sr-Backbone_742_15.1	**SrLHCX3h**	22.54				51101..51202,51287..51829
Sr-Backbone_263_11.1	**/**					32718..32914,33027..33065,33284..33413,33484..33534
Sr-Backbone_830_11.1	**SrLHCX4a**	20.81				40661..41248
Sr-Backbone_514_29.1	**SrLHCX4b**	20.83				77193..77497,77600..77882
Sr-Backbone_1740_5.1			97%	99%	98%	7218..7500,7604..7908
Sr-Backbone_53_45.1	**SrLHCX6**	32.82				166273..166944
Sr-Backbone_1602_3.1			60%	95%		8064..8469,8555..8967

Table 1: LHCX sequences in *S. robusta*. MW: molecular weight, Query cover: % coverage of the smaller by the larger contig. Seq identity: % identical base pairs on contig overlap. Gene seq id: % identical base pairs of transcripts. Not calculated in case of gene model uncertainty. Values are only reported for sequences considered alleles.

Table 2: primer specificity testing using FastPCR in silico PCR with default settings. Green represents an amplified PCR product, whereas orange represents the possibility of an amplified gene product, however with one of the primers having a melting temperature <50°C when binding on the corresponding *LHCX* transcript. As most *LHCX3* sequences are rather similar in the primer regions, the primer LHCX3 picks up multiple related transcripts.

Gene ID	Name	LHCX1a,b	LHCX2	LHCX3	LHCX3g	LHCX3h	LHCX4a	LHCX4b	LHCX6
Sr-Backbone_1106_30.1	**SrLHCX1a**								
Sr-Backbone_38_3.1	**SrLHCX1b**								
Sr-Backbone_1106_29.1	**SrLHCX2**								
Sr-Backbone_478_55.1	**SrLHCX3a**								
Sr-Backbone_785_13.1									
Sr-Backbone_392_6.1	**SrLHCX3b**								
Sr-Backbone_440_61.1	**SrLHCX3c**								
Sr-Backbone_1330_26.1	**SrLHCX3d**								
Sr-Backbone_514_62.1	**SrLHCX3e**								
Sr-Backbone_413_8.1									
Sr-Backbone_1430_6.1									
Sr-Backbone_335_3.1	**SrLHCX3f**								
Sr-Backbone_377_4.1	**SrLHCX3g**								
Sr-Backbone_757_9.1									
Sr-Backbone_742_15.1	**SrLHCX3h**								
Sr-Backbone_263_11.1	**/**								
Sr-Backbone_830_11.1	**SrLHCX4a**								
Sr-Backbone_514_29.1	**SrLHCX4b**								
Sr-Backbone_1740_5.1									
Sr-Backbone_53_45.1	**SrLHCX6**								
Sr-Backbone_1602_3.1									

LHCX gene expression

To identify which *SrLHCX* genes are responsive to high light, we exposed *S. robusta* cells to the same HL treatment as in (Blommaert et al. 2017), see section methods. The specificity of primer sets used in this experiment is given in Table 2, results are shown in Fig. 3. All *Sr LHCX* genes, were highly upregulated during the HL treatment. The highest upregulation was detected for *SrLHCX3g & 4b* (Fig. 3). Of all light induced *LHCX*s, only *SrLHCX2, 3g & 6* were significantly more highly upregulated after 15 min. of HL. After 30 min tested all *LHCX*s were significantly upregulated. Sr*LHCX2* reached the highest expression levels at 15 minutes, with subsequent significant decreases after both 30 and 60 min. Also *SrLHCX1a,b, 3g &6* showed a significant decline in expression between 30 and 60 minutes of HL.

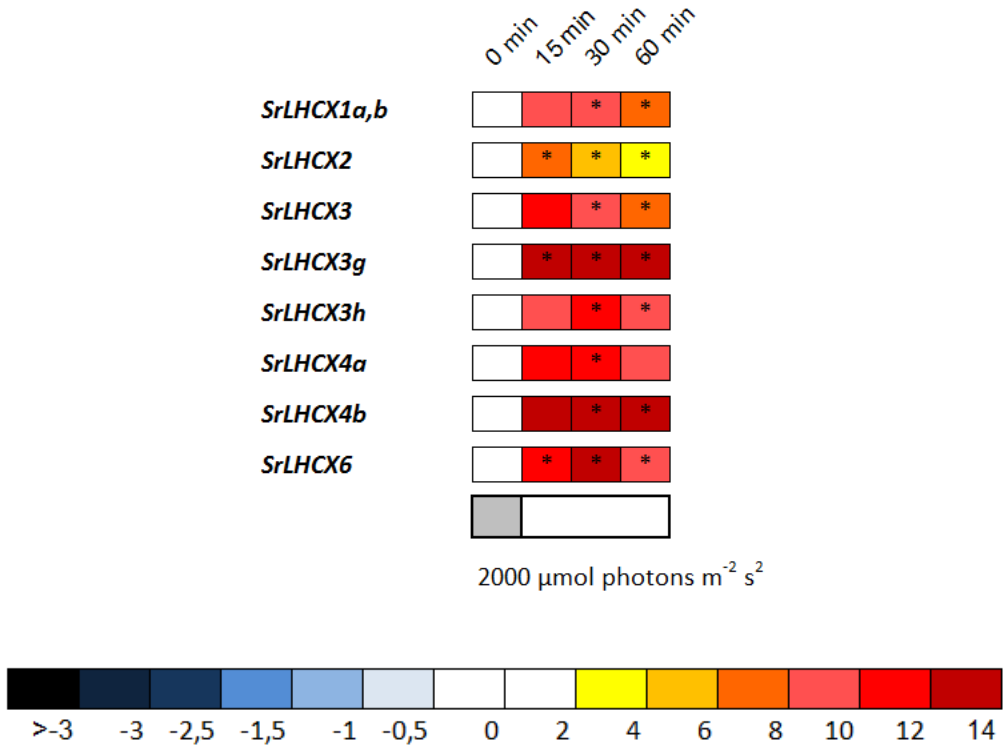

Figure 3: Expression ratios are log_2 transformed and indicated by the color chart. Values are averages of three independent replicates and relative to the respective initial values (LL). Significant changes at p<0.05 (Pairwise Fixed Reallocation Randomization Test performed by REST2013) are indicated with an asterisk.

In addition, we studied *LHCX* expression in *S. robusta* during 24 hours of a 16 h light (20 µmol photons m^2s^{-1}) 8 h dark cycle (Fig. 4a). Cultures kept in prolonged darkness were sampled in parallel (Fig. 4b). Gene expression was compared to expression levels in samples at the end of the previous light period (time point 0:00 in Fig. 4a-b). As in some replicates *SrLHCX2&4a* transcripts were not detected at the reference time point (0:00), transcription was compared to samples collected two hours before light onset (time point 6:00 in Fig. 4a-b). In the latter samples, no genes were significantly more highly

expressed. All *SrLHCX* genes showed a significant upregulation 15 minutes after the dark/light transition, with the exception of *SrLHCX6*. In the samples kept in prolonged darkness only *SrLHCX2* was significantly upregulated one hour after the light period would have started. All genes showed significantly higher expression values at 15 minutes of light exposure, compared to the samples kept in darkness (data not shown). This was also the case after one hour of light exposure, with exception of *SrLHCX3g* and *3h*. Only *SrLHCX2* was significantly more highly expressed 3 h after light onset, compared to unexposed samples (data not shown).

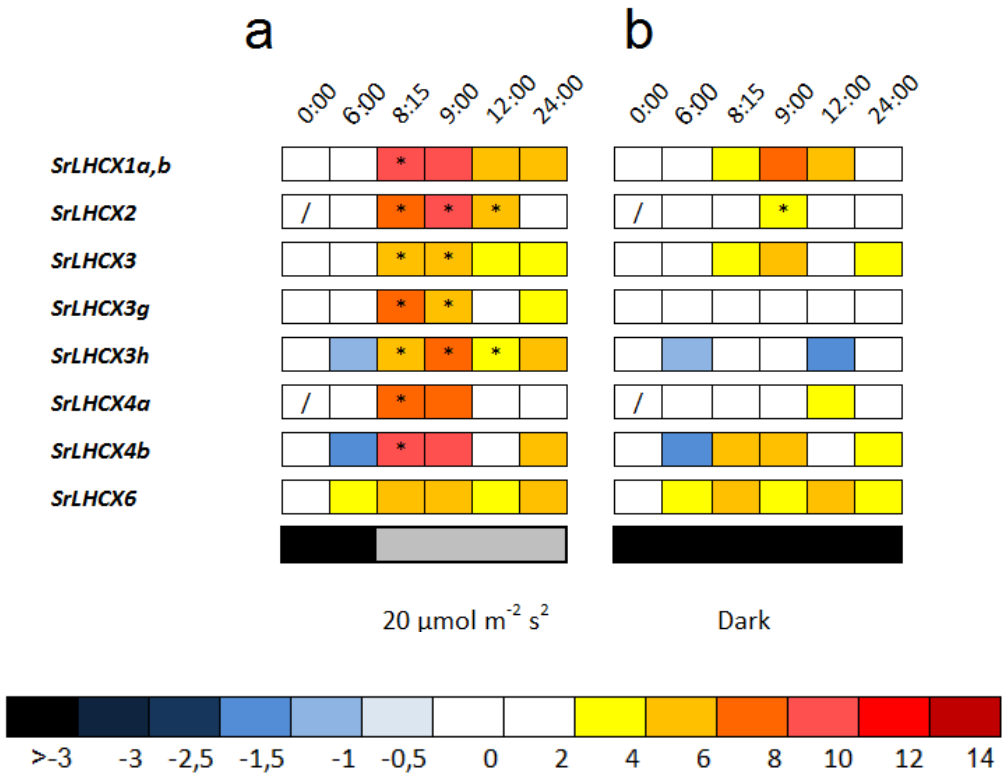

Figure 4: Expression ratios are log_2 transformed and values are indicated by the color chart. Values are averages of three independent biological replicates and are relative to the first time point (0:00), with the exception of *SrLHCX2* and *SrLHCX4a*, which are relative to the values at the second time point (6:00) as no transcripts were detected at (0:00). Therefore, the first time point (0:00) is represented by a '/'. Significant changes ($p<0.05$, Pairwise Fixed Reallocation Randomization Test performed by REST) are indicated with an asterisk. (a) *LHCX* expression during a 24 hour 16/8 hour day/night regime with light onset at 8:00. (b) *LHCX* expression during a 24-hour cycle with an extended dark period.

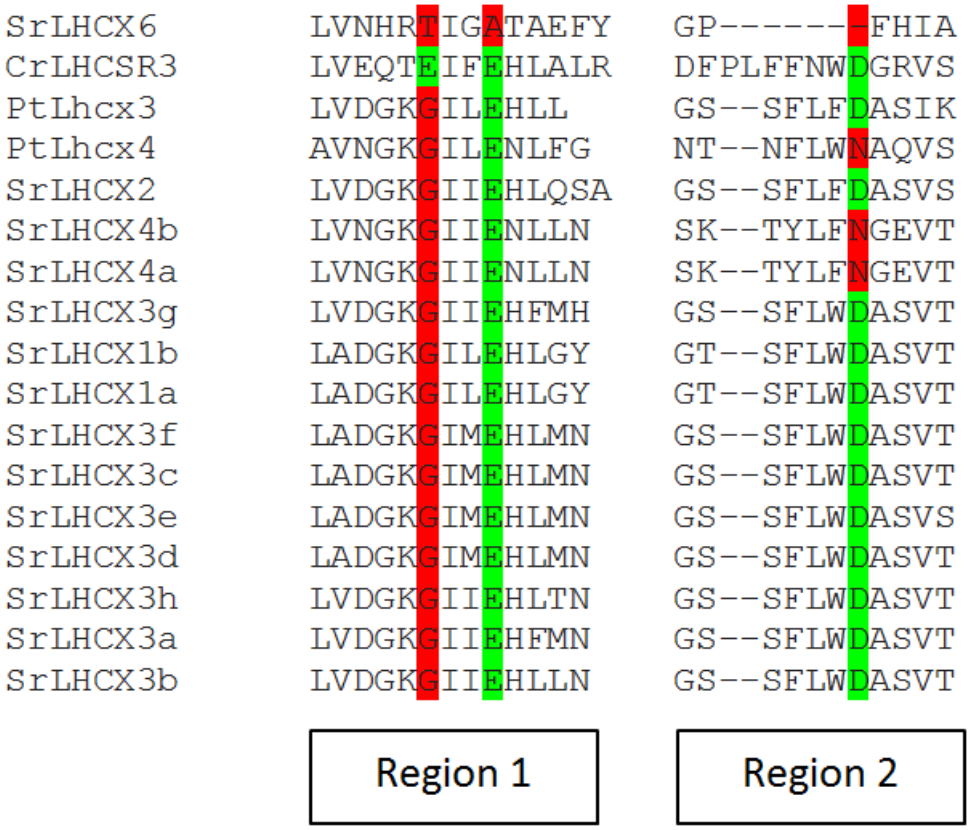

Figure 5: Alignment of regions 1 and 2 of *Chlamydomonas reinhardtii* LHCSR3, *P. tricornutum* LHCX3 and 4, and all LHCX sequences in *S. robusta*. The highlights in green represent conserved pH-sensing residues, whereas red highlights represent the absence of conserved pH-sensing residues.

We investigated the presence of three amino acid residues which are known to function as sensor of the thylakoid lumen pH in the LHCSR3 in *C. reinhardtii* and are indispensable for NPQ functioning (Ballottari et al. 2016), two of which are also present in all *P. tricornutum* LHCX sequences, except LHCX4 (Fig. 5). SrLHCX6 contains none of the protonable residues in *C. reinhardtii* as is the case for LHCX6 in *T. pseudonana* (not shown). The same residues are conserved in all SrLHCX sequences as in PtLHCX1,2&3, with the exception of SrLHCX4a,b which both lack the same residue as PtLHCX4.

Discussion

As LHCX proteins play a central role in the NPQ mechanism of planktonic diatoms (Bailleul et al. 2010; Zhu and Green 2010; Lepetit et al. 2013, 2017; Taddei et al. 2016) and light responsive LHCX-isoforms have been observed in benthic diatom isolates and communities (Laviale et al. 2015; Blommaert et al. 2017), we investigated the presence of *LHCX* genes in the benthic diatom *Seminavis robusta* and studied their transcriptional regulation during high light conditions and a darkness/low light transition.

We detected 14 *LHCX* genes and one possible pseudogene in *S. robusta*, a high number compared to the model diatoms *P. tricornutum* (4) and *T. pseudonana* (5), but in the same range of the psychrophilic sea ice diatom *F. cylindrus* (11) (Armbrust et al. 2004; Bowler et al. 2008; Mock et al. 2017). Even though a similar amount of LHCX genes was discovered, *LHCX* diversification in both species seems to have occurred independently as *LHCX* genes of both species were found in different clades. It has to be pointed out however that the relationships between SrLHCX proteins and isoforms in other diatom species, however, in general were not well resolved with bootstrap values being generally low. Using a cut-off value of 50%, for instance, strongly changes the tree topology (Fig. S3).

Even though a possible functional redundancy can be expected due to the high number of *LHCX* genes in *S. robusta*, transcription appears to be strongly light-regulated in all of the studied genes: all investigated *LHCX* transcripts were strongly upregulated in high light conditions, as was reported for planktonic diatoms (Nymark et al. 2009; Zhu and Green 2010; Lepetit et al. 2013) and in line with the observation of light responsive LHCX isoforms in benthic communities and the benthic diatoms *Navicula phyllepta* (Laviale et al. 2015) and *S. robusta* (Blommaert et al. 2017). In addition, the transcription of these genes, with the exception of *SrLHCX6*, peaked transiently after the dark/low light transition, confirming a possible regulating role in photosynthesis/photoprotection (Oeltjen et al. 2004; Nymark et al. 2009; Lepetit et al. 2013). Our results, however, do not allow to conclude why *S. robusta* has such a high number of *LHCX* genes (see below). One possibility, could be that a large set of *LHCX* genes is required to cope with variable light conditions. However, *P. tricornutum* only possesses four LHCX genes which still enable the species to rapidly adjust to a highly fluctuating light climate (Lepetit et al. 2017). The ability of motile epipelic diatoms to rapidly migrate away from strong light conditions, furthermore, could minimize the need for strong physiological photoprotection (Laviale et al. 2016).

Whereas the transcriptional response to changing light conditions was similar for most studied LHCX genes, a differential response was observed for *SrLHCX*2 and *SrLHCX*6. Interestingly, these genes are not closely related to the majority of *LHCX* genes in *S.*

robusta: *SrLHCX*6 clusters in a clade containing *LHCX*6 in the centric diatom *T. pseudonana* and the pennate diatom *F. cylindrus* (however with low bootstrap support). As *SrLHCX*6 was strongly upregulated in high light, whereas it was not upregulated from a dark to low light transition, it is possible that its gene product only accumulates in oversaturating conditions. Thus, together with Dtx binding, SrLHCX6 may play a role in sustained quenching (NPQs), as proposed for the LHCX6 in *T. pseudonana*. This matches the observation of sustained quenching and de novo Dtx synthesis in *S. robusta* under identical high light conditions. In *N. phyllepta*, which is phylogenetically related to *S. robusta* (Chepurnov et al. 2008), the anti-LHCX6 antibody raised against LHCX6 in *T. pseudonana* recognized a high light inducible LHCX isoform, whose size (~33KDa) is similar to the calculated size in *S. robusta*, Table 1, (Laviale et al. 2015). The same antibody, nonetheless, failed to recognize an isoform of any size in *S. robusta* (Blommaert et al. 2017).

In contrast to *SrLHCX*6, the *SrLHCX2* transcript was induced during the first 3 h after light onset and was the only gene being significantly induced when the dark/light transition was replaced by continuous darkness. Additional transcription upon a transition to high light, moreover, was only transiently induced. A similar light-regulation pattern was observed in Pt*LHCX1* (Nymark et al. 2009; Bailleul et al. 2010; Lavaud and Lepetit 2013; Lepetit et al. 2017) and could suggest that the gene product of Sr*LHCX2* is consistently present in the light harvesting antennae to provide a basal (but rather low) NPQ capacity (Barnett et al. 2015; Blommaert et al. 2017). As the difference in transcriptional regulation between *SrLHCX*2 and the other studied *SrLHCX* genes was less pronounced than in *P. tricornutum* and all transcripts, except *SrLHCX*6, were induced upon a light/dark transition, we cannot rule out that other SrLHCX proteins fulfill a similar role as PtLHCX1. The presence of *LHCX* transcripts in low light in *S. robusta* is consistent with the findings of Blommaert et al. (2017). The size of the observed isoform, nonetheless, is different from the calculated size of SrLHCX2 and is more likely to be an isoform of SrLHCX3. Linking transcriptional data and immuno-localization, in this case, is not straightforward as the used antibody (anti-LHCSR3, Bonente et al. 2011) was not specifically designed to recognize certain diatom LHCX isoforms. In addition, the large number of LHCX genes of similar sizes (Table 1) and differences in actual and predicted protein size (Bonente et al. 2011a) complicate the comparison of both datasets as was also observed for the observed discrepancies in transcriptional and translational regulation of LHCXs in *P. tricornutum* and *T. pseudonana* (Zhu and Green 2010; Lepetit et al. 2017).

One of the most highly upregulated transcripts in high light was Sr*LHCX*4b, which remained highly expressed even after 60 min of HL exposure. This gene is closely related to Sr*LHCX*4a and seems to be differentiated from the majority of *SrLHCX3*s. A major difference between the SrLHCX4a&b proteins and the other SrLHCX proteins (with the

exception of SrLHCX6) is that only one protonable instead of two protonable amino-acid residues (compared to the three amino-acids responsible for the switch to energy-dissipating mode in *C. reinhardtii*) is conserved. A similar difference in amino-acid sequence has been reported for PtLHCX4 and other *P. tricornutum* isoforms, the former, however, being induced only in prolonged darkness (Nymark et al. 2013; Taddei et al. 2016). Even though NPQ regulation by a light-induced luminal pH change in diatoms is as yet not clear (Blommaert et al. in prep, Chapter 6), the above findings may suggest that both SrLHCX4 as PtLHCX4 are not or less controlled by a trans-thylakoidal proton gradient and hence possibly could contribute to a more sustained NPQ component as was suggested for TpLHCX6 (Zhu and Green 2010), which completely lacks these residues.

In this study, we demonstrated the presence of multiple light-regulated *LHCX* genes, which may allow epipelic species to respond and/or acclimate to prolonged higher light conditions (Ezequiel et al. 2015; Barnett et al. 2015), either through an increase of the fast-responsive NPQ component 'qE' or through a more sustained quenching NPQs (Lavaud and Goss 2014). The differential involvement of SrLHCX proteins could be further discriminated using laboratory simulations of natural light conditions, such as a gradually increasing or rapidly fluctuating light regime (Lepetit et al. 2017) or during nutrient starvation conditions (Taddei et al. 2016). In addition, more specific antibodies could be designed or mass-spectrometry could be used to identify the proteins of the observed LHCX-isoforms, whereas knock-out mutants can give more details about the specific function. However, both approaches could also be complicated due to the high number of similar *LHCX* genes.

References

Admiraal, W. 1984. The ecology of estuarine sediment-inhabiting diatoms. Prog. Phycol. Res. **3**: 269–322.

Armbrust, E. V., J. A. Berges, C. Bowler, and others. 2004. The genome of the diatom *Thalassiosira pseudonana*: ecology, evolution, and metabolism. Science **306**: 79–86. doi:10.1126/science.1101156

Le Bail, A., S. M. Dittami, P.-O. de Franco, S. Rousvoal, M. J. Cock, T. Tonon, and B. Charrier. 2008. Normalisation genes for expression analyses in the brown alga model *Ectocarpus siliculosus*. BMC Mol. Biol. **9**: 75. doi:10.1186/1471-2199-9-75

Bailleul, B., A. Rogato, A. De Martino, S. Coesel, P. Cardol, C. Bowler, A. Falciatore, and G. Finazzi. 2010. An atypical member of the light-harvesting complex stress-related protein family modulates diatom responses to light. Proc. Natl. Acad. Sci. **107**: 18214–18219. doi:10.1073/pnas.1007703107

Ballottari, M., T. B. Truong, E. De Re, E. Erickson, G. R. Stella, G. R. Fleming, R. Bassi, and K. K. Niyogi. 2016. Identification of pH-sensing Sites in the Light Harvesting Complex Stress-related 3 Protein Essential for Triggering Non-photochemical Quenching in *Chlamydomonas reinhardtii*. J. Biol. Chem. **291**: 7334–46. doi:10.1074/jbc.M115.704601

Barnett, A., V. Méléder, L. Blommaert, and others. 2015. Growth form defines physiological photoprotective capacity in intertidal benthic diatoms. ISME J. **9**: 32–45. doi:10.1038/ismej.2014.105

Beer, A., K. Gundermann, J. Beckmann, and C. Büchel. 2006. Subunit Composition and Pigmentation of Fucoxanthin−Chlorophyll Proteins in Diatoms: Evidence for a Subunit Involved in Diadinoxanthin and Diatoxanthin Binding. Biochemistry **45**: 13046–13053. doi:10.1021/bi061249h

Blommaert, L., M. J. J. Huysman, W. Vyverman, J. Lavaud, and K. Sabbe. 2017. Contrasting NPQ dynamics and xanthophyll cycling in a motile and a non-motile intertidal benthic diatom. Limnol. Oceanogr. doi:10.1002/lno.10511

Bonente, G., M. Ballottari, T. B. Truong, T. Morosinotto, T. K. Ahn, G. R. Fleming, K. K. Niyogi, and R. Bassi. 2011a. Analysis of LhcSR3, a protein essential for feedback de-excitation in the green alga *Chlamydomonas reinhardtii*. T. Shikanai [ed.]. PLoS Biol. **9**: e1000577. doi:10.1371/journal.pbio.1000577

Bonente, G., M. Ballottari, T. B. Truong, T. Morosinotto, T. K. Ahn, G. R. Fleming, K. K. Niyogi, and R. Bassi. 2011b. Analysis of LhcSR3, a protein essential for feedback de-excitation in the green alga *Chlamydomonas reinhardtii*. PLoS Biol. **9**: e1000577. doi:10.1371/journal.pbio.1000577

Bowler, C., A. E. Allen, J. H. Badger, and others. 2008. The *Phaeodactylum* genome reveals the evolutionary history of diatom genomes. Nature **456**: 239–44. doi:10.1038/nature07410

Büchel, C. 2014. Non-Photochemical Quenching and Energy Dissipation in Plants, Algae and Cyanobacteria, Springer.

Cartaxana, P., S. Cruz, C. Gameiro, and M. Kühl. 2016. Regulation of intertidal

microphytobenthos photosynthesis over a diel emersion period is strongly affected by diatom migration patterns. Front. Microbiol. **7**: 872. doi:10.3389/fmicb.2016.00872

Chepurnov, V. A., D. G. Mann, P. Von Dassow, P. Vanormelingen, J. Gillard, D. Inzé, K. Sabbe, and W. Vyverman. 2008. In search of new tractable diatoms for experimental biology. BioEssays **30**: 692–702. doi:10.1002/bies.20773

Consalvey, M., D. M. Paterson, and G. J. C. Underwood. 2004. The ups and downs of life in a benthic biofilm: Migration of benthic diatoms. Diatom Res. **19**: 181–202.

Ezequiel, J., M. Laviale, S. Frankenbach, P. Cartaxana, and J. Serôdio. 2015. Photoacclimation state determines the photobehaviour of motile microalgae: The case of a benthic diatom. J. Exp. Mar. Bio. Ecol. **468**: 11–20. doi:10.1016/j.jembe.2015.03.004

Ghazaryan, A., P. Akhtar, G. Garab, P. H. Lambrev, and C. Büchel. 2016. Involvement of the Lhcx protein Fcp6 of the diatom *Cyclotella meneghiniana* in the macro-organisation and structural flexibility of thylakoid membranes. Biochim. Biophys. Acta - Bioenerg. **1857**: 1373–1379. doi:10.1016/j.bbabio.2016.04.288

Goss, R., and B. Lepetit. 2015. Biodiversity of NPQ. J. Plant Physiol. **172**: 13–32. doi:10.1016/j.jplph.2014.03.004

Guillard R. L. 1975. Culture of Marine Invertebrate Animals, W.L. Smith and M.H. Chanley [eds.]. Springer US.

Jeffrey, S. W., and G. S. Humphrey. 1975. New spectrophotometric equations for determining chlorophylls *a*, *b*, *c*1 and *c*2 in higher plants, algae and natural phytoplankton. Biochem Physiol Pflanz. Bd. **167**: 191–194.

Jesus, B., V. Brotas, L. Ribeiro, C. R. Mendes, P. Cartaxana, and D. M. Paterson. 2009. Adaptations of microphytobenthos assemblages to sediment type and tidal position. Cont. Shelf Res. **29**: 1624–1634. doi:10.1016/j.csr.2009.05.006

Lavaud, J., and R. Goss. 2014. The peculiar features of the non-photochemical fluorescence quenching in diatoms and brown algae, p. 421–443. *In* B. Demmig-Adams, G. Garab, W. Adams III, and Govindjee [eds.], Non-Photochemical Quenching and Energy Dissipation in Plants, Algae and Cyanobacteria. Springer.

Lavaud, J., and B. Lepetit. 2013. An explanation for the inter-species variability of the photoprotective non-photochemical chlorophyll fluorescence quenching in diatoms. Biochim. Biophys. Acta **1827**: 294–302. doi:10.1016/j.bbabio.2012.11.012

Lavaud, J., B. Rousseau, and a-L. Etienne. 2002. In diatoms, a transthylakoid proton gradient alone is not sufficient to induce a non-photochemical fluorescence quenching. FEBS Lett. **523**: 163–6.

Laviale, M., A. Barnett, J. Ezequiel, B. Lepetit, S. Frankenbach, V. Méléder, J. Serôdio, and J. Lavaud. 2015. Response of intertidal benthic microalgal biofilms to a coupled light-temperature stress: evidence for latitudinal adaptation along the Atlantic coast of Southern Europe. Environ. Microbiol. **17**: 3662–3677. doi:10.1111/1462-2920.12728

Laviale, M., S. Frankenbach, and J. Serôdio. 2016. The importance of being fast: comparative kinetics of vertical migration and non-photochemical quenching of benthic diatoms under light stress. Mar. Biol. **163**: 10. doi:10.1007/s00227-015-2793-7

van Leeuwe, M., V. Brotas, M. Consalvey, R. Forster, D. Gillespie, B. Jesus, J. Roggeveld, and W. Gieskes. 2008. Photoacclimation in microphytobenthos and the role of xanthophyll pigments. Eur. J. Phycol. **43**: 123–132. doi:10.1080/09670260701726119

Lepetit, B., G. Gélin, M. Lepetit, and others. 2017. The diatom *Phaeodactylum tricornutum* adjusts nonphotochemical fluorescence quenching capacity in response to dynamic light via fine-tuned Lhcx and xanthophyll cycle pigment synthesis. New Phytol. **214**: 205–218. doi:10.1111/nph.14337

Lepetit, B., S. Sturm, A. Rogato, A. Gruber, M. Sachse, A. Falciatore, P. G. Kroth, and J. Lavaud. 2013. High light acclimation in the secondary plastids containing diatom *Phaeodactylum tricornutum* is triggered by the redox state of the plastoquinone pool. Plant Physiol. **161**: 853–865. doi:10.1104/pp.112.207811

De Martino, A., A. Meichenin, J. Shi, K. Pan, and C. Bowler. 2007. Genetic and phenotypic characterization of *Phaeodactylum tricornutum* (Bacillariophyceae) accessions. J. Phycol. **43**: 992–1009. doi:10.1111/j.1529-8817.2007.00384.x

Mock, T., R. P. Otillar, J. Strauss, and others. 2017. Evolutionary genomics of the cold-adapted diatom *Fragilariopsis cylindrus*. Nature **541**: 536–540. doi:10.1038/nature20803

Moeys, S., J. Frenkel, C. Lembke, and others. 2016. A sex-inducing pheromone triggers cell cycle arrest and mate attraction in the diatom *Seminavis robusta*. Sci. Rep. **6**: 19252. doi:10.1038/srep19252

Niyogi, K. K., and T. B. Truong. 2013. Evolution of flexible non-photochemical quenching mechanisms that regulate light harvesting in oxygenic photosynthesis. Curr. Opin. Plant Biol. **16**: 307–14. doi:10.1016/j.pbi.2013.03.011

Nymark, M., K. C. Valle, T. Brembu, K. Hancke, P. Winge, K. Andresen, G. Johnsen, and A. M. Bones. 2009. An integrated analysis of molecular acclimation to high light in the marine diatom *Phaeodactylum tricornutum*. PLoS One **4**: e7743. doi:10.1371/journal.pone.0007743

Nymark, M., K. C. Valle, K. Hancke, P. Winge, K. Andresen, G. Johnsen, A. M. Bones, and T. Brembu. 2013. Molecular and photosynthetic responses to prolonged darkness and subsequent acclimation to re-illumination in the diatom *Phaeodactylum tricornutum*. PLoS One **8**: e58722. doi:10.1371/journal.pone.0058722

Oeltjen, A., J. Marquardt, and E. Rhiel. 2004. Differential circadian expression of genes fcp2 and fcp6 in *Cyclotella cryptica*. Int. Microbiol. **7**: 127–31.

Oeltjen, a., W. E. Krumbein, and E. Rhiel. 2002. Investigations on Transcript Sizes, Steady State mRNA Concentrations and Diurnal Expression of Genes Encoding Fucoxanthin Chlorophyll a/c Light Harvesting Polypeptides in the Centric Diatom *Cyclotella cryptica*. Plant Biol. **4**: 250–257. doi:10.1055/s-2002-25737

Park, S., G. Jung, Y. Hwang, and E. Jin. 2010. Dynamic response of the transcriptome of a psychrophilic diatom, *Chaetoceros neogracile*, to high irradiance. Planta **231**: 349–60. doi:10.1007/s00425-009-1044-x

Ribeiro, L., V. Brotas, Y. Rincé, and B. Jesus. 2013. Structure and diversity of intertidal benthic diatom assemblages in contrasting shores: a case study from the Tagus estuary. J. Phycol. **49**: 258–270. doi:10.1111/jpy.12031

Ruban, A., J. Lavaud, B. Rousseau, G. Guglielmi, P. Horton, and A.-L. Etienne. 2004. The super-excess energy dissipation in diatom algae: comparative analysis with higher plants. Photosynth. Res. **82**: 165–75. doi:10.1007/s11120-004-1456-1

Sabbe, K. 1993. Short-term fluctuations in benthic diatom numbers on an intertidal sandflat in the Westerschelde estuary (Zeeland, The Netherlands). Hydrobiologia **269–270**: 275–284. doi:10.1007/BF00028026

Serôdio, J., J. Ezequiel, a Barnett, J. Mouget, V. Méléder, M. Laviale, and J. Lavaud. 2012. Efficiency of photoprotection in microphytobenthos: role of vertical migration and the xanthophyll cycle against photoinhibition. Aquat. Microb. Ecol. **67**: 161–175. doi:10.3354/ame01591

Serôdio, J., S. Vieira, S. Cruz, and H. Coelho. 2006. Rapid light-response curves of chlorophyll fluorescence in microalgae: relationship to steady-state light curves and non-photochemical quenching in benthic diatom-dominated assemblages. Photosynth. Res. **90**: 29–43. doi:10.1007/s11120-006-9105-5

Taddei, L., G. R. Stella, A. Rogato, and others. 2016. Multisignal control of expression of the LHCX protein family in the marine diatom *Phaeodactylum tricornutum*. J. Exp. Bot. **67**: 3939–3951. doi:10.1093/jxb/erw198

Underwood, G. J. C., and J. Kromkamp. 1999. Primary production by phytoplankton and microphytobenthos in estuaries estuaries. Adv. Ecol. Res. **29**: 93–153. doi:10.1016/S0065-2504(08)60192-0

Zhu, S.-H., and B. R. Green. 2010. Photoprotection in the diatom *Thalassiosira pseudonana*: role of LI818-like proteins in response to high light stress. Biochim. Biophys. Acta **1797**: 1449–57. doi:10.1016/j.bbabio.2010.04.003

Acknowledgments

The authors would like to thank the Research Foundation Flanders (FWO project G.0222.09N), Ghent University (BOF-GOA 01G01911) and the Egide/Campus France-PHC Tournesol (n128992UA) exchange program for their financial support. J.L. also thanks the CNRS and the French consortium CPER Littoral for their financial support. M.J.J.H. acknowledges a Postdoctoral Fellowship of the Research Foundation Flanders.

Supplemental information

Table S1: primer sequences

ID	Left primer	Right primer
LHCX primers		
LHCXmerged1	CGGAGAAGCTGTTGAAGGGT	CAGTGACCAAGAGAGCCCAG
comp36360_c0_seq1	CAGTGGCCAAGGACTGTCAT	TCGGTGATTCATGGCTCCAG
comp48425_c0_seq1	CCCCTTGGATTGAAGCCTGA	TCCGTTGACAAGCTCCTGTG
comp48425_c0_seq2	GCCTGAGGATCCTGAAGAGC	TCCACCAACTCTTGTGCCAT
comp51532_c0_seq1	GGCTGATGTCAACACCCTCA	CAGTCACAGAGGCATCCCAG
comp66598_c0_seq1	ACCAGTTGATGTACCAGCGG	CCTGAGCCATGAATCCTGCA
comp66734_c0_seq1	GGTTGGTGAAGCTGTCGAGA	CCAGGCTTGTCAAATGGCAC
comp75154_c0_seq2	TCTTGTGGGATGCCAGTGTC	TCAGCACGCTTTTGTTCAGC
LHCX6	TACTAGACGAGCAAGGCAGC	ACAGTGAAGAAAGTAGCTTGTGT

Figure S1: mapped PACBIO reads on Backbone_757_9.1

Red reads with a '-' represent deletions, whereas blue and green reads are mapped sequences to the contig.

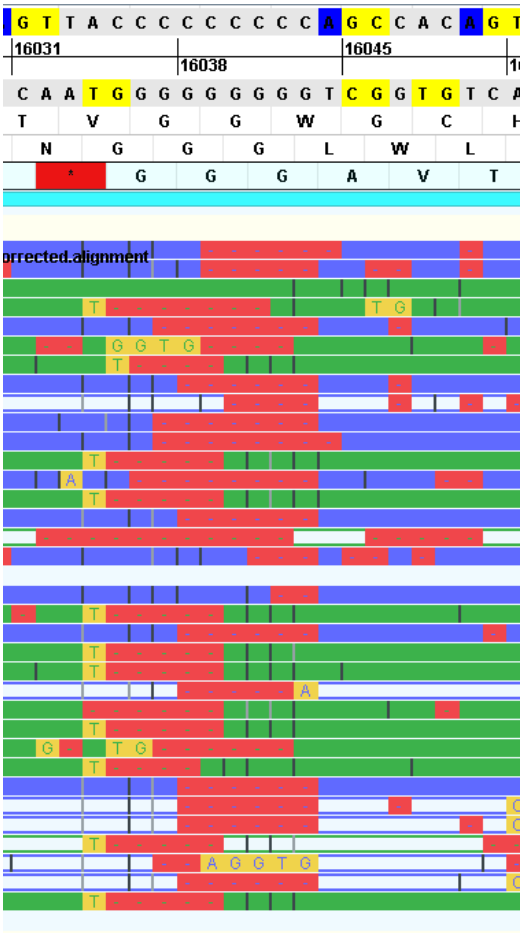

Figure S2a: Sr-Backbone_377_4.1 [2109..2881] contains a tandem repeat. Sequence and alignement of both sesquences

High within sequence similarity of two parts of this nucleotide sequence (highlighted in yellow and green in the Clustal Omega alignment below). 'part 2' yields an open reading frame, matching other LHCXs.

ATGAAGTTCGCTGCTGCCATCACTCTTTTTGCTGCTTCTGCCAGTGCTTTCAGCCCTTTTGGTGTTGCTTCC
AAGAAGGCTGCCACTGTGGCTCCGCTTCACTGTGAAACTATCTCCGACTCTGAGCCTGTGCACTGACCCTT
GTTGGCGACAAGTCTGAAGAAGACTGAAAGCGAACCGAGCTGACTTACCACATGACTGTGCCATGCTTG
CTGTGCCATTGGTTCTTGGCTGGAGAAGCGTTGAAGGATCCTCCTCTGTGGGATCCAGTGTTACCAGTCCT
GCCCATCCCACCTGCTCAGGTCCCACTTTCCCTGGGCTTGTTGTACGAATTGAAGCGCTGAACAAAAAGC
GGCGAGTATTGGATGCTTGCTGCCATTGGTTTCTTGGCTGGAGAAGCTGTTGAAGGATCCTCCTTCTTGT
GGGATGCCAGTGTTACCGGTCCTGCCATTTCCCACCTTGCTCAGGTCCCACCTCTTTTCTGGGCCTTGTTG
GTTACTGGAATTGGAGCTGCTGAACAAAAGCGTGCTGAGATTGGATGGGTTGATCCTGCTGATGTTCCAG
TTGACCAACCAGGCCTTCTCCGCGCTGATTACACTCCTGGTGACATTGGCTTTGACCCCCTTGGATTGAAG
CCTGAGGATCCTGAAGAGCTTTTGGTTCTCCAAAACAAGGAACTCCAGAACGGTCGCTTGGCCATGCTTG
CTGCTGCTGGATTCATGGCACAAGAGTTGGTGGATGGAAAGGGAATCATTGAGCACTTGATGCACTAA

```
part1      ATGCTTGCTGTGCCATTGGTTCTTGGCTGGAGAAGC-GTTGAAGGATCCTCC---TCTGT
part2      ATGCTTGCTGCC-ATTGGTTTCTTGGCTGGAGAAGCTGTTGAAGGATCCTCCTTCTTGTG
           **********     * * ***************** ***************   *

part1      GGGATCCAGTGTTACCAGTCCTGCCCATCCCACC--TGCTCAGGTCCCACTTTCC---CT
part2      GGATGCCAGTGTTACCGGTCCTGCCATTTCCCACCTTGCTCAGGTCCCACCTCTTTTCTG
           **   *********** ********  * **  *  ************** *

part1      GGGCT----TGTTGTACGAATTG-AAGCGCTGAACAAAAAGCGGCGAGTATTGG
part2      GGCCTTGTTGGTTACTGGAATTGGAGCTGCTGAACAAAAGCGTGCTGAGATTGG
           ** **     ***    ****** *   ***********    **    *****
```

Figure S2b: Sr-Backbone_377_4.1 mapped PACBIO reads as viewed in Genomviewer.

Red reads with a '-' represent deletions, whereas blue and green reads are mapped sequences to the contig. The smallest cyan bar represents the automatically annotated ORF, which was extended to a larger sequence (larger cyan bar).

Figure S3: The gene tree (Fig. 1) was collapsed with Treegraph 2, using a bootstrap value cut-off of 50%. Bootstrap values are shown at the nodes. LHCX sequences from *Thalassiosira pseudonana* (Tp), *Phaeodactylum tricornutum* (Pt), *Fragilariopsis cylindrus* (Fc) and *Pseudo-nitzschia multiseries* (PM, with kind permission of E. V. Armbrust) were obtained from the JGI database (http://genome.jgi.doe.gov/).

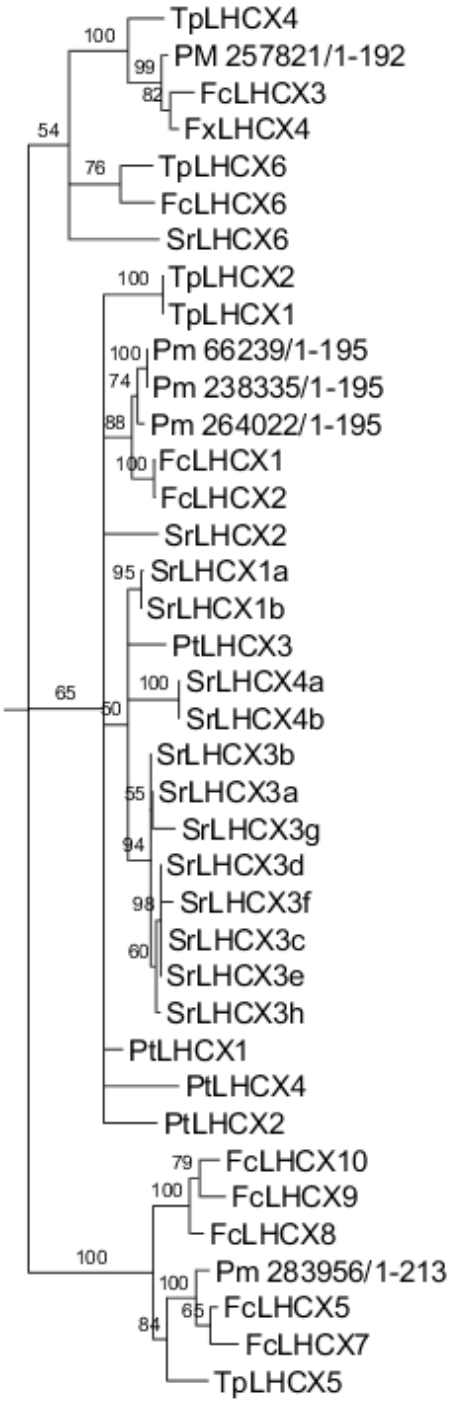

Chapter 6: The role of a trans-thylakoidal proton gradient in regulating Non-Photochemical Quenching in diatoms

Lander Blommaert[1,2], Wim Vyverman[1], Benjamin Bailleul[2] & Koen Sabbe[1]

1. Ghent University, Lab. Protistology & Aquatic Ecology, B-9000 Ghent, Belgium
2. Institut de Biologie Physico-Chimique (IBPC), UMR 7141, Centre National de la Recherche Scientifique (CNRS), Université Pierre et Marie Curie, 13 Rue Pierre et Marie Curie, F-75005 Paris, France

Abstract

Plants and algae organisms need light for photosynthesis, but absorption of too much light can lead to oxidative damage to the photosynthetic apparatus. Therefore, they can dissipate excess light energy harmlessly as heat in a process measured as Non-Photochemical Quenching (NPQ). In plants and green algae, this photoprotection mechanism is mainly controlled by the proton gradient across the thylakoid membrane (ΔpH), which is established during photosynthetic electron transfer. The magnitude of ΔpH has been estimated experimentally in plants and green algae, confirming its role as NPQ regulator. In diatoms the role of ΔpH in NPQ regulation is far less clear as it has never been measured experimentally. Therefore, in this preliminary study, we employed a method, established in plants, to determine ΔpH in the diatom *Opephora guenter-grassii* in conjunction with NPQ measurements. As observed in plants, the ElectroChromic Shift (ECS) signal of *O. guenter-grassii* exhibited a drop below the (dark) baseline (ECS inversion, ECS_{inv}), which is supposed to correlate with the magnitude of the ΔpH. Exposing *O. guenter-grassii* to a range of different light intensities, indeed, showed a strong relationship between NPQ, the xanthophyll cycle and ECS_{inv}. However, we exploited the sensitivity of *O. guenter-grassi* to the uncoupler nigericin, which at low concentrations dissipates ΔpH while keeping overall photosynthesis intact to test the validity of ECSinv as a ΔpH proxy. As at low concentrations of nigericin ECS_{inv} increases while NPQ decreases, it might be that NPQ is not regulated by the magnitude of ΔpH and/or the used method is not valid to measure ΔpH in diatoms and should be reevaluated in plants.

Introduction

Photosynthetic organisms often absorb more light than they can safely use for photosynthesis and have therefore developed mechanisms to protect themselves against excess light energy (Li et al. 2009; Goss and Lepetit 2015). One of the main photoprotection mechanisms is called Non-Photochemical Quenching of chlorophyll fluorescence (NPQ) in which excess light energy is dissipated as heat (Demmig-adams et al. 2014). A major component of the NPQ models in plants and algae is the proton gradient across the thylakoid membrane (ΔpH) (Goss and Lepetit 2015). This proton gradient is established during photosynthetic electron transport whereby protons are translocated from the thylakoid lumen to the stroma and are consequently used for ATP synthesis. In plants and green algae, the magnitude of ΔpH increases in strong light conditions and functions as a feedback control on light harvesting, as it triggers the switch in the light-harvesting antennae from a light-harvesting to an energy-dissipating state, which is observed as NPQ (Demmig-adams et al. 2014; Erickson et al. 2015; Ruban 2016; Sacharz et al. 2017).

In plants, a high ΔpH leads to protonation of the ΔpH sensor PSII subunit S (PsbS) which then undergoes a conformational change and induces rearrangement of the light-harvesting antennae (Ruban 2016; Sacharz et al. 2017). In green algae, ΔpH is sensed by Light-Harvesting Complex Stress Related (LHCSR) proteins (Peers et al. 2009). The LHCSR3 C-terminal domain in *C. reinhardtii* functions as a protonable pH sensor, controlling the quenching state of the light harvesting complexes (Liguori et al. 2013; Ballottari et al. 2016). Thylakoid lumen acidification in plants and green algae, furthermore, activates the de-epoxidation of the pigment violaxanthin (Vx) to zeaxanthin (Zx) in the xanthophyll cycle (XC). Zx is not essential for NPQ formation in both plants and green algae (Niyogi 1997; Bonente et al. 2011), but rather functions as an allosteric regulator in the NPQ formation in plants (Horton 2012).

In the PsbS protein as well as the LHCSR protein, protonable residues necessary for NPQ regulation have been identified using N,N' dicyclohexyl carbodiimide (DCCD) labeling and site-targeted mutations (Li et al. 2004; Ballottari et al. 2016). In plants and green algae, moreover, the magnitude of ΔpH has been estimated experimentally, confirming its role as NPQ regulator (Cruz et al. 2001, 2005; Kramer et al. 2003). The technique used to estimate the relative amplitude of ΔpH is based on the fact that protons are charged and proton accumulation in the lumen also generates an electric field (ΔΨ) across the thylakoid membrane (Kramer et al. 2003). Both the ΔpH and ΔΨ component make up the proton motive force (PMF), which drives ATP synthesis (Mitchell 1961). The ΔΨ component can be measured, based on the phenomenon that thylakoid pigments change their absorption spectrum under influence of a trans-thylakoidal electric field, called the Electro-Chromic Shift signal (ECS) (Bailleul et al. 2010a). Both components, however, are not equal as the thylakoid lumen is buffered and ΔΨ is (partly) dissipated

by counter-ion fluxes. The relaxation of ΔpH and ΔΨ upon an abrupt light-dark transition (which halts the proton influx) is thought to differ, which allows discrimination between both. In a first phase a fast decline in ECS signal is observed. Due to the low electric capacitance of the thylakoid membrane (Vredemberg 1976) and the high proton buffering capacity of the lumen (Junge and McLaughlin 1987), the PMF reaches its equilibrium value by decreasing mostly ΔΨ (the observed ECS signal), whereas the buffered ΔpH remains almost the same. As proton efflux continues until the PMF is completely dissipated, the observed ECS signal representing the transthylakoidal electric field, would be inverted (due to more positive charges on the stromal side) which is indicative of the magnitude of ΔpH. In a second phase when protons are freed from the "buffering network", ΔpH decreases while ΔΨ increases (the PMF being constant). Since what ECS follows is ΔΨ, these two phases translate into an ECS inversion (see Kramer et al. 2003, box 2 and Fig. 3 for a visual representation).

Diatoms possess a high capacity for NPQ (Ruban et al. 2004), which can respond rapidly to changes in light intensity (Lavaud and Goss 2014). The role of ΔpH as a NPQ regulator, however, is far from clear. As diatoms belong to a lineage that acquired photosynthesis mainly by incorporating a plastid of red algal origin (Archibald 2009), the NPQ regulatory components differ from those of the green lineage (reviewed by Goss & Lepetit, 2015). Diatom genomes lack the PsbS gene (Armbrust et al. 2004; Bowler et al. 2008) and the diadinoxanthin/diatoxanthin (Ddx/Dtx) cycle replaces the Vx cycle as the major xanthophyll cycle (Lohr and Wilhelm 1999). Like in the green lineage however, LHCX proteins (related to LHCSR proteins in green algae) are thought to be involved in the NPQ mechanism (Bailleul et al. 2010b; Zhu and Green 2010; Lepetit et al. 2013, 2017; Taddei et al. 2016).

Specific differences exist between plants/green algae and diatoms regarding the xanthophyll cycle and LHCX proteins. Therefore, a similar role for ΔpH as an NPQ regulator in diatoms as in the green algae and plants cannot be assumed: (1) LHCX proteins in diatoms only have two instead of three protonable residues, essential for ΔpH sensing in *C. reinhardtii* (with the exception of LHCX4 in *Phaeodactylum tricornutum*, in which only one residue is conserved (Ballottari et al. 2016; Taddei et al. 2016)); (2) The XC enzyme responsible for the de-epoxidation step (DDE) of Ddx to Dtx shows activity at a pH of 6.5 and higher (Jakob et al. 2001; Grouneva et al. 2006), while the activity of the Vx de-epoxidase in plants is strongly reduced at the same pH; (3) As a considerable PMF is present in darkness in diatoms (Bailleul et al. 2015), the thylakoid lumen might already be acidic in dark conditions. Therefore, the DDE enzyme already might be active in darkness and may therefore need an alternative regulator to become active in high light conditions.

The role of the ΔpH as an NPQ regulator in diatoms has been investigated using uncouplers (substances which artificially disrupt or increase ΔpH) and specific

illumination conditions, leading to the following model regarding the involvement of the ΔpH in NPQ in (pennate) diatoms (Lavaud and Goss 2014; Goss and Lepetit 2015): (1) A certain magnitude of ΔpH is needed for NPQ; (2) Once NPQ is established, only the presence of Dtx is sufficient to maintain a quenching state, even in the absence of a ΔpH; (3) Dtx is mandatory: NPQ is always accompanied by the de-epoxidized xanthophyll Dtx, however a XC-independent NPQ component has been observed in artificial conditions (Lavaud and Kroth 2006; Eisenstadt et al. 2008; Lepetit et al. 2013). To date, however, the magnitude of ΔpH in diatoms was not measured experimentally, making its role in NPQ difficult to investigate.

In the present study, we aimed to investigate in the relationship between NPQ and ΔpH in diatoms, by measuring both in vivo using the methodology previously used in plants (Cruz et al. 2001; Takizawa et al. 2007)(see above). The araphid pennate diatom *Opephora guenter-grassii* was chosen as a model organism, because its NPQ responds very rapidly to changes in irradiance (Blommaert et al. 2017) (Chapter 3), and because in contrast to the pennate model *Phaeodactylum tricornutum* its NPQ is sensitive to the uncoupler nigericin (found in a preliminary experiment) which dissipates ΔpH without affecting the ΔΨ, by equilibrating K^+ and H^+ across the thylakoid membrane (Harned et al. 1951; Graven et al. 1966; Reed 1979). The latter makes it possible to test the validity of ΔpH measurements in diatoms. As in diatoms, furthermore, both linear and quadratic ECS signals are present (Bailleul et al. 2015), and the ECS inversion method is based on a purely linear probe, we first identified at which wavelengths only a purely linear and quadratic signal is present.

Materials & Methods

Culture conditions

Opephora guenter-grassii was obtained from the diatom culture collection (BCCM/DCG) of the Belgian Coordinated Collection of Micro-organisms (http://bccm.belspo.be), accession number: DCG 0448, and grown in a CU-41L4 tissue culture chamber (Percival) in a 12 h light/12 h dark cycle with a Photosynthetically Available Radiation (PAR) of 10 µmol photons m^{-2} s^{-1}. Cells were cultured in Provasoli's enriched f/2 seawater (Guillard 1975) medium using Tropic Marin artificial sea salt (34.5 g L^{-1}) enriched with $NaHCO_3$ (80 mg L^{-1} final concentration) in 200 mL tissue culture flasks (Greiner).

Sample preparation

Cells were concentrated by centrifugation at 3000 RPM for 5 min at 20°C (J-E, Avanti), resuspended in a smaller volume of the supernatant and supplemented with 10% w/v ficoll (Sigma-Aldrich) to prevent sedimentation.

Deconvolution of linear and quadratic ECS components

Absorption difference signals were measured at different wavelengths with a home-made Joliot-type spectrophotometer equipped with a Varispec LC tunable filter (PerkinElmer, Ohio, USA), which allows to adjust wavelengths in the 500-600 nm range (7 nm bandwidth). To deconvolute the linear and quadratic contributions to the ECS signals, we used a low concentration of FCCP (Carbonyl cyanide 4-(trifluoromethoxy) phenylhydrazone, 10 µM) in order to ensure that there was no electric field (ΔΨ) in the dark. The buildup of the ΔΨ was then achieved with a short (duration ~10 ms) pulse of strong (4500 µmol photons m^{-2} s^{-1}) red illumination. We then followed the kinetics of the ECS signal decay over the 500-600 nm range and used the protocol described in Bailleul et al. (2015) to mathematically deconvolute the ECS signals into linear and quadratic components. Briefly, we assumed that the ΔΨ followed a mono- exponential decay:

$$\Delta\Psi(t) = \Delta\Psi_0 \,.\, \exp(-t/\tau)$$

where t is time after the end of the light pulse, $\Delta\Psi_0$ is the initial electric field at the end of the light pulse, and τ is the electric field decay lifetime. Given that the linear and quadratic ECS are theoretically proportional to ΔΨ and $\Delta\Psi^2$, respectively, the ECS signal's spectro-temporal matrices are described as a sum of two exponentials:

$$ECS(\lambda,t) = Al(\lambda) \cdot \exp(-t/\tau) + Aq(\lambda) \cdot \exp(-2.t/\tau)$$

The kinetics of ECS relaxation at all wavelengths were fitted by a global routine, using the Origin software, which considers the lifetime τ as a global (wavelength independent) variable, and the amplitudes of linear and quadratic components (Al and Aq, respectively) as local (wavelength dependent) variables. The plots of the Al and Aq amplitudes as functions of the wavelength provide the spectra of the linear and quadratic ECS components, respectively. This measurement was done only once because it was only a first step in the determination of the purely linear and quadratic wavelengths.

Measuring purely linear and quadratic ECS signals

The optimal wavelengths to probe linear and quadratic signals were determined around the approximated wavelengths identified by deconvolution (see previous paragraph). Wavelengths were selected using interference filters, which were rotated to transmit specific wavelengths. This was checked with an S2000 fiber optic spectrometer (Ocean Optics). Antimycin A (AA) and salicylhydroxamic acid (SHAM) were added to the darkened sample as it inhibits mitochondrial respiration and as such slows down the chloroplast ATP synthase activity (see Bailleul et al. 2015), which enhances the temporal resolution of the decay function. ECS signals were measured with a Joliot-type spectrophotometer (JTS-10, Biologic, Grenoble, France).

ECS measurements and contribution of ΔpH and ΔΨ to the PMF

Absorption differences during the transition from light to dark were measured as in Bailleul et al. (2015) with a Joliot-type spectrophotometer (JTS-10, Biologic, Grenoble, France) equipped with a white probing LED and an interference filter of 564 nm, rotated to transmit 560 nm light (this was checked with an S2000 fiber optic spectrometer, Ocean Optics). The photodiode was protected from actinic light using a Schott BG-39 filter. The same spectrophotometer was used to detect chlorophyll fluorescence (hence the measuring pulses had a wavelength of 560 nm) by placing a long-pass filter (Schott RG-695) in front of the photodiode detector. Saturating pulses (5000 µmol photons $m^{-2}s^{-1}$, 250 ms, 629 nm in wavelength) were provided each 30 s. The photosynthetic efficiency of PSII ($\Delta F/F_m'$) was calculated as $(F_m'-F')/F_m'$ with F' the minimal chlorophyll fluorescence yield in illuminated cells and F_m' the corresponding maximum chlorophyll fluorescence yield. The relative electron transport rate (rETR) was calculated as $(\Delta F/F_m')$*PAR. NPQ was calculated as $(F_m-F_m')/F_m'$, where F_m is the maximum chlorophyll fluorescence yield before high light exposure. NPQ was monitored until a steady state was reached (typically 5-7 min). The rate of PSII and PSI chemistry was calculated as the negative slope of the ECS signal, during 10 ms after light was shut off after steady state was reached (Joliot and Joliot 2002; Bailleul et al. 2010a). Five different light intensities were tested: 0, 135, 340, 800 and 1500 µmol photons $m^{-2}s^{-1}$, provided by a ring of red

(629 nm) LEDs. For each light intensity, NPQ was measured until a steady state was reached. A new sample was used for each light intensity. All experiments were replicated two times, with aliquots taken from a different stock culture each day.

Pigment analyses

After chlorophyll fluorescence and absorption difference measurements, one mL was sampled for pigments and analyzed as described by Blommaert et al. (2017). Diatom suspensions were rapidly filtered onto Isopore 1.2 µm RTTP filters (Merck Millipore), immediately frozen in liquid nitrogen and stored at -80°C. Samples were freeze-dried before adding -20°C cold 0.7 mL extraction buffer (90% methanol/0.2 M ammonium acetate (90/10 vol/vol) and 10% ethyl acetate). Pigment extraction was enhanced by adding glass beads (diameter 0.25–0.5 mm, Roth) and vortexing for 30 s. The extracts were sonicated for 60 s on ice at 40% amplitude with 2 s pulse, 1 s rest to pulverize the precipitated ficoll and filtered over a 0.2 µm filter. One hundred microliters were immediately injected into the HPLC system (Agilent). Samples were analyzed according to Van Heukelem and Thomas (2001). As buffered extraction medium was used, no additional TBAA buffer was injected. All pigment concentrations: diadinoxanthin (Ddx), diatoxanthin (Dtx) and chlorophyll *a* (Chl *a*) were calculated by comparison with pigment standards. All standards were obtained from DHI, with exception of Chl *a*, which was obtained from Sigma-Aldrich. Xanthophyll cycle pigments were normalized to 100 mol chlorophyll *a* (Chl *a*).

Results & discussion

Deconvolution of linear and quadratic ECS components

As in diatoms both linear and quadratic ECS components have been observed (Bailleul et al. 2015), we first identified the wavelengths at which wavelengths the ECS signal in *O. guenter-grassii* was either purely linear or quadratic, by following the kinetics of the ECS signal decay after a pulse of strong light (Fig. 1a) and estimated the contribution of the linear and quadratic component (Ai) (Fig. 1b). We found a wavelength around 560 nm where the signal was purely linear (i.e. the contribution from the quadratic component was null) and a wavelength around 580 nm where the contribution was purely quadratic (i.e. the linear contribution is null). These two wavelengths minimize contribution of cytochromes (Bailleul et al. 2015).

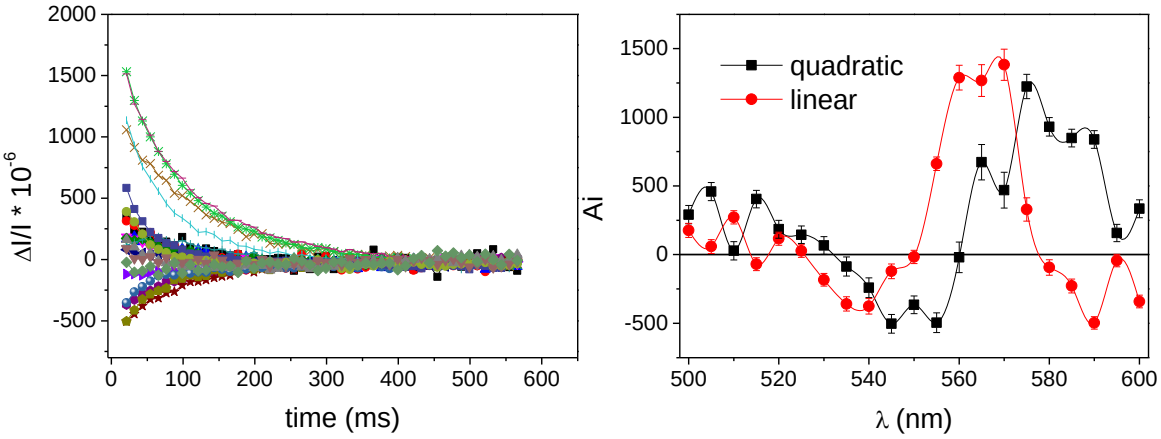

Fig. 1. (a, b). (a) Example of the decay of the ECS signal (the absorption difference ΔI/I), measured at different wavelengths (different colours) after a strong light pulse and (b) the contribution of quadratic (black) and linear (red) ECS signal (Ai) to the ECS signal amplitude.

The presence of a dark electric field

In diatoms the presence of both linear and quadratic components allows to measure the absolute electric field, as by plotting the relationship between ECS_{quad} and ECS_{lin} signals during the relaxation in the dark after a light pulse, a parabola can be observed (Bailleul et al. 2015). In diatoms, however, the ECS measurements do not reach the minimum of the parabola, suggesting the presence of a dark electric field $\Delta\Psi_d$ and the presence of a PMF (Bailleul et al. 2015). To determine this dark electric field ($\Delta\Psi_d$) in *O. guenter-grassii*, we used the same light perturbation as above and followed the kinetics of the ECS signal at 560 nm (linear signal) and 581 nm (quadratic signal). (Fig. 2). Unfortunately, the dark electric field could not be normalized to give a quantitative value, expressed in charge separations per PS (like in Bailleul et al 2015) because the laser was not operational at the time of the experiment. However, our results clearly showed that there was a dark electric field (and therefore a PMF), in the dark, due to the hydrolysis of ATP from mitochondrial origin, since it was suppressed in the presence of the cytochrome bc1

complex and AOX (Alternative OXidase) inhibitors, AA (Antimycin A) and salicylhydroxamic acid (SHAM) (Fig. 2) (as observed by Bailleul et al. 2015). The good fit of the experimental data with a parabolic equation in both control and mitochondria inhibited conditions, furthermore, validated the choice of the two wavelengths for the following experiments.

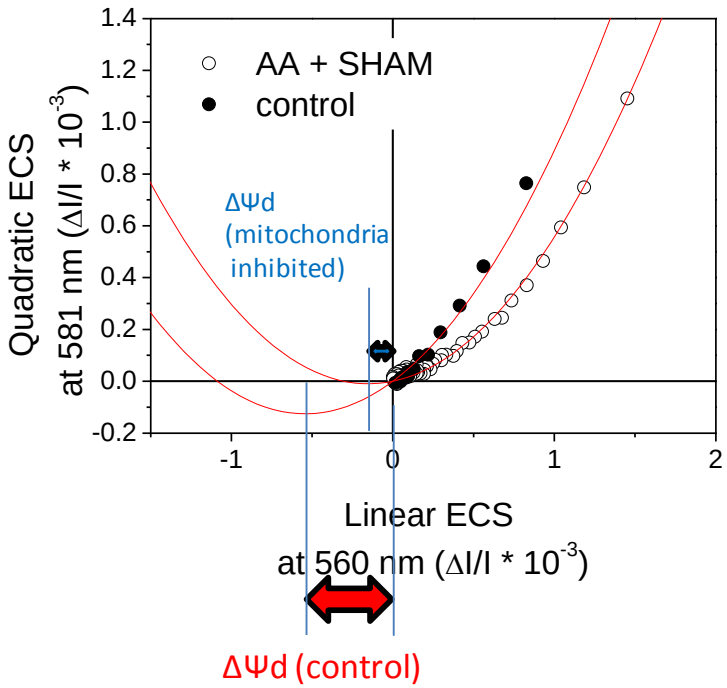

Fig. 2. The relationship between the linear and quadratic ECS signals in darkness in *Opephora guenter-grassii*: control (white symbols) and treated with 5 µM AA and 1 mM SHAM (black symbols). The red double arrow represents the extent of the dark electric field in an untreated sample ($\Delta\Psi_d$). Note that when mitochondria were inhibited a small electric field was still present (black double arrow), indicating that there remained some ATP generated by glycolysis/remaining mitochondrial respiration.

An ECS inversion was observed upon turning off illumination after a steady-state NPQ was reached.

When illumination was turned off, after a steady-state NPQ was reached, a fast decay of the linear ECS signal was observed (Fig. 3 a). The total decay has been interpreted as being equal to the PMF (Cruz et al 2001)(Fig. 3b), after which the signal increased again to reach a stable value, supposedly the dark-adapted level of electric field $\Delta\Psi_d$ (Cruz et al. 2001). The drop below the dark baseline represents an inversion of the ECS signal (ECS_{inv}) and has been related to the light-generated ΔpH fraction of the total PMF, whereas the difference between the signal during the light acclimated level and the supposed dark baseline ECS_{ss} has been related to the light-generated electric field (ΔΨ). As an ECS inversion has been observed in terrestrial plants and green algae (Cruz et al. 2001, 2005) and to our knowledge this work represents the first observation of an ECS inversion in diatoms (no ECS inversion has been observed in diatoms tested so far,

Bailleul, personal communication), the validity of the model/interpretation needs to be investigated in other diatoms before it can be used to probe ΔpH and ΔΨ.

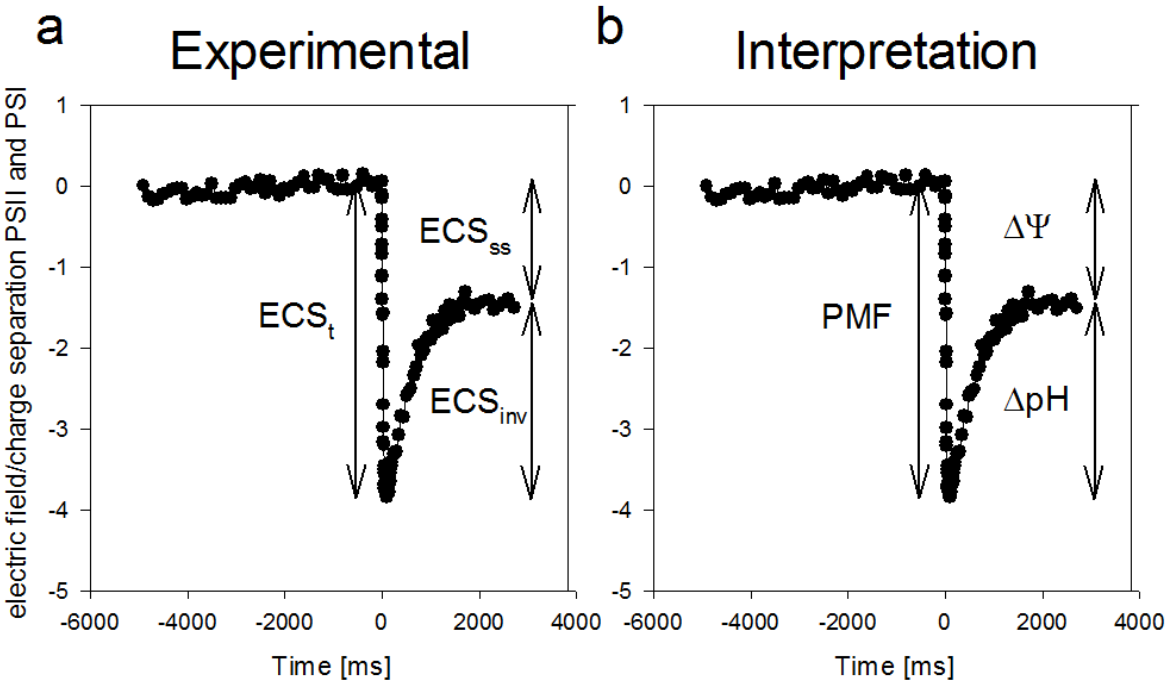

Fig. 3. (a,b) The ECS inversion observed in *O. guenter grassii* after exposure to 800 µmol photons $m^{-2} s^{-1}$. With the total ECS decline (ECS_t), steady state ECS in darkness (ECS_{ss}) and the ECS inversion ($ECS_{inv} = ECS_t - ECS_{ss}$) in (a) being related to the proton motive force (PMF), the light-generated electric field (ΔΨ) and the pH gradient (ΔpH) by Cruz et al. (2001) in (b).

The relationship between ΔpH and Dtx/NPQ

In order to characterize the light response of *O. guenter-grassii* we exposed it to different intensities of red light until a steady-state NPQ was reached. The relative ETR (rETR) (Fig. 4a) saturated above 350 µmol photons $m^{-2}s^{-1}$. A noticeable decay in rETR was observed at higher light intensities (800 and 1500 µmol photons $m^{-2}s^{-1}$). As this species has been shown to be able to withstand prolonged exposure to high light (e.g. 1 h, 2000 µmol photons $m^{-2}s^{-1}$, Blommaert et al. 2017) the observed decline in rETR was most probably due to a large development of NPQ during light exposure (Lefebvre et al. 2011), or to an underestimated $\Delta F/F_m'$ due to insufficienty high light pulses to reach F_m', instead of photoinhibition. Above saturating light conditions, diadinoxanthin (Ddx) de-epoxidation resulted in accumulation of diatoxanthin (Dtx) and NPQ development (Fig. 4b, c). Note that even though cells were acclimated to low light intensities, Dtx was present in significant amounts (about 1 mol (100 Chl *a*)$^{-1}$) before exposure to high light conditions, which could indicate that cells were not in an optimal (unstressed) condition before the experiments. The contributions of the putative 'ΔΨ' and 'ΔpH' component to the total PMF changed with increasing light intensity (Fig. 4d). Whereas the contribution of 'ΔpH' was low below light saturation, it was about 50% at 800 µmol photons $m^{-2} s^{-1}$. A

similar parsing have been observed in higher plants, where at the highest tested light intensity (1500 µmol photons $m^{-2} s^{-1}$) nearly all PMF consisted of 'ΔpH' (Klughammer et al. 2013). A small dip in 'PMF' and 'ΔpH' beyond the saturation point, as described by Klughammer et al. (2013) and Lyu and Lazár (2017) was not observed, possibly because we only have data for two light intensities beyond the saturation point. The above findings support the hypothesis that an increase in 'ΔpH' at the expense of 'ΔΨ' at oversaturating conditions (Kramer et al. 2003) regulates xanthophyll de-epoxidation and engages the NPQ mechanism in diatoms (Lavaud and Goss 2014).

a

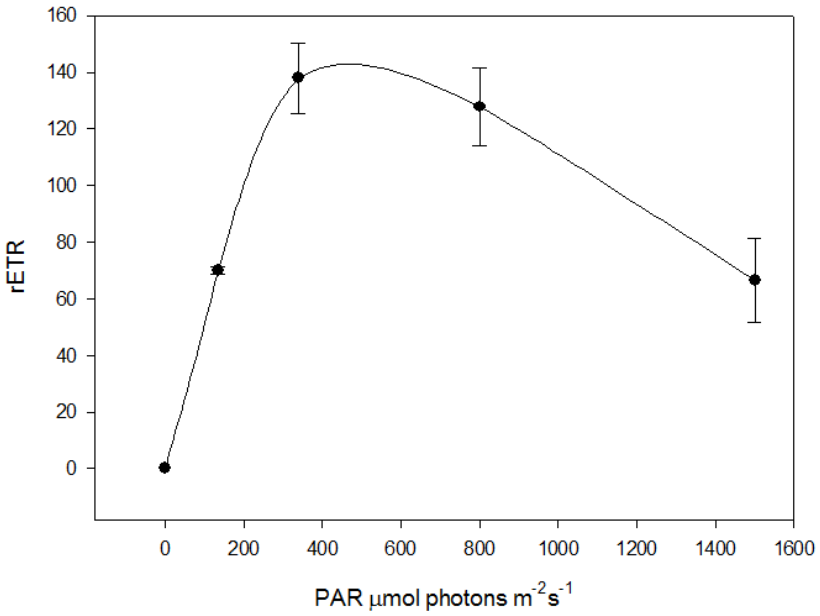

b

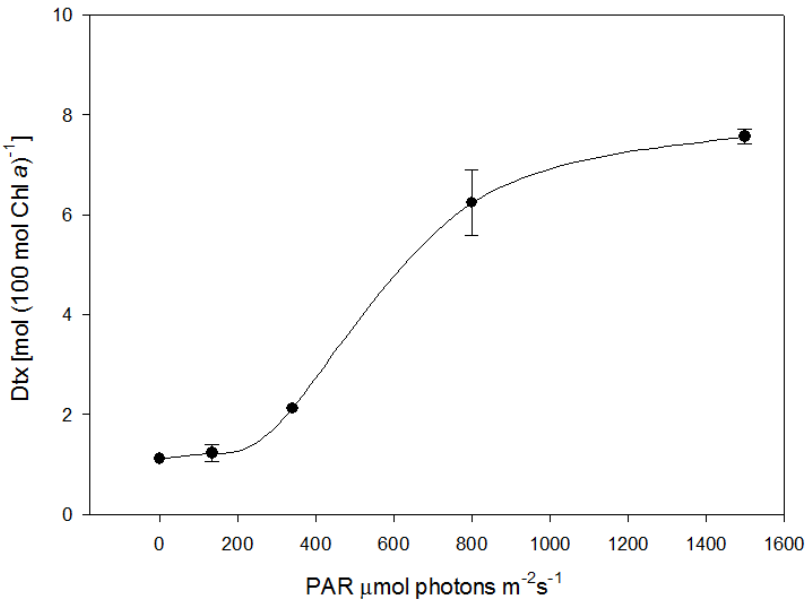

c

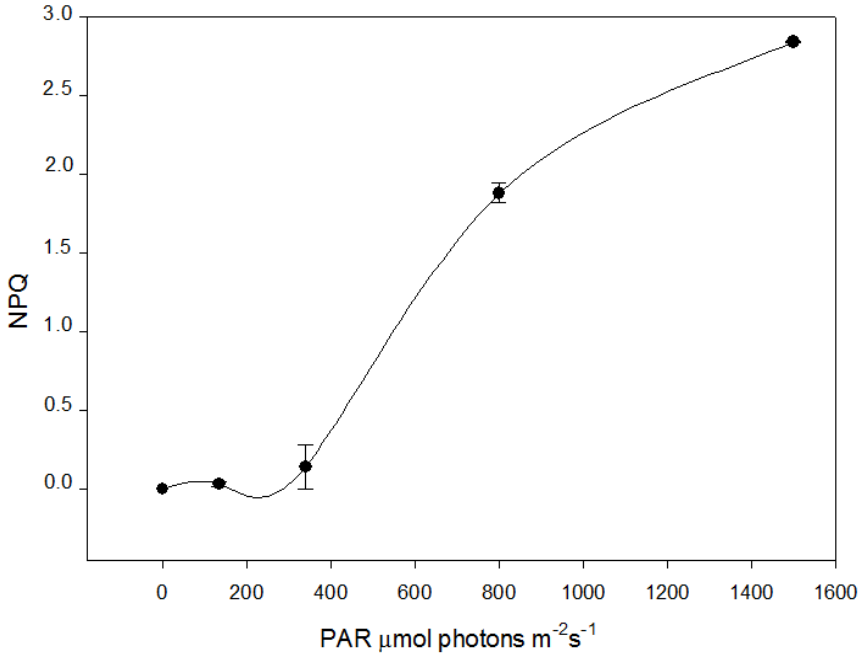

d

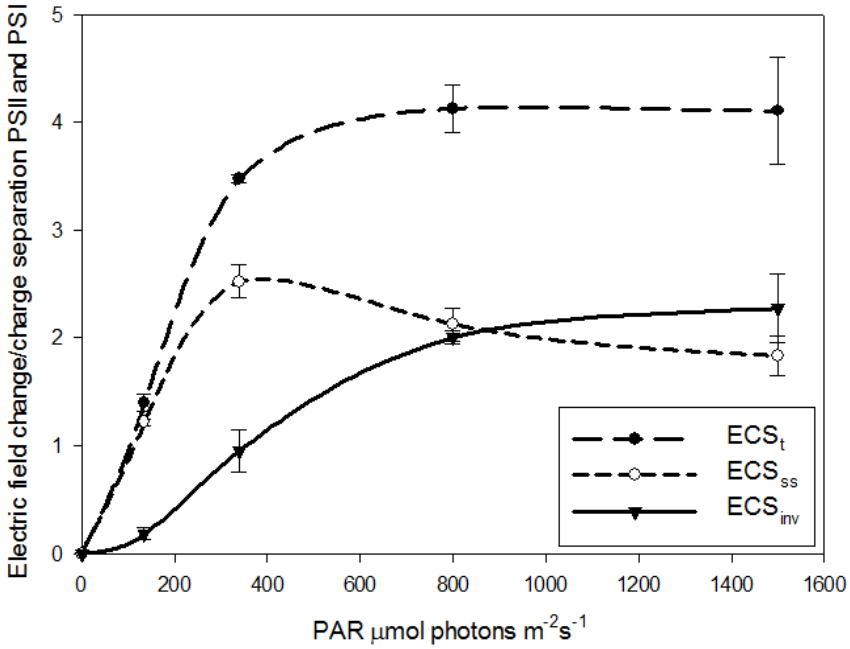

Fig.4. (a,b,c,d) The response of different photosynthetic parameters to increasing levels of Photosynthetically Available Radiation (PAR): (a) the relative Electron Transport Rate (rETR); (b) the diatoxanthin content (Dtx) normalized to Chl *a*; (c) Non-photochemical quenching (NPQ); and (d) the parsing of the PMF according to Cruz et al. (2001), see Fig. 3. Values are averages of two independent replicates, error bars represent standard deviations. A new sample was used for each data point.

Is ECS_{inv} a valid proxy for ΔpH?

The validity of ΔpH estimation as ECS_{inv}, as described by Cruz et al. (2001) was tested by using nigericin. This ionophore exchanges H^+ and K^+ (Reed 1979) and thus decreases the light-generated (here 800 µmol photons $m^{-2}s^{-1}$) transthylakoidal proton gradient while keeping the electric field component intact. As we wanted to be certain that nigericin modified only ΔpH, while not affecting other photosynthetic processes, we monitored the photochemical rate of PSII and PSI, R_{ph} (Joliot and Joliot 2002), and the photosynthetic efficiency of PSII ($\Delta F/F_m'$) (Fig.5 a,b). Especially above a nigericin concentration of 0.56 µM, a drastic decline in both photosynthetic parameters was observed. At higher nigericin concentrations, ECS_t decreased, concomitantly with the decrease in R_{ph} and $\Delta F/F_m'$, indicating that the electron transfer rate is altered in those conditions. Therefore, above 0.56 µM nigericin affects not only ΔpH, making it impossible to interpret its regulatory role in NPQ at the higher nigericin concentration ranges.

The largest decline in Dtx and NPQ (Fig. 5 c,d), however, was observed when using the lowest nigericin concentrations (0.14, 0.28 and 0.56 µM). As ECS_t, which has been interpreted as the light-generated PMF (Fig. 5e), did not decrease at the lowest nigericin concentrations (0.14-0.28 µM), but rather showed a small increase and similar R_{ph} and $\Delta F/F_m'$ values as in the untreated controls were observed, we can assume that in the lower concentration ranges nigericin only affects ΔpH. In contrast to what was expected however, ECS_{inv} showed a pronounced increase at a nigericin concentration of 0.14-0.28 µM, while ECS_{ss} decreased, suggesting an increase in ΔpH at the expense of ΔΨ (Cruz et al. 2001). Even though there was a positive relationship between ECS_{inv} or 'ΔpH' and NPQ and Dtx with increasing light intensity (Fig. 4), the opposite relationship was observed upon nigericin addition (Fig. 5c,d&e, Fig. 6). Furthermore, an increase in ECS_{inv} was also observed when nigericin was added in increasing doses after a steady state was reached at 800 µmol photons m^{-2} s^{-1} and waiting until NPQ stabilized before measuring ECS_{inv} (Fig. 7), as such confirming the results obtained from non-sequential observations. Interestingly, the small increase in ECS_t was observed as well. However, NPQ did not decrease at these nigericin concentrations (data not shown).

The correlation between NPQ and Dtx was strong, and remained similar in the presence of nigericin, as is commonly observed in diatoms (Lavaud et al. 2004; Schumann et al. 2007) (Fig. 8). Dtx, however, was not fully epoxidized to Ddx upon nigericin addition, but reached a level of about 1 mol (100 mol Chl *a*)$^{-1}$, similar to samples not exposed to 800 µmol photons $m^{-2}s^{-1}$ and as described above. NPQ on the other hand was completely abolished at the highest nigericin concentrations. Unfortunately, it was difficult to compare the relationship between nigericin treated and untreated samples as data points for the latter (obtained upon exposure to different light intensities) in the same Dtx range were lacking. This could be alleviated by sampling in light conditions between

350 and 800 µmol photons m^{-2} s^{-1}. Interestingly, in rather artificial conditions, small deviations in the NPQ/Dtx relationship have been observed in *P. tricornutum*, by decreasing the thylakoid lumen pH with NH_4Cl (Lavaud et al. 2002) or using DCCD, which increases ΔpH by inhibiting the ATP synthase. Additional deviations, moreover, were observed when increasing Dtx content by addition of exogenous ascorbate (shifting the pH optimum of the de-epoxidase) or a stepwise pre-illumination protocol at moderate light intensities (Lavaud and Kroth 2006).

a

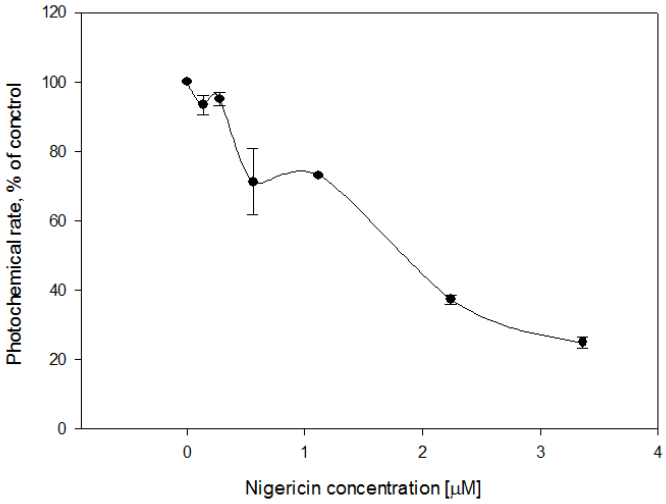
Photochemical rate, % of conctrol
120
100
80
60
40
20
0
0
1
2
3
4
Nigericin concentration [μM]

b

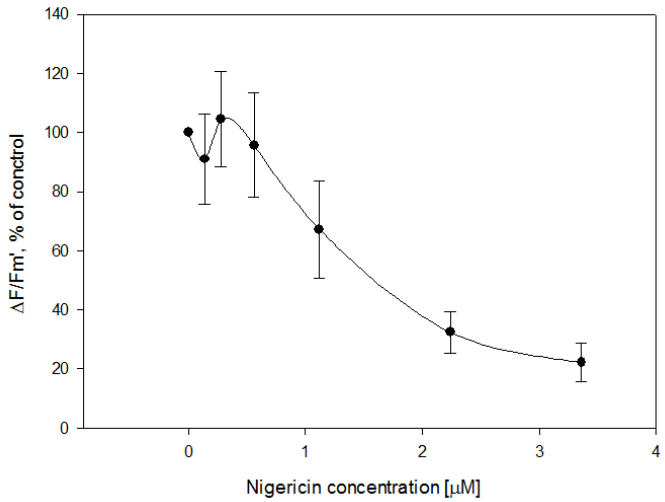
ΔF/Fm', % of conctrol
140
120
100
80
60
40
20
0
0
1
2
3
4
Nigericin concentration [μM]

c

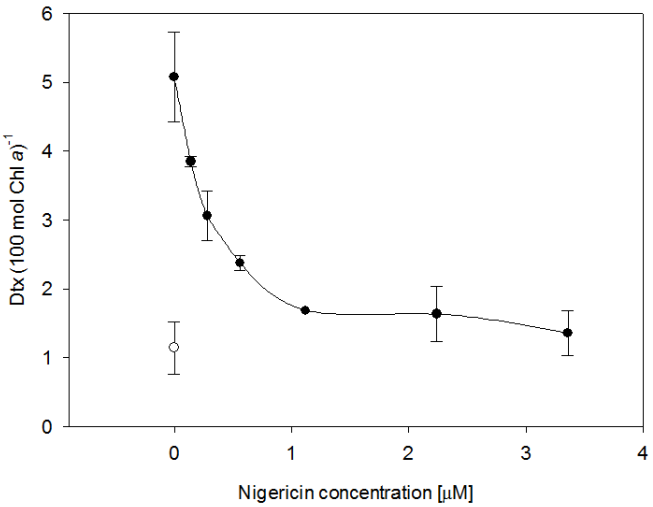
Dtx (100 mol Chl a)-1
6
5
4
3
2
1
0
0
1
2
3
4
Nigericin concentration [μM]

d

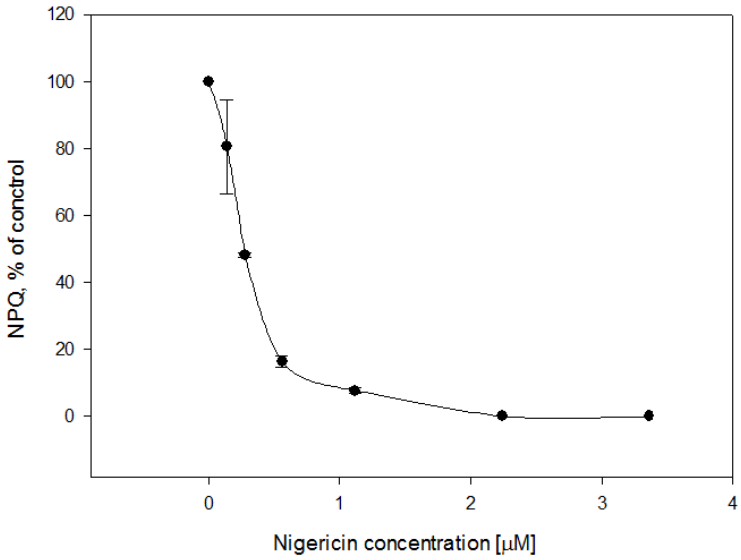

e

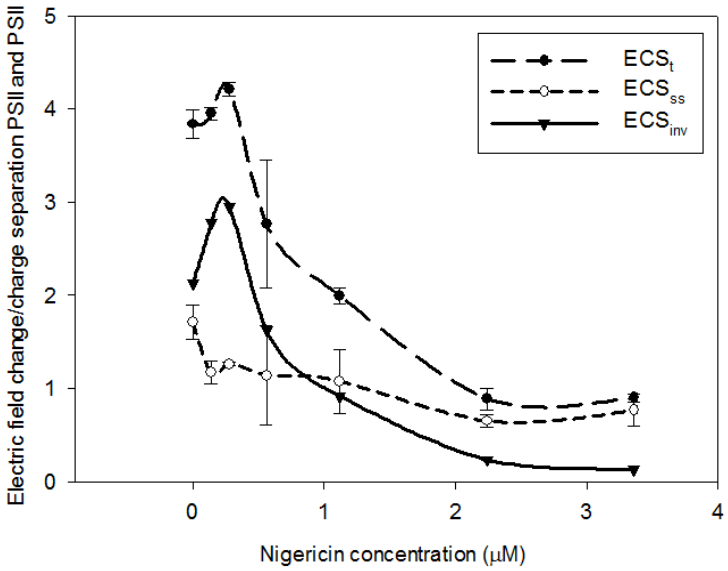

Fig. 5. (a,b,c,d,e) The response of different photosynthetic parameters at 800 µmol photons m^{-2} s^{-1} to different concentrations of nigericin: (a) the photochemical rate of PSII and PSI, relative to the untreated control; (b) The effective quantum efficiency of PSII photochemistry, relative to the untreated control; (c) the diatoxanthin content (Dtx) normalized to 100 mol Chl *a*. The white symbol represents samples not exposed to 800 µmol photons m^{-2} s^{-1} and without nigericin; (d) Non-photochemical quenching (NPQ) relative to the control; and (e) the parsing of the PMF according to Cruz et al. (2001), see Fig. 3. All Values are averages of two independent replicates, error bars represent standard deviations.

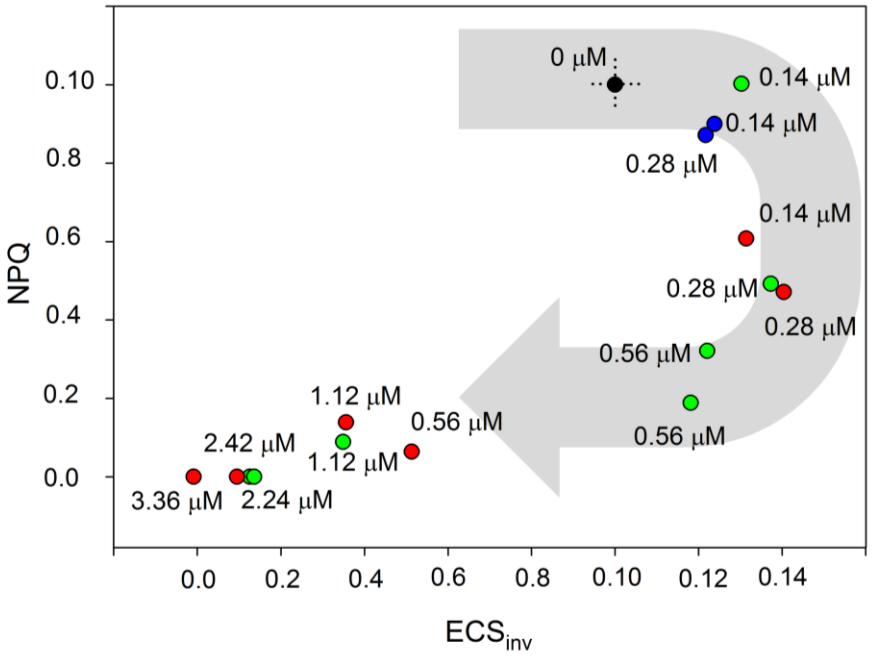

Fig. 6. Non-photochemical quenching (NPQ) in function of ECS_{inv}, see Fig. 3. Both NPQ and ECS_{inv} were normalized to 1 (black data point with cross hairs) for the control values for demonstrative purposes. Different colors represent different biological replicates. A fresh sample was used for each data point. The grey arrow represents increasing nigericin concentration.

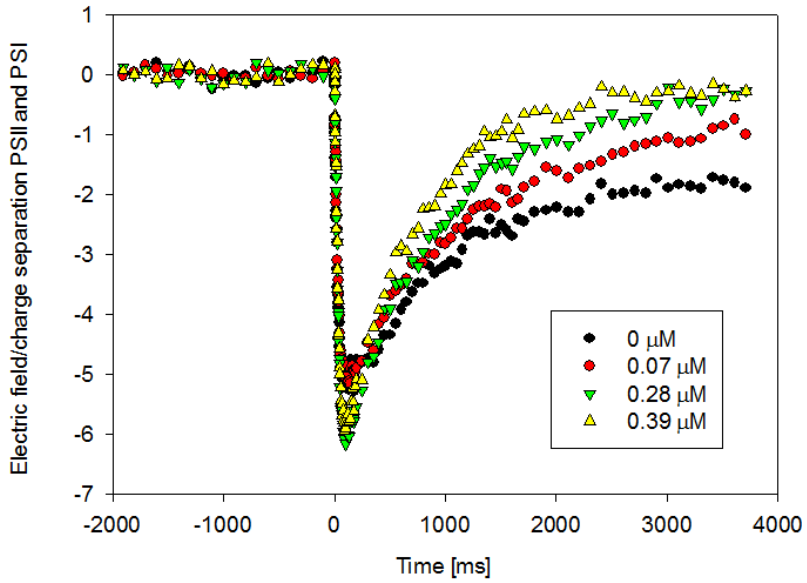

Fig. 7. The ECS inversion observed after turning off illumination (800 µmol photons m^{-2} s^{-1}) with increasing doses of nigericin applied to the same sample.

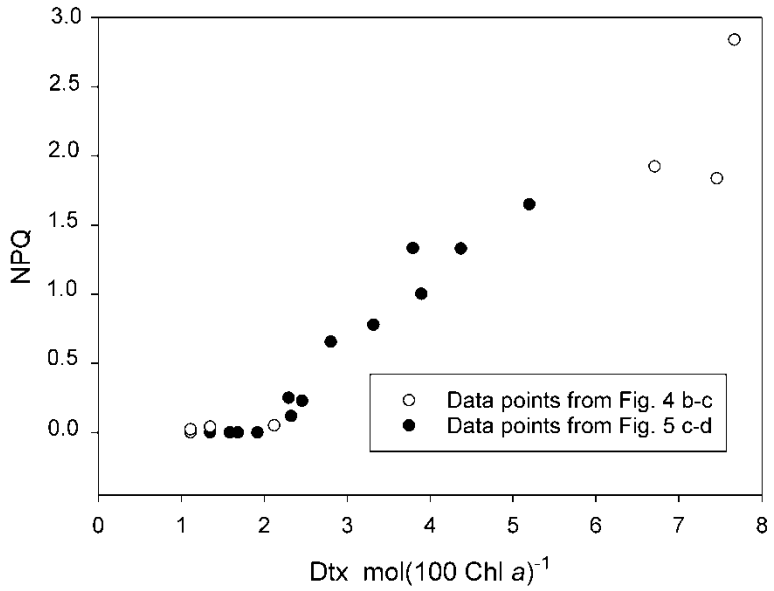

Figure 8: The relationship between Non-photochemical quenching (NPQ) and diatoxanthin (Dtx) normalized to 100 mol Chl *a*, black symbols represent data points from Fig. 5 c-d, whereas the white symbols represent data points from Fig. 4b-c.

Using small concentrations of nigericin we observed an increase ECS_{inv} while both NPQ and Dtx decreased. These observations could be explained by two alternative hypotheses: 1) the ECS-based method to measure ΔpH as ECS_{inv} is not valid in diatoms, or 2) NPQ is not regulated by ΔpH. However, as our results comprise only two replicated sets of experiments on one diatom species, more replication on the studied species and experiments on more diatom representatives are required to evaluate the above hypotheses.

We suggest that the method of Cruz et al. (2001) should be used with caution. Even though this method is commonly applied to determine ΔpH in plants and green algae (Cruz et al. 2001, 2005; Kanazawa and Kramer 2002; Klughammer et al. 2013; Lyu and Lazár 2017), its findings (e.g. the presence of a light-generated ΔΨ in steady state conditions) have been recently disputed by Johnson and Ruban (2014). They argued that the observed ΔΨ in steady state conditions (as evidenced by ECS measurements at 515 nm) might be (at least partly) due to overlap with absorption changes around 535 nm, associated with the formation of qE. At the light intensity used in this study (700 µmol photons m^{-2} s^{-1}), the contribution of ΔΨ to the PMF nonetheless is considered to be low (Klughammer et al. 2013). Recent modeling of the light-induced ΔΨ (Lyu and Lazár 2017), however, agrees with the presence of a generally low ΔΨ. In diatoms, a qE associated 535 nm absorption change has not been observed, but an analogous absorption band has been observed at 522 nm (Ruban et al. 2004). As in our study we measured (linear) absorption changes at 560 nm, it is very unlikely that our signal is contaminated by qE related absorption changes. Either way, it would be informative to

test the ECS-based ΔpH determination in plants using similarly low nigericin concentrations.

An alternative methods to determine ΔpH is the use of the fluorescent dye 9-aminoacridine as a pH indicator (Johnson and Ruban 2011). The use of 9-aminoacridine, however, is mostly applied to chloroplasts. Therefore, to resolve the function of a ΔpH in the regulation of NPQ in diatoms, a new method should be developed. The presence of both a linear and quadratic ECS signal in diatoms (Bailleul et al. 2010a, this study), allows measuring the absolute value of the electric component ΔΨ of the PMF. As, at least in plants, it is possible to determine the total PMF (Joliot and Joliot 2008), applying this method in combination with determining its electric component ΔΨ, the ΔpH can be calculated as the difference between PMF and ΔΨ. By developing this method in diatoms the role of ΔpH in regulating NPQ can be further dissected.

References

Archibald, J. M. 2009. The Puzzle of Plastid Evolution. Curr. Biol. **19**: 81–88. doi:10.1016/j.cub.2008.11.067

Armbrust, E., J. Berges, and C. Bowler. 2004. The genome of the diatom T*halassiosira pseudonana*: ecology, evolution, and metabolism. Science (80-.). **306**: 79–86.

Bailleul, B., N. Berne, O. Murik, and others. 2015. Energetic coupling between plastids and mitochondria drives CO_2 assimilation in diatoms. Nature **524**: 366–369. doi:10.1038/nature14599

Bailleul, B., P. Cardol, C. Breyton, and G. Finazzi. 2010a. Electrochromism: a useful probe to study algal photosynthesis. Photosynth. Res. **106**: 179–89. doi:10.1007/s11120-010-9579-z

Bailleul, B., A. Rogato, A. De Martino, S. Coesel, P. Cardol, C. Bowler, A. Falciatore, and G. Finazzi. 2010b. An atypical member of the light-harvesting complex stress-related protein family modulates diatom responses to light. Proc. Natl. Acad. Sci. **107**: 18214–18219. doi:10.1073/pnas.1007703107

Ballottari, M., T. B. Truong, E. De Re, E. Erickson, G. R. Stella, G. R. Fleming, R. Bassi, and K. K. Niyogi. 2016. Identification of pH-sensing sites in the Light Harvesting Complex Stress-related 3 protein essential for triggering Non-photochemical Quenching in *Chlamydomonas reinhardtii*. J. Biol. Chem. **291**: 7334–46. doi:10.1074/jbc.M115.704601

Blommaert, L., M. J. J. Huysman, W. Vyverman, J. Lavaud, and K. Sabbe. 2017. Contrasting NPQ dynamics and xanthophyll cycling in a motile and a non-motile intertidal benthic diatom. Limnol. Oceanogr. doi:10.1002/lno.10511

Bonente, G., M. Ballottari, T. B. Truong, T. Morosinotto, T. K. Ahn, G. R. Fleming, K. K. Niyogi, and R. Bassi. 2011. Analysis of LhcSR3, a protein essential for feedback de-excitation in the green alga *Chlamydomonas reinhardtii*. PLoS Biol. **9**: e1000577. doi:10.1371/journal.pbio.1000577

Bowler, C., A. E. Allen, J. H. Badger, and others. 2008. The *Phaeodactylum* genome reveals the evolutionary history of diatom genomes. Nature **456**: 239–44. doi:10.1038/nature07410

Cruz, J. A., A. Kanazawa, N. Treff, and D. M. Kramer. 2005. Storage of light-driven transthylakoid proton motive force as an electric field (Δψ) under steady-state conditions in intact cells of *Chlamydomonas reinhardtii*. Photosynth. Res. **85**: 221–233. doi:10.1007/s11120-005-4731-x

Cruz, J. A., C. A. Sacksteder, A. Kanazawa, and D. M. Kramer. 2001. Contribution of electric field (Δψ) to steady-state transthylakoid proton motive Force (PMF) in vitro and in vivo. Control of PMF parsing into Δψ and ΔpH by ionic Strength. Biochemistry **40**: 1226–1237. doi:10.1021/bi0018741

Demmig-adams, B., C. M. Cohu, J. J. Stewart, W. W. A. III, and Govindjee. 2014. Non-Photochemical Quenching and Energy Dissipation in Plants, Algae and Cyanobacteria, B. Demmig-Adams, G. Garab, W. Adams III, and Govindjee [eds.]. Springer Netherlands.

Eisenstadt, D., I. Ohad, N. Keren, and A. Kaplan. 2008. Changes in the photosynthetic reaction centre II in the diatom *Phaeodactylum tricornutum* result in non-photochemical fluorescence quenching. Environ. Microbiol. **10**: 1997–2007. doi:10.1111/j.1462-2920.2008.01616.x

Erickson, E., S. Wakao, and K. K. Niyogi. 2015. Light stress and photoprotection in *Chlamydomonas reinhardtii*. Plant J. **82**: 449–465. doi:10.1111/tpj.12825

Goss, R., and B. Lepetit. 2015. Biodiversity of NPQ. J. Plant Physiol. **172**: 13–32. doi:10.1016/j.jplph.2014.03.004

Graven, S. N., S. Estrada-O, and H. A. Lardy. 1966. Alkali metal cation release and respiratory inhibition induced by nigericin in rat liver mitochondria. Proc. Natl. Acad. Sci. U. S. A. **56**: 654–8.

Grouneva, I., T. Jakob, C. Wilhelm, and R. Goss. 2006. Influence of ascorbate and pH on the activity of the diatom xanthophyll cycle-enzyme diadinoxanthin de-epoxidase. Physiol. Plant. **126**: 205–211. doi:10.1111/j.1399-3054.2006.00613.x

Guillard, R. R. . 1975. Culture of phytoplankton for feeding marine invertebrates, p. 26–60. *In* W.L. Smith and M.L. Chanley [eds.], Culture of Marine Invertebrate Animals. Planum Press.

Harned, R. L., P. H. Hidy, C. J. Corum, and K. L. Jones. 1951. Nigericin a new crystalline antibiotic from an unidentified *Streptomyces*. Antibiot. Chemother. (northf. III.) **1**: 594–596.

Van Heukelem, L., and C. S. Thomas. 2001. Computer-assisted high-performance liquid chromatography method development with applications to the isolation and analysis of phytoplankton pigments. J. Chromatogr. A **910**: 31–49. doi:10.1016/S0378-4347(00)00603-4

Horton, P. 2012. Optimization of light harvesting and photoprotection: molecular mechanisms and physiological consequences. Philos. Trans. R. Soc. Lond. B. Biol. Sci. **367**: 3455–65. doi:10.1098/rstb.2012.0069

Jakob, T., R. Goss, and C. Wilhelm. 2001. Unusual pH-dependence of diadinoxanthin de-epoxidase activation causes chlororespiratory induced accumulation of diatoxanthin in the diatom *Phaeodactylum tricornutum*. J. Plant Physiol. **158**: 383–390. doi:10.1078/0176-1617-00288

Johnson, M. P., and A. V. Ruban. 2011. Restoration of rapidly reversible photoprotective energy dissipation in the absence of PsbS protein by enhanced DeltapH. J. Biol. Chem. **286**: 19973–19981. doi:10.1074/jbc.M111.237255

Johnson, M. P., and A. V. Ruban. 2014. Rethinking the existence of a steady-state $\Delta\psi$ component of the proton motive force across plant thylakoid membranes. Photosynth. Res. **119**: 233–242. doi:10.1007/s11120-013-9817-2

Joliot, P., and A. Joliot. 2002. Cyclic electron transfer in plant leaf. Proc. Natl. Acad. Sci. **99**: 10209–10214. doi:10.1073/pnas.102306999

Joliot, P., and A. Joliot. 2008. Quantification of the electrochemical proton gradient and activation of ATP synthase in leaves. Biochim. Biophys. Acta - Bioenerg. **1777**: 676–683. doi:10.1016/j.bbabio.2008.04.010

Junge, W., and S. McLaughlin. 1987. The role of fixed and mobile buffers in the kinetics of proton movement. Biochim. Biophys. Acta **890**: 1–5.

Kanazawa, A., and D. M. Kramer. 2002. In vivo modulation of nonphotochemical exciton quenching (NPQ) by regulation of the chloroplast ATP synthase. Proc. Natl. Acad. Sci. **99**: 12789–12794. doi:10.1073/pnas.182427499

Klughammer, C., K. Siebke, and U. Schreiber. 2013. Continuous ECS-indicated recording of the proton-motive charge flux in leaves. Photosynth. Res. **117**: 471–487. doi:10.1007/s11120-013-9884-4

Kramer, D. M., J. A. Cruz, and A. Kanazawa. 2003. Balancing the central roles of the thylakoid proton gradient. Trends Plant Sci. **8**: 27–32. doi:10.1016/S1360-1385(02)00010-9

Lavaud, J., and R. Goss. 2014. The peculiar features of the non-photochemical fluorescence quenching in diatoms and brown algae, p. 421–443. *In* B. Demmig-Adams, G. Garab, W. Adams III, and Govindjee [eds.], Non-Photochemical Quenching and Energy Dissipation in Plants, Algae and Cyanobacteria. Springer.

Lavaud, J., and P. G. Kroth. 2006. In diatoms, the transthylakoid proton gradient regulates the photoprotective non-photochemical fluorescence quenching beyond its control on the xanthophyll cycle. Plant Cell Physiol. **47**: 1010–6. doi:10.1093/pcp/pcj058

Lavaud, J., B. Rousseau, and A.-L. Etienne. 2002. In diatoms, a transthylakoid proton gradient alone is not sufficient to induce a non-photochemical fluorescence quenching. FEBS Lett. **523**: 163–166.

Lavaud, J., B. Rousseau, and A.-L. Etienne. 2004. General features of photoprotection by energy dissipation in planktonic diatoms (Bacillariophyceae). J. Phycol. **40**: 130–137. doi:10.1046/j.1529-8817.2004.03026.x

Lefebvre, S., J.-L. Mouget, and J. Lavaud. 2011. Duration of rapid light curves for determining the photosynthetic activity of microphytobenthos biofilm in situ. Aquat. Bot. **95**: 1–8. doi:10.1016/j.aquabot.2011.02.010

Lepetit, B., G. Gélin, M. Lepetit, and others. 2017. The diatom *Phaeodactylum tricornutum* adjusts nonphotochemical fluorescence quenching capacity in response to dynamic light via fine-tuned Lhcx and xanthophyll cycle pigment synthesis. New Phytol. **214**: 205–218. doi:10.1111/nph.14337

Lepetit, B., S. Sturm, A. Rogato, A. Gruber, M. Sachse, A. Falciatore, P. G. Kroth, and J. Lavaud. 2013. High light acclimation in the secondary plastids containing diatom *Phaeodactylum tricornutum* is triggered by the redox state of the plastoquinone pool. Plant Physiol. **161**: 853–865. doi:10.1104/pp.112.207811

Li, X.-P., A. M. Gilmore, S. Caffarri, R. Bassi, T. Golan, D. Kramer, and K. K. Niyogi. 2004. Regulation of photosynthetic light harvesting involves intrathylakoid lumen pH sensing by the PsbS Protein. J. Biol. Chem. **279**: 22866–22874. doi:10.1074/jbc.M402461200

Li, Z., S. Wakao, B. B. Fischer, and K. K. Niyogi. 2009. Sensing and responding to excess light. Annu. Rev. Plant Biol. **60**: 239–60. doi:10.1146/annurev.arplant.58.032806.103844

Liguori, N., L. M. Roy, M. Opacic, G. Durand, and R. Croce. 2013. Regulation of light harvesting in the green alga *Chlamydomonas reinhardtii*: the C-terminus of LHCSR is the knob of a dimmer switch. J. Am. Chem. Soc. **135**: 18339–42. doi:10.1021/ja4107463

Lohr, M., and C. Wilhelm. 1999. Algae displaying the diadinoxanthin cycle also possess the violaxanthin cycle. Proc. Natl. Acad. Sci. **96**: 8784–8789. doi:10.1073/pnas.96.15.8784

Lyu, H., and D. Lazár. 2017. Modeling the light-induced electric potential difference (ΔΨ), the pH difference (ΔpH) and the proton motive force across the thylakoid membrane in C3 leaves. J. Theor. Biol. **413**: 11–23. doi:10.1016/j.jtbi.2016.10.017

Mitchell, P. 1961. Coupling of Phosphorylation to Electron and Hydrogen Transfer by a Chemi-Osmotic type of Mechanism. Nature **191**: 144–148. doi:10.1038/191144a0

Niyogi, K. K. 1997. *Chlamydomonas* xanthophyll cycle mutants identified by video imaging of chlorophyll fluorescence quenching. Plant Cell **9**: 1369–1380. doi:10.1105/tpc.9.8.1369

Peers, G., T. B. Truong, E. Ostendorf, A. Busch, D. Elrad, A. R. Grossman, M. Hippler, and K. K. Niyogi. 2009. An ancient light-harvesting protein is critical for the regulation of algal photosynthesis. Nature **462**: 518–521. doi:10.1038/nature08587

Reed, P. W. 1979. Ionophores, p. 435–454. *In* Methods in enzymology.

Ruban, A., J. Lavaud, B. Rousseau, G. Guglielmi, P. Horton, and A.-L. Etienne. 2004. The super-excess energy dissipation in diatom algae: comparative analysis with higher plants. Photosynth. Res. **82**: 165–75. doi:10.1007/s11120-004-1456-1

Ruban, A. V. 2016. Nonphotochemical chlorophyll fluorescence quenching: Mechanism and effectiveness in protecting plants from photodamage. Plant Physiol. **170**: 1903–16. doi:10.1104/pp.15.01935

Sacharz, J., V. Giovagnetti, P. Ungerer, G. Mastroianni, and A. V. Ruban. 2017. The xanthophyll cycle affects reversible interactions between PsbS and light-harvesting complex II to control non-photochemical quenching. Nat. Plants **3**: 16225. doi:10.1038/nplants.2016.225

Schumann, A., R. Goss, T. Jakob, and C. Wilhelm. 2007. Investigation of the quenching efficiency of diatoxanthin in cells of *Phaeodactylum tricornutum* (Bacillariophyceae) with different pool sizes of xanthophyll cycle pigments. Phycologia **46**: 113–117. doi:10.2216/06-30.1

Taddei, L., G. R. Stella, A. Rogato, and others. 2016. Multisignal control of expression of the LHCX protein family in the marine diatom *Phaeodactylum tricornutum*. J. Exp. Bot. **67**: 3939–3951. doi:10.1093/jxb/erw198

Takizawa, K., J. A. Cruz, A. Kanazawa, and D. M. Kramer. 2007. The thylakoid proton motive force in vivo. Quantitative, non-invasive probes, energetics, and regulatory consequences of light-induced PMF. Biochim. Biophys. Acta **1767**: 1233–44. doi:10.1016/j.bbabio.2007.07.006

Vredemberg, W. J. 1976. Electrostatic interactions and gradients between chloroplast compartments ands cytoplasm., p. 53–87. *In* J. Barber [ed.], The intact chloroplast. Elservier, Amsterdam, The Netherlands.

Zhu, S.-H., and B. R. Green. 2010. Photoprotection in the diatom *Thalassiosira pseudonana*: role of LI818-like proteins in response to high light stress. Biochim. Biophys. Acta **1797**: 1449–1457. doi:10.1016/j.bbabio.2010.04.003

Acknowledgments

The authors would like to thank the Research Foundation Flanders (FWO project G.0222.09N), Ghent University (BOF-GOA 01G01911).

Chapter 7: General discussion

In this dissertation we studied photoprotection strategies in the major benthic diatom growth forms present in intertidal sediments. One of the main photoprotection mechanisms, Non-Photochemical Quenching (NPQ), and its regulation (comprising the xanthophyll cycle and LHCX proteins) to date have been mainly characterized in (tycho)planktonic diatoms and to a lesser degree also in motile epipelic diatoms (Lavaud and Goss 2014). Very little is known about NPQ regulation in epipsammic diatoms (Jesus et al. 2009; Cartaxana et al. 2011; Pniewski et al. 2015). While NPQ as a photoprotection strategy in intertidal diatoms has been studied in natural communities, the results of these measurements on natural communities (on sediment), are difficult to interpret. This can be due to rapid micromigration and bulk vertical migration of epipelic diatoms, which may affect the fluorescence signal, especially using long (≥30 s) illumination steps (Jesus et al. 2006; Perkins et al. 2011). In addition, pre-existing NPQ levels, induced by in situ light conditions (Perkins et al. 2011), may interfere with NPQ determination. Diatom communities on sandy sediments, furthermore, often contain a mix of both epipsammic and epipelic diatoms (Hamels et al. 1998; Ribeiro et al. 2013; Cartaxana et al. 2016b), making it difficult to draw conclusions about growth-form specific photoprotection traits.

In this study, therefore, we obtained and/or established cultures of the four major morphological diatom growth form of the microphytobenthos (epipelon, tychoplankton and motile as well as non-motile epipsammon). This enabled us to compare NPQ and XC characteristics comprehensively between these growth forms. In Chapters 2,3 and 4 we observed a generally higher NPQ capacity due to a larger XC pigment pool in non-motile epipsammic diatoms in comparison with epipelic and tychoplanktonic species, while motile epipsammic diatoms showed intermediate values. NPQ relaxation differences between epipsammic and epipelic species, moreover, became obvious during low light conditions following high light (Chapters 3 & 4). Epipsammic diatoms rapidly relaxed NPQ in response to a switch to non-saturating light conditions, a feature particularly evident in the non-motile epipsammic model *Opephora guenter-grassii*, which showed very fast Dtx epoxidation kinetics (Chapter 3). Epipelic diatoms, which are able to migrate away from high light (Chapter 4) generally showed a slower NPQ relaxation or even sustained a considerable NPQ portion (Chapter 4). In the epipelic model *Seminavis robusta*, this was due to slower Dtx epoxidation kinetics (Chapter 3). Immuno-localization revealed the presence of LHCX isoforms in low light conditions in *O. guenter-grassii* as well as in *S. robusta*. When both species were exposed to high light conditions, accumulation of additional isoforms could only be detected in *S. robusta* (Chapter 3). The genome of *S. robusta*, moreover, contains fourteen *LHCX* genes, of which all investigated genes showed distinct upregulation during (high) light exposure. Combining our results, with the results from studies, mainly conducted in situ or on natural

communities (see Table 1) we come to the photoprotection models below (Fig. 1&2). The main NPQ regulators in diatoms: the xanthophyll cycle and LHCX proteins are discussed in detail in their respective sections

Conceptual models of photoprotection in microphytobenthic diatoms

Epipelic diatoms

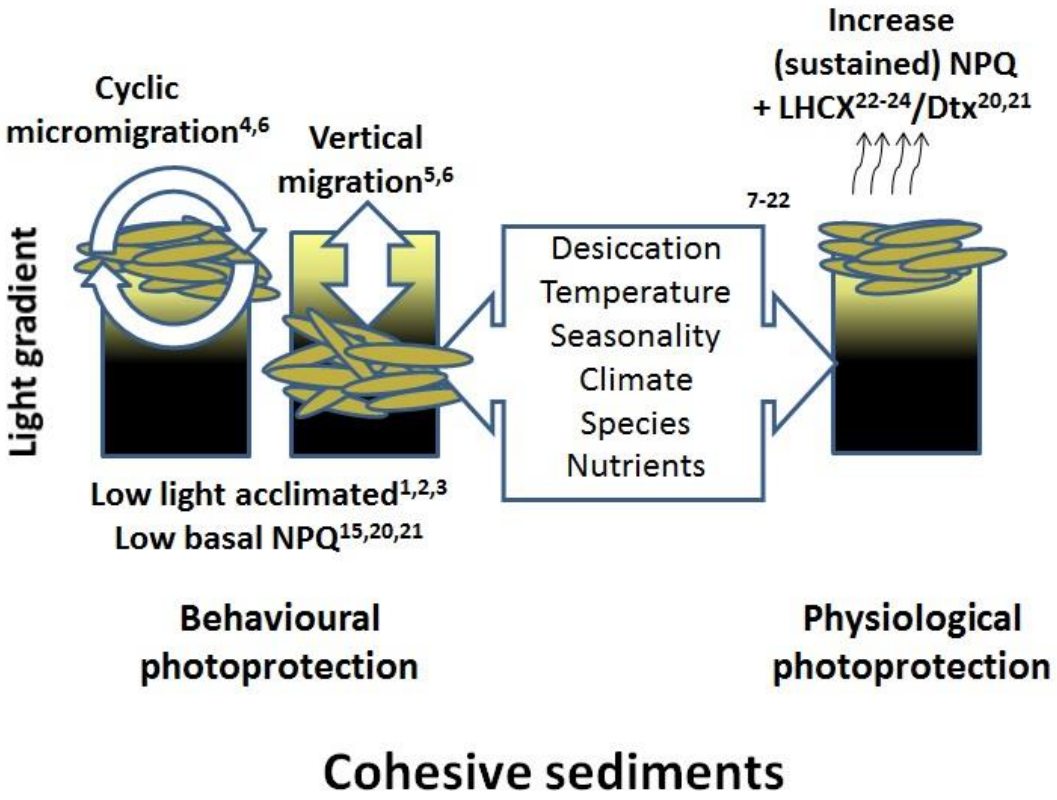

Figure 1: A conceptual model of photoprotection in epipelic diatoms on cohesive sediments. References are added in superscript and compiled in Table 1. See text for details.

Epipelic diatoms, dominating cohesive sediments, position themselves within steep sediment light gradient (Kühl et al. 1994) to avoid overexposure (Admiraal 1984; Serôdio et al. 2006; Cartaxana et al. 2016a). Both cyclic micromigration in the upper sediment layers (Kromkamp et al. 1998; Underwood et al. 2005; Cartaxana et al. 2016a) and bulk downward migration (vertical migration, VM) (Consalvey et al. 2004; Serôdio et al. 2006; Perkins et al. 2010; Laviale et al. 2016) can reduce the light climate experienced by epipelic diatoms at a rate, fast enough to influence the acclimation state and physiological photoprotection (Laviale et al. 2016), Chapter 4. This may explain why epipelic species in situ generally show characteristics of being low light acclimated: (1) they have a higher fucoxanthin/chlorophyll *a* ratio (Jesus et al. 2009; Pniewski et al.

2015), (2) a lower light saturation point (Pniewski et al. 2015; Cartaxana et al. 2016b), and (3) are more vulnerable to photoinhibition compared to epipsammic communities (Pniewski et al. 2015), Chapters 3-4. In addition, the formation of dense epipelic diatom biofilms can result in strong self-shading and lead to the above characteristics (Jesus et al. 2009).

The ability to avoid high light in epipelic diatoms 'behavioural photoprotection', may explain the generally low NPQ capacity and higher photoinhibition/NPQs after strong light conditions in these species, as observed in Chapters 2-4. The NPQ capacity measured in epipelic communities, freshly obtained from the field, nonetheless, can be up to 4 times higher than in our experiments, whereas photoinhibition/NPQs in general is lower (Serôdio et al. 2005, 2012; Laviale et al. 2015), indicating that epipelic species use a combination of both physiological and behavioural photoprotection to cope with fluctuating light intensities (Cartaxana et al. 2011). Indeed, epipelic benthic diatoms can increase their NPQ capacity according to the light climate to which they are exposed (Cruz and Serôdio 2008; Ezequiel et al. 2015) by increasing their cellular Dtx content (Laviale et al. 2015), Chapters 2&3 and/or accumulation of LHCX proteins (Laviale et al. 2015), Chapters 3&5 and below. This may especially be relevant in harsh conditions when vertical migration is restricted by high temperatures and/or sediment desiccation (Laviale et al. 2015).

Epipsammic diatoms

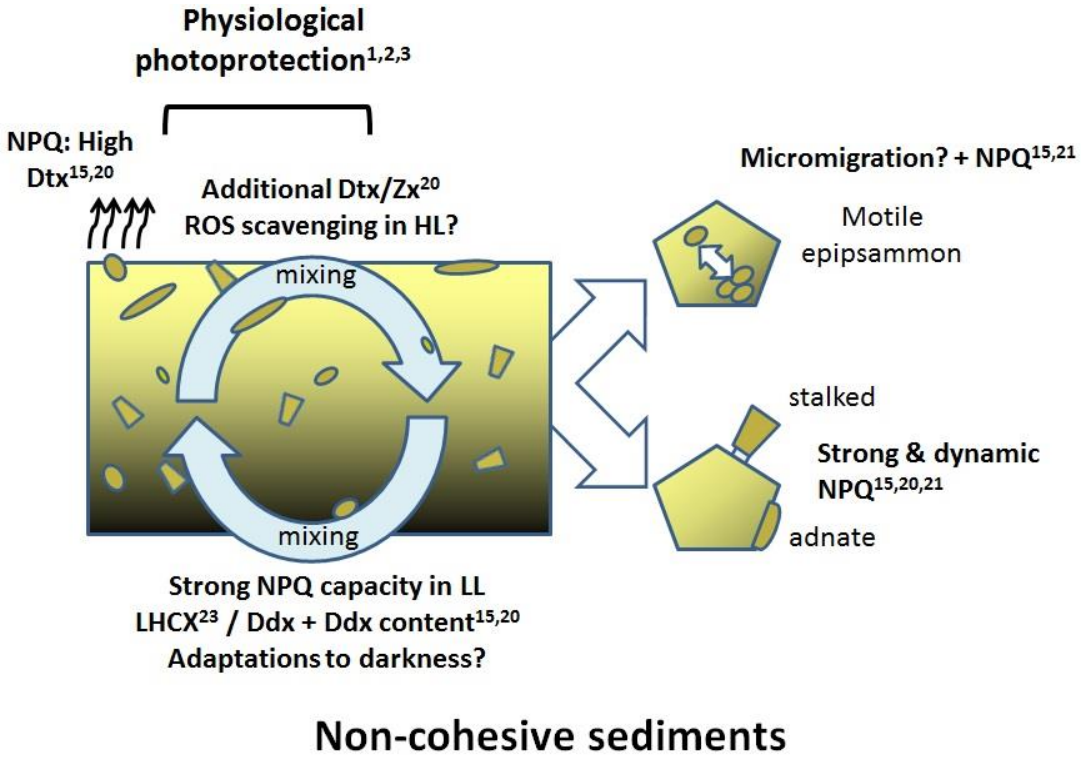

Figure 2: A conceptual model of photoprotection in epipsammic diatoms in non-cohesive sediments. References are added in superscript and compiled in Table 1. See text for details.

While the epipsammic species in this work were grown in the same low light intensities as the epipelic species, they showed a consistently higher NPQ capacity, associated with stronger XC characteristics, see further (Chapters 2,3,4). This may compensate for the lack of vertical migration in the epipsammic growth form (Jesus et al. 2009; Cartaxana et al. 2011, 2016b), Chapter 4. Epipsammic species, moreover, were able to cope with light conditions similar in intensity to in situ light (Chapters 3&4), which is in line with the lack of photoinhibition in natural epipsammic communities (Pniewski et al. 2015). Transitions from prolonged low light conditions to strong light conditions may be common in sandy sediments that are constantly reworked by tidal forces and bioturbation (Hamels et al. 1998; Cartaxana et al. 2006). Additional differences in NPQ capacity and dynamics were also observed between araphid and raphid (hence potentially motile) epipsammic species (Chapter 2&4) (E.g. Higher NPQ values Chapter 2 and a faster NPQ relaxation rate, Chapter 4). Raphid epipsammic species can theoretically use their motility to move to more optimal light conditions within the sphere of individual sand grains. Pronounced vertical migration, as observed in epipelic diatoms, however, was not observed in the raphid epipsammic species in Chapter 4 and in epipsammic communities (Cartaxana et al. 2011, 2016b). The strong light scattering and deeper penetration in sandy sediments, furthermore, makes VM a less effective photoprotection strategy than in silty sediments (Cartaxana et al. 2016b).

Ref		Epipelon	epipsammon	References
	Acclimation in situ	**low light acclimated**	**High light acclimated**	
1		higher fucoxanthin/chlorophyll rario	lower fucoxanthin/chlorophyll rario	Jesus et al. 2009; Pniewski et al. 2015
2		lower light acclimation index (Ek)	Higher light acclimation index (Ek)	Cartaxana et al. 2016b; Pniewki et al. 2015, not observed in Cartaxana 2011
3		higher photoinhibition	lack of photoinhibition	Pniewski et al. 2015
4	**Behavioural photoprotection**	**vertical migration (VM)**	/	Admiraal 1984
5		**cyclic micromigration**	/	Kromkamp et al. 1998
6				Both reviewed in Consalvey et al. 2004
7	**Balance Behavioural/NPQ & XC**	high amplitude migration patterns	lower amplitude migration (sandy mud)	Serodio et al. 2006
8		migration affects determination of PAM-parameters	/	Jesus et al. 2006
9		migratory patterns during emersion	no migratory pattern	Jesus et al. 2009
10		lower Dtx/Ddx	higher Dtx/Ddx	Jesus et al. 2009; Cartaxana; Pniewski et al. 2015
11		vertical migration primary response	/	Perkins et al. 2010
12		both migratory and XC response	lack of migratory response	Cartaxana et al. 2011
13		equal, but low contribution, seasonal differences	/	Serôdio et al. 2012
14		XC important when motility is inhibited	/	Cartaxana et al. 2013
15		**low NPQ, small Ddx + Dtx pool, increase both in HL**	**High NPQ, large Ddx + Dtx pool**	**Barnett et al. 2015, Chapter 2**
16		balance depends on lattitidunal pattern	/	Laviale et al. 2015
17		photoacclimation affects both NPQ and migratory behaviour	/	Ezequiel et al. 2015
18		VM optimizes photosynthesis, when inhibitted higher Dtx/Ddx	/	Cartaxana 2016a
19		VM is fast enough to affect the XC/NPQ		Laviale et al. 2016
20		**less dynamic NPQ/XC, photoinhibition/NPQs**	**Dynamic NPQ and XC, no photoinhibition**	**Blommaert et al. 2017, Chapter 3**
21		**vertical migration in all species, high photoinhibition/NPQs**	**Dynamic NPQ, lack of vertical migration**	**Chapter 4**
22	**LHCX proteins**	isoform present in low light + high light responsive isoforms	/	Laviale et al. 2015
23		**isoform present in low light + high light responsive isoforms**	**isoform present in low light, light responsive**	**Blommaert et al. 2017, Chapter 3**
24		**multiple light regulated LHCX genes in *S. robusta***	**/**	**Chapter 5**

Table 1: An overview of photoprotection strategy studies in intertidal benthic diatoms

The xanthophyll cycle

As the xanthophyll cycle and its kinetics can explain NPQ capacity differences in planktonic diatoms, originating from habitats experiencing different degrees of light fluctuations (Lavaud et al. 2007; Dimier et al. 2007; Lavaud and Lepetit 2013), it was the main focus in both chapters 2 and 3. The main findings are that (1) NPQ in epipsammic diatoms is generally higher compared to epipelic species, both acclimated to low light conditions, as they possess larger Ddx + Dtx pools and as such de-epoxidize more Dtx in high light conditions, rather than showing a larger de-epoxidation state as observed in situ (Jesus et al. 2009; Cartaxana et al. 2011). (2) During exposure to higher light intensities, both epipelic as epipsammic species increase their XC pools. (3) the epipsammic species *O. guenter-grassii* accumulates, besides Dtx, significant amounts of Vx-cycle pigments when exposed to a relatively short period of strong light conditions (2000 µM photons m^{-2} s^{-1}, 1 h). (4) Epoxidation in this epipsammic species is very fast enabling it to relax its NPQ rapidly in low light conditions.

The XC pool in epipsammic species is larger, compared to epipelic species, when both grown in low light conditions (20 µmol photons m^{-2} s^{-1}), this results in higher Dtx content and NPQ capacity in the former when exposed to high light (Barnett et al. 2015; Blommaert et al. 2017). Dtx was absent or only present in very low concentrations (Chapters 2&3) in epipelic as well as epipsammic species, in above culture conditions, whereas in field conditions it is usually present, even in low/moderate light conditions (van Leeuwe et al. 2008; Jesus et al. 2009; Chevalier et al. 2010; Cartaxana et al. 2011). The total Ddx + Dtx content in these cultures, moreover, was rather low, compared planktonic species exposed to prolonged high light conditions (Lohr and Wilhelm 1999; Dimier et al. 2007). Therefore, we studied Ddx + Dtx content in cultures acclimated to 75 µmol photons m^{-2} s^{-1} (Barnett et al. 2015) or exposed to 2000 µmol photons m^{-2} s^{-1} (Chapter 3). Both conditions resulted in a significant increase in the Ddx + Dtx pool in both epipelic as epipsammic species, generally resulting in higher NPQ capacity, as has been observed in natural (epipelic) communities (Laviale et al. 2015). In some cases, however, a decline in the NPQ/Dtx slope was observed. This was especially the case at high Dtx concentrations and may be due to the fact that the additional Dtx may be dissolved in the lipid shield surrounding the FCPs, where it may play a role as antioxidant, preventing lipid peroxidation rather than participating in NPQ (Lepetit et al. 2010; Lavaud and Lepetit 2013), or regulating membrane fluidity as has been observed for Zx in plants (Havaux and Gruszecki 1993).

Accumulation of significant amounts of Zx in the epipsammic diatom *O. guenter-grassii* during one hour of 2000 µmol photons $m^{-2}s^{-1}$ was a rather unexpected finding and represents the first observation of both XCs in benthic diatoms, as Zx accumulation in diatoms has been only reported in (tycho)planktonic diatoms exposed to prolonged (up to 6 hours) strong light conditions (Lohr and Wilhelm 1999, 2001; Dimier et al. 2007). The

generality and function of Zx in (epipsammic) benthic diatoms, however, is not entirely clear. As proposed by Lohr and Wilhelm (1999, 2001) Zx could mainly be an intermediate in Dtx synthesis and was observed in species that have a high rate of carotenoid de novo synthesis in combination with high de-epoxidation activity, which fits our observations (Lohr and Wilhelm 1999). Vx-cycle pigments, moreover, disappeared rapidly and possibly were converted via the intermediate neoxanthin to the Ddx-cycle pool (Dambek et al. 2012), arguing for their possible role as intermediates. Alternatively, de-epoxidized xanthophylls may play a role in scavenging reactive oxygen species or membrane stability as mentioned above. However, we have no reasons to assume that Zx would be better at either functions as the more abundant Dtx.

Another major characteristic of the XC in relation to NPQ is the epoxidation reaction, which is crucial to switch the light harvesting system from an energy dissipating state back to a light harvesting state (Goss and Jakob 2010; Lavaud and Goss 2014). The fast epoxidation reaction in the epipsammic species *O. guenter-grassii* during low light allowed this species to rapidly relax its NPQ and as such to optimize light harvesting. This is in contrast to the epipelic species *S. robusta*, in which both epoxidation of Dtx and NPQ relaxation occurred more gradually. Even though Dtx epoxidation was only studied in two species (Chapter 3), a generally faster NPQ relaxation in epipsammic diatoms in contrast to epipelic species after high light illumination implicate faster epoxidation in the former, as described in Chapter 4. Interestingly, NPQ relaxation was substantially faster in the araphid and thus non-motile species *O. guenter-grassii*, compared to the other raphid and possibly motile epipsammic species. Hence, monitoring Dtx epoxidation in other araphid epipsammic species could resolve whether the fast epoxidation in *O. guenter-grassii* is rather exceptional or common in araphid epipsammic diatoms.

LHCX proteins

While LHCX proteins are a crucial component of the NPQ mechanism in diatoms (Bailleul et al. 2010b; Taddei et al. 2016; Ghazaryan et al. 2016), current knowledge about their function is mostly based on studies in planktonic diatoms (Lavaud and Goss 2014; Goss and Lepetit 2015), with the exception of an immuno-localization study of LHCX proteins in epipelic communities and in the epipelic diatom *Navicula phyllepta* (Laviale et al. 2015). As we observed NPQ differences between epipsammic and epipelic species, we studied light-regulation of LHCX isoforms in a representative of each group (Chapter 3). In addition we investigated the presence of LHCX genes in the epipelic model *S. robusta* and their transcriptional regulation in response to a day/night light climate and to oversaturating light conditions (Chapter 5).

As the used antibodies were not specifically designed to recognize LHCX isoforms in our benthic model diatoms, we could not quantitatively compare LHCX content between species.

However, we could detect an isoform present in low light in both species, which could provide both benthic diatoms with a basal NPQ to cope with a sudden increase in light intensity (Chapter 3). In the pennate model diatom *P. tricornutum*, LHCX1 fulfills this function (Bailleul et al. 2010b). The molecular weight of both isoforms, present in low light conditions in our studied benthic diatoms, seems to be higher than PtLHCX1. Moreover, we did not find a close homolog to LHCX1 in the genome of *S. robusta* (Chapter 5). As we showed that NPQ capacity is strongly correlated to Dtx content (Chapter 2&3) and Dtx molecules need pigment-binding proteins (probably LHCXs or certain LHCFs) to be involved in the NPQ mechanism (Lepetit et al. 2013, 2017) we do suspect that in general, LHCX proteins are abundant in epipsammic diatoms acclimated to low light conditions, in contrast to in epipelic diatoms. This hypothesis is also supported by relatively high NPQ/Dtx slopes in most epipsammic diatoms (Chapter 2).

When exposed to prolonged moderate/high light conditions, benthic diatoms (epipelic as well as epipsammic species) are able to increase their NPQ capacity (Ezequiel et al. 2015; Barnett et al. 2015). Besides de novo XC pigment synthesis (Lavaud et al. 2004; Schumann et al. 2007; Dimier et al. 2007), accumulation of specific LHCX proteins may play a role in adjusting the NPQ capacity to the experienced light climate (Lepetit et al. 2013, 2017; Laviale et al. 2015). In the only studied epipsammic diatom (*O. guenter-grasssii*), one LHCX isoform was detected in low light conditions, which seemed to increase in abundance during high light conditions (Blommaert et al. 2017). Lack of detection of other light-inducible isoforms in this species may be due to the fact that the antibody was not specific and might not be able to recognize particular LHCX isoforms (Lepetit et al. 2017). Alternatively, epipsammic species already have a relatively high and flexible NPQ capacity when acclimated to low light conditions (Barnett et al. 2015; Blommaert et al. 2017) as described in Chapters 2-4, which may alleviate the need for additional NPQ capacity.

The opposite situation is observed in epipelic diatoms. When acclimated to low light intensities, they generally have lower NPQ capacities, which increases during acclimation to higher light conditions (See Chapters 2-4, Ezequiel et al. 2015). These findings are in line with high light inducible transcription of *LHCX* genes (Chapter 5) and accumulation of additional LHCX isoforms (Chapter 4) in *S. robusta* and natural epipelic communities (Laviale et al. 2015) upon high light exposure. Interestingly, in contrast to epipsammic diatoms, a sustained quenching is generally observed after prolonged exposure to strong light conditions (Laviale et al. 2015), (Chapter 3&4), which may be partly attributed to photoinhibition and to the slow epoxidation of Dtx (Lavaud and Goss 2014). In *Thalassiosira pseudonana*, the observed sustained quenching might be associated with accumulation of the TpLHCX6 protein which may be responsible for additional Dtx binding. A protein, with similar characteristics as TpLHCX6, seems to be present in epipelic diatoms and may fulfill a similar function during prolonged light stress (Laviale et al. 2015), Chapter 5.

NPQ in the intertidal: macro-algae vs. benthic diatoms

While microphytobenthic diatoms dominate intertidal sediments (Underwood and Kromkamp 1999), rocky shores are dominated by dense populations of macro-algae. On temperate coasts of the northern hemisphere, these populations exhibit a strong vertical zonation with fucoid algae thriving on the high to the low mid-shore and laminarians occurring on the lower shore (Migné et al. 2015). These brown algae experience a similar light climate as benthic diatoms when emerged (Lavaud and Goss 2014). Therefore, they may require similar flexible photoprotection strategies.

While both diatoms and brown algae are capable of strong excess light energy dissipation as heat (measured as NPQ) (Lavaud and Goss 2014) and both belong to the Stramenopila (Kooistra et al. 2007), they differ in the main xanthophyll cycle pigments. Whereas in diatoms Dtx is involved in NPQ, Zx is responsible for NPQ in brown algae. Similar to our findings in benthic diatoms (Barnett et al. 2015; Blommaert et al. 2017), the total xanthophyll pool and the ability to produce de-epoxidized xanthophylls (Zx in the case of brown algae) is correlated with inter-species NPQ differences, with species living higher on the shore exhibiting higher NPQ/XC capacities than lower shore/subtidal species (Harker et al. 1999; Rodrigues et al. 2002).

A common feature of the respective xanthophyll cycles in brown algae and diatoms is that xanthophylls have to be converted to their epoxy-form (epoxidation) in order to relax NPQ in low light conditions, whereas in plants and green algae a change in the transthylakoidal proton gradient (ΔpH) is sufficient to accomplish NPQ relaxation, disregarding the slow Zx epoxidation in the green lineage (Goss and Jakob 2010; Goss and Lepetit 2015). While diatoms are capable of rapid Dtx epoxidation in low light conditions (Goss et al. 2006), a feature particularly evident in the epipsammic diatom *O. guenter-grassii* (Blommaert et al. 2017), the epoxidation reaction in brown algae is as slow as in plants (Goss and Jakob 2010). Therefore, also NPQ relaxation in brown algae is slow and unable to track fast fluctuations in light intensity (García-Mendoza and Colombo-Pallotta 2007). According to Goss and Jacob (2010), large kelps (and especially their deeper thallus parts) do not need flexible photoprotection mechanisms as they are exposed to relatively slowly changing light conditions. However, it would be interesting to assess the Zx epoxidation rate in brown algae living high in the intertidal, as they may experience more light fluctuations and/or a higher overall light climate. Additionally, as a similarly strong relationship between NPQ and de-epoxidized xanthophylls in diatoms and brown algae exists (see above), it would be valuable to assess the relationship between NPQ and ΔpH as we have attempted in a diatom in Chapter 6. Using a brown macro-alga, instead of a diatom suspension would have the additional advantages that the ElectroChromic Shift (ECS) signal would not drift as much (due to cell sedimentation in the case of diatoms) and that an optically dense macro-algal sample increases the signal to noise ratio.

The function of LHCSR proteins in photoprotection is less well-studied in brown algae than in diatoms. Sequencing of the *Ectocarpus siliculosus* genome, however, revealed 13 isoforms (Dittami et al. 2010). This is a high copy number, compared to the planktonic model diatoms *Thalassiosira pseudonana* and *Phaeodactylum tricornutum*, but in the range of the sea-ice associated diatom *Fragilariopsis cylindrus* and the epipelic benthic diatom *Seminavis robusta* (see Taddei et al. 2016; Mock et al. 2017 and Chapter 5 for an overview). Functional evidence for these proteins in NPQ regulation is scarce. In the giant kelp *Macrocystis pyrifra* members of the *LHCSR* family show a higher expression in blades near the surface than at 18 m depth. Targeted mutagenesis in brown algae (which is at present not possible; Lipinska, pers. comm.) may help to resolve whether LHCSR proteins share a similar NPQ regulatory function as in diatoms.

Finally, besides brown algae, red algae are also found in the intertidal. Even though NPQ has been measured in these organisms, the regulatory mechanism is far from clear as they do not seem to possess LHCSR proteins (Dittami et al. 2010) and have no functional xanthophyll cycle (Goss and Lepetit 2015).

Conclusion & future perspectives

Contribution of NPQ and XC to overall photoprotection in benthic diatoms

We showed that in epipsammic diatoms possess a high capacity for NPQ, and in combination with a high accumulation of de-epoxidized xanthophylls, this possibly leads to the a low vulnerability to photoinhibition, as observed in epipsammic communities in the field (Chapters 2-4 Pniewski et al. 2015). The contribution of the XC and NPQ to photoprotection, however, is not clear. Therefore, blocking the XC cycle using DTT (dithiothreitol), which inhibits Ddx de-epoxidase enzyme, in epipsammic species and/or communities could resolve the actual contribution of NPQ to overall photoprotection in this growth form (Lavaud et al. 2002). In addition, the contribution of NPQ- XC (and of migratory behavior) to the overall photoprotection in epipelic diatoms is not equivocal (Serôdio et al. 2012; Cartaxana et al. 2013; Laviale et al. 2015) and may depend, besides on in situ conditions, on the method used to quantify photoinhibition: recovery of photosynthetic efficiency during recovery in low light (Serôdio et al. 2012; Laviale et al. 2015) or quantifying the PSII core protein D1 (Cartaxana et al. 2013). In the case of photosynthetic efficiency recovery, it was shown that the total contribution of vertical migration and xanthophyll-cycle based photoprotection was relatively low (~20%) in epipelic communities from the Tagus estuary (Serôdio et al. 2012; Laviale et al. 2015). This is in contrast with the study of Cartaxana et al. (2013), where blocking the xanthophyll cycle with DTT decreased the D1 protein content 60%, compared to 20% in a control exposed to high light. As in diatoms a sustained NPQ component involving Dtx and LHCX proteins (Lavaud and Goss 2014; Laviale et al. 2015, Chapters 3&4) decreases the efficiency of PSII, it does not necessarily involve damage to the PSII core. Interestingly, a new PAM-based technique which allows discriminating between a protective and photoinhibitory NPQ component in a non-destructive and rapid (e.g. not requiring prolonged dark or low light conditions) manner. has recently been developed in plants (Ruban and Murchie 2012; Ruban 2016).

Species-specific balance behavioural/physiological photoprotection strategies in situ

Even though we observed general differences between epipelic and epispammic growth forms, our findings also suggest the existence of pronounced species-specific responses to high light conditions within each growth form, such as the accumulation of high amounts of Ddx + Dtx which are not involved in NPQ in the epipsammic diatom *Plagiogramma staurophorum*, (Chapter 2), a significantly stronger migratory response in the epipelic diatom *Navicula phyllepta* than in other epipelic species, or the fast relaxation of NPQ in the epipelic species *Navicula arenaria*, which is almost similar to that observed in epipsammic species (Chapter 4). These observations corroborate the observation of different surfacing peaks of epipelic diatom species during tidal emersion, suggesting different light niches (Underwood et al. 2005) and/or photoprotective capacities. Species-specific differences in NPQ capacity can be further investigated using imaging chlorophyll fluorescence microscopy (Oxborough

et al. 2000; Underwood et al. 2005, Jesus, pers comm) in cells freshly obtained from sandy and silty sediments . This could allow assessing whether some epipelic species couple a stronger capacity for NPQ with a less pronounced migratory response (high light avoidance) or whether epipelic and epipsammic species in sandy sediments have equally high NPQ capacities. To our knowledge, photophysiological features of epipelic species typical of sandy sediments (which are different from those typically present in silty sediments, e.g. representatives of the genus *Petroneis*, Sabbe 1997) have not yet been investigated.

Other photoprotective mechanisms

In this work the we studied mainly fast-regulatory photoprotective mechanism. Whereas NPQ and vertical migration clearly differed between the growth forms, this was not the case for PSII cyclic electron transfer (CET, Chapter 2). Other alternative electron pathways such as PSI CET (Bailleul et al. 2015) and the water-to-water cycle (Waring et al. 2010; Bailleul et al. 2015) could be evaluated in a set of epipelic and epipsammic species. In addition, the release of organic carbon could play a role during prolonged illumination as in both epipsammic (Cook et al. 2007) and epipelic communities (Smith and Underwood 2000) a considerable part of fixed carbon is excreted through the apical pore field or through the raphe slit (which is present only in raphid diatoms) in the form of carbohydrate rich extracellular polymeric substances (Hoagland et al. 1993). A comprehensive comparative study between both growth forms, however, is lacking. The photoprotective potential for this 'overflow' mechanism, moreover, is not clearly proven.

Adaptation to prolonged darkness in epipsammic diatoms

Epipsammic diatoms seem to be well-adapted to episodic high light conditions. However, they probably also spend long periods of time buried below the photic zone (Jewson et al. 2006; Cartaxana et al. 2011), and this without noticeable pigment degradation (Steele and Baird 1968). They must therefore possess adaptations to cope with long dark periods. It is known that benthic diatoms can respire nitrate to survive dark and anoxic conditions (Kamp et al. 2011). Anoxic conditions, however, may be less of an issue in sandy sediments (Anil et al. 2007). The uptake of amino acids, indeed seems to be higher in attached species, compared to motile species (Nilsson and Sundbäck 1996). The heterotrophic use of amino acids and other organic substrates in epipsammic diatoms could enable these species to survive for prolonged time periods, as has been shown in freshwater species (Tuchman et al. 2006).

Function of LHCX proteins as NPQ regulator in diatoms

Even though a crucial function for LHCX proteins has been implicated by the use of knock-down mutants (Bailleul et al. 2010b; Taddei et al. 2016; Ghazaryan et al. 2016), the exact contribution of LHCX proteins to the NPQ mechanism and to photoprotection in general is

unclear. Therefore, we suggest the use of knock-out mutants by targeted mutation in *P. tricornutum* (Serif et al. 2017). The presence of only four LHCX isoforms and their characterization in different conditions (Nymark et al. 2009, 2013; Bailleul et al. 2010b; Lepetit et al. 2013, 2017; Valle et al. 2014; Taddei et al. 2016), furthermore, make it the ideal model species for the time being, in contrast to *S. robusta* for which a standardized transformation protocol is not yet developed (Gust Bilcke, personal communication) and which contains 14 different LHCX genes. In addition, the differential conservation of protonable residues in *C. reinhardtii, P. tricornutum* and *S. robusta* raises interesting questions about their function in the regulation of NPQ in response to a trans-thylakoidal proton gradient (ΔpH). It is, for instance, unclear whether conserved protonable residues in diatoms LHCXs indeed have an NPQ regulatory function and whether LHCX4 in *P. tricornutum* and *S. robusta* (in which only one protonable residue is conserved) have a function in sustained NPQ. Introducing an LHCX1 construct, lacking one or both 'protonable residues' in an LHCX knockout context in *P. tricornutum*, as has been done for LHCSR3 in *C. reinhardtii*, could possibly resolve the first question. Overexpression of LHCX4 in a *P. tricornutum* strain lacking all other LHCXs, could possibly answer the second question.

Function of a trans-thylakoidal proton gradient as NPQ regulator

A new method to measure ΔpH in diatoms in vivo should be developed. The presence of both a linear and quadratic ECS signal in diatoms (Bailleul et al. 2010a) including *O. guenter-grassii* (Chapter 6), allows to measure the absolute value of the electric component ΔΨ of the PMF. As, at least in plants, it is possible to determine the total PMF (Joliot and Joliot 2008), applying this method in combination with determining its electric component ΔΨ, the ΔpH can be calculated as the difference between PMF and ΔΨ. By developing this method in diatoms the role of ΔpH in regulating NPQ can be further dissected.

References

Admiraal, W. 1984. The ecology of estuarine sediment-inhabiting diatoms. Prog. Phycol. Res. **3**: 269–322.

Anil, A. C., S. Mitbavkar, M. S. D'Silva, S. Hegde, P. M. D'Costa, S. S. Meher, and D. Banerjee. 2007. Effect of ageing on survival of benthic diatom propagules. J. Exp. Mar. Bio. Ecol. **343**: 37–43. doi:10.1016/j.jembe.2006.11.006

Bailleul, B., N. Berne, O. Murik, and others. 2015. Energetic coupling between plastids and mitochondria drives CO2 assimilation in diatoms. Nature **524**: 366–369. doi:10.1038/nature14599

Bailleul, B., P. Cardol, C. Breyton, and G. Finazzi. 2010a. Electrochromism: a useful probe to study algal photosynthesis. Photosynth. Res. **106**: 179–89. doi:10.1007/s11120-010-9579-z

Bailleul, B., A. Rogato, A. De Martino, S. Coesel, P. Cardol, C. Bowler, A. Falciatore, and G. Finazzi. 2010b. An atypical member of the light-harvesting complex stress-related protein family modulates diatom responses to light. Proc. Natl. Acad. Sci. **107**: 18214–18219. doi:10.1073/pnas.1007703107

Barnett, A., V. Méléder, L. Blommaert, and others. 2015. Growth form defines physiological photoprotective capacity in intertidal benthic diatoms. ISME J. **9**: 32–45. doi:10.1038/ismej.2014.105

Blommaert, L., M. J. J. Huysman, W. Vyverman, J. Lavaud, and K. Sabbe. 2017. Contrasting NPQ dynamics and xanthophyll cycling in a motile and a non-motile intertidal benthic diatom. Limnol. Oceanogr. doi:10.1002/lno.10511

Cartaxana, P., S. Cruz, C. Gameiro, and M. Kühl. 2016a. Regulation of intertidal microphytobenthos photosynthesis over a diel emersion period is strongly affected by diatom migration patterns. Front. Microbiol. **7**: 872. doi:10.3389/fmicb.2016.00872

Cartaxana, P., N. Domingues, S. Cruz, B. Jesus, M. Laviale, J. Serôdio, and J. Marques da Silva. 2013. Photoinhibition in benthic diatom assemblages under light stress. Aquat. Microb. Ecol. **70**: 87–92. doi:10.3354/ame01648

Cartaxana, P., C. R. Mendes, M. A. van Leeuwe, and V. Brotas. 2006. Comparative study on microphytobenthic pigments of muddy and sandy intertidal sediments of the Tagus estuary. Estuar. Coast. Shelf Sci. **66**: 225–230. doi:10.1016/j.ecss.2005.08.011

Cartaxana, P., L. Ribeiro, J. Goessling, S. Cruz, and M. Kühl. 2016b. Light and O2 microenvironments in two contrasting diatom-dominated coastal sediments. Mar. Ecol. Prog. Ser. **545**: 35–47. doi:10.3354/meps11630

Cartaxana, P., M. Ruivo, C. Hubas, I. Davidson, J. Serôdio, and B. Jesus. 2011. Physiological versus behavioral photoprotection in intertidal epipelic and epipsammic benthic diatom communities. J. Exp. Mar. Bio. Ecol. **405**: 120–127. doi:10.1016/j.jembe.2011.05.027

Chevalier, E. M., F. Gévaert, and A. Créach. 2010. In situ photosynthetic activity and xanthophylls cycle development of undisturbed microphytobenthos in an intertidal mudflat. J. Exp. Mar. Bio. Ecol. **385**: 44–49. doi:10.1016/j.jembe.2010.02.002

Consalvey, M., D. M. Paterson, and G. J. C. Underwood. 2004. The ups and downs of life in a benthic biofilm: Migration of benthic diatoms. Diatom Res. **19**: 181–202.

Cook, P. L. M., B. Veuger, S. Böer, and J. J. Middelburg. 2007. Effect of nutrient availability on carbon and nitrogen incorporation and flows through benthic algae and bacteria in near-shore sandy sediment. Aquat. Microb. Ecol. **49**: 165–180.

Cruz, S., and J. Serôdio. 2008. Relationship of rapid light curves of variable fluorescence to photoacclimation and non-photochemical quenching in a benthic diatom. Aquat. Bot. **88**: 256–264. doi:10.1016/j.aquabot.2007.11.001

Dambek, M., U. Eilers, J. Breitenbach, S. Steiger, C. Büchel, and G. Sandmann. 2012. Biosynthesis of fucoxanthin and diadinoxanthin and function of initial pathway genes in *Phaeodactylum tricornutum*. J. Exp. Bot. **63**: 5607–5612. doi:10.1093/jxb/ers211

Dimier, C., F. Corato, F. Tramontano, and C. Brunet. 2007. Photoprotection and xanthophyll cycle activity in three marine diatoms. J. Phycol. **43**: 937–947. doi:10.1111/j.1529-8817.2007.00381.x

Dittami, S. M., G. Michel, J. Collén, C. Boyen, and T. Tonon. 2010. Chlorophyll-binding proteins revisited - a multigenic family of light-harvesting and stress proteins from a brown algal perspective. BMC Evol. Biol. **10**: 365. doi:10.1186/1471-2148-10-365

Ezequiel, J., M. Laviale, S. Frankenbach, P. Cartaxana, and J. Serôdio. 2015. Photoacclimation state determines the photobehaviour of motile microalgae: The case of a benthic diatom. J. Exp. Mar. Bio. Ecol. **468**: 11–20. doi:10.1016/j.jembe.2015.03.004

García-Mendoza, E., and M. F. Colombo-Pallotta. 2007. The giant kelp *Macrocystis pyrifera* presents a different nonphotochemical quenching control than higher plants. New Phytol. **173**: 526–536. doi:10.1111/j.1469-8137.2006.01951.x

Ghazaryan, A., P. Akhtar, G. Garab, P. H. Lambrev, and C. Büchel. 2016. Involvement of the Lhcx protein Fcp6 of the diatom *Cyclotella meneghiniana* in the macro-organisation and structural flexibility of thylakoid membranes. Biochim. Biophys. Acta - Bioenerg. **1857**: 1373–1379. doi:10.1016/j.bbabio.2016.04.288

Goss, R., and T. Jakob. 2010. Regulation and function of xanthophyll cycle-dependent photoprotection in algae. Photosynth. Res. **106**: 103–122. doi:10.1007/s11120-010-9536-x

Goss, R., and B. Lepetit. 2015. Biodiversity of NPQ. J. Plant Physiol. **172**: 13–32. doi:10.1016/j.jplph.2014.03.004

Goss, R., E. A. Pinto, C. Wilhelm, and M. Richter. 2006. The importance of a highly active and ΔpH-regulated diatoxanthin epoxidase for the regulation of the PS II antenna function in diadinoxanthin cycle containing algae. J. Plant Physiol. **163**: 1008–1021. doi:10.1016/j.jplph.2005.09.008

Hamels, I., K. Sabbe, K. Muylaert, C. Barranguet, C. Lucas, P. Herman, and W. Vyverman. 1998. Organisation of microbenthic communities in intertidal estuarine flats, a case study from the molenplaat (Westerschelde estuary, The Netherlands). Eur. J. Protistol. **34**: 308–320. doi:10.1016/S0932-4739(98)80058-8

Harker, M., C. Berkaloff, Y. Lemoine, G. Britton, A. Young, J.-C. Duval, N.-E. Rmiki, and B. Rousseau. 1999. Effects of high light and desiccation on the operation of the xanthophyll cycle in two marine brown algae. Eur. J. Phycol. **34**: 35–42. doi:10.1080/09670269910001736062

Havaux, M., and W. I. Gruszecki. 1993. Heat and light induced chlorophull a fluorescence changes in potato leaves containign high or low levels of the carotenoid zeaxanthin: indications of a regulatory effect of zeaxanthin on thylakoid fluidity. Photochem. Photobiol. **58**: 607–614.

doi:10.1111/j.1751-1097.1993.tb04940.x

Hoagland, K. D., J. R. Rosowski, M. R. Gretz, and S. C. Roemer. 1993. Diatom extracellular polymeric substances: function, fine structure, chemistry and physiology. J. Phycol. **29**: 537–566. doi:10.1111/j.0022-3646.1993.00537.x

Jesus, B., V. Brotas, L. Ribeiro, C. R. Mendes, P. Cartaxana, and D. M. Paterson. 2009. Adaptations of microphytobenthos assemblages to sediment type and tidal position. Cont. Shelf Res. **29**: 1624–1634. doi:10.1016/j.csr.2009.05.006

Jesus, B., R. G. Perkins, M. Consalvey, V. Brotas, and D. M. Paterson. 2006. Effects of vertical migrations by benthic microalgae on fluorescence measurements of photophysiology. Mar. Ecol. Prog. Ser. **315**: 55–66. doi:10.3354/meps315055

Jewson, D. H., S. F. Lowry, and R. Bowen. 2006. Co-existence and survival of diatoms on sand grains. Eur. J. Phycol. **41**: 131–146. doi:10.1080/09670260600652903

Joliot, P., and A. Joliot. 2008. Quantification of the electrochemical proton gradient and activation of ATP synthase in leaves. Biochim. Biophys. Acta - Bioenerg. **1777**: 676–683. doi:10.1016/j.bbabio.2008.04.010

Kamp, A., D. de Beer, J. L. Nitsch, G. Lavik, and P. Stief. 2011. Diatoms respire nitrate to survive dark and anoxic conditions. Proc. Natl. Acad. Sci. U. S. A. **108**: 5649–54. doi:10.1073/pnas.1015744108

Kooistra, W. H. C. F., R. Gersonde, L. K. Medlin and D. G. Mann. 2007. The origin and the evolution of the diatoms: their adaptation to a planktonic existence, p. 207-249. *In* P. G. Falkowski, and A. H. Knoll [eds.], Evolution of Primary Producers in the Sea. Elsevier Academic Press, Burlington.

Kromkamp, J. C., C. Barranguet, and J. Peene. 1998. Determination of microphytobenthos PSII quantum efficiency and photosynthetic activity by means of variable chlorophyll fluorescence. Mar. Ecol. Prog. Ser. **162**: 45–55. doi:10.3354/meps162045

Kuhl, M., C. Lassen, and B. B. Jorgensen. 1994. Light penetration and light intensity in sandy marine sediments measured with irradiance and scalar irradiance fiber-optic microprobes. Mar. Ecol. Prog. Ser. **105**: 139–148. doi:10.3354/meps105139

Lavaud, J., and R. Goss. 2014. The peculiar features of the non-photochemical fluorescence quenching in diatoms and brown algae, p. 421–443. *In* B. Demmig-Adams, G. Garab, W. Adams III, and Govindjee [eds.], Non-Photochemical Quenching and Energy Dissipation in Plants, Algae and Cyanobacteria. Springer.

Lavaud, J., and B. Lepetit. 2013. An explanation for the inter-species variability of the photoprotective non-photochemical chlorophyll fluorescence quenching in diatoms. Biochim. Biophys. Acta **1827**: 294–302. doi:10.1016/j.bbabio.2012.11.012

Lavaud, J., B. Rousseau, and A.-L. Etienne. 2004. General features of photoprotection by energy dissipation in planktonic diatoms (Bacillariophyceae). J. Phycol. **40**: 130–137. doi:10.1046/j.1529-8817.2004.03026.x

Lavaud, J., B. Rousseau, and A-L. Etienne. 2002. In diatoms, a transthylakoid proton gradient alone is not sufficient to induce a non-photochemical fluorescence quenching. FEBS Lett. **523**: 163–6.

Lavaud, J., R. F. Strzepek, and P. G. Kroth. 2007. Photoprotection capacity differs among diatoms :

Possible consequences on the spatial distribution of diatoms related to fluctuations in the underwater light climate. Limnol. Oceanogr. **52**: 1188–1194.

Laviale, M., A. Barnett, J. Ezequiel, B. Lepetit, S. Frankenbach, V. Méléder, J. Serôdio, and J. Lavaud. 2015. Response of intertidal benthic microalgal biofilms to a coupled light-temperature stress: evidence for latitudinal adaptation along the Atlantic coast of Southern Europe. Environ. Microbiol. **17**: 3662–3677. doi:10.1111/1462-2920.12728

Laviale, M., S. Frankenbach, and J. Serôdio. 2016. The importance of being fast: comparative kinetics of vertical migration and non-photochemical quenching of benthic diatoms under light stress. Mar. Biol. **163**: 10. doi:10.1007/s00227-015-2793-7

van Leeuwe, M., V. Brotas, M. Consalvey, R. Forster, D. Gillespie, B. Jesus, J. Roggeveld, and W. Gieskes. 2008. Photoacclimation in microphytobenthos and the role of xanthophyll pigments. Eur. J. Phycol. **43**: 123–132. doi:10.1080/09670260701726119

Lepetit, B., G. Gélin, M. Lepetit, and others. 2017. The diatom *Phaeodactylum tricornutum* adjusts nonphotochemical fluorescence quenching capacity in response to dynamic light via fine-tuned Lhcx and xanthophyll cycle pigment synthesis. New Phytol. **214**: 205–218. doi:10.1111/nph.14337

Lepetit, B., S. Sturm, A. Rogato, A. Gruber, M. Sachse, A. Falciatore, P. G. Kroth, and J. Lavaud. 2013. High light acclimation in the secondary plastids containing diatom *Phaeodactylum tricornutum* is triggered by the redox state of the plastoquinone pool. Plant Physiol. **161**: 853–865. doi:10.1104/pp.112.207811

Lepetit, B., D. Volke, M. Gilbert, C. Wilhelm, and R. Goss. 2010. Evidence for the existence of one antenna-associated, lipid-dissolved and two protein-bound pools of diadinoxanthin cycle pigments in diatoms. Plant Physiol. **154**: 1905–1920. doi:10.1104/pp.110.166454

Lohr, M., and C. Wilhelm. 1999. Algae displaying the diadinoxanthin cycle also possess the violaxanthin cycle. Proc. Natl. Acad. Sci. **96**: 8784–8789. doi:10.1073/pnas.96.15.8784

Lohr, M., and C. Wilhelm. 2001. Xanthophyll synthesis in diatoms: quantification of putative intermediates and comparison of pigment conversion kinetics with rate constants derived from a model. Planta **212**: 382–391. doi:10.1007/s004250000403

Migné, A., G. Delebecq, D. Davoult, N. Spilmont, D. Menu, and F. Gévaert. 2015. Photosynthetic activity and productivity of intertidal macroalgae: In situ measurements, from thallus to community scale. Aquat. Bot. **123**: 6–12. doi:10.1016/j.aquabot.2015.01.005

Mock, T., R. P. Otillar, J. Strauss, and others. 2017. Evolutionary genomics of the cold-adapted diatom Fragilariopsis cylindrus. Nature **541**: 536–540. doi:10.1038/nature20803

Nilsson, C., and K. Sundbäck. 1996. Amino acid uptake in natural microphytobenthic assemblages studied by microautoradiography. Hydrobiologia **332**: 119–129. doi:10.1007/BF00016691

Nymark, M., K. C. Valle, T. Brembu, K. Hancke, P. Winge, K. Andresen, G. Johnsen, and A. M. Bones. 2009. An integrated analysis of molecular acclimation to high light in the marine diatom *Phaeodactylum tricornutum*. PLoS One **4**: e7743. doi:10.1371/journal.pone.0007743

Nymark, M., K. C. Valle, K. Hancke, P. Winge, K. Andresen, G. Johnsen, A. M. Bones, and T. Brembu. 2013. Molecular and photosynthetic responses to prolonged darkness and subsequent acclimation to re-illumination in the diatom *Phaeodactylum tricornutum*. PLoS One **8**: e58722. doi:10.1371/journal.pone.0058722

Oxborough, K., A. R. M. Hanlon, G. J. C. Underwood, and N. R. Baker. 2000. In vivo estimation of the photosystem II photochemical efficiency of individual microphytobenthic cells using high-resolution imaging of chlorophyll *a* fluorescence. Limnol. Oceanogr. **45**: 1420–1425. doi:10.4319/lo.2000.45.6.1420

Perkins, R. G., J. C. Kromkamp, J. Serôdio, J. Lavaud, B. Jesus, J.-L. Mouget, S. Lefebvre, and R. M. Forster. 2011. The application of variable chlorophyll fluorescence to microphytobenthic biofilms, p. 237–275. *In* D.J. Suggett, M.A. Borowitzka, and O. Prášil [eds.], Chlorophyll *a* Fluorescence in Aquatic Sciences: Methods and Applications. Springer Netherlands.

Perkins, R. G., J. Lavaud, J. Serôdio, and others. 2010. Vertical cell movement is a primary response of intertidal benthic biofilms to increasing light dose. Mar. Ecol. Prog. Ser. **416**: 93–103. doi:10.3354/meps08787

Pniewski, F. F., P. Biskup, I. Bubak, P. Richard, A. Latała, and G. Blanchard. 2015. Photo-regulation in microphytobenthos from intertidal mudflats and non-tidal coastal shallows. Estuar. Coast. Shelf Sci. **152**: 153–161. doi:10.1016/j.ecss.2014.11.022

Ribeiro, L., V. Brotas, Y. Rincé, and B. Jesus. 2013. Structure and diversity of intertidal benthic diatom assemblages in contrasting shores: a case study from the Tagus estuary. J. Phycol. **49**: 258–270. doi:10.1111/jpy.12031

Rodrigues, M. A., C. Pereira Dos Santos, A. J. Young, D. Strbac, and D. O. Hall. 2002. A smaller and impaired xanthophyll cycle makes the deep sea macroalgae *Laminaria abyssalis* (Phaeophyceae) highly sensitive to daylight when compared with shallow water *Laminaria digitata*. J. Phycol. **38**: 939–947. doi:10.1046/j.1529-8817.2002.t01-1-01231.x

Ruban, A. V. 2016. Nonphotochemical chlorophyll fluorescence quenching: Mechanism and effectiveness in protecting plants from photodamage. Plant Physiol. **170**: 1903–16. doi:10.1104/pp.15.01935

Ruban, A. V., and E. H. Murchie. 2012. Assessing the photoprotective effectiveness of non-photochemical chlorophyll fluorescence quenching: A new approach. Biochim. Biophys. Acta - Bioenerg. **1817**: 977–982. doi:10.1016/j.bbabio.2012.03.026

Sabbe, K. 1997. Systematics and ecology of intertidal benthic diatoms of the Westerschelde estuary (The Netherlands). Ghent University.

Schumann, A., R. Goss, T. Jakob, and C. Wilhelm. 2007. Investigation of the quenching efficiency of diatoxanthin in cells of *Phaeodactylum tricornutum* (Bacillariophyceae) with different pool sizes of xanthophyll cycle pigments. Phycologia **46**: 113–117. doi:10.2216/06-30.1

Serif, M., B. Lepetit, K. Weißert, P. G. Kroth, and C. Rio Bartulos. 2017. A fast and reliable strategy to generate TALEN-mediated gene knockouts in the diatom *Phaeodactylum tricornutum*. Algal Res. **23**: 186–195. doi:10.1016/j.algal.2017.02.005

Serôdio, J., S. Cruz, S. Vieira, and V. Brotas. 2005. Non-photochemical quenching of chlorophyll fluorescence and operation of the xanthophyll cycle in estuarine microphytobenthos. J. Exp. Mar. Bio. Ecol. **326**: 157–169. doi:10.1016/j.jembe.2005.05.011

Serôdio, J., J. Ezequiel, A. Barnett, J.-L. Mouget, V. Méléder, M. Laviale, and J. Lavaud. 2012. Efficiency of photoprotection in microphytobenthos: role of vertical migration and the xanthophyll cycle against photoinhibition. Aquat. Microb. Ecol. **67**: 161–175. doi:10.3354/ame01591

Serôdio, J., S. Vieira, S. Cruz, and H. Coelho. 2006. Rapid light-response curves of chlorophyll

fluorescence in microalgae: relationship to steady-state light curves and non-photochemical quenching in benthic diatom-dominated assemblages. Photosynth. Res. **90**: 29–43. doi:10.1007/s11120-006-9105-5

Smith, D. J., and G. J. C. Underwood. 2000. The production of extracellular carbohydrates by estuarine benthic diatoms: The effects of growth phase and light and dark treatment. J. Phycol. **36**: 321–333. doi:10.1046/j.1529-8817.2000.99148.x

Steele, J. H., and I. E. Baird. 1968. Production ecology of a sandy beach. Limnol. Oceanogr. **13**: 14–25. doi:10.4319/lo.1968.13.1.0014

Taddei, L., G. R. Stella, A. Rogato, and others. 2016. Multisignal control of expression of the LHCX protein family in the marine diatom *Phaeodactylum tricornutum*. J. Exp. Bot. **67**: 3939–3951. doi:10.1093/jxb/erw198

Tuchman, N. C., M. A. Schollett, S. T. Rier, and P. Geddes. 2006. Differential heterotrophic utilization of organic compounds by diatoms and bacteria under light and dark conditions. Hydrobiologia **561**: 167–177. doi:10.1007/s10750-005-1612-4

Underwood, G. J. C., and J. Kromkamp. 1999. Primary production by phytoplankton and microphytobenthos in estuaries estuaries. Adv. Ecol. Res. **29**: 93–153. doi:10.1016/S0065-2504(08)60192-0

Underwood, G. J. C., R. G. Perkins, M. C. Consalvey, A. R. M. Hanlon, K. Oxborough, N. R. Baker, and D. M. Paterson. 2005. Patterns in microphytobenthic primary productivity: Species-specific variation in migratory rhythms and photosynthesis in mixed-species biofilms. Limnol. Oceanogr. **50**: 755–767. doi:10.4319/lo.2005.50.3.0755

Valle, K. C., M. Nymark, I. Aamot, and others. 2014. System Responses to Equal Doses of Photosynthetically Usable Radiation of Blue, Green, and Red Light in the Marine Diatom *Phaeodactylum tricornutum* R. Subramanyam [ed.]. PLoS One **9**: e114211. doi:10.1371/journal.pone.0114211

Waring, J., M. Klenell, U. Bechtold, G. J. C. Underwood, and N. R. Baker. 2010. Light-induced responses of oxygen photoreduction, reactive oxygen species production and scavenging in two diatom species. J. Phycol. **46**: 1206–1217. doi:10.1111/j.1529-8817.2010.00919.x

Chapter 8: Summary

Benthic diatoms are dominant primary producers in intertidal marine sediments and are roughly divided into two main growth forms: the epipelon comprises mainly larger raphid motile diatoms and dominates silty sediments, whereas the epipsammon mainly consists of small motile and non-motile species that live in close association with single sand particles. As intertidal sediments are characterized by rapidly fluctuating and often extreme light conditions, benthic diatoms display behavioural as well as physiological photoprotection mechanisms. Vertical migration into the sediment (behavioural photoprotection), however, is largely restricted to epipelic diatoms, whereas epipsammic diatoms have to undergo changes in light conditions. As in natural communities (in situ studies) it is hard to characterize the photoprotective strategies of diatom growth forms (as natural communities can contain both epipelic and epipsammic growth forms), we studied the photoprotection capacity of unialgal isolates belonging to the main growth forms under controlled lab conditions.

One of the major physiological photoprotection mechanisms is to dissipate excess light energy as heat which can be measured as Non-Photochemical Quenching (NPQ). The capacity of this mechanism is mainly defined by the xanthophyll cycle (XC) pigment diatoxanthin and Light-harvesting Complex X (LHCX) proteins. We show that epipelic and epipsammic diatoms show fundamentally different photoprotective responses: epipsammic diatoms have a higher NPQ and associated XC capacities compared to epipelic diatoms. In the latter group, the behavioural response (vertical migration) is more important which may alleviate the need for strong physiological photoprotection. The regulation and performance of NPQ was further studied using model representatives of each functional group during and after exposure to high light. The epipsammic species *Opephora guenter-grassii* could rapidly switch NPQ on and off by relying on fast XC kinetics. This species also demonstrated high de novo synthesis of xanthophylls within a relatively short period of time (1 h), including significant amounts of zeaxanthin, a feature not observed before in other diatoms. In contrast, the epipelic representative *Seminavis robusta* showed slower NPQ and associated XC kinetics, partly relying on NPQ conferred by de novo synthetized diatoxanthin molecules and synthesis of Light-Harvesting Complex X (LHCX) isoforms. The genome of *S. robusta* contains fourteen *LHCX* genes. For eight *LHCX* genes we could show distinct upregulation during (strong) light exposure.

While overall our results support the a trade-off between behavioural and physiological photoprotection mechanisms other factors besides growth form, such as environmental factors, cell size, substrate type and photoacclimation, may influence photoprotective

strategies and explain species-specific photoregulation traits in intertidal benthic diatoms.

Samenvatting

Benthische (bodem bewonende) kiezelwieren zijn de dominante primaire producenten in de sedimenten van mariene intergetijdengebieden. Ze worden doorgaans opgedeeld in twee grote groepen: Epipelische soorten leven meestal op fijne, slibrijke sedimenten en zijn in staat om te bewegen. Epipsammische soorten zijn doorgaans kleiner en leven vastgehecht aan zandkorrels of kunnen rond bewegen op één zo'n zandkorrel. Gezien in intertidale sedimenten het lichtklimaat sterk kan fluctueren en er vaak hoge licht condities voorkomen, hebben deze kiezelwieren beschermingsmechanismes ontwikkeld tegen de extreme, en snel veranderende lichtcondities. Zowel gedragsmatige- als fysiologische mechanismes zijn gekend. Gedragsmatige mechanismes (het verticaal in het sediment migreren bij te sterk light), is echter alleen mogelijk in epipelische soorten, terwijl epipsammische soorten veranderingen in lichtklimaat moeten doorstaan. Studies met natuurlijke gemeenschappen suggereerden inderdaad dat gemeenschappen op zandige sedimenten, in vergelijking met modderige sedimenten sterkere fysiologische beschermingsmechanismes bezitten. Op zandige sedimenten, komen echter zowel epipelische als epipsammische soorten voor en is het meten van fysiologische beschermingsmechanismes niet evident. Daarom hebben we in deze studie fysiologische beschermingsmechanismes bestudeerd in monoclonale celculturen in een gecontroleerde labo omgeving.

Eén van de belangrijkste fysiologische beschermingsmechanismes bij hoog licht in kiezelwieren is de overtollige lichtenergie kwijt spelen als warmte, tijdens een proces genaamd Non-Photochemical Quenching, 'NPQ'. Zowel het xanthofylcyclus-pigment diatoxanthine als Light-Harvesting Complex (LHCX) eiwitten spelen hierbij een rol. In deze studie toonden we aan dat epipelische en epipsammische kiezelwieren duidelijk verschillen in het gebruik van beschermingsprocessen tegen sterke lichtcondities. Epipsammische kiezelwieren hebben een sterkere NPQ capaciteit dan epipelische kiezelwieren, doordat ze meer diatoxanthine kunnen aanmaken. Gezien epipelische soorten weg kunnen bewegen van hoog licht, hebben ze vermoedelijk geen nood aan sterke fysiologische bescherming. We onderzochten de regulatie van NPQ verder voor een vertegenwoordiger van elke groep. Hierbij toonden we aan dat de epipsammische soort zijn NPQ mechanisme zeer snel aan- en af kan zetten, afhankelijk van het lichtklimaat. Dit door zeer snel (1 uur) diatoxanthine aan te maken en terug om te vormen tot zijn precursor wanneer nodig. Opmerkelijk was dat deze soort ook een ander xanthofyl pigment aanmaakt: zeaxanthine. Dit werd bij kiezelwieren nog nooit eerder waargenomen op eenzelfde tijdsperiode. De epipelische soort *Seminavis robusta* reageerde trager en minder sterk op een verandering in lichtintensiteit. We namen echter wel waar dat deze soort zijn NPQ capaciteit kan opdrijven door nieuwe xanthofylcyclus pigmenten en LHCX eiwitten aan te maken. Er zitten dan ook 14 *LHCX*

genen in het genoom van *S. robusta*. Voor acht ervan konden we aantonen dat deze werden opgereguleerd bij hoge lichtintensiteiten.

Hoewel onze resultaten bevestigen dat epipelische en epipsammische kiezelwieren er verschillende strategieën op na houden om met sterke lichtintensiteiten om te gaan, zijn er ook duidelijke verschillen binnen de grote groepen. Deze verschillen zijn vermoedelijk te wijten aan onder andere omgevingsfactoren, celgrootte en sedimenttype.

Acknowledgements - Dankwoord

First of all, I would like to thank Koen and Wim for granting me the opportunity to start a Ph.D. in the Protistology and Aquatic Ecology research group. Koen, first of all, many thanks for the constant support, advice (work and non-work related) and maybe most of all, for all your patience during the last six years and a half. The work you have put into the different chapters of this thesis and constructive criticism was highly appreciated and necessary. Thanks as well for allowing me to join international conferences and to visit the labs of experts in the field of diatom photophysiology. Wim, many thanks for the confidence during all these years, research ideas and advice.

Johann, I'm really grateful to you for inviting me to your lab in La Rochelle and for introducing me to diatom photophysiology, together with Alex and Bernard. Your technical advice during publication writing was crucial.

Benjamin, first of all, many thanks for the scientific discussions (we got a whiteboard in Ghent as well) and for introducing me to electrochromism. Furthermore, I cannot say how thankful I am for granting me the opportunity to join your lab.

Pieter and Bart, thanks for learning me the basics of diatom culturing techniques. It was really essential for this work.

I would also like to sincerely acknowledge to work of the technical staff of PAE (Olga, Tine, Sofie, Ilse and Renaat) who's expertise was essential for this thesis.

Marie, Emmelien and Klaas, many thanks for the valuable advice on the molecular aspects of the LHCX story.

Fredje, Sofie and Frédéric, thanks for all the fun we had during the practicals (mostly during sampling though).

A special thanks Anja, for support on things I had no clue about.

A big thank you to all the other past and present colleagues of PAE, Phycology, Marbiol, Limnology, Botany and Limnology for making me feel welcome at S8 as well as at the Ledeganck. It was a real pleasure to work with you all. In particular, I would like to thank Willem for sharing the office with me until the end and listening to all my complaints, while all other Amniota fled to better places, and Céline for all the support during the last six years, and for practical advice these last months.

A sincere thanks to the members of the jury committee Bart Braeckman, Graham Underwood, Bruno Jesus, Lieven De Veylder and Olivier De Clerck for the constructive criticism, which substantially improved the final version of this work.

Ik zou graag uitdrukkelijk mijn ouders, schoonouders, broers Adriaan en Florian (en George), familie en schoonfamilie en vrienden in Temse en Gent willen bedanken voor al hun steun en afleiding tijdens mijn assistentschap.

Ten slotte kan een welgemeend dankwoord aan Anneke niet ontbreken. Anneke, van harte bedankt om er steeds voor mij te zijn, ook al was ik soms moeilijk te verdragen de voorbije jaren en in het bijzonder de laatste maanden. Op nog vele mooie momenten samen!

Veel liefs

Lander